TECHNISCHE UNIVERSITÄT MÜNCHEN
Max-Planck-Institut für Plasmaphysik

Nonlinear Triad Interactions in Three-Dimensional Magnetohydrodynamic Plasma Turbulence

Yasser Saad Abdel-Halim Rammah

Vollständiger Abdruck der von der Fakultät für Physik der Technischen Universität München zur Erlangung des akademischen Grades eines Doktors der Naturwissenschaften (Dr. rer. nat.) genehmigten Dissertation.

Vorsitzender: Univ.-Prof. Dr. Reiner Krücken
Prüfer der Dissertation: 1. Hon.-Prof. Dr. Sibylle Günter
2. Univ.-Prof. Dr. Katharina Krischer

Die Dissertation wurde am 05.10.2010 bei der Technischen Universität München eingereicht und durch die Fakultät für Physik am 20.01.2011 angenommen.

To

My parants

My wife and daughters (Basant and Jana)

Physcis Department, Faculty of science, Menoufia University, Egypt

My brothers, sisters and relatives

and

My colleagues and friends

Abstract

The spectral properties of nonlinear turbulent dynamics, *i.e.,* transfer functions, triad interactions, and cascade direction of ideal quadratic invariants are studied by analyzing data from high-resolution direct numerical simulations of incompressible two and three-dimensional hydrodynamic (HD) and magnetohydrodynamic (MHD) turbulence. The goal of our numerical studies is to improve the understanding of the dynamics of such flows. An accurate numerical approach toward analyzing nonlinear turbulent transfer functions and triad interactions is presented. In this approach, every wavenumber triad in the inertial range associated with the nonlinear terms of the differential equations of Navier-Stokes and MHD equations is numerically examined. The technique allows us to compute the spectral transfer functions, fluxes, and the spectral locality of the transfer functions. To this end, the geometrical shape of each underlying wavenumber triad that contributes to the statistical transfer density function is examined to infer the locality of the ideal invariant transport. In isotropic two-dimensional hydrodynamic turbulence, the kinetic energy transfer is found to be nonlocal through nonlocal triad interactions with an inverse cascade. The enstrophy transfer is found to be local through nonlocal interactions with a direct cascade. In three-dimensional hydrodynamic turbulence, the kinetic energy and helicity transfer functions are local through nonlocal triad interactions with a direct cascade.

The total energy and cross helicity transfer functions are local through nonlocal interactions with a direct cascade in decaying macroscopically isotropic 2D and 3D-MHD turbulence. Mean square magnetic vector potential transfer is nonlocal through nonlocal interactions with an inverse cascade in 2D-MHD turbulence. Magnetic helicity transfer is nonlocal with an inverse cascade in isotropic 3D-MHD turbulence. In anisotropic 3D-MHD turbulence subject to a strong mean magnetic field, the nonlinear total energy and cross helicity transfer functions are generally weak with a weak direct cascade. They exhibit a moderate increase of nonlocality in both perpendicular and parallel directions compared to the isotropic case. These results support the recent mathematical findings which also find that nonlinear transfer functions in hydro- and magnetohydrodynamic turbulence are local and will help setting this controversial issue.

Kurzfassung

Die spektralen Eigenschaften der nichtlinearen turbulenten Dynamik, d.h. Transferfunktionen, Triadenwechselwirkungen und Kaskadenrichtung der idealen quadratischen Invarianten, werden durch die Analyse hoch aufgelöster direkter numerischen Simulationen inkompressibler zwei- und dreidimensionaler hydrodynamischer (HD) und magnetohydrodynamischer (MHD) Turbulenz betrachtet. Das Ziel der durchgeführten numerischen Untersuchungen ist ein besseres Verständnis der Dynamik solcher Strömungen. Es wird ein präziser numerischer Zugang zur Analyse nichtlinearer turbulenter Transferfunktionen und Triadenwechselwirkung vorgestellt. Im Rahmen dieses Zugangs wird jede Wellenzahltriade im Inertialbereich, die vom nichtlinearen Term der zugrunde liegenden Navier-Stokes bzw. MHD Gleichungen herrührt, numerisch untersucht. Die verwendete Methode erlaubt die Berechnung der spektralen Transferfunktionen, der Flüsse und der spektralen Lokalität der Transferfunktionen. Zur Bestimmung der Lokalität des resultierenden Transports wird dabei die geometrische Gestalt jeder zugrundeliegenden Wellenzahltriade, die zur statistischen Transferdichtefunktion beiträgt, untersucht. Der kinetische Energietransfer verläuft in Simulationen der isotropen zweidimensionalen hydrodynamischen Turbulenz nichtlokal vermittelt durch nichtlokale Triadenwechselwirkung mit einer inversen Kaskade. Der Enstrophietransfer vollzieht sich lokal über nichtlokale Wechselwirkungen mit einer direkten Kaskade. In der dreidimensionalen hyrdodynamischen Turbulenz sind die kinetische Energie- und Helizitätstransferfunktionen lokal und kommen durch die nichtlokale Triadenwechselwirkung mit einer direkten Kaskade zustande. In Fall der zerfallenden, makroskopischen, isotropen 2D und 3D MHD-Turbulenz sind die Gesamtenergie- und Kreuzhelizität-Transferfunktionen lokal und kommen durch die nichtlokale Wechselwirkung mit einer direkten Kaskade zustande. Der Transfer des mittleren magnetischen Vektorpotentials ist nichtlokal und läuft in der 2D MHD über nichtlokale Wechselwirkung mit einer inversen Kaskade ab. In der isotropen 3D MHD verläuft der Transfer magnetischer Helizität nichtlokal über eine inverse Kaskade. In der aufgrund eines starken magnetischen Feldes anisotropen 3D MHD Turbulenz sind die nichtlinearen Transferfunktionen der Gesamtenergie und der Kreuzhelizität im Allgemeinen schwächer als ohne ein mittleres Feld und besitzen eine schwache direkten Kaskade. Sie weisen eine schwache Zunahme der Nichtlokalität sowohl senkrecht, als auch parallel zum Magnetfeld gegenüber dem isotropen Fall auf. Die vorgestellten Ergebnisse unterstützen neueste mathematische Untersuchungen, die ebenfalls die Lokalität der nichtlinearen Transferfuktionen für hydrodynamische und magnetohydrodynamische Turbulenz zeigen und werden zu Klärung dieses kontrovers diskutierten Aspekts der turbulenten nichtlinearen Dynamik beitragen.

Contents

Introduction

Turbulence is a widespread phenomenon in which a fluid flow is characterized by apparently random, unsteady, irregular, and chaotic motions. Turbulent flows can be observed on Earth in the atmosphere and the water of rivers and oceans. Structures formed in the flow are called eddies. The motion of eddies is unpredictable [1], and they can span length scales of kilometers or only a few centimeters. A turbulent flow is a flow that is disordered in time and space. It may be three-dimensional or sometimes quasi two-dimensional, and may exhibit well-organized structures or not [1].

The most common electrically conducting medium is an ionized gas called a plasma. In the universe, plasmas constitute 99% of the visible material [2]. Electrically conducting media can be described as fluids, if the dynamical time and length scales of interest are large compared to those of the microscopic plasma constituents. In the context of this work, the single-fluid approximation is used for studying turbulent systems. Experimental examples where this approximation is justified are for example, the reversed-field pinch fusion experiment and dynamo experiments investigating turbulence of electrically conducting fluids by using liquid metals. Turbulent motions are also significant in many astrophysical systems: the convective zone in stars, interstellar media (ISM), planetary cores, the intergalactic medium (IGM), and the solar wind [2, 3]. The size of turbulent structures in astrophysical systems can span many light years as in the ISM or IGM, or less than a kilometer size as in sub-structure of the plasma in stars or cores of planets.

In the following two basic forms of turbulence will be studied: hydrodynamic (HD) Navier-Stokes (NS) turbulence involving the velocity field only and magnetohydrodynamic (MHD) turbulence which additionally features the magnetic field. In the study of turbulence, a set of differential equations must be simultaneously solved to gain an understanding of the flow. This set of equations includes nonlinear terms and so in general cannot be solved analytically. It is conventionally characterized by certain non-dimensional parameters: the kinetic Reynolds number in the case of HD turbulence, and in the case of MHD turbulence both kinetic and magnetic Reynolds numbers and the Alfv́en number. The value of these numbers distinguishes the type of flow. Beynod a critical Reynolds number, the flow is termed as turbulent. If the Reynolds number is increased, the smaller scale motions survive [2]. There are several methods for solving the differential equations of the HD and MHD systems approximately. Some of these methods are the eddy damped quasi-normal Markovian (EDQNM) approximation and large eddy simulations (LES). The target of these methods is to get a solution of the equations which to a certian degree resembles the systems in nature. These methods usually involve

additional assumptions to solve the equations. However, the non-dimensional parameters in the equations are not achievable numerically with the current computing facilities. Although, the results from the methods mentioned above are far from the reality of what is seen in nature, they give insights into the physical aspects of the turbulent flows. In this thesis, direct numerical simulations (DNS) methods are used to solve the equations of turbulent systems. DNS methods do not use any additional physical approximations to the equations, but solve them as they are in their true form. Numerical simulations methods represent a valuable tool that provide more detailed information about the examined systems compared to other methods. The DNS methods stay closest to the underlying differential equations describing the turbulent systems although they are computationally expensive. Therefore, we prefer to use data obtained by DNS.

The physics of magnetohydrodynamic (MHD) turbulence is more complex than hydrodynamic turbulence. There are two coupled vector fields, velocity and magnetic, and also two dissipative parameters, viscosity and resistivity. In addition, when the system is exposed to a mean magnetic field which cannot be transformed away like a mean velocity, the turbulence becomes anisotropic. For simplicity of the MHD description, a simple single-fluid approximation is used, and the mass density of the magnetofluid is assumed to be constant in time and spatially uniform. In addition, relativistic effects are neglected and fluid velocities are assumed to be much smaller than the magnetosonic speeds in the plasma [4].

Phenomenological models exist to describe the nonlinear dynamics of Navier-Stokes and MHD turbulence. These models were developed to understand certain aspects of turbulent flows. They assume different mechanisms through which structures in the fields act to build-up or destroy turbulence. The Kolmogorov (K41), Iroshnikov-Kraichnan (IK), and Goldreich-Sridhar (GS) phenomenologies are presented in details in Chapter two of this work.

To understand the spectral properties, especially the dynamics of energy transfer in turbulent systems, it is advantageous to solve the HD and MHD equations in Fourier space. Any nonlinear term, *e.g.,* a product of two functions in configuration space, transforms into a convolution integral in Fourier space. In the case of the discrete Fourier transform, the convolution integral becomes a convolution sum. Thus the nonlinear terms of the HD and MHD equations couple group of three wavevectors in Fourier space, forming a triad which satisfies the relation $\mathbf{k} + \mathbf{p} + \mathbf{q} = 0$. These triads are key to understanding the phenomenon of energy transfer in turbulent flows. This phenomenon is central to the concept of triad interactions and is a consequence of the quadratic nonlinearities of both HD and MHD equations. There are ideal quadratic invariants in both incompressible HD and MHD [2]. Each of these quantities is exchanged conservatively between the wavenumbers. Understanding the difference between local and nonlocal traid interactions, local and nonlocal transfer function of an ideal quadratic invariant is instrumental to understanding turbulent dynamical processes in the inertial range.

Kraichnan [5, 6] studied the locality of the energy transfer and triad interactions analytically using an 'almost Markovian Galilean invariant' turbulence model in the inertial range of 2D and 3D hydrodynamic fluid turbulence. Numerically, Domaradzki and Rogallo [7] computed the strength of triad interactions and the energy transfers in fluid turbulence. The energy

transfer is described in terms of shell-to-shell transfer functions and spherical energy-fluxes in isotropic MHD turbulence by for example: Alexakis *et al.* [8] using numerical simulations. Theoretically, the energy fluxes in MHD turbulence have been studied by Verma [9, 10] using field-theoretic arguments. Alexakis *et al.* [11] have studied the locality of energy transfer functions and the spectral interactions in anisotropic MHD turbulence.

The goal of this work to study the spectral properties of nonlinear turbulent dynamics, *i.e,* transfer functions, triad interactions, and cascade direction of ideal quadratic invariants in incompressible two and three-dimensional hydrodynamic and magnetohydrodynamic turbulence by analyzing data from high-resolution direct numerical simulations. Nonlinear dynamical processes help us to understand the nature and the sturcture formation of the turbulent. This work introduces an accurate numerical approach for analyzing nonlinear turbulent transfer functions and interactions. This approach includes the direct numerical examination of every wavenumber triad in the inertial range associated with nonlinear terms in the differential equations of Navier-Stokes turbulence and MHD turbulence. This technique allows to compute the spectral transfer functions, fluxes, and the spectral locality of the transfer functions. The geometrical shape of each underlying wavenumber triad that contributes to the statistical transfer density function $Q(v)$ (where v is the ratio of the smallest wavenumber to the middle wavenumber in the interacting triad) is examined to infer the locality of the ideal invariant transport. Quantitatively, the locality function $W(v)$ is computed to represent the nature of the nonlinear transfer function. This function measures the part of the total transfer that passes through the inertial range, that is due to all triad interactions in which the ratio of the smallest wavenumber to the middle wavenumber is greater than v. The Fortran code made for this purpose is based on an existing program developped by T. Hertkorn for 2D-HD simulations [12] and M. Haslehner for 3D-HD simulations [13]. In this work, we have modified the program to implement the analysis of two- and three-dimensional magnetohydrodynamic turbulence. Analysis of fully-developed, driven turbulence stemming from large pseudospectral simulations with high resolution conducted by A. Busse and W.-C. Müller is used to investigate all turbulent systems which studied in this work.

The work is organized as follows. Chapter 1 introduces the basic concepts of fluid and magnetohydrodynamics turbulence, including the set of dynamical equations governing the investigated systems, and the nonlinear quadratic invariants. Chapter 2 explains current phenomenological models that explain the spectral and spatial properties of hydrodynamic and magnetohydrodynamic turbulence. These models result in simple power laws, which play an important role in understanding the dynamical processes of turbulence. Chapter 3 discuss the energy transfer function, nonlinear triad interaction, and detailed conservation in HD and MHD turbulence. In addition, this chapter shows the difference between locality and nonlocality of transfer function and triad interactions, and analyses the different types of cascade directions. Chapter 4 outlines the numerical procedure employed to solve the equations of HD and MHD turbulence. Chapters 5 presents the results of our calculations for the spectral locality of transfer functions, triad interactions, and the type of cascade direction for ideal invariants in two- and three-dimensional hydrodynamic turbulence. Chapters 6 presents the results for the spectral locality of transfer functions, triad interactions, and the type of cascade

direction for ideal invaraints in two- and three-dimensional MHD turbulence. This chapter also includes the results of our calculations for the spectral properties of ideal invariants in forced-inverse cascade turbulence system.

Chapter 1

Theoretical concepts of fluid and magnetohydrodynamic turbulence

In this chapter, basic concepts of fluid turbulence such as continuity and the Euler equations of an ideal fluid[1] are introduced. A derivation of the Navier-Stokes equations is presented. The basic equations of magnetohydrodynamic (MHD) turbulence are discussed. Energy equations in both fluid and magnetohydrodynamic turbulence are presented. Homogenous isotropic and anisotropic turbulence are discussed. Navier-Stokes and magnetohydrodynamic equations in spectral Fourier space are presented.

1.1 Fundamental equations of neutral fluids

1.1.1 Continuity and Euler equations of an ideal Fluid

Fluids obey the general laws of continuum mechanics, conservation of mass, energy and linear momentum [14, 15]. The conservation of mass is expressed by the continuity equation, which is a mathematical statment that, in a steady state process, the rate at which mass of fluid enters the system is equal to the rate at which mass leaves the system. The differential form of the continuity equation is

$$\frac{\partial}{\partial t}\rho + \nabla \cdot (\rho \mathbf{v}) = 0, \tag{1.1}$$

where ρ is the fluid density, t is the time, and $\mathbf{v}$ is the fluid velocity vector. If the density ρ is a constant, as in the case of incompressible flow, the mass continuity equation simplifies to a volume continuity equation

$$\nabla \cdot \mathbf{v} = 0, \tag{1.2}$$

which means that the divergence of velocity field is zero everywhere.
The derivation of the **Euler equation** is based on the conservation of momentum, $\mathbf{P}$. Let us consider a small volume element in the fluid. The total force acting on this volume element is given by the integral

$$\mathbf{F} = \frac{d}{dt}\mathbf{P} = -\oint_{\partial \mathbf{V}} p \, d\mathbf{f}, \tag{1.3}$$

[1] Ideal fluid is the fluid without viscosity; viscosity is the quantity that describes a fluid's inner friction.

where the integration domain is the boundary surface of the volume, and p is the scalar pressure .
Transforming this integral over a closed surface into a volume integral using Gauss's formula, we find

$$-\oint_{\partial V} p\, d\mathbf{f} = -\int_V \nabla p\; dV. \tag{1.4}$$

where the force $-\nabla p$ acts on unit volume of the fluid.
Since the force can also be expressed as $\mathbf{F} = m\,\frac{d\mathbf{v}}{dt}$, Thus we have

$$\rho dV \frac{d\mathbf{v}}{dt} = -\nabla p dV \tag{1.5}$$

and therefore,

$$\frac{d}{dt}\mathbf{P}(t) = -\int_V \nabla p\; dV = \int_V \rho\,\frac{d\mathbf{v}}{dt}\; dV. \tag{1.6}$$

The notation $\frac{d\mathbf{v}}{dt} = \frac{\partial \mathbf{v}}{\partial t} + (\mathbf{v}\cdot\nabla)\mathbf{v}$ refers to a substantial derivative, *i.e.,* not the change of velocity of the fluid at a fixed point, but at moving points in space. Then Eq.(1.6) can be written

$$\int_V \left(-\nabla p - \rho\,\frac{\partial \mathbf{v}}{\partial t} - \rho\,(\mathbf{v}\cdot\nabla)\,\mathbf{v}\right)\, dV = 0. \tag{1.7}$$

Because this is valid for any arbitrary volume V, the integrand is also equal to zero.

$$\frac{\partial \mathbf{v}}{\partial t} + (\mathbf{v}\cdot\nabla)\mathbf{v} = -\frac{1}{\rho}\nabla p. \tag{1.8}$$

This equation is called the Euler equation. It describes the motion of a volume element in an ideal fluid. The state of a moving field is determined by five quantities (the three components of the velocity, and for example, by the pressure and the density) that constitute complete system of equations of an ideal fluid. They are thus given by the Euler, the continuity, and a thermodynamic equations of state.

1.1.2 Navier-Stokes equations of a fluid flow

The equations for a viscous liquid can be derived from the equations of an ideal fluid by taking into consideration the effects of an irreversible momentum transfer due to friction between fluid particles. By fluid particle we mean elements of volume which are small compared with the volume of the body but large in comparison with the distances between the molecules [14]. Finite viscosity leads to energy dissipation. Although we are not primarily interested in dissipation effects in this work, viscosity plays an essential role in the derivation of the Navier-Stokes equations.
The most general form of the equations of motion for a viscous Newtonian fluid is given by [14]

$$\rho\left(\frac{\partial \mathbf{v}}{\partial t} + (\mathbf{v}\cdot\nabla)\mathbf{v}\right) = -\nabla p + \mu\Delta\mathbf{v} + (\zeta + \frac{\mu}{3})\nabla(\nabla\cdot\mathbf{v}), \tag{1.9}$$

where ρ is the fluid density, μ and ζ are the shear and volume viscosity, respectively. These viscosities are set constant in space and are functions of the pressure and of the temperature. However, In many cases, they may be regarded as constant [16]. The above equation can

be simplified by assuming that the fluid is incompressible. This means that the density ρ is constant

$$\frac{d\rho}{dt} = 0. \tag{1.10}$$

The continuity equation simplifies then to

$$\nabla \cdot \mathbf{v} = 0. \tag{1.11}$$

Finally,

$$\frac{\partial \mathbf{v}}{\partial t} + (\mathbf{v} \cdot \nabla)\mathbf{v} = -\frac{1}{\rho}\nabla p + \frac{\mu}{\rho}\Delta \mathbf{v}, \tag{1.12}$$

introducing the kinematic viscosity ν, which is defined as the dynamic viscosity of the fluid divided by the density of the fluid,

$$\nu := \frac{\mu}{\rho}. \tag{1.13}$$

We can write,

$$\frac{\partial \mathbf{v}}{\partial t} + (\mathbf{v} \cdot \nabla)\mathbf{v} = -\frac{1}{\rho}\nabla p + \nu\Delta \mathbf{v}. \tag{1.14}$$

and

$$\nabla \cdot \mathbf{v} = 0. \tag{1.15}$$

Eqs.(1.14) and (1.15), first found by Navier in 1827, are the Navier-Stokes equations in the case of steady flow of an incompressible fluid. In this case (see Eq.1.11), the viscosity is determined only by the so-called dynamic viscosity coefficient μ. Since $\nabla \cdot \mathbf{v} = 0$, the velocity is determined by $(\nabla \times \mathbf{v})$, according to the splitting into the sum of a rotation-free and a divergence-free part.

1.1.3 Energy equation

Energy equations can be derived for compressible fluid turbulence and also in the incompressible limit. For an incompressible fluid the energy equation can be constructed by using Eq.(1.14). The energy equation for the kinetic energy can be written [14]

$$\frac{\partial}{\partial t}\left(\frac{1}{2}\rho v^2\right) = -\nabla \cdot \left[\left(\frac{1}{2}v^2\right)\rho \mathbf{v}\right] - \nabla \cdot p\mathbf{v} + \mathbf{\Phi}. \tag{1.16}$$

The l.h.s. of Eq.(1.16) is the rate of change of the kinetic energy in the fluid. The first term on the r.h.s. is the energy flux, the second term is the work done by pressure and the third term (Φ) is the energy change due to surface forces. For an incompressible fluids we can choose $\rho = 1$, and treat the value $\frac{1}{2}v^2$ as the total energy. For an ideal incompressible fluid ($\nu = 0$), the energy evolution equation is

$$\frac{\partial}{\partial t}\frac{1}{2}v^2 = -\nabla \cdot \left[\left(\frac{1}{2}v^2 + p\right)\mathbf{v}\right].$$

By integrating the above equation over volume and applying Gauss′s law, we obtain

$$\frac{\partial}{\partial t}\int_V \frac{1}{2}v^2 dV = -\oint \left[\left(\frac{1}{2}v^2 + p\right)\mathbf{v}\right] \cdot dS. \tag{1.17}$$

For the boundary conditions, $v_n = 0$ (*i.e.,* the component of the fluid velocity normal to the bounding surface must vanish if that surface is at rest) or periodic boundary condition, the total energy is given by

$$E = \int_V \frac{1}{2} v^2 dV \tag{1.18}$$

and it is conserved. Several other conserved quantities in 2D and 3D Navier-Stokes turbulence will be discussed in section 1.7.

1.2 Concepts and fundamental equations in magnetohydrodynamic (MHD) turbulence

1.2.1 Magnetohydrodynamic (MHD) equations

Magnetohydrodynamic (MHD) or hydromagnetics is a branch which studies the dynamics of electrically conducting fluids. In a MHD fluid, the local charges ions and electrons are almost balance each other. The conductivity of MHD fluid is very high. As a consequence, the magnetic field lines are frozen into the fluid. Ions and electrons are find to the field, and the slight imbalance in the motion creates electric currents which in turn generate the magnetic fields. In the MHD picture, the heavier ions are considered to carry momentum, and the lighter electrons carry electric current. In an electromagnetic field with electric and magnetic fields $\mathbf{E}$ and $\mathbf{b}$ respectively, a particle of charge q_i is subjected to the Lorentz force $q_i\left(\mathbf{E} + \mathbf{v_i} \times \mathbf{b}/c\right)$, where c is the speed of light. The force on a macroscopic fluid element is the sum of the forces acting on the individual particles in this element $\delta q \times \mathbf{E} + \delta \mathbf{j} \times \mathbf{b}/c$, where δq is the net charge and $\delta \mathbf{j}$ the electric current density carried by the the fluid element. In the rest frame of the fluid element, the electric field $\mathbf{E}' = \mathbf{j}/\sigma$, where σ is the electrical conductivity. In the laboratory reference frame, the fluid element is moving by velocity $\mathbf{v}$ and the electric field is obtained by the Lorentz transformation for nonrelativistic flows,

$$\mathbf{E}' = \mathbf{E} + \frac{\mathbf{v} \times \mathbf{b}}{c} = \frac{1}{\sigma}\mathbf{j}. \tag{1.19}$$

Since, Ampere's law states that

$$\nabla \times \mathbf{b} = \frac{c}{4\pi}\mathbf{j} + \frac{1}{c}\frac{\partial \mathbf{E}}{\partial \mathbf{t}}.$$

The last term of the above equation can be ignored, because it is $(\mathbf{v}/c)^2$ times smaller than $(\nabla \times \mathbf{b})$. Therefore,

$$\mathbf{j} = \frac{c}{4\pi}\nabla \times \mathbf{b}. \tag{1.20}$$

Hence both $\mathbf{E}$ and $\mathbf{j}$ are dependent variables, and can be written in terms of $\mathbf{b}$ and $\mathbf{v}$. In MHD both magnetic and velocity fields are dynamic, so to determine the magnetic field we can use Faraday's equation which states that

$$\frac{\partial \mathbf{b}}{\partial t} = -c\nabla \times \mathbf{E}. \tag{1.21}$$

By applying Eqs.(1.19) and (1.20) in Eq.(1.21), we have the induction equation

$$\frac{\partial \mathbf{b}}{\partial t} = \nabla \times (\mathbf{v} \times \mathbf{b}) + \eta \nabla^2 \mathbf{b}.$$

Then we can write

$$\frac{\partial \mathbf{b}}{\partial t} + (\mathbf{v} \cdot \nabla)\mathbf{b} = (\mathbf{b} \cdot \nabla)\mathbf{v} + \eta \nabla^2 \mathbf{b}. \tag{1.22}$$

The parameter $\eta = c^2/(4\pi\sigma)$ is called the magnetic diffusivity and σ is the electrical conductivity. The magnetic field obeys the constraint:

$$\nabla \cdot \mathbf{b} = 0. \tag{1.23}$$

The time evolution of the velocity field is given by the momentum balance, which is [14, 17]

$$\rho \left(\frac{\partial \mathbf{v}}{\partial t} + (\mathbf{v} \cdot \nabla)\mathbf{v} \right) = -\nabla p_{\rm th} + \frac{1}{c}\mathbf{j} \times \mathbf{b} + \mu \nabla^2 \mathbf{v} \tag{1.24}$$

where ρ is the density of the fluid, $p_{\rm th}$ is the thermal pressure, and μ is the dynamic viscosity. Substituting kinematic viscosity of the fluid, $\nu = \mu/\rho$, and of $\mathbf{j}$ in terms of $\mathbf{b}$ from Eq.(1.20) into Eq.(1.24) we can obtain

$$\frac{\partial \mathbf{v}}{\partial t} + (\mathbf{v} \cdot \nabla)\,\mathbf{v} = \frac{1}{\rho}\left[-\nabla \left(p_{\rm th} + \frac{\mathbf{b}^2}{8\pi} \right) + \frac{1}{4\pi}\,(\mathbf{b} \cdot \nabla)\,\mathbf{b} \right] + \nu \nabla^2 \mathbf{v}. \tag{1.25}$$

In the above equation, the value $(p_{\rm th} + \frac{\mathbf{b^2}}{8\pi}) = p$ is called total pressure and the ratio $p_{\rm th} 8\pi/\mathbf{b^2}$ describes the strength of the magnetic pressure relative to thermal pressure. Mass conservation yields the continuity equation (cf. Eq.1.1) Pressure can be computed from ρ by using an equation of state,

$$p = f(\rho). \tag{1.26}$$

Eqs.(1.22),(1.25),(1.15) and (1.23) are the basic equations of magnetohydrodynamics (MHD). The incompressibility approximation can be interpreted as the limit when mass density of a fluid element does not change along its path, *i.e.,* $d\rho/dt = 0$. From the continuity equation (1.1), the incompressibility condition reduces to

$$\nabla \cdot \mathbf{v} = 0. \tag{1.27}$$

Incompressibility does not imply spatially constant density, but for simplicity one can take the density to be spatially homogenous and equal to unity. Under this condition, Eqs. (1.22) and (1.25) reduce to

$$\frac{\partial \mathbf{v}}{\partial t} + (\mathbf{v} \cdot \nabla)\mathbf{v} = -\nabla p + \frac{1}{4\pi}(\mathbf{b} \cdot \nabla)\mathbf{b} + \nu \nabla^2 \mathbf{v}, \tag{1.28}$$

$$\frac{\partial \mathbf{b}}{\partial t} + (\mathbf{v} \cdot \nabla)\mathbf{b} = (\mathbf{b} \cdot \nabla)\mathbf{v} + \eta \nabla^2 \mathbf{b}. \tag{1.29}$$

Then the incompressible magnetohydrodynamic (MHD) equations are Eqs. (1.28), (1.29), (1.27) and (1.23). Poisson's equation for the pressure can be obtained by taking divergence of Eq.(1.28) giving

$$\nabla \cdot [(\mathbf{v} \cdot \nabla)\mathbf{v} - (\mathbf{b} \cdot \nabla)\mathbf{b}] = -\nabla^2 p. \tag{1.30}$$

Hence one can compute p subject to the constraints of Eqs. (1.27) and (1.23) for the velocity and the magnetic field. Therefore, p is a passive quantity in the incompressible limit.
It is advantageous to work with a non-dimensional form of the set of magnetohydrodynamic equations [Eqs. (1.28), (1.29), (1.27) and (1.23)]. The mean magnetic field is assumed to be zero [18, 19]. The pressure term is eliminated from the equations by writing Eq.(1.28) in terms of vorticity $\boldsymbol{\omega} = \nabla \times \mathbf{v}$. The quantities are written in non-dimensional form, in terms of the characteristic length scale L_0 and velocity V_0 of the configuration under consideration as:

$$\mathbf{r}' \equiv \frac{\mathbf{r}}{L_0}, \quad \mathbf{v}' \equiv \frac{\mathbf{v}}{V_0}, \quad t' \equiv \frac{V_0}{L_0} t, \quad \mathbf{b}' \equiv \frac{\mathbf{b}}{\sqrt{4\pi}\, V_0} \qquad \text{and} \qquad p' \equiv \frac{p}{V_0^2} \quad . \tag{1.31}$$

With these operations, the set of MHD equations (1.28), (1.29), (1.27) and (1.23) becomes:

$$\partial_t \boldsymbol{\omega} - \nabla \times (\mathbf{v} \times \boldsymbol{\omega} + S_B \mathbf{j} \times \mathbf{b}) = \mathrm{Re}^{-1} \boldsymbol{\Delta} \boldsymbol{\omega}, \tag{1.32}$$

$$\partial_t \mathbf{b} = \nabla \times (\mathbf{v} \times \mathbf{b}) + \mathrm{Rm}^{-1} \boldsymbol{\Delta} \mathbf{b}, \tag{1.33}$$

$$\boldsymbol{\omega} = \nabla \times \mathbf{v}, \tag{1.34}$$

$$\mathbf{j} = \nabla \times \mathbf{b}, \tag{1.35}$$

$$\nabla \cdot \mathbf{v} = \nabla \cdot \mathbf{b} = 0. \tag{1.36}$$

The quantities are written without their respective primes (*i.e.,* $\mathbf{v}'$ as $\mathbf{v}$ and so on). This set of equations contains three dimensionless parameters S_B, Re and Rm which characterize the system. S_B is the interaction parameter (squared Alfvén number) and defined as $S_B = \frac{V_A^2}{V_0^2}$ where V_A is characteristic Alfvén velocity[2] [2, 4]. This parameter determines the relative dynamical importance of the velocity compared to magnetic field and for the rest of the work is set equal to 1. This means the magnetic field is measured in units of the characteristic Alfvén velocity. Re and Rm are given by the dissipation coefficients ν and η and the characteristic length L_0 and velocity V_0 as

$$\mathrm{Re} = \frac{L_0 V_0}{\nu} = \tilde{\nu}^{-1}, \qquad \mathrm{Rm} = \frac{L_0 V_0}{\eta} = \tilde{\eta}^{-1}, \tag{1.37}$$

and are called the kinetic Reynolds number and the magnetic Reynolds number, respectively. These Reynolds numbers are rough estimates of the strength of the nonlinearities compared to the dissipative terms in Eqs.(1.32) and (1.33). The ratio between the the magnetic Reynolds number and the kinetic Reynolds number is called the magnetic Prandtl number, $\mathrm{Pr_m} = \mathrm{Rm}/\mathrm{Re} = \nu/\eta$ which is another significant parameter of incompressible MHD, for example of importance in studies of magnetic field generation by MHD turbulence (turbulent dynamo

[2]The phase velocity of an Alfvén wave is given by $\frac{\mathbf{b}}{\sqrt{4\pi}\, V_0}$

effect, see *e.g.,* [20]). With the set of definitions given by Eq.(1.37), the final form of the non-dimensional MHD equations read:

$$\partial_t \boldsymbol{\omega} = \nabla \times (\mathbf{v} \times \boldsymbol{\omega} - \mathbf{b} \times \mathbf{j}) + \tilde{\nu} \boldsymbol{\Delta} \boldsymbol{\omega}, \tag{1.38}$$

$$\partial_t \mathbf{b} = \nabla \times (\mathbf{v} \times \mathbf{b}) + \tilde{\eta} \boldsymbol{\Delta} \mathbf{b}, \tag{1.39}$$

$$\nabla \cdot \mathbf{v} = \nabla \cdot \mathbf{b} = 0. \tag{1.40}$$

$\tilde{\nu}$ and $\tilde{\eta}$ are now the dimensionless dissipation coefficients.
By introducing Elsässer fields $\mathbf{z}^{\pm} = \mathbf{v} \pm \mathbf{b}$, an equivalent formulation of the MHD equations is also possible (*e.g.,* [21, 22, 23]). The Elsässer variables are well studied for analyses of nonlinear dynamics because the velocity and magnetic field equations in the Elsässer variables possess an almost symmetric form

$$\partial_t \mathbf{z}^{\pm} = -\mathbf{z}^{\mp} \cdot \nabla \mathbf{z}^{\pm} - \nabla p + \frac{\mathrm{Re}^{-1} + \mathrm{Rm}^{-1}}{2} \boldsymbol{\Delta} \mathbf{z}^{\pm} + \frac{\mathrm{Re}^{-1} - \mathrm{Rm}^{-1}}{2} \boldsymbol{\Delta} \mathbf{z}^{\mp}, \tag{1.41}$$

$$\nabla \cdot \mathbf{z}^{\pm} = 0. \tag{1.42}$$

where $p = (p_{th} + \frac{b^2}{2})$ is the total pressure. These equations can be solved, and lead to exact solutions in the form of counter-propagating Alfvén waves z^- and z^+ traveling in the same and in the opposite direction along the mean field, respectively. The nonlinear dynamics in the Elsässer picture is therefore represented by an ensemble of interacting Alfvén wave packets. It follows from the structure of the nonlinear term that only counter-propagating wave packets interact. In systems without mean magnetic field, it is supposed that the wave packets propagate along a large-scale magnetic field that plays the role of a guide field [19].

1.2.2 Important significance of MHD equations

Of the non-dimensional MHD equations the first Eq.(1.38) is called the vorticity equation, it represents the balance of momentum in the system. The first term on the r.h.s. of the vorticity equation describes the advection by the velocity field. The second term represents the influence of magnetic field on the velocity dynamics via the Lorentz force. It is responsible for energy transfer between the magnetic field and the velocity field, resulting in driving or suppression of velocity fluctuations [19].
Eq.(1.39) is the induction equation. The first term on the r.h.s. indicates to the nonlinear interaction between velocity and the magnetic field, which influences the evolution of magnetic field fluctuations. This term not only exchanges the energy between both the fields but also redistributes this energy over different spatial scales of the magnetic field [19]. The non-dimensional dissipation coefficients $\tilde{\nu}$ and $\tilde{\eta}$ in both Eqs.(1.38) and (1.39) are related to the Reynolds numbers in Eq.(1.37). In the hydrodynamic case, the Reynolds number Re must be greater than some critical Reynolds number (*i.e,* the critical Reynolds marks the transition from laminar to turbulent flow), $\mathrm{Re}^{\mathrm{crit}}$ for turbulence generation to occur. This is because its inverse, the normalized kinematic viscosity has a damping effect on turbulent fluctuations. The critical kinetic Reynolds number depends on the geometry of the flow and typically

$\mathrm{Re}^{\mathrm{crit}} \sim 10^2$ [2]. This parameter determines the transition to turbulence at low Re and properties of the turbulence itself at high Re of hydrodynamic flow. Additionally, very low values of the magnetic Reynolds number Rm implies that the domination of the magnetic dissipation, whereas very high Rm means that the magnetic flux through a surface moving with the fluid remains almost constant. In other words, the parameter Rm quantifies the frozen in property of magnetic fields, *i.e.,* how much the magnetic field is dragged by the velocity field, and how much it can slip through [24, 21]. Reynolds numbers determine the ratio of large and dissipation scales in a flow and thereby their separation (see chapter 2). Turbulent flows are characterized by large Reynolds numbers. Typically, the Reynolds numbers range from 10^6 for laboratory plasmas to 10^{12-20} or more in the case of astrophysical systems [19]. These large Reynolds number regimes are not achievable in direct numerical simulations with the current computational capabilities. Nevertheless the computations performed to give a reliable impression of the inherent properties of these systems to a large extent. Another parameter called the magnetic Prandtl number is introduced and defined as the ratio of the two Reynolds numbers:

$$\mathrm{Pr_m} = \frac{\mathrm{Rm}}{\mathrm{Re}}. \tag{1.43}$$

This parameter measures the relative importance of viscous and Ohmic dissipation. The typical values are on the order of 10^{-10} to 10^{-5} in the interiors of certain celestial bodies. $\mathrm{Pr_m}$ can be 10^2 in fusion plasma and 10^{14} for interstellar medium [19].
In this thesis the magnetic Prandtl number is always set to unity to achieve a formally symmetric configuration with regard to $\mathbf{v}$ and $\mathbf{b}$ [4]. Thus only the case where both the kinetic and magnetic diffusivities are equal is considered. The terms in Eq.(1.40) signify the fact that both the velocity and magnetic fields are solenoidal. Eqs.(1.41) and (1.42) contain Elsässer fields $\mathbf{z}^{\pm} = \mathbf{v} \pm \mathbf{b}$. These quantities are mathematically interesting in incompressible MHD because their equations are symmetric in nature [18, 2]. Ideal invariants (see section 1.7) and some properties like residual energy can also be expressed in terms of Elsässer fields (*e.g.,* see [2]). From Eq.(1.41), it can be seen that there is no self coupling in the nonlinear term but a cross coupling of $\mathbf{z}^+$ and $\mathbf{z}^-$ [2]. This forms the basis of the Alfvén effect, that describes a fundamental nonlinear process. Where Kraichnan [25] noticed that in the presence of large scale magnetic energy, Alfvén waves can bring small scale velocity and magnetic energies to equipartition and relax triple correlations which due to triad interactions in a time which may be shorter than the local eddy turnover time [26].

1.2.3 Energy equations and conserved quantities in magnetohydrodynamic (MHD) turbulence

Using Eqs.(1.22) and (1.25), we can construct energy equations for incompressible fluids. The energy equation for the kinetic energy is [14]

$$\frac{\partial}{\partial t}\left(\frac{1}{2}v^2\right) = -\nabla \cdot \left[\left(\frac{1}{2}v^2\right)\mathbf{v}\right] - \nabla \cdot (p\mathbf{v}) + \frac{1}{c}\mathbf{v} \cdot (\mathbf{j} \times \mathbf{b}) + \mathbf{\Phi}. \tag{1.44}$$

The first term on the r.h.s. is the nonlinear energy flux, and the second term is the work done by the pressure. The third term on the r.h.s is work done by magnetic force on the fluid. Φ is a complex function of the strain tensor, that represents the energy change due to surface forces.
Similarly we can use Eq.(1.21) to obtain an equation for the evolution of magnetic energy [17]

$$\begin{aligned}\frac{\partial}{\partial t}\frac{1}{8\pi}b^2 &= -\frac{c}{4\pi}\mathbf{b}\cdot\nabla\times\mathbf{E}\\ &= -\nabla\cdot\left[\frac{c}{4\pi}\mathbf{E}\times\mathbf{b}\right]-\mathbf{j}\cdot\mathbf{E}.\end{aligned} \tag{1.45}$$

The first term on the r.h.s is the Poynting flux (energy flux of the electro-magnetic field), and the second term is the work done by the electro-magnetic field on fluid. The second term is the Joule dissipation term. The dynamical equation for the energy in MHD can be obtained by combining equations (1.44) and (1.45)

$$\frac{\partial}{\partial t}\left(\frac{1}{2}v^2+\frac{1}{8\pi}b^2\right) = -\nabla\cdot\left[\left(\frac{1}{2}v^2\right)\mathbf{v}+\frac{c}{4\pi}\mathbf{E}\times\mathbf{b}\right]-\nabla\cdot(p\mathbf{v})+\mathbf{\Phi}+\mathbf{j^2}/\sigma. \tag{1.46}$$

In the above equation, $\left(\frac{1}{2}v^2+\frac{1}{8\pi}b^2\right)$ is the total energy. Eq.(1.46) simply says that the rate of change of total energy is the sum of energy flux, the work done by the pressure, and losses from viscous and resistive dissipation. Using a new variable for magnetic field $\mathbf{b}=\mathbf{b_{CGS}}/\sqrt{4\pi}$. In the terms of the new variable, the total energy is $\left(\frac{1}{2}v^2+\frac{1}{2}b^2\right)$. For an incompressible MHD fluid we can treat with the value $(v^2+b^2)/2$ as the total energy. For ideal incompressible MHD (where $\nu=\eta=0$) the energy evolution equation is then

$$\frac{\partial}{\partial t}\frac{1}{2}(v^2+b^2) = -\nabla\cdot\left[\left(\frac{1}{2}v^2+\frac{1}{2}b^2+p\right)\mathbf{v}\right]-2\nabla\cdot\left[(\mathbf{b}\cdot\mathbf{v})\,\mathbf{b}\right]. \tag{1.47}$$

By integrating this equation over some volume and appling Gauss′s law to the r.h.s., we find

$$\frac{\partial}{\partial t}\int_V\frac{1}{2}(v^2+b^2)dV = -\oint\left[\left(\frac{1}{2}v^2+\frac{1}{2}b^2+p\right)\mathbf{v}+(\mathbf{b}\cdot\mathbf{v})\mathbf{b}\right]dS. \tag{1.48}$$

For $v_n=b_n=0$ or periodic boundary condition, the total energy in incompressible MHD is conserved

$$E=\int_V\frac{1}{2}(v^2+b^2)dV. \tag{1.49}$$

Additional conserved quantities in 2D and 3D-MHD turbulence will be discussed in section 1.7.

1.3 Homogeneous isotropic turbulence

A turbulent flow (see the introduction of this thesis) is said to be homogeneous if it is statistically invariant under translation. For example the total energy of the turbulent fluctuations, $E=\frac{1}{2}\langle\mathbf{v_i}(\mathbf{x})\mathbf{v_i}(\mathbf{x})\rangle$, and the probability density function of the fluctuating velocity, $f(\delta\mathbf{v_i})(\mathbf{x},\mathbf{t})$, where $\delta\mathbf{v_i}(\mathbf{x},\mathbf{t})=\mathbf{v_i}(\mathbf{x},\mathbf{t})-\langle\mathbf{v_i}(\mathbf{x},\mathbf{t})\rangle$ are average quantities and thus translation invariant. Correlation functions such as $C_{ij}(\mathbf{r})=\langle\mathbf{v_i}(\mathbf{x})\mathbf{v_j}(\mathbf{x}+\mathbf{r})\rangle$ are independent of x and depend only on $\mathbf{r}$. Turbulence is isotropic if, it is spatially homogenous and the velocity

field is statistically invariant under rotation, meaning the field has no preferred direction, then $C_{ij} = C_{ij}(\mathbf{r})$. Isotropy implies that there is no mean velocity, since a nonzero mean velocity would create a preferred direction. The simplest setting for studying turbulence is a homogeneous isotropic field, which can be modelled by the flow behind a homogeneous grid in a water or a wind tunnel. The grid is placed at right angles to the uniform stream of the tunnel. One of the first experiments of this kind was devised in 1934 by Orszag [27] and Simmons and Salter [28]. Each bar of the grid generates a wake, and wakes due to different bars mingle leading to a turbulent velocity field downstream of the grid. The field, though highly non-isotropic at the beginning, becomes more and more isotropic as it decays. The motion far downstream consists of a nearly isotropic homogeneous random velocity field superposed on the uniform stream velocity [27]. In addition, the turbulence is observed to be accurately homogeneous in planes normal to the stream direction.
In hydrodynamic turbulence, homogeneous isotropic fields do not correspond to physical reality. Turbulent fields in nature must be anisotropic, because they have boundaries, and because turbulence is typically caused by mean gradients of velocity undergoing variations. Despite these effects of inhomogeneity, turbulent flows are locally homogeneous at sufficiently small scales. Homogenous isotropic fields constitute a way of simplifying the mathematical problem. This simplification allows for the isolation of the self-interaction of fluctuating components from the interaction between fluctuating components and the mean velocity field [27]. Isotropy in MHD turbulence should therefore be considered as a theoretical concept generalizing isotropic hydrodynamic turbulence.
When the fluid system is subjected to a mean magnetic field, this field has a strong effect on the turbulent dynamics, the fluid and the flow becomes highy anisotropic [21]. The motion perpendicular to the mean magnetic field may develop small-scale structure that give rise to turbulent dissipation and spatial variations along the mean magnetic field. In presence of a mean magnetic field, isotropy can only be expected in the perpendicular plane.

1.4 Fourier represention of a flow

Fourier transforms can convert the differential operators into multipliers. Although the Navier-Stokes equations have no known exact mathematical solution in the general case, the use of Fourier transformations allows simplification of the whole problem by converting differential operators into algebraic ones [29]. Fourier transforms also permit the resolution of the velocity field into spectral components. The Fourier component is a collective coordinate that specifies the total excitation scale over the whole flow [27]. The concept of scale L of turbulent fluctuations characterizes the size of the vortices via the relation $L = \frac{2\pi}{k}$, where $k = |\mathbf{k}|$ is the appropriate wavenumber and in turbulent state. This allows vortices of different scales to be identified. The velocity fields must be homogeneous isotropic, because the existence of a wall would be a contradiction to homogeneity. This causes a mathematical problem for the expansion of the velocity components into an infinite series. Any periodic continuous function can be expanded into an infinite Fourier series [1]. In typical flow realizations, $\mathbf{v}$ is not periodic, however this difficulty can be avoided by virtually confining the turbulent flow to a cubic box of size $L \times L \times L$ with periodic boundary conditions. Any space can be filled

with an infinite number of identical boxes, so that one obtains a periodic flow of period L in three directions of space. Thus this flow within a box is a periodic flow, filling the whole space, and whose features for scales smaller than L are close to the features of the real flow. Let $v_i(\mathbf{x}, t)$ be the periodic velocity field. Since it is periodic of period L, it can be expanded as an infinite series as:

$$v_i(\mathbf{x}, t) = (2\pi)^3 (L^{-3}) \sum_{n_1,n_2,n_3=-\infty}^{+\infty} e^{(2i\pi/L)(n_1 x_1 + n_2 x_2 + n_3 x_3)} \hat{v}_i(n_1, n_2, n_3, t)$$

where, n_1, n_2, n_3 are integers. The coefficient in front of the r.h.s. of above equation has been chosen for reasons of normalization. We introduce a wave-vector $\mathbf{k}$ of components,

$$\mathbf{k} = \left[\frac{2\pi}{L} n_1, \frac{2\pi}{L} n_2, \frac{2\pi}{L} n_3\right], \quad n_1, n_2, n_3 \in \mathbb{Z}.$$

The above equation can be rewritten by

$$v_i(\mathbf{x}, t) = (2\pi)^3 (L^{-3}) \sum_k \hat{v}_i(\mathbf{k}, t) e^{i\mathbf{k}\cdot\mathbf{x}}, \tag{1.50}$$

where the sum is taken over the discrete set of $\mathbf{k}$-vectors. The $\hat{v}_i(\mathbf{k}, t)$ are the velocity components in Fourier space of the functions $v_i(\mathbf{x}, t)$ and written as

$$\hat{v}_i(\mathbf{k}, t) = (2\pi)^{-3} \int_{\text{box}} v_i(\mathbf{x}, t) e^{-i\mathbf{k}\cdot\mathbf{x}} d^3x. \tag{1.51}$$

with the volume element is $dV = dx_1 dx_2 dx_3 = dx^3$. In the limit $L \to \infty$, the sum in Eq.(1.50) is [1]

$$\sum_k \Leftrightarrow V_{\text{box}} (2\pi)^{-3} \int d^3k, \tag{1.52}$$

Thus, we obtain the Fourier inversion formula to (1.51)

$$v_i(\mathbf{x}, t) = \int_{\mathbb{R}^3} \hat{v}_i(\mathbf{k}, t) e^{i\mathbf{k}\cdot\mathbf{x}} d^3k. \tag{1.53}$$

1.5 Navier-Stokes equations in Fourier space

As we mentiond in section 1.1, the Navier-Stokes equations can be represented by Eqs.(1.14) and (1.15). These two equations can be expressed again by,

$$\frac{\partial \mathbf{v}}{\partial t} + \mathbf{v} \cdot \nabla \mathbf{v} = -\frac{\mathbf{1}}{\rho} \nabla p + \nu \nabla^2 \mathbf{v}. \tag{1.54}$$

$$\nabla \cdot \mathbf{v} = \mathbf{0}. \tag{1.55}$$

For a function $f(x_1, x_2, x_3, t)$, we write the Fourier transform $\hat{f}$. The Fourier transform of the derivative, $\frac{\partial f}{\partial x_i}$, is $ik_i \hat{f}(k_1, k_2, k_3, t)$, where k_i is the i-component of the wavevector $\mathbf{k}$. The

sybmol $\mathcal{F}$ represents the Fourier transform operator [1], we note

$$\mathcal{F}(f(\mathbf{x},t)) = \hat{f}(\mathbf{k},t).$$

$$\mathcal{F}\left(\frac{\partial f}{\partial x_i}\right) = ik_i\hat{f}(\mathbf{k},t).$$

$$\mathcal{F}(\nabla f) = i\hat{f}(\mathbf{k},t)\mathbf{k}.$$

$$\mathcal{F}(\nabla^2 f) = \mathcal{F}\left(\frac{\partial^2 f}{\partial x_1^2} + \frac{\partial^2 f}{\partial x_2^2} + \frac{\partial^2 f}{\partial x_3^2}\right) = -(k_1^2 + k_2^2 + k_3^2)\hat{f} = -k^2\hat{f}.$$

Thus, we have

$$\mathcal{F}(\nabla \cdot \mathbf{v}) = i\mathbf{k} \cdot \hat{\mathbf{v}}(\mathbf{k},t).$$

$$\mathcal{F}(\nabla \times \mathbf{v}) = i\mathbf{k} \times \hat{\mathbf{v}}(\mathbf{k},t).$$

Fourier transformation of the product of two functions $f(\mathbf{x},t)$ and $g(\mathbf{x},t)$ is given by

$$\mathcal{F}\left[f(\mathbf{x},t)g(\mathbf{x},t)\right] = [\hat{f} * \hat{g}](\mathbf{k},t).$$

where $*$ is the convolution product $\int_{\mathbf{k}=\mathbf{p}+\mathbf{q}} \hat{f}(\mathbf{p},t)\hat{g}(\mathbf{q},t)d\mathbf{p}$. The incompressibility condition $\nabla \cdot \mathbf{v} = \mathbf{0}$ implies

$$\mathbf{k} \cdot \hat{\mathbf{v}}(\mathbf{k},t) = 0.$$

and the velocity $\hat{\mathbf{v}}(\mathbf{k},t)$ is in a plane perpendicular to $\mathbf{k}$.
Applying the above Fourier transformations to the Navier-Stokes equations (1.54) and (1.55), we have the Navier-Stokes equations in Fourier space

$$\frac{\partial \hat{\mathbf{v}}}{\partial t}(\mathbf{k},t) + \hat{\mathbf{v}}(\mathbf{k},t) \cdot i\hat{\mathbf{v}}(\mathbf{k},t)\mathbf{k} = -\frac{1}{\rho}i\hat{p}(\mathbf{k},t)\mathbf{k} - \nu k^2\hat{\mathbf{v}}(\mathbf{k},t). \tag{1.56}$$

Because $\hat{\mathbf{v}}(\mathbf{k},t)$ is in the plane perpendicular to $\mathbf{k}$, $\frac{\partial \hat{\mathbf{v}}}{\partial t}(\mathbf{k},t)$ and $\nu k^2\hat{\mathbf{v}}(\mathbf{k},t)$ also belong to that plane. However the pressure gradient $i\hat{p}(\mathbf{k},t)$ is parallel to $\mathbf{k}$. As a consequence the Fourier transform of the quantity $\mathbf{v} \cdot \nabla\mathbf{v} + \frac{\mathbf{1}}{\rho}\nabla\mathbf{p}$ is the projection on the plane perpendicular to $\mathbf{k}$ of the Fourier transform of $(\mathbf{v} \cdot \nabla\mathbf{v})$. To make this projection clear, introducing the tensor,

$$P_{ij}(\mathbf{k}) = \delta_{ij} - \frac{k_i k_j}{k^2}.$$

which allows a vector such as $\mathbf{v}$ to be projected on a plane perpendicular to $\mathbf{k}$. Thus, $P_{ij}(\mathbf{k})\mathbf{v}_j$ is the i-component of the projection of the vector $\mathbf{v}$ upon the plane perpendicular to $\mathbf{k}$. We use the Einstein convention of summation over repeated indices. Then due to incompressibility

$$\mathcal{F}\left(\mathbf{v_j}\frac{\partial \mathbf{v_i}}{\partial x_j}\right) = \mathcal{F}\left(\frac{\partial(\mathbf{v_i}\mathbf{v_j})}{\partial x_j}\right) = ik_j\int_{\mathbf{k}=\mathbf{p}+\mathbf{q}} \hat{\mathbf{v}}_\mathbf{i}(\mathbf{p},t)\hat{\mathbf{v}}_\mathbf{j}(\mathbf{q},t)d\mathbf{p}.$$

Then the i-component of $\mathbf{v} \cdot \nabla\mathbf{v} + \frac{\mathbf{1}}{\rho}\nabla\mathbf{p}$ in Fourier space is equal to

$$ik_m P_{ij}(\mathbf{k})\int_{\mathbf{k}=\mathbf{p}+\mathbf{q}} \hat{\mathbf{v}}_\mathbf{j}(\mathbf{p},t)\hat{\mathbf{v}}_\mathbf{m}(\mathbf{q},t)d\mathbf{p}.$$

Finally the Navier-Stokes equation in Fourier space is written by

$$\left(\frac{\partial}{\partial t}+\nu k^2\right)\hat{\mathbf{v}}_\mathbf{i}(\mathbf{k},t)=-ik_m P_{ij}(\mathbf{k})\int_{\mathbf{k}=\mathbf{p}+\mathbf{q}}\hat{\mathbf{v}}_\mathbf{j}(\mathbf{p},t)\hat{\mathbf{v}}_\mathbf{m}(\mathbf{q},t)d\mathbf{p}.$$

The pressure has thus been eliminated by projection on the incompressibility plane. *The nonlinear interactions* involve triad interactions between wavevectors such that $\mathbf{k}=\mathbf{p}+\mathbf{q}$. A structure of wavelength $\frac{2\pi}{k}$ will also often be associated with a wavenumber k.

1.6 MHD equations in the spectral domain

Nonlinear triad interactions and many other properties in MHD turbulence are best explained in the spectral domain. Hence the flow Eqs.(1.38)-(1.40) are expressed by Fourier transformation by the same way as the Navier-Stokes equations. For example a quantity like vorticity $\boldsymbol{\omega}$ is transformed into the spectral domain as:

$$\boldsymbol{\omega}(\mathbf{x},t)=\int d^3k\hat{\boldsymbol{\omega}}(\mathbf{k},t)e^{i\mathbf{k}\cdot\mathbf{x}} \tag{1.57}$$

here, the l.h.s. is the real space quantity and on the r.h.s. $\hat{\boldsymbol{\omega}}(\mathbf{k},t)$ is its Fourier space counterpart, $e^{i\mathbf{k}\cdot\mathbf{x}}$ is the basis function for the Fourier space and $\mathbf{k}$ is the spectral wavevector, with $\mathbf{x}$ and $\mathbf{k}$ being the Fourier transform pair $\mathbf{x}=2\pi/\mathbf{k}$. For simplicity of notation, the quantities $\boldsymbol{\omega}(\mathbf{x},t)$ and $\hat{\boldsymbol{\omega}}(\mathbf{k},t)$ will generally be referred to $\boldsymbol{\omega}$ and $\hat{\boldsymbol{\omega}}$ respectively. With this formulation the set of Eqs.(1.38)-(1.40) read

$$\partial_t\hat{\boldsymbol{\omega}}=i\mathbf{k}\times[\widehat{\mathbf{v}\times\boldsymbol{\omega}}-\widehat{\mathbf{b}\times(\nabla\times\mathbf{b})}]-\tilde{\nu}k^2\hat{\boldsymbol{\omega}}, \tag{1.58}$$

$$\partial_t\hat{\mathbf{b}}=i\mathbf{k}\times\widehat{\mathbf{v}\times\mathbf{b}}-\tilde{\eta}k^2\hat{\mathbf{b}}, \tag{1.59}$$

$$i\mathbf{k}\cdot\hat{\mathbf{v}}=i\mathbf{k}\cdot\hat{\mathbf{b}}=0. \tag{1.60}$$

Here the symbol $\widehat{(...)}$ means the convolution integral, for example

$$\widehat{(\mathbf{v}\times\boldsymbol{\omega})(\mathbf{k})}=\int d^3k'\hat{\mathbf{v}}(\mathbf{k}')\times\hat{\boldsymbol{\omega}}(\mathbf{k}-\mathbf{k}'). \tag{1.61}$$

When no mean magnetic field is imposed on a homogenous incompressible MHD system of Eqs.(1.58)-(1.60), this system is called an isotropic MHD turbulent system. When a constant mean magnetic field with a given strength is imposed on a MHD system, it is anisotropic MHD turbulent system. The mean magnetic field greatly influences the turbulent flow and its characteristics (ideal invariants). Nonlinear triad interactions are studied in both isotropic and anisotropic cases.

1.7 Ideal invariants in Navier-Stokes and MHD turbulence

In order to describe and obtain more information about the turbulent dynamics in Navier-Stokes (NS) and MHD systems, in particular the spectral nonlinear energy transfer, triad interactions, and cascading directions processes, a number of ideal invariants are considered [2]. This is especially for the ideal fluid (ν=0 in NS, and $\nu=\eta=0$ in MHD). Quadratic

invariants are particularly important since they remain invariant when truncating the spatial Fourier representation of the turbulent system at a finite wavenumber [30].

1.7.1 Ideal invariants in Navier-Stokes turbulence

- **In 2D-NS:** there are two ideal quadratic invariants

  1- Kinetic energy: It is the kinetic energy of the system

$$E^K = \frac{1}{2}\int_S dS v^2. \tag{1.62}$$

  2- Enstrophy: It is half the squared vorticity, it also called mean square vorticity

$$\Omega = \frac{1}{2}\int_S dS \omega^2. \tag{1.63}$$

where $\omega = \nabla \times \mathbf{v}$ is the vorticity and S denotes the surface of the fully periodic domain.

- **In 3D-NS:** there are two ideal quadratic invariants

  1- Kinetic energy

$$E^K = \frac{1}{2}\int_V dV v^2. \tag{1.64}$$

  2- Kinetic helicity: It represents the twist of vortex lines and is defined as the volume integral of the dot product of vorticity and velocity fields,

$$H^K = \frac{1}{2}\int_V dV (\mathbf{v} \cdot \boldsymbol{\omega}). \tag{1.65}$$

where V is the volume of the system under consideration. The results of direct numerical simultions (DNS) of 3D-NS turbulence show that the turbulent structures are thin tubes of high vorticity. This occurs due to vortex stretching and leads to the invariance of the kinetic helicity in an ideal fluid 3D-NS turbulence [1]. In 2D-NS turbulence, vortex stretching is not present but since vorticity is conserved, this leads to an inverse cascade of kinetic energy and direct cascade of enstrophy [2]. We will discuss this in detail in Chapter five.

1.7.2 Ideal invariants in MHD turbulence

- **In 2D-MHD:** there are three quadratic ideal invariants

  1- Total energy is the sum of the kinetic energy and magnetic energy of the system

$$E^{\text{tot}} = E^K + E^M = \frac{1}{2}\int_S dS (v^2 + b^2). \tag{1.66}$$

  2-Mean square vector potential: It represents half squared magnetic vector potential

$$A = \frac{1}{2}\int_S dS a^2 \tag{1.67}$$

  where $\mathbf{a}$ is the magnetic vector potential which is related to the magnetic field by $\mathbf{b} = \nabla \times \mathbf{a}$.

  3- Cross helicity: It is the surface integral of the dot product of the velocity field and magnetic field. It gives the overall correlation of velocity and magnetic fields and it

expressed dy:

$$H^C = \frac{1}{2}\int_S dS(\mathbf{v}\cdot\mathbf{b}). \tag{1.68}$$

- **In 3D-MHD:** there are three important quadratic invariants [18] which give a fair idea of the large-scale dynamics of the system. These ideal invariants are:
  1- Total energy is the sum of the kinetic energy and magnetic energy of the system

$$E^{\text{tot}} = E^K + E^M = \frac{1}{2}\int_V dV(v^2 + b^2). \tag{1.69}$$

  2- Magnetic helicity: It is the volume integral of the dot product of the magnetic vector potential and the magnetic field. It measures the linkage and twist of the magnetic field lines [31]

$$H^M = \frac{1}{2}\int_V dV(\mathbf{a}\cdot\mathbf{b}) \tag{1.70}$$

  3- Cross helicity: It is the volume integral of the dot product of the velocity field and magnetic field.

$$H^C = \frac{1}{2}\int_V dV(\mathbf{v}\cdot\mathbf{b}). \tag{1.71}$$

As mentioned above in section 1.6, the three ideal invariants in 3D-MHD in spectral space read as :

$$E_k^{\text{tot}} = \frac{1}{2}\int d^3k(|\hat{\mathbf{v}}|^2 + |\hat{\mathbf{b}}|^2), \tag{1.72}$$

$$H_k^C = \frac{1}{2}\int d^3k\hat{\mathbf{v}}^*\cdot\hat{\mathbf{b}}, \tag{1.73}$$

$$H_k^M = \frac{1}{2}\int d^3k\hat{\mathbf{a}}\cdot\hat{\mathbf{b}}^*. \tag{1.74}$$

Here * is the usual complex conjugate notation. In the Eqs.(1.73) and (1.74) the symmetry property of the Fourier transforms for the real-valued functions *e.g.*, $f(-k) = f^*(k)$ has been used. Using these flow equations in the Fourier space, the nonlinear triad interactions in HD and MHD are studied.

1.7.3 Selective decay

Turbulence occurs only in non-ideal systems, meaning systems with viscosity present. Viscosity dissipates energy and thus the global energy of a system will decay unless it is sustained by a driving mechanism. In decaying turbulent system it is interesting to quantify the rate of decay of each of the ideal invariants. These decay rates are called selective dissipation and their derivation is given in [2, 21].

- **In 2D-HD:** The decay rates of the energy and enstrophy are given by:

$$\dot{E}^K = -\epsilon^K = -D_{E^K} = -\nu\int_S dS\omega^2 = -2\nu\Omega, \tag{1.75}$$

$$\dot{\Omega} = -\beta = -D_\Omega = -\nu\int_S dS(\nabla\boldsymbol{\omega})^2. \tag{1.76}$$

- **In 3D-HD:** The decay rates of the energy and kinetic helicity are given by:

$$\dot{E}^K = -\epsilon^K = -D_{E^K} = -\nu \int_V dV\omega^2, \tag{1.77}$$

$$\dot{H}^K = -\alpha = -D_{HK} = -\nu \int_V dV\boldsymbol{\omega} \cdot (\nabla \times \boldsymbol{\omega}). \tag{1.78}$$

- **In 2D-MHD:** The decay rates of the total energy, mean square vector potential and cross helicity are given by:

$$\dot{E}^{\rm tot} = -\epsilon^{\rm tot} = -D_{E^{\rm tot}} = -\int_S dS(\nu\omega^2 + \eta j^2), \tag{1.79}$$

$$\dot{A} = -D_A = -\eta \int_S dS\mathbf{b^2}, \tag{1.80}$$

$$\dot{H}^C = -D_{HC} = -\frac{\nu+\eta}{2} \int_S dS(\mathbf{j} \cdot \omega). \tag{1.81}$$

where $\mathbf{j} = \nabla \times \mathbf{b}$ is the current density of the system under consideration.

- **In 3D-MHD:** The decay rates of the total energy, magnetic helicity and cross helicity are given by:

$$\dot{E}^{\rm tot} = -\epsilon^{\rm tot} = -D_{E^{\rm tot}} = -\int_V dV(\nu\omega^2 + \eta j^2), \tag{1.82}$$

$$\dot{H}^M = -D_{HM} = -\eta \int_V dV(\mathbf{j} \cdot \mathbf{b}), \tag{1.83}$$

$$\dot{H}^C = -D_{HC} = -\frac{\nu+\eta}{2} \int_V dV(\mathbf{j} \cdot \boldsymbol{\omega}). \tag{1.84}$$

where the dot in above decay-rate equations represents the time derviative and ϵ represents the dissipation. From the total rate of energy dissipation $\dot{E}^{\rm tot} = -\epsilon^{\rm tot}$ in the 3D-MHD case, one can obtain both of the rate of kinetic energy dissipation, $\dot{E}^K = -\epsilon^K = -\nu \int_V dV\omega^2$ and the rate of magnetic energy dissipation, $\dot{E}^M = -\epsilon^M = -\eta \int_V dV j^2$.

Chapter 2

Hydrodynamic and magnetohydrodynamic turbulence phenomenological models

To understand the way that turbulent structures form, nonlinearly interact, and dissipate in both hydrodynamic and MHD turbulence, there are several standard models: Kolmogorov(K41), Iroshnikov-Kraichnan(IK) and Goldreich-Sridhar(GS). Each approach gives rise to a different phenomenological description of turbulent flows. Kolmogorov's phenomenology has eddy interactions at it's basis. In contrast the IK and GS phenomenologies have Alfvén wave interactions as the central idea. Before these models are explained, important terms that appear in them are discussed first. The concentration is only on briefly defining scales, ranges, nonlinear triad interactions, and interaction time scales, which will later be used to describe the phenomenologies.

2.1 Aspects of the turbulence phenomenologies

2.1.1 Different scales and ranges

In order to understand the physical processes in different eddies of turbulence, eddies[1] can be classified by length scale and then interactions among eddies of different scales can be studied. These eddies are described as large, intermediate, and small-scale. Here the word scale approximately represents the wavelength considered in these structures (in turbulence studies the inverse of the wavelength, *i.e.*, wavenumber, k is generally used). This classification is highly subjective to the system under consideration [1, 32]. Intermediate eddies would have sizes in between the largest and the smallest scaled eddies. Interaction between eddies of various sizes, spanning over several orders of magnitude (in size).

Usually energy is injected into the system by some large-scale gradient. In the numerical simulations of forced turbulence, the driving mechanisms are placed in large-scales. Hence the range associated with these scales is termed as 'the drive range'. The large structures break into smaller and smaller structures due to the shear stresses. In this process intermediate

[1] An eddy is a fluid current whose flow direction differs from that of the general flow; the motion of the whole fluid is the net result of the movements of the eddies that compose it.

size eddies are created, which in turn create small eddies. In an established turbulent flow, structures of all scales can be observed. At small scales, dissipative processes such as heat generation or radiation are dominant. This range is called 'the dissipation range'. During the transition from large scales to small scales and eventual dissipation, the eddies exhibit self-similar behavior in some physical quantities, not influenced by either energy injection or dissipation. The range over which self-similar behavior is present in the flow is called 'the inertial range' and in this range large-scale driving and small-scale dissipation are negligible. The inertial range gets its name from hydrodynamic turbulence studies where in this range, the dynamics are supposed to be determined by nonlinear inertia terms of the Navier-Stokes equation [1].

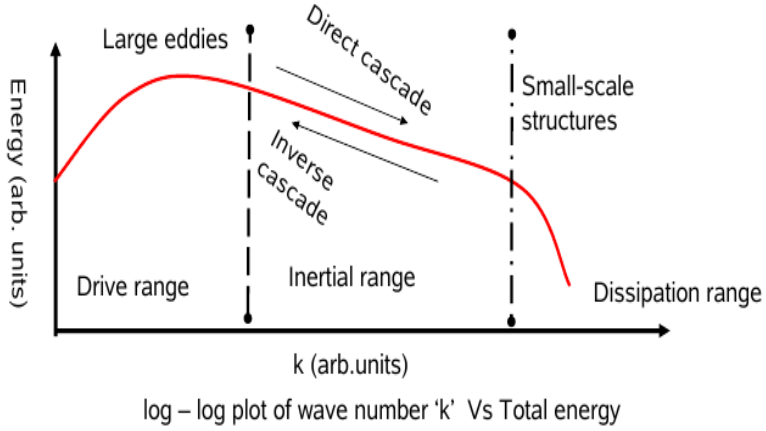

Figure 2.1: Schematic view of the Kolmogorov (K41) picture of turbulence using the energy spectrum as an example from Müller and Biskamp [30].

Fig.2.1 shows the different rangs, scales and two ways by the energy can be transferred in the inerial range: a direct cascade or an inverse cascade. Generally, the word cascade means flow, but in this context it means nonlinear spectral transport. In the inertial range, it has been observed that certain physical quantities transport smoothly from large scales to small scales, without the influence of either of these two scales. Such quantities are said to have shown a direct cascade. There exist some other quantities which spectrally transport from small scales to large scales once again uninfluenced by either of the scales, such quantities are said to have shown an inverse cascade behavior. A cascade can exit in both directions only if the flux of the quantity remained constant over the inertial range of transport. This means that the ideal invariants would show a cascade by virtue of their invariance (*i.e.*, they possess constant dissipation rates similar to transfer rate), which results in constant spectral flux. In addition, Fig.2.1 shows that the energy in turbulent structures can span many orders of magnitude between the small and the large scales. Because of the self-similar behavior of the physical quantity in the inertial range, the observed curve is a straight line with a specific slope when plotted in a log-log plot.

2.1.2 Local and nonlocal interactions

The method which used to discretize the MHD equations in the Fourier domain is explained in section 1.6. This discretization not only allows us to numerically solve the equations but also is useful in applying the formalism of equilibrium statistical mechanics to continuum fluid turbulence [2]. In this process, ideal invariants are not strictly conserved. However, quadratic invariants remain invariant in the truncated system. To understand this property we must examine the Fourier transform more closely. For any nonlinear term, *e.g.,* a product of two functions $f(x)g(x)$ in configuration space, there corresponds a convolution integral in the Fourier space

$$\hat{f} * \hat{g} = \int \hat{f}(\mathbf{p})\hat{g}(\mathbf{k}-\mathbf{p})d^3\mathbf{p} = \int\int \hat{f}(\mathbf{p})\hat{g}(\mathbf{q})\delta(\mathbf{k}-\mathbf{p}-\mathbf{q})d^3\mathbf{p}d^3\mathbf{q} \tag{2.1}$$

where $\int \delta(\mathbf{k})d\mathbf{k}$=1, for the Dirac delta function $\delta(\mathbf{k})$. Here $\mathbf{k}$, $\mathbf{p}$, and $\mathbf{q}$ are three wavevectors. By using a discrete Fourier transform, the convolution integral becomes a convolution sum. Thus the nonlinear terms of HD and MHD equations which are shown in section 1.6, make three wavenumbers (*i.e.*, three scales) appear in the Fourier space, defining *a triad*. By the detailed conservation relation for elementary interaction between any triad of wavevectors $\mathbf{k}$, $\mathbf{p}$, and $\mathbf{q}$ forming a triangle, *i.e.*, $\mathbf{k}+\mathbf{p}+\mathbf{q}$=0, a quadratic invariant, *e.g.,* energy $E(\mathbf{k})$ satisfies

$$\dot{E}(\mathbf{k}) + \dot{E}(\mathbf{p}) + \dot{E}(\mathbf{q}) = T(\mathbf{k},\mathbf{p},\mathbf{q}) + T(\mathbf{p},\mathbf{q},\mathbf{k}) + T(\mathbf{q},\mathbf{k},\mathbf{p}) = 0 \tag{2.2}$$

where the dotted quantity represents time differentiation and T is the nonlinear transfer function. These interactions are called *triad interactions* and can be inferred from the nonlinear terms of the MHD equations. These interactions are intrinsically related to the mathematical nature of the MHD equations. They are classified into local and nonlocal types on the basis of the topology of the triangle formed from the three wave vectors [33]. Different types of nonlinear transfer and triad interactions will be discussed in detail in section 3.4.

2.1.3 Fluctuations and interaction time

Turbulent structures can be of various sizes and they can interact either locally or nonlocally in spectral space. This work attemps to quantify these interactions. To this end, various properties of turbulent flow are statistically measured and the interaction time scales quantified. The velocity field $\mathbf{v}$ is used as an example to illustrate this approach. This velocity field is viewed as a superposition of eddies characterized by a spatial scale, $\boldsymbol{l}$. The associated velocity fluctuation is given by

$$\delta v_l \simeq [\mathbf{v}(\mathbf{r}+\boldsymbol{l}) - \mathbf{v}(\mathbf{r})] \cdot \boldsymbol{l}/l. \tag{2.3}$$

On small scales statistical isotropy of the field is assumed. This assumption is valid because of random mixing, where the fluid forgets the anisotropic way that turbulence is generated [2]. The fluctuation in amplitude only depends on l, thus allowing the characteristic eddy velocity to be defined as:

$$v_l \sim \left\langle \delta v_l^2 \right\rangle^{1/2}. \tag{2.4}$$

In the inertial range, the statistical moments of the two-point probability distribution of the turbulent field, the structure function of order p, is defined based on the velocity fluctuations

$$S_p^v(l) \sim \langle \delta v_l \rangle^p \sim l^{\zeta_p}, \tag{2.5}$$

where ζ_p is a constant scaling exponent that can differ depending on the order of the structure function. This family of constants characterize the intermittency of flow structures by establishing a connection between inertial range and dissipative range physics (see, [2]).
With the help of the spatial scale and the characteristic eddy velocity, the eddy turnover time τ_l is now defined as:

$$\tau_l \sim \frac{l}{v_l}. \tag{2.6}$$

Here τ_l is the typical time for a structure of size l to undergo a significant distortion due to shear stresses. As incompressibility has been assumed, it is also the time for the transfer of an excitation from one scale to another (*i.e.*, a cascade time). It is achieved by the changes in the shapes of the structures in order to preserve incompressibility. Typically in the case of a direct cascade (*i.e.*, physical quantity getting transferred to smaller scales), *e.g.*, for energy in 3D-HD, the flux can be defined

$$\Pi_l' \sim \frac{v_l^2}{t_l} \sim \frac{v_l^3}{l} \sim \epsilon. \tag{2.7}$$

Here ϵ is the energy dissipation rate. Dimensional considerations are used in deriving Eq.(2.7) (for more details see, [34]).
In the MHD case, the energy transfer is driven by shear Alfvén waves (the central idea of the IK phenomenology). If $\mathbf{b_0}$ is a magnetic guide field, interacting with the eddies of size l, then

$$\tau_A \sim l/b_0, \tag{2.8}$$

is the duration of a collision of two counter-propagating shear-Alfvén wave packets. Since the magnetic field is measured in Alfvén speed units, $|\mathbf{b_0}| = b_0$, τ_A is typically much shorter than τ_l, so the change in amplitude during one scattering event is small and many such events are needed in order to produce a relative change of order unity [2].
In cases where a mean magnetic field is applied, the turbulent system is no longer isotropic, leading to anisotropic MHD turbulence. In this case, the excitations are not uniformly transferred, but have a preferred direction. Typically if the wavevector $\mathbf{k}$ is resolved into parallel and perpendicular components, $k_{||}$ and $k_\perp$ respectively, small-scale modes are excited primarily perpendicular to the magnetic field [2]. In this set up, the time scales corresponding to the two components of $\mathbf{k}$ are different and are defined by

$$\tau_A \sim l_{||}/v_A, \tag{2.9}$$

and

$$\tau_{l_\perp} \sim l_\perp / z_{l_\perp}. \tag{2.10}$$

The length scale l is resolved into parallel and perpendicular directions $l_{||}$ and $l_{\perp}$ being, v_A is the Alfvén velocity, and $z_{l_\perp}$ is the Elsässer field in the perpendicular direction. τ_A is called Alfvén time and $\tau_{l_\perp}$ the eddy turnover time of the system.

2.2 Kolmogorov's 1941 theory for fluid turbulence

The K41 phenomenology is useful to explain the turbulence phenomena in hydrodynamic. Some predictions from this phenomenology have also been confirmed for the MHD case (*e.g.*, [35, 36, 37, 38]), though the interaction mechanisms leading to such results are different from the hydrodynamic case and still not well understood. The important aspects of this theory in the hydrodynamic case are described below briefly, more detailed presentation can be found in Müller and Biskamp [30], and Verma [39].
For the most ideal case, *i.e*, steady-state, large Reynolds number (Re $\to \infty$), and incompressible isotropic turbulence, Kolmogorov derived the well-known the four-fifth law [40, 41, 42, 14]

$$\left\langle (\Delta v)_{\|}^3 \right\rangle = -\frac{4}{5}\epsilon l. \tag{2.11}$$

where $(\Delta v)_{\|}$ is the component of $\mathbf{v}(\mathbf{x}+\mathbf{l}) - \mathbf{v}(\mathbf{x})$ parallel to the direction of the spatial increment $\mathbf{l}$. Here $\mathbf{x}$, $\langle ... \rangle$ is a standard notation for ensemble average[2], ϵ is the dissipation rate, and l lies between characterize forcing scale L and dissipative scale l_d, *i.e.*, $l_d \ll l \ll L$. This intermediate range of scales is called *the inertial range*. Fig.2.1 shows a schematic representation of K41 picture, which uses three spatial scale ranges: (a) the energy containing range at large-scales (small wavenumbers, k) where energy is supplied to the system by an external force or an instability, (b) the dissipation range at smallest-scales (large wavenumbers, k) where dissipative effects dominate and energy is removed from the system by viscosity or resistivity, and (c) an intermediate region known as the inertial-range. In the inertial range it is assumed that the influence of driving and dissipation are negligible and nonlinear interactions that govern the dynamics of energy transfer. More convenient than Eq.(2.11) is its equivalent statement on the energy spectrum. If we assume (Δv) to be fractal[3], and ϵ to be independent of scale, we have

$$\left\langle (\Delta v)^2 \right\rangle \sim \epsilon^{2/3} l^{2/3}.$$

Under the assumption of quasi-stationarity condition, the nonlinear energy flux in the inertial range is scale independent and equal to the energy dissipation as shown in Eq.(2.7). This relatioin helps to determine the velocity scaling as

$$v_l \sim (\epsilon l)^{1/3}.$$

[2]For a random variable x, the n^{th} realization of x is x_n. The ensemble average of x is denoted as X or $\langle x \rangle$, and is defined as

$$\langle x \rangle = \lim_{N\to\infty} \frac{1}{N} \sum x_n.$$

[3]Mathematically, fractal means a geometric pattern that is repeated at every scale and so cannot be represented by classical geometry.

Thus Eq.(2.11) can be written as [34]

$$S_3^v(l) = -\frac{4}{5}\epsilon l. \tag{2.12}$$

Using (2.12), a relation $v_l^3 \sim l$ is obtained and it can be written in general form as:

$$S_p^v(l) \sim (\epsilon l)^{p/3}. \tag{2.13}$$

In the spectral space, where $k \sim l^{-1}$, for the hydrodynamic case, the angle-integrated energy spectrum $E(k)$ is given by

$$E(k) = \frac{1}{2}\int d^3k' \delta(|\mathbf{k}'| - k)|\mathbf{v}(\mathbf{k}')|^2, \tag{2.14}$$

with $\mathbf{v}(\mathbf{k}')$ being the Fourier counter part of the velocity $\mathbf{v}$. With the relation $v_l^2 \simeq kE(k)$, the scaling exponent of $S_2^v(l)$, ζ_2 and the inertial range scaling of $E(k) \sim k^{-x}$ can be linked to get a relation between the two exponents as $x = -(1 + \zeta_2)$. This particular relation yields the most important K41-spectrum in incompressible hydrodynamic turbulence

$$E(k) = K_{K_0}\epsilon^{2/3}k^{-5/3}, \tag{2.15}$$

where $K_{K_0} \approx 1.6$ is a universal constant, commonly known as Kolmogorov's constant. It is to be noted that this power law could also be arrived using only the dimensional analysis of the relation $E(k) \sim \epsilon^y k^x$, where x and y are the constants to be determined. This spectral relation has been verified experimentally and also seen in several natural phenomena like atmospheric turbulences and ocean wave turbulences [34].
Eqs. (2.11) and (2.15) can be derived using scaling arguments (dimensional analysis) under the following assumptions,

(i) The energy spectrum in the inertial range does not depend on the large-scaling forcing processes and the small-scale dissipative processes, hence there must be a power-law in the local wavenumber.

(ii) Energy transfer in fluid turbulence is local in the wavenumber space in the inertial range. The energy supplied to the fluid at the forcing scale cascades to smaller scales. Under steady state turbulence the energy cascade rate (the energy flux) is constant in the wavenumber space and equal to the rate of energy dissipation, *i.e.*, $\Pi(k)$= constant $=\epsilon$.

Complex interactions among fluid eddies in various different situations can be well approximated by Eq.(2.15).
From Kolmogorov's theory we learn:

(i) Kolmogorov's theory assumes homogeneity and isotropy. In real flows, large scales (forcing) as well as dissipative scales do not satisfy these properties. However, experiments and numerical simulations show that in the inertial range ($l_d \ll l \ll L$), the fluid flows

are typically homogeneous and isotropic. So K41 is usually valid in the inertial range of neutral fluid turbulence.

(ii) The velocity fluctuations at any scale l satisfy: $v_l \sim (\epsilon l)^{1/3}$. Therefore, the effective time-scale for the interaction among eddies of size l is: $\tau_l \sim \frac{l}{v_l} \sim \epsilon^{-1/3} l^{2/3}$.

(iii) An extrapolation of Kolmogorov's scaling to the forcing and the dissipative scales yields

$$\epsilon \sim \frac{v_L^3}{L} \sim \frac{v_d^3}{l_d}.$$

Taking $\nu \sim v_d l_d$ one obtains

$$l_d \sim \left(\frac{\nu^3}{\epsilon}\right)^{1/4}.$$

This dissipation scale, also known as Kolmogorov's length scale, depends on the large-scale quantity ϵ apart from kinematic viscosity, ν.

(iv) From the definition of the Reynolds number

$$\mathrm{Re} \sim \frac{V_L L}{\nu} \sim \frac{V_L L}{v_{l_d} l_d} \sim \left(\frac{L}{l_d}\right)^{4/3},$$

where V_L is the velocity in the forcing scale L. Onset of turbulence depends on geometry, initial conditions, noise, etc. In most experiments turbulence becomes fully developed above Re of 2000 or more. In three dimensions the number of active modes $(L/l_d)^3$ is large, which makes the problem computationally complex and challenging.

2.3 Iroshnikov-Kraichnan(IK) phenomenology

In magnetohydrodynamic turbulence, the velocity field is coupled to a magnetic field. Iroshnikov and Kraichnan [43, 25] independently developed a phenomenology, called IK phenomenology, that takes into account both velocity and magnetic fields. The important features of this theory are explained briefly here following [2, 18]. This theory based is on the idea that only oppositely directed Alfvén waves interact in incompressible MHD. Other important assumptions of the IK theory are:

(i) Turbulence is statistically isotropic, and

(ii) The dominant interactions are those which couple three waves (*i.e.,* triad interactions).

In the IK theory, the energy transfer is driven by Alfvén wave interactions. Energy is redistributed between different length scales by nonlinear scattering of colliding Alfvén-wave packets, along a magnetic field line, traveling in opposite directions. Here the Elsässer quantity z_l is used in defining the major relations analogously to v_l in the hydrodynamic case. Elsässer variables have the special property that $\mathbf{z}^{\pm} = 0$ are exact nonlinear solutions of the ideal incompressible MHD equations. The Elsässer variables represent Alfvén wave pulses on a mean magnetic field. There is no distinction made between $\mathbf{z}^-$ and $\mathbf{z}^+$ as the mean alignment between the magnetic and velocity fields is restricted to small values. If a magnetic

guide field $\mathbf{b_0}$ is present in the system, and if the perturbations $\delta\mathbf{v}$ and $\delta\mathbf{b}$ are small compared to $\mathbf{b_0}$ then it is seen that $\delta\mathbf{v} \simeq \pm\delta\mathbf{b}$ [2, 18]. The interaction time of eddies of size l is

$$\tau_A \sim (l/b_0).$$

The non-magnetic eddy-distortion time $\tau_l \sim l/\delta z_l$ is much longer than the interaction time τ_A.

With the above differences, the IK phenomenology follows the same logic as the K41 phenomenology, but with two dynamic time scales: the Alfvén time, and the time for distortion of a wave packet by a counter propagating eddy, $\tau_A \ll \tau_l$. Both time scales are associated with the same scale l. Since the interaction time of two oppositely propagating wave packets is τ_A, the change of amplitude $\triangle\delta z_l$ during a single collision of two wave packets is small

$$\frac{\triangle\delta z_l}{\delta z_l} \sim \frac{\tau_A}{\tau_l} \ll 1.$$

Because of the random nature of the interaction process, the number of elementary interactions needed to produce a relative change in amplitude of order unity is $N \sim (\frac{\delta z_l}{\triangle\delta z_l})^2$ [2]. Hence the energy-transfer time is defined by $\tau_{\rm in} \sim \tau_l^2/\tau_A$. and if $\tau_l \to \tau_{\rm in}$ then the dissipation rate is defined by

$$\epsilon \sim \delta z_l^4 \tau_A / l^2. \tag{2.16}$$

With the approximations presented above, and $v_l \to z_l$, all of the K41 results can be modified to the IK results. The basic inertial range scaling of the Elsässer fields in IK case is given by

$$z_l \sim (\epsilon b_0 l)^{1/4}$$

and this leads to

$$S_p^z(l) \sim (\epsilon b_0 l)^{p/4}. \tag{2.17}$$

Eq.(2.17) for the non-intermittent inertial range scaling leads to the spectral relation for total energy

$$E(k) \sim C_{IK}(b_0\epsilon)^{1/2}k^{-3/2}, \tag{2.18}$$

with a dissipation length

$$l_{IK} = \left(\frac{b_0\tilde{\eta}^2}{\epsilon}\right)^{1/3}. \tag{2.19}$$

The IK phenomenology relies on the isotropic nature of the turbulent fields. However the magnetic field does not satisfy Galilean invariance and hence this assumption is not valid. Although IK phenomenology appears to explain many aspects of the MHD turbulence, anisotropy that sets in because of a mean magnetic field remains a major challenge. However, the triad interaction assumption, which is fundamental to this phenomenology forms the basis for a stochastic description of 3D-MHD through eddy-damped quasi-normal Markovian (EDQNM) approximation [1, 26].

The IK phenomenology is valid in 2D-MHD turbulence, several numerical simulations confirm that the scaling law for the energy is consistent with Eq.(2.18).

2.4 Goldreich-Sridhar (GS) phenomenology

In both the isotropic K41 and the IK pictures, turbulent fluctuations are characterized by a single length scale l. However, the presence of a magnetic field renders the turbulence locally anisotropic. Alfvén wave packets on the scale of λ propagate along the mean magnetic field $\mathbf{b_0}$ with a characteristic time scale $\tau_\lambda \sim \lambda/b_0$. Simultaneously, the field-lines are subject to eddy-scrambling perpendicular to the mean magnetic field b_0 on the turnover time-scale $\tau_l \sim l/z_l$, where l is the field perpendicular extent and z_l the amplitude of the fluctuations. In addition, it has been found that the nonlinear energy flux is much weaker along the direction of the magnetic field [44, 45, 46, 47].

Goldreich and Sridhar take into account the anisotropic nature of the magnetic field, while formulating the phenomenology for MHD turbulence [2, 48, 49, 18]. The wavevector $\mathbf{k}$ is split into its parallel and perpendicular components with respect to the mean magnetic field. The fundamental assumption in this phenomenology is that there exists a critical balance between τ_A and τ_l defined as above in IK phenomenology, *i.e.,* $\tau_A \sim \tau_l$. This means that the magnetic field deformations associated with the field-perpendicular turnover time τ_l propagate with Alfvén speed b_0 over a parallel distance $\lambda = b_0\tau_A$ in the same time. The nonlinear energy flux is much weaker along the direction of the magnetic field.

Thus from the strong and intermediate MHD turbulence arguments, power law behavior similar to the K41 spectra in the perpendicular direction and a new power law behavior in the parallel direction, respectively, were predicted by the GS theory. The derived power law behaviors are

$$E(k_\perp) \sim \frac{1}{2}\int dk_1 \int dk_2 (|\mathbf{v}(\mathbf{k})|^2 + |\mathbf{b}(\mathbf{k})|^2) \sim k_\perp^{-5/3}, \tag{2.20}$$

and

$$E(k_\parallel) \sim k_\parallel^{-2}. \tag{2.21}$$

Here $k_\perp \sim l^{-1}$ while $k_1 = k_\parallel \sim \lambda^{-1}$ and $k_2 \perp k_\parallel, k_\perp$. However in numerical simulations of strong MHD turbulence, this 5/3 law is not observed and instead a 3/2 behavior is found [50, 35, 45]. Boldyrev [51] suggested an explaination of this deviation from the GS theory: an increasingly parallel polarization of Alfvénic fluctuations results in weakening of nonlinear turbulent interaction.

Recently, Gogoberidze [52] modified the IK model for anisotropic incompressible MHD so that it yields a 3/2 spectrum in the perpendicular direction for the energy spectrum. In the context of our own work, neither IK or GS phenomenologies are directly relevant, but due to their importance for MHD turbulence, they have been briefly introduced here. They are also not capable of explaining all the features observed in numerical simulations and observations inspite of the recent modifications. In fact, no unique phenomenological model exists for this purpose. Explaining all the features of 3D-MHD turbulence using an unique phenomenological model is currently an area of research.

Chapter 3

Nonlinear triad interactions and detailed conservation

In this chapter, the concept of nonlinear triad interactions is introduced. The model of energy transfer, the formulae of the combined energy transfer rate, and detailed conservation in both hydrodynamic (HD) and magnetohydrodynamic (MHD) turbulence are explained. The energy cascade rates or flux and how it plays an important role for studying the locality and nonlocality of the nonlinear energy transfer and triad interactions in both HD and MHD turbulence are discussed. Definition of the locality and nonlocality of the nonlinear transfer function and triad interactions are presented. Different types of turbulent cascade directions are shown. Finally, the transfer density function $Q(v)$ and locality function $W(v)$ of Kraichnan [5, 6] are discussed.

3.1 The concept of nonlinear triad interactions

In this section, the importance of triad interactions in turbulence will be shown in more details. As mentioned before that the set of equations of both hydrodynamic and magnetohydrodynamic turbulence systems includes nonlinear terms, these equations set must be solved in Fourier space to understand the spectral properties and dynamics of energy transfer in these systems of turbulence.
The Fourier transform of the nonlinear term, for example a product of two functions $f(\mathbf{x})g(\mathbf{x})$ can be computed using the series expansion of $f(\mathbf{x})$ and $g(\mathbf{x})$ (cf. section 1.4), and appyling Eq.(1.51) on the nonlinear term $f(\mathbf{x})g(\mathbf{x})$, we have

$$\begin{aligned}\mathcal{F}(fg)(\mathbf{k}) &= \frac{1}{(2\pi)^3}\int_V f(\mathbf{x})g(\mathbf{x})e^{-i\mathbf{k}\cdot\mathbf{x}}d^3x \\ &= \frac{(2\pi)^3}{L^6}\sum_{\mathbf{p}}\sum_{\mathbf{q}} f(\mathbf{p})g(\mathbf{q})\int_V e^{-i(\mathbf{k}-\mathbf{p}-\mathbf{q})\cdot\mathbf{x}}d^3x. \end{aligned} \tag{3.1}$$

Using the distribution definition of the Dirac delta-function,

$$\delta(\mathbf{k}) = \frac{1}{V}\int_V e^{-i\mathbf{k}\cdot\mathbf{x}}d\mathbf{x} = \frac{1}{V}\int_V e^{i\mathbf{k}\cdot\mathbf{x}}d\mathbf{x},$$

where $V = L^3$. This function is zero when $\mathbf{k} \neq 0$, and when $\mathbf{k} = 0$ it is infinite in such a way as to make

$$\int \delta(\mathbf{k}) d\mathbf{k} = 1.$$

Thus Eq.(3.1) can be written as

$$\mathcal{F}(fg)(\mathbf{k}) = \frac{(2\pi)^3}{L^3} \sum_{\mathbf{p}} \sum_{\mathbf{q}} f(\mathbf{p}) g(\mathbf{q}) \delta(\mathbf{k} - \mathbf{p} - \mathbf{q}). \tag{3.2}$$

The sum and the integral signs were changeable here, because the Fourier series are converging by definition of periodic functions. In Eq.(3.2) $\delta(\mathbf{k} - \mathbf{p} - \mathbf{q})$ is the Kronecker delta symbol, which is zero unless

$$\mathbf{k} = \mathbf{p} + \mathbf{q}.$$

Now, taking the limit $V \to \infty$, Eq.(3.2) becomes

$$\mathcal{F}(fg)(\mathbf{k}) = \frac{V}{(2\pi)^3} \iint f(\mathbf{p}) g(\mathbf{q}) \delta(\mathbf{k} - \mathbf{p} - \mathbf{q}) d^3\mathbf{p}\, d^3\mathbf{q}. \tag{3.3}$$

This because the delta function in Eq.(3.2) is still discrete, and the continuous delta function satisfies the relation

$$\delta_c(\mathbf{k} - \mathbf{p} - \mathbf{q}) = \frac{(2\pi)^3}{V} \delta_d(\mathbf{k} - \mathbf{p} - \mathbf{q}).$$

which is obtained by computing the discrete and the continuous expressions:

$$\sum_{\mathbf{k}} \delta_d(\mathbf{k}) \mathbf{f}(\mathbf{k}) = \mathbf{f}(\mathbf{0})$$

and

$$\int f(\mathbf{k}) \delta(\mathbf{k}) d\mathbf{k} = \frac{(2\pi)^3}{V} \sum_{\mathbf{k}} \mathbf{f}(\mathbf{k}) \delta(\mathbf{k}) = \mathbf{f}(\mathbf{0}).$$

This finally leads to the expression for the Fourier transform of the nonlinear term $f(\mathbf{x})\mathbf{g}(\mathbf{x})$,

$$\mathcal{F}(fg)(\mathbf{k}) = \int \int f(\mathbf{p}) g(\mathbf{q}) \delta(\mathbf{k} - \mathbf{p} - \mathbf{q}) d^3\mathbf{p} d^3\mathbf{q}. \tag{3.4}$$

The expression in Eq.(3.4) is nonzero only when the three vectors $\mathbf{k}$, $\mathbf{p}$, and $\mathbf{q}$ form a triangle, *i.e.,* when $\mathbf{k} - \mathbf{p} - \mathbf{q} = 0$. The interpretaion of the double integral on the r.h.s. of Eq.(3.4) is that the Fourier modes belonging to wavenumbers $\mathbf{p}$ and $\mathbf{q}$ can interact, *e.g.,* exchange energy with the third mode belonging to wavenumber $\mathbf{k}$, provided that the three vectors form a triangle.

Thus, the nonlinear terms of HD and MHD equations which are shown in section 1.6, makes three wavevectors appear in the Fourier space, forming a triad and only the triads which satisfy the relation $\mathbf{k} + \mathbf{p} + \mathbf{q} = 0$. These triads are the key of understanding the phenomenon of energy transfer in turbulent flows, this phenomenon is the central to the concept of "triad interactions" and is a consequence of the quadratic nonlinearities of both hydrodynamic and magnetohydrodynamic equations.

3.2 Energy transfer in fluid turbulence

3.2.1 Combined energy transfer rate in fluid turbulence

In fluid and MHD turbulence, eddies of various sizes interact amongst themselves. The energy exchange takes place between various Fourier modes during their interactions. These interactions arise due to the nonlinearities present in these systems. The fundamental interactions in turbulence involve a wavenumber triad $(\mathbf{k}, \mathbf{p}, \mathbf{q})$ satisfying $\mathbf{k} + \mathbf{p} + \mathbf{q} = 0$ as mentioned in section 3.1. The formulae for combined energy transfer rate were used to study energy transfer rates in HD and MHD by many authors (see, for example [53, 26, 54, 55, 56, 57]). Usually energy gained by a mode (wavenumber) in the triad is computed using the combined energy transfer from the other two modes [58].
The evolution equation for the kinetic energy in turbulent fluid in periodic box can be written in simple form (see appendix A and more details in [59, 1])

$$\left(\frac{\partial}{\partial t} + 2\nu k^2\right) \frac{1}{2} \left\langle |\mathbf{v}(\mathbf{k})|^2 \right\rangle = \frac{1}{2} \sum_{\mathbf{k}+\mathbf{p}+\mathbf{q}=0} -\Im \left[\langle (\mathbf{k}\cdot\mathbf{v}(\mathbf{q}))(\mathbf{v}(\mathbf{p})\cdot\mathbf{v}(\mathbf{k})) \rangle + \langle (\mathbf{k}\cdot\mathbf{v}(\mathbf{p}))(\mathbf{v}(\mathbf{q})\cdot\mathbf{v}(\mathbf{k})) \rangle \right]. \tag{3.5}$$

where $\Im$ denotes the imaginary part.
In this work, an ideal hydrodynamic case is considered where viscous dissipation is zero ($\nu = 0$), then the evolution of energy equation is given in Lesieur [58]

$$\frac{\partial}{\partial t} \frac{1}{2} |v(\mathbf{k})|^2 = \frac{1}{2} \sum_{\mathbf{k}+\mathbf{p}+\mathbf{q}=0} -\Im \left[(\mathbf{k}\cdot\mathbf{v}(\mathbf{q}))(\mathbf{v}(\mathbf{p})\cdot\mathbf{v}(\mathbf{k})) + (\mathbf{k}\cdot\mathbf{v}(\mathbf{p}))(\mathbf{v}(\mathbf{q})\cdot\mathbf{v}(\mathbf{k})) \right]. \tag{3.6}$$

The evolution equation of kinetic energy does not include any contribution from the pressure field. This is because in incompressible flows, the pressure force is always perpendicular to the velocity field, thus the incompressibility condition can be obtained $\mathbf{k}\cdot\mathbf{v}(\mathbf{k}) = 0$. Indeed, the pressure force may however indirectly influence the evolution of the energy, $\left\langle |\mathbf{v}(\mathbf{k})|^2 \right\rangle$. Consider a case in which only three modes $\mathbf{v}(\mathbf{k}), \mathbf{v}(\mathbf{p}), \mathbf{v}(\mathbf{q})$ and their conjugates are nonzero, Eq.(3.6) yields

$$\frac{\partial}{\partial t} \frac{1}{2} |v(\mathbf{k})|^2 = \frac{1}{2} T(\mathbf{k}|\mathbf{p}, \mathbf{q}), \tag{3.7}$$

with

$$T(\mathbf{k}|\mathbf{p}, \mathbf{q}) = -\Im \left[(\mathbf{k}\cdot\mathbf{v}(\mathbf{q}))(\mathbf{v}(\mathbf{p})\cdot\mathbf{v}(\mathbf{k})) + (\mathbf{k}\cdot\mathbf{v}(\mathbf{p}))(\mathbf{v}(\mathbf{q})\cdot\mathbf{v}(\mathbf{k})) \right]. \tag{3.8}$$

Eq.(3.8) gives the nonlinear quantity, which represents the combined energy transfer rate from the modes $\mathbf{p}$ and $\mathbf{q}$ to the mode $\mathbf{k}$ (see, *e.g.,* [39, 60, 58, 61, 62]). The evolution equations for $|v(\mathbf{p})|^2$ and $|v(\mathbf{q})|^2$ are similar to that for $|v(\mathbf{k})|^2$. By adding the energy equations for all the three modes, we obtain

$$\begin{aligned} \frac{\partial}{\partial t} \frac{1}{2} \left[|v(\mathbf{k})|^2 + |v(\mathbf{p})|^2 + |v(\mathbf{q})|^2 \right] &= T(\mathbf{k}|\mathbf{p}, \mathbf{q}) + T(\mathbf{p}|\mathbf{q}, \mathbf{k}) + T(\mathbf{q}|\mathbf{k}, \mathbf{p}) \\ &= \Im \left[(\mathbf{q}\cdot\mathbf{v}(\mathbf{q}))(\mathbf{v}(\mathbf{k})\cdot\mathbf{v}(\mathbf{p})) + (\mathbf{p}\cdot\mathbf{v}(\mathbf{p}))(\mathbf{v}(\mathbf{k})\cdot\mathbf{v}(\mathbf{q})) + (\mathbf{k}\cdot\mathbf{v}(\mathbf{k}))(\mathbf{v}(\mathbf{p})\cdot\mathbf{v}(\mathbf{q})) \right]. \end{aligned} \tag{3.9}$$

According to incompressibilty condition $\mathbf{k} \cdot \mathbf{v}(\mathbf{k})$ for incompressible fluid, the r.h.s of Eq.(3.9) is identically zero. Hence the energy in each of the interacting triad is conserved, *i.e.*,

$$|v(\mathbf{k})|^2 + |v(\mathbf{p})|^2 + |v(\mathbf{q})|^2 = \text{constant} \tag{3.10}$$

3.2.2 Effective mode-to-mode energy transfer rate in fluid turbulence

Dar *et al.* [61] tried to specify the combined energy transfer rate formula from two modes to the third one in a triad (cf. Eq.3.8) by a formalism that takes in consideration the energy transfer between a pair of modes in a triad with the third mode mediating the transfer, *e.g.,* the quantity $T(\mathbf{k}|\mathbf{p}|\mathbf{q})$ represents the energy transfer from mode $\mathbf{p}$ to mode $\mathbf{k}$ via mode $\mathbf{q}$ which acts as a mediator, the quantity by this formalism is called "mode-to-mode energy transfer". They showed that mode-to-mode energy transfer formalism to be unique apart from an irrelevant arbitrary constant. Even though they talk about mode-to-mode transfer, they are still within the framework of triad interaction, *i.e.*, a triad is still the fundamental entity of interaction. Fig.3.1 shows the mode-to-mode energy transfer in a triad of fluid turbulence, *e.g.,* the kinetic energy transfer from mode $\mathbf{p}$ to kinetic energy in mode $\mathbf{k}$ with the mode $\mathbf{q}$ acts as the mediator, $T^{vv}(\mathbf{k}|\mathbf{p}|\mathbf{q})$ and the kinetic energy transfer from mode $\mathbf{q}$ to kinetic energy in mode $\mathbf{k}$ with the mode $\mathbf{p}$ acts as the mediator, $T^{vv}(\mathbf{k}|\mathbf{q}|\mathbf{p})$. In addition, Fig.3.1 shows the combined energy transfer of these two mode-to-mode quantities, $T^{vv}(\mathbf{k}|\mathbf{p},\mathbf{q})$ in the same triad. Dar *et al.* [61] and Verma [39] showed that the nonlinear term of combined energy transfer rate $T^{vv}(\mathbf{k}|\mathbf{p},\mathbf{q})$ can be split into a sum of two terms as

$$T^{vv}(\mathbf{k}|\mathbf{p},\mathbf{q}) = R^{vv}(\mathbf{k}|\mathbf{p}|\mathbf{q}) + R^{vv}(\mathbf{k}|\mathbf{q}|\mathbf{p}), \tag{3.11}$$

The superscript symbol vv represents the kinetic energy transfer from one mode to kinetic energy in another mode via the third mode in a triad. The r.h.s of Eq.(3.11) includes two terms, the first one $R^{vv}(\mathbf{k}|\mathbf{p}|\mathbf{q})$ denotes to the rate of kinetic energy transfer from the mode $\mathbf{p}$ to the mode $\mathbf{k}$ via the mediator $\mathbf{q}$, whereas the second one denotes to the rate of energy transfer from the mode $\mathbf{q}$ to the mode $\mathbf{k}$ via the mediator $\mathbf{p}$. Similarly, the nonlinear terms of combined energy transfer rate $T^{vv}(\mathbf{p}|\mathbf{q},\mathbf{k})$ and $T^{vv}(\mathbf{q}|\mathbf{k},\mathbf{p})$ can be given by

$$T^{vv}(\mathbf{p}|\mathbf{q},\mathbf{k}) = R^{vv}(\mathbf{p}|\mathbf{q}|\mathbf{k}) + R^{vv}(\mathbf{p}|\mathbf{k}|\mathbf{q}), \tag{3.12}$$

$$T^{vv}(\mathbf{q}|\mathbf{k},\mathbf{p}) = R^{vv}(\mathbf{q}|\mathbf{k}|\mathbf{p}) + R^{vv}(\mathbf{q}|\mathbf{p}|\mathbf{k}), \tag{3.13}$$

The R quantities in Eqs.(3.11)-(3.13) are required to satisfy another condition, is that the energy transfer from one mode to another should be equal and opposite to the energy transfer from the latter to the former. Thus, the kinetic energy transferred from mode $\mathbf{p}$ to mode $\mathbf{k}$ via mode $\mathbf{q}$, $R^{vv}(\mathbf{k}|\mathbf{p}|\mathbf{q})$ must be equal and opposite to the kinetic energy transferred from mode $\mathbf{k}$ to mode $\mathbf{p}$ via mode $\mathbf{q}$, $R^{vv}(\mathbf{p}|\mathbf{k}|\mathbf{q})$. Thus,

$$R^{vv}(\mathbf{k}|\mathbf{p}|\mathbf{q}) + R^{vv}(\mathbf{p}|\mathbf{k}|\mathbf{q}) = 0, \tag{3.14}$$

$$R^{vv}(\mathbf{p}|\mathbf{q}|\mathbf{k}) + R^{vv}(\mathbf{q}|\mathbf{p}|\mathbf{k}) = 0, \tag{3.15}$$

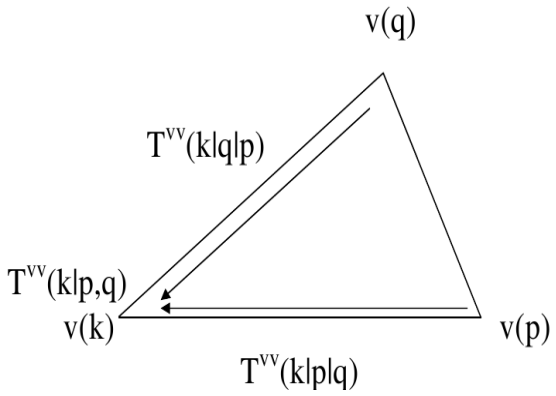

Figure 3.1: Schematic view of both the mode-to-mode, $T^{vv}(\ |\ |\ )$ and the combined, $T^{vv}(\ |\ ,\ )$ energy transfer in a triad of fluid turbulence.

$$R^{vv}(\mathbf{q}|\mathbf{k}|\mathbf{p}) + R^{vv}(\mathbf{k}|\mathbf{q}|\mathbf{p}) = 0, \tag{3.16}$$

Then there are six equations from Eq.(3.11) to Eq.(3.16) with six unknowns. However, the value of the determinant fromed from these equations is zero. Therefore it is difficult to find a unique R^{vv} just given these equations, but it is possible to expect that there is a definite amount of energy transfer from one mode to another in the triad. Thus Dar *et al.* [61, 63] used constraints based on invariance and symmetries to get a definite amount of R^{vv} using Eqs.(3.11)-(3.16). They supposed that one solutions is given by the function,

$$T^{vv}(\mathbf{k}|\mathbf{p}|\mathbf{q}) = -\Im\left[(\mathbf{k}\cdot\mathbf{v}(\mathbf{q}))(\mathbf{v}(\mathbf{p})\cdot\mathbf{v}(\mathbf{k}))\right]. \tag{3.17}$$

From the above definition of the quantity $T^{vv}(\mathbf{k}|\mathbf{p}|\mathbf{q})$, it directly satisfies the properties in Eqs.(3.11)-(3.13). Using the triad relationship $\mathbf{k}+\mathbf{p}+\mathbf{q} = 0$ and because of the incompressibilty constraint, $[\mathbf{k}\cdot\mathbf{v}(\mathbf{k})] = 0$, the quantity $T^{vv}(\mathbf{k}|\mathbf{p}|\mathbf{q})$ also satisfies the conditions in Eqs.(3.14)-(3.16). These results imply that the set of $T^{vv}(\ |\ |\ )$'s is one instance of the $R^{vv}(\ |\ |\ )$'s, *i.e.*, $R^{vv}(\mathbf{k}|\mathbf{p}|\mathbf{q}) = T^{vv}(\mathbf{k}|\mathbf{p}|\mathbf{q})$. However, $T^{vv}(\mathbf{k}|\mathbf{p}|\mathbf{q})$ is not a unique solution. The second solution is $R^{vv}(\mathbf{k}|\mathbf{p}|\mathbf{q})$ differs from the first solution $T^{vv}(\mathbf{k}|\mathbf{p}|\mathbf{q})$ by an arbitrary function α_Δ, *i.e.*, $R^{vv}(\mathbf{k}|\mathbf{p}|\mathbf{q}) = T^{vv}(\mathbf{k}|\mathbf{p}|\mathbf{q}) + \alpha_{\mathbf{\Delta}}$, then if we look at the equations that describe the energy transfer, one can easily see that the solution of Eqs.(3.11)-(3.16) must be of the form

$$R^{vv}(\mathbf{k}|\mathbf{p}|\mathbf{q}) = T^{vv}(\mathbf{k}|\mathbf{p}|\mathbf{q}) + \alpha_{\mathbf{\Delta}}, \tag{3.18}$$

$$R^{vv}(\mathbf{q}|\mathbf{k}|\mathbf{p}) = T^{vv}(\mathbf{q}|\mathbf{k}|\mathbf{p}) + \alpha_{\mathbf{\Delta}}, \tag{3.19}$$

$$R^{vv}(\mathbf{p}|\mathbf{q}|\mathbf{k}) = T^{vv}(\mathbf{p}|\mathbf{q}|\mathbf{k}) + \alpha_{\mathbf{\Delta}}, \tag{3.20}$$

$$R^{vv}(\mathbf{q}|\mathbf{p}|\mathbf{k}) = T^{vv}(\mathbf{q}|\mathbf{p}|\mathbf{k}) - \alpha_{\mathbf{\Delta}}, \tag{3.21}$$

$$R^{vv}(\mathbf{k}|\mathbf{q}|\mathbf{p}) = T^{vv}(\mathbf{k}|\mathbf{q}|\mathbf{p}) - \alpha_{\mathbf{\Delta}}, \tag{3.22}$$

$$R^{vv}(\mathbf{p}|\mathbf{k}|\mathbf{q}) = T^{vv}(\mathbf{p}|\mathbf{k}|\mathbf{q}) - \alpha_{\mathbf{\Delta}}. \tag{3.23}$$

where, $T^{vv}(\mathbf{k}|\mathbf{p}|\mathbf{q}) + \alpha_{\mathbf{\Delta}}$ gets transferred from mode $\mathbf{p}$ to mode $\mathbf{k}$, $T^{vv}(\mathbf{q}|\mathbf{k}|\mathbf{p}) + \alpha_{\mathbf{\Delta}}$ gets

transferred from mode $\mathbf{k}$ to mode $\mathbf{q}$ and $T^{vv}(\mathbf{p}|\mathbf{q}|\mathbf{k}) + \alpha_{\mathbf{\Delta}}$ gets transferred from mode $\mathbf{q}$ to mode $\mathbf{p}$. From Eqs.(3.18)-(3.20), it can be observed that the quantity α_Δ flows from $\mathbf{p}$ along $\mathbf{k}$ to $\mathbf{q}$ and again to $\mathbf{p}$, circulating around the entire triad without changing the energy of any of the modes. This quantity is called *circulating transfer*. The total energy transfer between two modes, as from $\mathbf{p}$ to $\mathbf{k}$ is $T^{vv}(\mathbf{k}|\mathbf{p}|\mathbf{q}) + \alpha_{\mathbf{\Delta}}$, but only $T^{vv}(\mathbf{k}|\mathbf{p}|\mathbf{q})$ can bring about a change in modal energy. The quantity α_Δ transferred from mode $\mathbf{p}$ to mode $\mathbf{k}$ is transferred back to mode $\mathbf{p}$ via mode $\mathbf{q}$, *i.e.*, the mode $\mathbf{p}$ transfers α_Δ directly to mode $\mathbf{k}$, and mode $\mathbf{k}$ transfers α_Δ back to $\mathbf{p}$ indirectly through mode $\mathbf{q}$. By the same way the quantity $-\alpha_\Delta$ in Eqs.(3.21)-(3.23) flows from $\mathbf{p}$ along $\mathbf{q}$ to $\mathbf{k}$ and again to $\mathbf{p}$, thus this quantity $-\alpha_\Delta$ transfers from mode $\mathbf{p}$ directly to mode $\mathbf{q}$, and mode $\mathbf{q}$ transfers it back to mode $\mathbf{p}$ indirectly througth mode $\mathbf{k}$. Thus the energy that is effectively transferred from mode $\mathbf{p}$ to mode $\mathbf{k}$ is just $T^{vv}(\mathbf{k}|\mathbf{p}|\mathbf{q})$. Therefore $T^{vv}(\mathbf{k}|\mathbf{p}|\mathbf{q})$ can be termed as "the effective mode-to-mode energy transfer" from mode $\mathbf{p}$ to mode $\mathbf{k}$ mediated by mode $\mathbf{q}$. Hence

$$R^{vv}_{eff.}(\mathbf{k}|\mathbf{p}|\mathbf{q}) = T^{vv}(\mathbf{k}|\mathbf{p}|\mathbf{q}). \tag{3.24}$$

Note that the quantity α_Δ depends on the wavenumbers triad $\mathbf{k}$, $\mathbf{p}$, $\mathbf{q}$ and the Fourier components $\mathbf{v}(\mathbf{k})$, $\mathbf{v}(\mathbf{p})$, $\mathbf{v}(\mathbf{q})$. It also must satisfy rotational invariance, galilean invariance, and it should be finite. Dar *et al.* [61] attempted to obtain the quantity α_Δ, but they showed that α_Δ is zero to linear order in the expansion. However, a general solution for α_Δ could not be found (for more details, see [63, 7]).

3.2.3 Energy cascade rates in fluid turbulence

The kinetic energy cascade rate (or flux) $\Pi(r)$ in fluid turbulence is defined as the rate of kinetic energy loss by the modes inside/outside a sphere of radius r in k-space to the modes outside/inside the same sphere. Kraichnan [64] and Leslie [29], and others have computed the quantity of the kinetic energy cascade rate or the kinetic energy flux $\Pi(r)$ in fluid turbulence using $T^{vv}(\mathbf{k}|\mathbf{p}|\mathbf{q})$. They have reported that the kinetic energy flux given by

$$\Pi(r) = -\sum_{|\mathbf{k}|<r}\sum_{|\mathbf{p}|>r} \frac{1}{2} T^{vv}(\mathbf{k}|\mathbf{p}|\mathbf{q}). \tag{3.25}$$

where r is the radius of the sphere. Dar *et al.* [61] obtained an equivalent expression for the flux in terms of the effective mode-to-mode energy transfer. This expression depends on the quantity $R^{vv}(\mathbf{k}|\mathbf{p}|\mathbf{q})$, which represents energy transfer from $\mathbf{p}$ to $\mathbf{k}$ with $\mathbf{q}$ as the mediator. The energy loss from a sphere can be written as

$$\Pi(r) = \sum_{|\mathbf{k}|>r}\sum_{|\mathbf{p}|<r} R^{vv}(\mathbf{k}|\mathbf{p}|\mathbf{q}). \tag{3.26}$$

Note that, $R^{vv}(\mathbf{k}|\mathbf{p}|\mathbf{q}) = T^{vv}(\mathbf{k}|\mathbf{p}|\mathbf{q}) + \alpha_{\mathbf{\Delta}}$ and the circulating transfer α_Δ makes no contribution to the energy flux from the sphere because the energy lost from modes inside the sphere

through α_Δ returns to the sphere again. Hence, one can write the kinetic energy flux

$$\Pi(r) = \sum_{|\mathbf{k}|>r} \sum_{|\mathbf{p}|<r} T^{vv}(\mathbf{k}|\mathbf{p}|\mathbf{q}). \tag{3.27}$$

Dar *et al.* [63] showed that Eqs.(3.25) and (3.27) are equivalent. The kinetic energy cascade in fluid turbulence Eq.(3.27) with Eq.(3.17) can be written as

$$\Pi(r) = \sum_{|\mathbf{k}|>r} \sum_{|\mathbf{p}|<r} -\Im\left[(\mathbf{k}\cdot\mathbf{v}(\mathbf{q}))(\mathbf{v}(\mathbf{p})\cdot\mathbf{v}(\mathbf{k}))\right]. \tag{3.28}$$

and this is the energy cascade rate from modes $\mathbf{v}(\mathbf{p})$ inside a sphere of radius r to modes $\mathbf{v}(\mathbf{k})$ that are outside the same sphere.

3.3 Energy transfer in magnetohydrodynamic turbulence

3.3.1 Combined energy transfer rate in the magnetohydrodynamic triad

As mentioned in section 1.2, the equation for the incompressible MHD turbulence in real space are written as

$$\frac{\partial \mathbf{v}}{\partial t} + (\mathbf{v}\cdot\nabla)\mathbf{v} = -\nabla p + (\mathbf{b}\cdot\nabla)\mathbf{b} + \nu\nabla^2\mathbf{v}, \tag{3.29}$$

$$\frac{\partial \mathbf{b}}{\partial t} + (\mathbf{v}\cdot\nabla)\mathbf{b} = (\mathbf{b}\cdot\nabla)\mathbf{v} + \eta\nabla^2\mathbf{b}, \tag{3.30}$$

$$\nabla\cdot\mathbf{v} = 0, \tag{3.31}$$

$$\nabla\cdot\mathbf{b} = 0. \tag{3.32}$$

where $\mathbf{v}$ and $\mathbf{b}$ are the velocity and magnetic fields respectively, p is the total (kinetic+magnetic) pressure divided by the density, and ν and η are the fluid kinematic viscosity and magnetic diffusivity respectively. In Fourier space, the kinetic energy and magnetic energy evolution equations are given by [59]

$$\frac{\partial E^v(\mathbf{k})}{\partial t} + 2\nu k^2 E^v(\mathbf{k}) = \sum_{\mathbf{k}+\mathbf{p}+\mathbf{q}=0} \frac{1}{2} T^{vv}(\mathbf{k}|\mathbf{p},\mathbf{q}) + \sum_{\mathbf{k}+\mathbf{p}+\mathbf{q}=0} \frac{1}{2} T^{vb}(\mathbf{k}|\mathbf{p},\mathbf{q}), \tag{3.33}$$

$$\frac{\partial E^b(\mathbf{k})}{\partial t} + 2\eta k^2 E^b(\mathbf{k}) = \sum_{\mathbf{k}+\mathbf{p}+\mathbf{q}=0} \frac{1}{2} T^{bb}(\mathbf{k}|\mathbf{p},\mathbf{q}) + \sum_{\mathbf{k}+\mathbf{p}+\mathbf{q}=0} \frac{1}{2} T^{bv}(\mathbf{k}|\mathbf{p},\mathbf{q}). \tag{3.34}$$

where, $E^v(\mathbf{k}) = |\mathbf{v}(\mathbf{k})|^2/2$ is the kinetic energy, $E^b(\mathbf{k}) = |\mathbf{b}(\mathbf{k})|^2/2$ is the magnetic energy, and the superscript YX (where X, Y= v or b) represents the energy transfer from the field X to the field Y. Eqs.(3.33) and (3.34) include four nonlinear terms, which are

$$T^{vv}(\mathbf{k}|\mathbf{p},\mathbf{q}) = -\Im\left[(\mathbf{k}\cdot\mathbf{v}(\mathbf{q}))(\mathbf{v}(\mathbf{p})\cdot\mathbf{v}(\mathbf{k})) + (\mathbf{k}\cdot\mathbf{v}(\mathbf{p}))(\mathbf{v}(\mathbf{q})\cdot\mathbf{v}(\mathbf{k}))\right], \tag{3.35}$$

$$T^{bb}(\mathbf{k}|\mathbf{p},\mathbf{q}) = -\Im\left[(\mathbf{k}\cdot\mathbf{v}(\mathbf{q}))(\mathbf{b}(\mathbf{p})\cdot\mathbf{b}(\mathbf{k})) + (\mathbf{k}\cdot\mathbf{v}(\mathbf{p}))(\mathbf{b}(\mathbf{q})\cdot\mathbf{b}(\mathbf{k}))\right], \tag{3.36}$$

$$T^{vb}(\mathbf{k}|\mathbf{p},\mathbf{q}) = \Im\left[(\mathbf{k}\cdot\mathbf{b}(\mathbf{q}))(\mathbf{b}(\mathbf{p})\cdot\mathbf{v}(\mathbf{k})) + (\mathbf{k}\cdot\mathbf{b}(\mathbf{p}))(\mathbf{b}(\mathbf{q})\cdot\mathbf{v}(\mathbf{k}))\right], \tag{3.37}$$

$$T^{bv}(\mathbf{k}|\mathbf{p},\mathbf{q}) = \Im\left[(\mathbf{k}\cdot\mathbf{b}(\mathbf{q}))(\mathbf{v}(\mathbf{p})\cdot\mathbf{b}(\mathbf{k})) + (\mathbf{k}\cdot\mathbf{b}(\mathbf{p}))(\mathbf{v}(\mathbf{q})\cdot\mathbf{b}(\mathbf{k}))\right]. \tag{3.38}$$

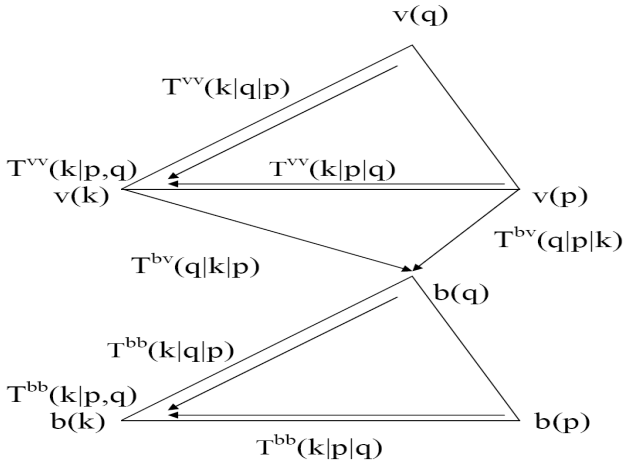

Figure 3.2: An example for the mode-to-mode $T^{YX}(\ |\ |\ )$ and the combined, $T^{YX}(\ |\ ,\ )$ energy transfer in a triad MHD, X, Y= v or b.

These nonlinear terms are conventionally taken to represent the nonlinear energy transfer rates from the modes $\mathbf{p}$ and $\mathbf{q}$ to the mode $\mathbf{k}$ of a triad formed by three wavenumbers $\mathbf{k}$, $\mathbf{p}$, $\mathbf{q}$, such that $\mathbf{k}+\mathbf{p}+\mathbf{q}=0$ in MHD turbulence [58, 59]. The term $T^{vv}(\mathbf{k}|\mathbf{p},\mathbf{q})$ represents the net transfer of kinetic energy from the modes $\mathbf{p}$ and $\mathbf{q}$ to the mode $\mathbf{k}$, the term $T^{vb}(\mathbf{k}|\mathbf{p},\mathbf{q})$ is the net magnetic energy transferred from the modes $\mathbf{p}$ and $\mathbf{q}$ to the kinetic energy in the mode $\mathbf{k}$, the term $T^{bv}(\mathbf{k}|\mathbf{p},\mathbf{q})$ is the net kinetic energy transferred from the modes $\mathbf{p}$ and $\mathbf{q}$ to the magnetic energy in the mode $\mathbf{k}$, and the term $T^{bb}(\mathbf{k}|\mathbf{p},\mathbf{q})$ represents the transfer of magnetic energy from the modes $\mathbf{p}$ and $\mathbf{q}$ to the mode $\mathbf{k}$. Fig.3.2 shows an example for the different mode-to-mode $T^{YX}(\ |\ |\ )$ and the combined, $T^{YX}(\ |\ ,\ )$ energy transfer in a triad MHD.

It can be shown (see *e.g.,* Stanišic [59]) that these nonlinear terms satisfy the following detailed conservation properties:

$$T^{vv}(\mathbf{k}|\mathbf{p},\mathbf{q})+T^{vv}(\mathbf{p}|\mathbf{k},\mathbf{q})+T^{vv}(\mathbf{q}|\mathbf{k},\mathbf{p})=0, \tag{3.39}$$

$$T^{bb}(\mathbf{k}|\mathbf{p},\mathbf{q})+T^{bb}(\mathbf{p}|\mathbf{k},\mathbf{q})+T^{bb}(\mathbf{q}|\mathbf{k},\mathbf{p})=0, \tag{3.40}$$

$$T^{vb}(\mathbf{k}|\mathbf{p},\mathbf{q})+T^{vb}(\mathbf{p}|\mathbf{k},\mathbf{q})+T^{vb}(\mathbf{q}|\mathbf{k},\mathbf{p})+T^{bv}(\mathbf{k}|\mathbf{p},\mathbf{q})+T^{bv}(\mathbf{p}|\mathbf{k},\mathbf{q})+T^{bv}(\mathbf{q}|\mathbf{k},\mathbf{p})=0. \tag{3.41}$$

Eqs.(3.39) and (3.40) imply that the kinetic (magnetic) energy are transferred conservatively between the velocity (magnetic) modes of a wavenumber triad and Eq.(3.41) implies that the cross energy transfers of kinetic and magnetic energy within a triad in MHD turbulence are also energy conservative. The quantities in Eqs.(3.39)-(3.41) represent the combined energy transfer in a MHD triad. In the next section, we will show the effective mode-to-mode energy transfer rate in a MHD triad.

3.3.2 Effective mode-to-mode energy transfer in MHD turbulence

Dar *et al.* [61, 63] showed that the formalism of the effective mode-to-mode in a MHD triad is similar to that of a HD triad. They considered an ideal MHD fluid ($\nu = \eta = 0$). The basic unit of nonlinear interaction in MHD is a triad involving modes $\mathbf{v}(\mathbf{k})$, $\mathbf{v}(\mathbf{p})$, $\mathbf{v}(\mathbf{q})$, $\mathbf{b}(\mathbf{k})$, $\mathbf{b}(\mathbf{p})$ and $\mathbf{b}(\mathbf{q})$ with $\mathbf{k}+\mathbf{p}+\mathbf{q} = 0$, and the mode-to-mode energy transfer is from velocity to velocity, magnetic to magnetic, velocity to magnetic, and magnetic to velocity mode. We will discuss these transfers briefly below.

Effective mode-to-mode energy transfer between two velocity modes

The transfer of kinetic energy between the velocity modes is due to the term $(\mathbf{v}\cdot\nabla\mathbf{v})$ in both the Navier-Stokes (cf. Eq.1.14) and MHD equations (cf. Eq.3.29). Therefore, the expression for the combined kinetic energy transfer in HD and MHD triad is the same (cf. subsection 3.2.1). Consequently, the quantity $R^{vv}(\ |\ |\ )$ for MHD triad will satisfy the constraints given in Eqs.(3.11)-(3.16). As a result, the quantity $R^{vv}(\mathbf{k}|\mathbf{p}|\mathbf{q})$ in a MHD triad can be expressed as a sum of a circulating transfer α_Δ and the effective mode-to-mode energy transfer $T^{vv}(\mathbf{k}|\mathbf{p}|\mathbf{q})$, which defined in Eq.(3.17). So, we can write

$$R^{vv}(\mathbf{k}|\mathbf{p}|\mathbf{q}) = T^{vv}(\mathbf{k}|\mathbf{p}|\mathbf{q}) + \alpha_{\boldsymbol{\Delta}}. \tag{3.42}$$

The circulating transfer α_Δ is irrelevant for the effective energy transfer as shown in subsection 3.2.2. Therefore, the quantity $T^{vv}(\mathbf{k}|\mathbf{p}|\mathbf{q})$ as the energy transfer rate from the mode $\mathbf{v}(\mathbf{p})$ to the mode $\mathbf{v}(\mathbf{k})$ with the mediation of the mode $\mathbf{v}(\mathbf{q})$. Hence,

$$R^{vv}_{eff.}(\mathbf{k}|\mathbf{p}|\mathbf{q}) = T^{vv}(\mathbf{k}|\mathbf{p}|\mathbf{q}). \tag{3.43}$$

Effective mode-to-mode energy transfer between two magnetic modes

In MHD turbulence, there is a magnetic energy transfer from magnetic mode to another one. This transfer is due to the term $\mathbf{v}\cdot\nabla\mathbf{b}$ of induction equation (3.30), where the magnetic field changes due to the field line stretching and to compression [2]. Consider the quantity $R^{bb}(\mathbf{k}|\mathbf{p}|\mathbf{q})$ represents the magnetic transfer from mode $\mathbf{b}(\mathbf{p})$ to mode $\mathbf{b}(\mathbf{k})$ in the triad $(\mathbf{k},\mathbf{p},\mathbf{q})$ as shown in Fig.3.2. The function $R^{bb}(\mathbf{k}|\mathbf{p}|\mathbf{q})$ should satisfy the same relationships as in Eqs.(3.11)-(3.16) with R^{vv} and T^{vv} replaced by R^{bb} and T^{bb} respectively. Similarly, as we mentioned in subsection 3.2.2 the solution of R^{bb} is not unique and from following arguments, we can show that

$$R^{bb}(\mathbf{k}|\mathbf{p}|\mathbf{q}) = T^{bb}(\mathbf{k}|\mathbf{p}|\mathbf{q}) + \beta_{\boldsymbol{\Delta}}. \tag{3.44}$$

with

$$T^{bb}(\mathbf{k}|\mathbf{p}|\mathbf{q}) = -\Im\left[(\mathbf{k}\cdot\mathbf{v}(\mathbf{q}))(\mathbf{b}(\mathbf{p})\cdot\mathbf{b}(\mathbf{k}))\right], \tag{3.45}$$

β_Δ is the circulating energy transfer that is transferred from $\mathbf{b}(\mathbf{p}) \to \mathbf{b}(\mathbf{k}) \to \mathbf{b}(\mathbf{q})$ and back to $\mathbf{b}(\mathbf{p})$. Then, β_Δ does not cause any change in modal energy. Hence, the magnetic energy effectively transferred from mode $\mathbf{b}(\mathbf{p})$ to mode $\mathbf{b}(\mathbf{k})$ is only given by the quantity $T^{bb}(\mathbf{k}|\mathbf{p}|\mathbf{q})$, *i.e.*,

$$R^{bb}_{eff.}(\mathbf{k}|\mathbf{p}|\mathbf{q}) = T^{bb}(\mathbf{k}|\mathbf{p}|\mathbf{q}). \tag{3.46}$$

Then the quantity $T^{bb}(\mathbf{k}|\mathbf{p}|\mathbf{q})$ is "the effective mode-to-mode magnetic energy transfer" from mode $\mathbf{b}(\mathbf{p})$ to mode $\mathbf{b}(\mathbf{k})$ mediated by the velocity mode $\mathbf{v}(\mathbf{q})$.

Effective velocity mode to magnetic mode and effective magnetic mode to velocity mode energy transfer

Consider the functions $R^{vb}(\mathbf{k}|\mathbf{p}|\mathbf{q})$ represents the energy transfer from mode $\mathbf{b}(\mathbf{p})$ to mode $\mathbf{v}(\mathbf{k})$ and $R^{bv}(\mathbf{k}|\mathbf{p}|\mathbf{q})$ represents the energy transfer from mode $\mathbf{v}(\mathbf{p})$ to mode $\mathbf{b}(\mathbf{k})$ in a MHD triad. These functions satisfy the same relationships as in Eqs.(3.11)-(3.16). For example, energy comes from to the mode $\mathbf{v}(\mathbf{k})$ from other two modes $\mathbf{b}(\mathbf{p})$ and $\mathbf{b}(\mathbf{q})$, we have

$$T^{vb}(\mathbf{k}|\mathbf{p},\mathbf{q}) = R^{vb}(\mathbf{k}|\mathbf{p}|\mathbf{q}) + R^{vb}(\mathbf{k}|\mathbf{q}|\mathbf{p}), \tag{3.47}$$

and

$$R^{vb}(\mathbf{k}|\mathbf{p}|\mathbf{q}) + R^{bv}(\mathbf{p}|\mathbf{k}|\mathbf{q}) = 0, \tag{3.48}$$

The solutions of these equations are not unique. Using arguments similar to those in subection 3.2.2, we can show that the general solution of R's are

$$R^{bv}(\mathbf{k}|\mathbf{p}|\mathbf{q}) = T^{bv}(\mathbf{k}|\mathbf{p}|\mathbf{q}) + \gamma_{\mathbf{\Delta}}, \tag{3.49}$$

$$R^{vb}(\mathbf{k}|\mathbf{q}|\mathbf{p}) = T^{vb}(\mathbf{k}|\mathbf{q}|\mathbf{p}) - \gamma_{\mathbf{\Delta}}, \tag{3.50}$$

with

$$T^{bv}(\mathbf{k}|\mathbf{p}|\mathbf{q}) = \Im\left[(\mathbf{k}\cdot\mathbf{b}(\mathbf{q}))(\mathbf{v}(\mathbf{p})\cdot\mathbf{b}(\mathbf{k}))\right], \tag{3.51}$$

$$T^{vb}(\mathbf{k}|\mathbf{p}|\mathbf{q}) = \Im\left[(\mathbf{k}\cdot\mathbf{b}(\mathbf{q}))(\mathbf{b}(\mathbf{p})\cdot\mathbf{v}(\mathbf{k}))\right]. \tag{3.52}$$

γ_{Δ} is the circulating transfer, in this case the energy transfer from mode $\mathbf{v}(\mathbf{p}) \to \mathbf{b}(\mathbf{k}) \to \mathbf{v}(\mathbf{q}) \to \mathbf{b}(\mathbf{p}) \to \mathbf{v}(\mathbf{k}) \to \mathbf{b}(\mathbf{q})$ and back to $\mathbf{v}(\mathbf{p})$ without resulting in any change in modal energy. This circulating transfer does not affect on the net energy transfer, we deal with the functions T^{bv} and T^{vb} as "the effective mode-to-mode energy transfer rates". Then we have

$$R^{bv}_{eff.}(\mathbf{k}|\mathbf{p}|\mathbf{q}) = T^{bv}(\mathbf{k}|\mathbf{p}|\mathbf{q}). \tag{3.53}$$

$$R^{vb}_{eff.}(\mathbf{k}|\mathbf{p}|\mathbf{q}) = T^{vb}(\mathbf{k}|\mathbf{p}|\mathbf{q}). \tag{3.54}$$

From the different types of mode-to-mode energy transfer in MHD turbulence, we can summarize that

1- The energy evolution equations for a triad $(\mathbf{k},\mathbf{p},\mathbf{q})$ in MHD turbulence as

$$\frac{\partial}{\partial t}\frac{1}{2}|v(\mathbf{k})|^2 = T^{vv}(\mathbf{k}|\mathbf{p}|\mathbf{q}) + T^{vv}(\mathbf{k}|\mathbf{q}|\mathbf{p}) + T^{vb}(\mathbf{k}|\mathbf{p}|\mathbf{q}) + T^{vb}(\mathbf{k}|\mathbf{q}|\mathbf{p}), \tag{3.55}$$

$$\frac{\partial}{\partial t}\frac{1}{2}|b(\mathbf{k})|^2 = T^{bb}(\mathbf{k}|\mathbf{p}|\mathbf{q}) + T^{bb}(\mathbf{k}|\mathbf{q}|\mathbf{p}) + T^{bv}(\mathbf{k}|\mathbf{p}|\mathbf{q}) + T^{bv}(\mathbf{k}|\mathbf{q}|\mathbf{p}), \tag{3.56}$$

2- The function $T^{YX}(\mathbf{k}|\mathbf{p}|\mathbf{q})$, where (X, Y $=v$ or b) is the mode-to-mode energy transfer rate from the mode $\mathbf{p}$ of field X to the mode $\mathbf{k}$ of field Y with the mode $\mathbf{q}$ acting as a mediator.

3- The nonlinear triads interactions can also be written in terms of Elsässer variables. Here

the participating modes are $\mathbf{z}(\mathbf{k})$, $\mathbf{z}(\mathbf{p})$ and $\mathbf{z}(\mathbf{q})$. The energy equations for these modes are

$$\frac{\partial}{\partial t}\frac{1}{2}|z^{\pm}(\mathbf{k})|^2 = T^{\pm}(\mathbf{k}|\mathbf{p}|\mathbf{q}) + T^{\pm}(\mathbf{k}|\mathbf{q}|\mathbf{p}), \tag{3.57}$$

where, $z^{\pm} = v \pm b$ and

$$T^{\pm}(\mathbf{k}|\mathbf{p}|\mathbf{q}) = -\Im\left[(\mathbf{k}\cdot\mathbf{z}^{\mp}(\mathbf{q}))(\mathbf{z}^{\pm}(\mathbf{p})\cdot\mathbf{z}^{\pm}(\mathbf{k})\right]. \tag{3.58}$$

The energy transfer functions $T^{YX}(\mathbf{k}|\mathbf{p}|\mathbf{q})$ in an ideal MHD triad have the following interesting properties:
1- Energy transfer rate from $X(\mathbf{p})$ to $Y(\mathbf{k})$ is equal and opposite to that from $Y(\mathbf{k})$ to $X(\mathbf{p})$, *i.e.*,

$$T^{YX}(\mathbf{k}|\mathbf{p}|\mathbf{q}) = -T^{XY}(\mathbf{p}|\mathbf{k}|\mathbf{q}) \tag{3.59}$$

2- Sum of all energy transfer rates along $v \to v$, $b \to b$, $z^+ \to z^+$, and $z^- \to z^-$ channels are zero, *i.e.*,

$$T^{XX}(\mathbf{k}|\mathbf{p}|\mathbf{q}) + T^{XX}(\mathbf{k}|\mathbf{q}|\mathbf{p}) + T^{XX}(\mathbf{p}|\mathbf{k}|\mathbf{q}) + T^{XX}(\mathbf{p}|\mathbf{q}|\mathbf{k}) + T^{XX}(\mathbf{q}|\mathbf{k}|\mathbf{p}) + T^{XX}(\mathbf{q}|\mathbf{p}|\mathbf{k}) = 0 \tag{3.60}$$

where, X represents any vector field among $\mathbf{v}$, $\mathbf{b}$, $\mathbf{z}^+$ or $\mathbf{z}^-$.
3- Sum of all energy transfer rates along $v \to b$ and $b \to v$ channels is zero, *i.e.*,

$$\begin{aligned} T^{bv}(\mathbf{k}|\mathbf{p}|\mathbf{q}) + T^{bv}(\mathbf{k}|\mathbf{q}|\mathbf{p}) + T^{bv}(\mathbf{p}|\mathbf{k}|\mathbf{q}) + T^{bv}(\mathbf{p}|\mathbf{q}|\mathbf{k}) + T^{bv}(\mathbf{q}|\mathbf{k}|\mathbf{p}) + T^{bv}(\mathbf{q}|\mathbf{p}|\mathbf{k}) + \\ T^{vb}(\mathbf{k}|\mathbf{p}|\mathbf{q}) + T^{vb}(\mathbf{k}|\mathbf{q}|\mathbf{p}) + T^{vb}(\mathbf{p}|\mathbf{k}|\mathbf{q}) + T^{vb}(\mathbf{p}|\mathbf{q}|\mathbf{k}) + T^{vb}(\mathbf{q}|\mathbf{k}|\mathbf{p}) + T^{vb}(\mathbf{q}|\mathbf{p}|\mathbf{k}) = 0 \end{aligned} \tag{3.61}$$

4- The total energy in a triad interaction is conserved, *i.e.*,

$$E^v(\mathbf{k}) + E^v(\mathbf{p}) + E^v(\mathbf{q}) + E^b(\mathbf{k}) + E^b(\mathbf{p}) + E^b(\mathbf{q}) = \text{const} \tag{3.62}$$

Note that kinetic and magnetic energies are not conserved individually.

3.4 Important definitions of the nonlinear interactions

In order to understand and investigate the nonlinear processes in the spectral space, it is important to distinguish between local and nonlocal transfer, local and nonlocal triad interactions, local and nonlocal cascade, and cascade directions of an ideal quadratic invariant. We will explain these concepts in this section as following

3.4.1 Locality and nonlocality of nonlinear transfer and triad interactions

Because of the quadratic form of the nonlinear terms in the incompressible hydrodynamic and MHD equations, three wavenumbers are involved in any basic triad interaction (see, Appendix A), with the ideal invariant being transferred between two of the wavenumbers (say $\mathbf{k}$ and $\mathbf{p}$) while the third wavenumber (say $\mathbf{q}$) is acting as a mediator for the transfer [39, 8, 54]. Because of the triad wavenumbers satisfy the condition $\mathbf{k}+\mathbf{q}+\mathbf{p}=0$, at least two of the wavenumbers have to be of the same order, while the

third can either be of the same order or much smaller than the other two. In order to investigate the dynamics of the energy transfer processes, there are two aspects must be considered: (1) The transfer process it self, and (2) Interactions beteen different scales of motion which result in such energy transfers.

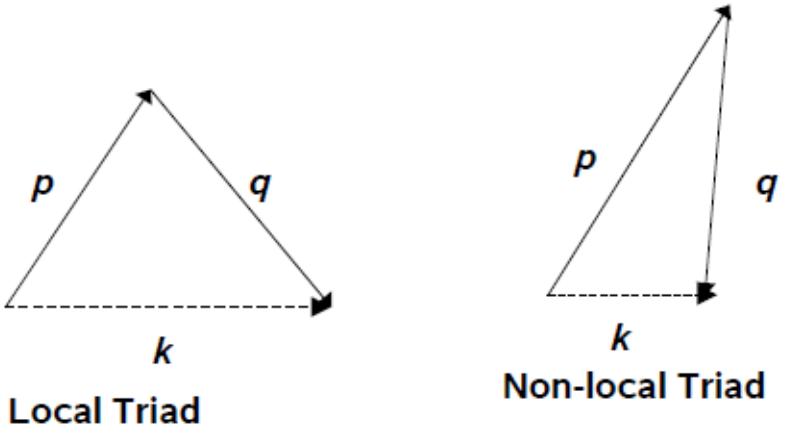

Figure 3.3: Local and Nonlocal triad interactions adapted from [33].

The spectral energy transfer in the turbulence is often implicitly assumed to involve only two scales of motion, it is then possible following Domaradzki and Rogallo [7], to introduce the following definitions:
(i) If the transfer takes place between two scales with similar sizes, *i.e.*, the transfer exchanges between two wavenumbers with similar sizes, then the transfer process is called *local transfer*,
(ii) If the transfer takes place between two scales with different sizes, *i.e.*, the transfer exchangs between two wavenumbers with different sizes, then the transfer is called *nonlocal transfer*.
A wavenumber triad represents interactions among three different scales of motion, and such triad interactions can be classified on the basis of the topology of the triangle formed from the three wavevectors [33] as Fig.3.3:
(i) *Local triad interactions*, in which all three scales are similar in size, *i.e.*, all three legs of the wavenumber triangle are of comparable lengths, $k \approx p \approx q$ (where $k = |\mathbf{k}|, p = |\mathbf{p}|, q = |\mathbf{q}|$);
(ii) *Nonlocal triad interactions*, in which one scale is much larger than the remaining two scales, *i.e.*, one leg of the wavenumber triangle is much shorter than the other two, $k \approx p \gg q$, $k \approx q \gg p$, or $p \approx q \gg k$.
With these definitions, it is possible to state the following facts:
(i) *Local triad interactions* always imply *local transfer*,
(ii) *Nonlocal energy transfer* (as an example) due to *nonlocal triad interactions* is possible only when the energy is exchanged between a large scale and two small scales,
(iii) *Local energy transfer* can take place through *nonlinear triad interactions* if the energy is exchanged between two small scales (large wavenumbers) in the *nonlocal triad*, without affecting the remaining large scale (small wavenumber).

3.4.2 Nonlinear cascade directions

The nonlinear triad interaction results in transport quasi-randomly directed towards smaller scales (larger wavenumbers) or larger scales (smaller wavenumbers), on average the transfer has a preferred direction which depends on the kind and number of ideal invariants as well as

on the dimensionality of the system under consideration. The spectral nonlinear transfer proceeds in small steps, motivating the name *turbulent cascade* depending on its direction. There are two types of nonlinear cascades in k-space. The cascade is called *forward or direct* cascade, when the ideal quadratic invariant transfer takes place from large scales (small wavenumbers) to small scales (large wavenumbers) and called *inverse or indirect* cascade, when it transfer takes place from small scales to large scales [62, 65, 54]. According these types of nonlinear energy cascade, one observed that when the energy cascade rate or flux $\Pi(r)$ is positive, this implies that the energy transfer occurs from modes with small wavenumber to modes with large wavenumber *direct cascade*. when the energy cascade rate is negative, this implies that the energy transfer occurs from modes with large wavenumber to modes with small wavenumber *inverse cascade*. Table 3.1 shows the cascading of different ideal quadratic invariants in NS and MHD turbulence [2, 4].

	Cascade direction in 2D	Cascade direction in 3D
Navier-Stokes	E^K inverse	E^K direct
Navier-Stokes	Ω direct	H^K direct
MHD	E^{tot} direct	E^{tot} direct
MHD	H^C direct	H^C direct
MHD	$A2$ inverse	H^M inverse

Table 3.1: Cascade directions of the different ideal quadratic invariants in NS and MHD turbulence.

3.5 The Q-graphs of Kraichnan

In this section, we will show how Kraichnan [5, 6] measured the locality of the energy transfer and triad interactions in the inertial range of both two and three dimensions incompressible isotropic hydrodynamic turbulence. In order to determine the localness of the energy transfer and triad interactions, Kraichnan introduced a new function, $Q(v)$ that depends on the ratio of the norm of the vector with the smallest length of a given triad, and the norm of the vector of middle length, in other words the ratio of the smallest wavenumber to the middle wavenumber in the interacting triad [5]. This function serves to measure the contributions of the energy transfer due to different triads in the inertial range, this function derived from the flux $\Pi(k)$ as following:
The energy balance equation in both two and three dimensions incompressible stationary isotropic hydrodynamic turbulence is given by [6]

$$(\frac{\partial}{\partial t} + 2\nu k^2)E(k) = T(k), \tag{3.63}$$

and

$$T(k) = \frac{1}{2}\iint_{\mathbb{R}^6} T(\mathbf{k},\mathbf{p},\mathbf{q})\, d^3p d^3q. \tag{3.64}$$

where $E(k)$ is the turbulent spectral function, which contains the energy in the modes with scalar wavenumbers lying in $[k, k+\delta k]$, and it is the distribution of the turbulence intensity over spatial scales [66]. In Eq.(3.64), $T(k)$ is the nonlinear transfer term with the quantity $T(\mathbf{k},\mathbf{p},\mathbf{q})$ which defined in Eq.(3.8). The integrand on the r.h.s of Eq.(3.64) is a function of

the scalar variables k, p, and q. Since the intergrals of the form

$$I(k,p,q) = \iint f(k,p,q)\delta(\mathbf{k}-\mathbf{p}-\mathbf{q})d^3pd^3q \tag{3.65}$$

are known as bipolar integrals are effectively double integrals over the scalar variables p and q. Thus Eq.(3.65) can be written as

$$I(k,p,q) = \iint (2\pi pq/k)f(k,p,q)dpdq \tag{3.66}$$

The above integration is restricted to the part of the p, q plane in which k, p and q can form a triad. The quantity $(2\pi pq/k)$ depends on k that comes from the intergration over spherical coordinates (for more details, see appendix in [29]). Applying Eqs.(3.65 and 3.66), Eq.(3.64) can be written as

$$T(k) = \frac{1}{2}\int_0^\infty \int_0^\infty T(k,p,q)dpdq. \tag{3.67}$$

Through the transfer function only the energy can be transferred between the modes (it does not destroy or create) and this is the basis for the existence of the cascade. The integration of the transfer term over all modes is zero and it represents the energy conservation law

$$\int_0^\infty T(k)dk = 0.$$

In addition, in Eq.(3.67) the quantity $T(k,p,q) = T(k,q,p)$ is the net rate of energy transfer into mode k from interactions with modes p and q ($\mathbf{k} = \mathbf{p}+\mathbf{q}$, $k = |\mathbf{k}|$, $p = |\mathbf{p}|$, $q = |\mathbf{q}|$). Also, this quantity is zero if k, p and q are cannot form the sides of a triangle [6, 67], and it represents the combined energy transfer in fluid turbulence. According to conservation of the total energy in both two and three dimensions of HD and MHD turbulence, we can write

$$T(k,p,q) + T(p,q,k) + T(q,k,p) = 0.$$

From the energy transfer function, the flux of kinetic energy through wavenumber k, $\Pi(k)$ can be derived, which is proportional to the transfer rate from wavenumbers smaller than k to wavenumbers larger than k, and expreesed as

$$\Pi(k) = \int_k^\infty T(k')dk'. \tag{3.68}$$

where $T(k')$ is the nonlinear transfer term of the energy equation (see, appendix A) which has to be brought into a more convenient from the integration over the scalars k, p, and q [29]. Using Eq.(3.68), the general form of the energy flux directly can be written by the energy transfer function of the triads as in Eq.(3.27) (cf. subsection 3.2.3).
Thus by using Eq.(3.68) with Eq.(3.67), the mean rate of energy transfer (the flux $\Pi(k)$) into

wavenumbers above k from wavenumbers below k becomes

$$\Pi(k) = \int_k^\infty T(k^{'})dk^{'} = \frac{1}{2}\int_k^\infty \left(\int_0^\infty \int_0^\infty T(k^{'},p,q)dpdq\right)dk^{'}.$$
$$= \frac{1}{2}\int_k^\infty dk^{'}\int_0^k \int_0^k T(k^{'},p,q)dpdq - \frac{1}{2}\int_0^k dk^{'}\int_k^\infty \int_k^\infty T(k^{'},p,q)dpdq. \quad (3.69)$$

where the first term at the end of Eq.(3.69) gives the total rate of energy gained into the range $k^{'} > k$ after triad interactions with p and q that are smaller than k, whereas the second term gives the total rate loss of energy in the range $k^{'} < k$ after triad interactions with p and q that are bigger than k.
Using the symmetry of $T(k^{'},p,q)$, where $T(k^{'},p,q)$=$T(k^{'},q,p)$ we can write $2\int_0^k dp\int_0^p dq$ instead of $\int_0^k dp\int_0^k dq$ in the first integral and $2\int_k^\infty dp\int_p^\infty dq$ instead of $\int_k^\infty dp\int_k^\infty dq$ in the second integral, then we can write,

$$\Pi(k) = \int_k^\infty dk^{'}\int_0^k \int_0^p T(k^{'},p,q)dpdq - \int_0^k dk^{'}\int_k^\infty \int_p^\infty T(k^{'},p,q)dpdq. \quad (3.70)$$

Choosing the following variable changes, $p = \frac{k}{u}$, $k^{'} = pw$, $q = pv$ in the first term and $p = \frac{k}{u}$, $k^{'} = pv$, $q = pw$ in the second term of the right hand side of Eq.(3.70), we have

$$\Pi(k) = \int_0^1 dv\int_1^\infty du\int_u^\infty dw\frac{1}{u}\left(\frac{k}{u}\right)^3 T(\frac{k}{u}w,\frac{k}{u},\frac{k}{u}v)$$
$$- \int_0^1 du\int_1^\infty dw\int_0^u dv\frac{1}{u}\left(\frac{k}{u}\right)^3 T(\frac{k}{u}v,\frac{k}{u},\frac{k}{u}w). \quad (3.71)$$

This choice for the variable changes reveals the aim of expressing the ratios of the smallest to the middle wavenumber (with $v = q/p$ in the first, $v = k/p$ in the second integral) and of the largest to the middle wavenumber (with $w = k/p$ in the first, $w = q/p$ in the second integral). Kraichnan assumed that the second and third order moments at the instant considered satisfy the similarity laws [6]

$$E(k)/E(k) = a^{-n},$$
$$\frac{T(ak,ap,aq)}{T(k,p,q)} = a^{-(1+3n)/2}. \quad (3.72)$$

where a is an arbitrary scaling factor and n is at first undetermined. The scaling factor of $T(k,p,q)$ in Eq.(3.72) is the same as that of $[E(k)]^{3/2}k^{-1/2}$ (which has the same dimensions) and corresponds to a independence of the appropriately defined triple correlation cofficients of the distribution on the Fourier amplitudes in the neighborhoods of the wavenumber arguments. Eq.(3.72) is connecting directly to the inverse cascade, taking the scaling of energy $n = 5/3$ in hydrodynamic turbulence (see section 2.2), so Eq.(3.72) becomes

$$\frac{T(ak,ap,aq)}{T(k,p,q)} = a^{-3} \Rightarrow T(ak,ap,aq) = a^{-3}T(k,p,q). \quad (3.73)$$

Using Eq.(3.73) with $a = k/u$, then Eq.(3.71) can be written by

$$\begin{aligned}\Pi(k) &= \int_0^1 dv \int_1^\infty du \int_u^\infty dw \frac{1}{u} a^3 T(aw, a, av) - \int_0^1 du \int_1^\infty dw \int_0^u dv \frac{1}{u} a^3 T(av, a, aw). \\ &= \int_0^1 dv \int_1^\infty du \int_u^\infty dw \frac{1}{u} T(w, 1, v) - \int_0^1 du \int_1^\infty dw \int_0^u dv \frac{1}{u} T(v, 1, w). \end{aligned} \tag{3.74}$$

Because of $\int_1^\infty du \int_u^\infty dw$ is equivalent to $\int_1^\infty dw \int_1^w du$ in first integral and $\int_0^1 du \int_0^u dv$ is equivalent to $\int_0^1 dv \int_v^1 du$ in the second integral, Eq.(3.74) can be written by

$$\begin{aligned}\Pi(k) &= \int_0^1 dv \int_1^\infty dw \int_1^w du \frac{1}{u} T(w, 1, v) - \int_0^1 dv \int_1^\infty dw \int_v^1 du \frac{1}{u} T(v, 1, w) \\ &= \int_0^1 dv \int_1^\infty dw \ln(w) T(w, 1, v) + \int_0^1 dv \int_1^\infty dw \ln(v) T(v, 1, w) \\ &= \int_0^1 dv \int_1^\infty dw \left[\ln(w) T(w, 1, v) + \ln(v) T(v, 1, w)\right]. \end{aligned} \tag{3.75}$$

With the consideration that T is non-zero only if w, 1 and v are form a triangle and w in the first term in the r.h.s. of Eq.(3.70) can never reach infinity because of the triangle constraint, $w = k^{'}/p < (p+q)/p = 1 + v$, thus in Eq.(3.75) the integration border ∞ replaced by $1 + v$, then we can write

$$\Pi(k) = \int_0^1 dv \int_1^{1+v} dw \left[\ln(w) T(w, 1, v) + \ln(v) T(v, 1, w)\right] \tag{3.76}$$

Introducing a new function, which is

$$Q(v) = \frac{v}{\epsilon} \int_1^{1+v} dw \left[\ln(w) T(w, 1, v) + \ln(v) T(v, 1, w)\right]. \tag{3.77}$$

we get

$$\Pi(k) = \epsilon \int_0^1 \frac{dv}{v} Q(v). \tag{3.78}$$

where ϵ is the total rate of energy dissipation. Therefore, the function $Q(v)$ serves as a measure of the localness of energy transfer, showing the structure of the inertial range energy transfer, where v is the ratio of the smallest to middle wavenumber in the interacting triad. The integrand in Eq.(3.77) represents to the total contribution to the energy transfer across k from all possible shapes of the triangles formed by the wavenumbers $k^{'}, p, q$ in Eq.(3.69). Since $v \leq 1$ and $1 < w \leq 1 + v$, each pair of values v and w corresponds uniquely to a possible shape of the triangle formed by the triad of interacting wavenumbers [5, 6]. The factors of T in the mentioned integrand give the weights of the contributions of the different triangle shapes and arise from integration over triangle size.

3.6 Direct calculation of $Q(v)$-graphs

In this work, we introduce a new and accurate approach of analyzing the nonlinear turbulent interactions. This approach involves the direct numerical (not analtyical and model dependent like Kraichnan [5]) examination of every wavenumber triad that is associated with

the nonlinear terms in the differential equations of HD and MHD in inertial range of turbulence. This technique allows us to compute the spectral energy transfer and the energy fluxes as well as the spectral locality property of energy transfer by computing the transfer density function $Q(v)$ in Eq.(3.78). The basis of our approach depends on in the inertial range of incompressible isotropic HD and 3D-MHD turbulence, the scaling factor is $n = 5/3$ as many authors showed that the energy spectrum of incompressible isotropic HD [5, 6] and 3D-MHD with no or small mean magnetic field [35, 37, 68] turbulence is Kolmogrov-like ($k^{-5/3}$), where the similarity range yields a k-independent energy flux $\Pi(k)$. The convergence of the integrals in this range implies that the energy transfer is accomplished locally in space, and this local transfer is associated with the distortion of the fields by their own shear [6, 67]. This implies that in the inertial range the total energy flux $\Pi(k)$ is equal to the total rate of energy dissipation ϵ [64], so Eq.(3.78) can be written by:

$$\int_0^1 \frac{dv}{v} Q(v) = 1 \tag{3.79}$$

The above equation gives us a new meaning of $Q(v)$ as a probability density function of v, which measures the probability density of contributions to the nonlinear energy transfer of the different shapes of triangles of interacting modes in k-space.

3.7 The $W(v)$-graphs of Kraichnan

Another useful way of quantitatively presenting the nature of the nonlinear transfer functions and nonlinear triad interactions is to consider the contributions based on the geometry of a triad, as was done by Kraichnan [5] using an analytical closure model. For a given k, the geometry of a triad can be partially expressed as the ratio of the length of the smallest side to the length of the middle side in a given triad. Thus, it is possible to measure the part of the total energy transfer that passes through the inertial-range in different cases of incompressible isotropic Navier-Stokes turbulence, isotropic and anisotropic MHD trubulence, that is due to all triad interactions in which the ratio of the smallest to the middle wavenumber is greater than a given value of v ($v \leq 1$), namely by introducing a new function is called the locality function $W(v)$, where this function is given by,

$$W(v) = \int_v^1 Q(s) \frac{ds}{s}. \tag{3.80}$$

Chapter 4

Numerical Simulation Methods

In this chapter the numerical methods employed for the simulation of two and three dimensional HD and MHD turbulence are described. First the calculation of the necessary turbulent fields is outlined. Then the spectral scheme used for the simulation is discussed with the aliasing error problem and its solution. Next the integration scheme with the Leapfrog method is discussed. A spectral calculation of quadratic nonlinearities is presented. Finally, the numerical code is described, and a detailed account of the nonlinear terms is given.

4.1 Calculation of turbulent fields

To obtain the required turbulent fields such as velocity in hydrodynamic, or velocity and magnetic fields in MHD, it is necessary to solve the Navier-Stokes and MHD equations numerically. This is accomplished with a pseudospectral code. Both of vorticity and magnetic vector potential are represented by a discrete Fourier series and solved in a regular cubic box of length size 2π with N points in each direction, more details in next section.

4.2 Direct Numerical simulations (DNS)

Spectral properties of the nonlinear processes such as nonlinear transfer functions, triad interactions, and cascade direction of the quadratic nonlinear invariants in hydrodynamic and magnetohydrodynamics turbulence are best understood in the spectral domain. Hydrodynamic flows demonstrate an inertial range of wavenumbers in the spectra of certian quantities like kinetic energy, the enstrophy, and the kinetic helicity (cf. section 2.2). In MHD turbulence, there is an inertial range for total energy, cross helicity, mean squared potential, and magnetic helicity. In the inertial range, the spectra show self-similar power law behavior, which is a predictable property of a randomly fluctuating system. The investigation of inertial ranges and the universality of the power laws form one of the important aspects of turbulence studies. Numerical simulations of turbulence in the spectral domain are performed using several methods like large eddy simulations (LES)[1], shell models[2], or direct numerical

[1]Large eddy simulation (LES) is a popular technique for simulating turbulent flows. An implication of Kolmogorov's (1941) theory of self similarity is that the large eddies of the flow are dependant on the geometry while the smaller scales more universal. This feature allows one to explicitly solve for the large eddies in a calculation and implicitly account for the small eddies by using a subgrid-scale model (SGS model), for more details, see [1].

[2]Shell models of turbulence are methods with simplified caricatures of the equations of the fluid mechanics in wave-vector representation. Their main advantage is that they can be studied via fast and accurate numerical

simulations (DNS) [1]. LES methods and shell models approximate the nonlinear terms of Eqs.(1.58 - 1.60) in one or other form (see for *e.g.,* [69]), whereas DNS methods do not use any such approximations and deal with the equations in their true form. Thus methods other than DNS usually involve additional assumptions. If the equation set is studied without any additional physical approximations, a better understanding of the turbulent flows could be obtained. The DNS methods stay closest to the underlying differential equations describing the turbulent systems although they are computationally expensive. With appropriate choice of numerical methods however the computational overhead can be reduced.
In the Fourier domain, the spatial derivatives are transformed into simple multiplications with wavevectors. Here, the time evolution of the equations directly yields the spectra of the physical quantities. Fourier methods have several advantages, they also have a major drawback: the Gibbs phenomenon. The Gibbs phenomenon manifests itself as characteristic oscillations of Fourier series near steep gradients. The incompressibility assumption eliminates [19]. For incompressible flows, spectral methods are more accurate than finite difference schemes. They require fewer discretization points to achieve the same accuracy (for a detailed description of different numerical schemes, see [70]).

4.3 Pseudospectral scheme

The HD and MHD equations are solved in the Fourier space. The computational domain is a periodic square or cubic box with sides of length 2π. The domain is uniformly discretized with N points in each direction. This corresponds to the Fourier wavenumber range $\frac{-N}{2}+1 \leq k \leq \frac{N}{2}-1$. In the pseudospectral scheme, all physical fields are approximated by a finite Fourier series, *e.g.,* the velocity field

$$\mathbf{v}(\mathbf{x},t) = \sum_{\mathbf{k}} \hat{\mathbf{v}}(\mathbf{k},t) e^{i\mathbf{k}.\mathbf{x}}.$$

In its Fourier transformed form, the vorticity equation is

$$\partial_t \hat{\boldsymbol{\omega}} = i\mathbf{k} \times \widehat{(\mathbf{v} \times \omega)} - \nu k^2 \hat{\boldsymbol{\omega}}.$$

The velocity field is algebraic in Fourier space from the vorticity field can be calculated as

$$\hat{\mathbf{v}}(\mathbf{k},t) = i\frac{\mathbf{k} \times \hat{\boldsymbol{\omega}}(\mathbf{k},t)}{|k|^2}.$$

The incompressibility condition is satisfied with the calculation accuracy. Nonlinear terms as $\mathbf{v} \times \omega$ become convolutions in Fourier space

$$\widehat{\mathbf{v} \times \boldsymbol{\omega}}(\mathbf{k},t) = \sum_{\mathbf{k}'} \hat{\mathbf{v}}(\mathbf{k}',t) \times \hat{\boldsymbol{\omega}}(\mathbf{k}-\mathbf{k}',t).$$

All physical quantities are approximated by truncated Fourier series, *e.g.,* for the Fourier

simulation, in which the values of the scaling exponents can be determined precisely.

counterpart of the real quantity $\boldsymbol{\omega}(\mathbf{x}_j, t)$,

$$\hat{\boldsymbol{\omega}}(\mathbf{k}, t) = \frac{1}{N^3} \sum_j \boldsymbol{\omega}(\mathbf{x}_j, t) e^{-i\mathbf{k}\cdot\mathbf{x}_j} \quad \text{where} \quad x_j = \frac{2\pi j}{N} \quad j = 0, ..., \mathrm{N} - 1 \ \text{ for each direction.} \tag{4.1}$$

The mode $\mathbf{k} = (0, 0, 0)$ of all physical quantities, *i.e.,* their spatial average, is set to zero. Where the original physical quantities are real-valued functions, they satisfy additional relations of symmetry in Fourier space, $(\hat{\boldsymbol{\omega}}_{-\mathbf{k}}(t) = \hat{\boldsymbol{\omega}}^*_{\mathbf{k}}(t))$ in Fourier space, hence it is enough to only store one half of Fourier modes. This symmetry property reduces the memory requirement and also speeds up the calculations. Additionally, in Fourier space all spatial derivations are replaced by multiplications with wavevectors. The nonlinear terms in Eqs.(1.58) and (1.59) are convolution sums arising from the nonlinearities. In general form these may be represented as

$$\widehat{[a \ \ b]}_{\mathbf{k}} = \sum_{\mathbf{k}=\mathbf{p}+\mathbf{q}} \widehat{a_{\mathbf{p}}} \ \widehat{b_{\mathbf{q}}} \quad \text{where} \quad |\mathbf{k}|, |\mathbf{p}|, |\mathbf{q}| \leq \frac{N}{2} - 1. \tag{4.2}$$

Direct calculation of the above expression in two dimensions requires $O(N^4)$ operations and in three dimensions requires $O(N^6)$ operations [71]. This limits the application of spectral methods to small Fourier data sets [16]. To overcome this limitation the variables in Eq.(4.2) are first transformed into real space. The multiplication is performed and the value retransformed into the Fourier space. This mathematical operation is facilitated by the fact that a convolution in Fourier domain is a multiplication in real space. This the basic idea of the method which called the pseudospectral scheme [16]. This method reduces the complexity of the order of operations performed to $O(N^3 \log_2 N)$, which is only possible with FFT (Fast Fourier Transform). But this method suffers from aliasing error caused by the finite discretization, the technique applied to remove the aliasing error is discussed in the next section.

4.3.1 Treatment of Aliasing Errors

The aliasing error of the pseudospectral scheme is removed by a truncation technique known as de-aliasing [16]. This technique utilizes the calculation of extended Fourier fields of size $M \geq \frac{3N}{2}$ instead of the original size of N. To this end, a Fourier variable resulting from the pseudospectral procedure can be expressed as a sum of two contributions (for simplicity only a one-dimensional convolution is considered). So, Eq.(4.2) is written as:

$$\widehat{[a \ \ b]}_k = \sum_{k=p+q} \widehat{a_p} \ \widehat{b_q} + \sum_{k \pm N = p+q} \widehat{a_p} \ \widehat{b_q}. \tag{4.3}$$

In the r.h.s of Eq.(4.3), the first term is the correct result of the convolution that is required and the second term is the aliasing error. If original Fourier variables are padded with zeros in the extra wavenumber range $\frac{M}{2} - 1 \geq |p|, |q| \geq \frac{N}{2} - 1$, the second term in the equation (4.3) vanishes and the exact result of the convolution is obtained. This de-aliasing procedure is sometimes called the 3/2 rule. However, the number of operations performed in this case is higher than in the normal pseudospectral calculation. In one dimension the truncation technique requires $\approx 50\%$ more numerical operations. The computational effort increases with number of dimensions, because modes that do not carry any physical information have to be

included and evaluated [19].
The performance of the dealiasing step can be improved by reducing the number of extra modes, this can be accomplished by introduced the spherical truncation of the Fourier variables in three dimensions. In this dealiasing method, a sphere of physical Fourier modes is assumed that are padded to a square in 2D or cubic in 3D shape. The aliasing error due to the modes in this sphere was empirically found to be of the order of discretization error, and is negligible. This reduces the number of additional calculations by a factor of more than 2/3 compared to the full 3/2 dealiasing [72, 19].

4.4 Leapfrog Integration

The equation set (1.14)-(1.15) of the HD case and (1.58)- (1.60) of the MHD case is evolved in time using a leapfrog scheme. The leapfrog scheme is a fast, explicit two-step algorithm that uses a constant time step. The scheme is second order accurate, and suitable for non-dissipative problems. However, the algorithm is unstable in the presence of diffusion terms. A modification in the form of an integrating factor, is therefore required to avoid this property. This method treats the linear diffusion term exactly [19, 18]. We integrate Eqs.(1.58) and (1.59) of the MHD case in the form

$$\partial_t(\hat{\boldsymbol{\omega}}_{\mathbf{k}} e^{\tilde{\mu}k^2 t}) = e^{\tilde{\mu}k^2 t} i\mathbf{k} \times [\widehat{\mathbf{v} \times \boldsymbol{\omega}} - \widehat{\mathbf{b}} \times (\nabla \times \mathbf{b})] \tag{4.4}$$

$$\partial_t(\hat{\mathbf{b}}_{\mathbf{k}} e^{\tilde{\eta}k^2 t}) = e^{\tilde{\eta}k^2 t} i\mathbf{k} \times \widehat{\mathbf{v} \times \mathbf{b}} \tag{4.5}$$

Here the dissipation term is included implicitly, and does not appear explicitly in the equations. The stability and accuracy properties do not depend on the dissipation term, and are given solely by the nonlinear term [16]. With this modification the leapfrog scheme for the Eqs.(4.4) and (4.5) is:

$$\hat{\boldsymbol{\omega}}_{n+1} = \hat{\boldsymbol{\omega}}_{n-1}\, e^{-\tilde{\mu}k^2 \Delta t} + 2\Delta t e^{-\tilde{\mu}k^2 \Delta t} [\widehat{\mathbf{v} \times \boldsymbol{\omega}} - \widehat{\mathbf{b} \times (\nabla \times \mathbf{b})}]_n \tag{4.6}$$

$$\hat{\mathbf{b}}_{n+1} = \hat{\mathbf{b}}_{n-1}\, e^{-\tilde{\eta}k^2 \Delta t} + 2\Delta t e^{-\tilde{\eta}k^2 \Delta t} [\widehat{\mathbf{v} \times \mathbf{b}}]_n \tag{4.7}$$

where n is a time step index and Δt denotes the time interval of one time step. The solution obtained with this scheme is often modified by temporal oscillations with the period $2\Delta t$ (*e.g.,* [16]). These oscillations arise due to inaccuracies in the approximation of time derivatives. Temporal averaging of the obtained solution over every two subsequent time steps eliminates the oscillations (see, [19, 18]). For nonlinear partial differential equations like the ones under consideration there are no clear rules to guarantee the numerical stability of a simulation, and therefore no recipes to indicate how small Δt ought to be. The Courant-Friedrichs-Lewy (CFL) condition, an estimate originally developed for advection, provides the upper bound as:

$$\Delta t \leq \frac{\Delta x}{v_{\max}} \sim \frac{\pi}{k_{\max} v_{\max}} \tag{4.8}$$

where $v_{\max}$ is the maximal speed of propagation in the system. Incompressibility is assumed, so magneto-acoustic waves are excluded. A good estimate for the maximum speed of propagation is $v_{\max} = \sqrt{E^{\mathrm{tot}}}$. Although the CFL criterion in Eq.(4.8) provides a basic estimate

for stability, the time step can be adjusted in particular simulations for maximum stability [19, 18, 73].

4.5 Simulation program and Diagnostics

To gain a better understanding of the characteristics of nonlinear energy transfer and triad interactions between turbulent flctuations, the analysis of fully-developed driven turbulence stemming from a large direct numerical pseudospectral simulation is carried out.
To study the spectral properties of the quadratic nonlinearity invariants in incompressible 2D and 3D for both of hydrodynamic and magnetohydrodynamic turbulence, we extend the approach of Smith and Lee [67]. They introduced a strategy for calculating the nonlinearity of the Navier-Stokes equations over a finite number of triad interactions in wavenumber space. An extension Fortran program developped by T. Hertkorn for 2D-HD simulations [12] and M. Haslehner for 3D-HD simulations [13]. In this work, we have modified the program to implement the analysis of two- and three-dimensional magnetohydrodynamic turbulence. Analysis of fully-developed, driven turbulence stemming from large pseudospectral simulations with high resolution is used to investigate all turbulent systems which studied in this work. The extension we develop is outlined below. We show the 3D case as an example.
Step 1: Consider a three-dimensional periodic cubic grid in Fourier space, and a set of wavevectors $\mathbf{k}$ within this cubic grid in Fourier space given by,

$$K = \{\mathbf{k} = (k_x, k_y, k_z)\,|k_x, k_y, k_z \in \{-k_{\max}, -k_{\max}+1, ..., k_{\max}\}\}\,,$$

We define the domains K^+ and K^-, respectively as

$$K^+ = \{\mathbf{k} = (k_x, k_y, k_z)\,|\mathbf{\Delta}_k\,\{k_x > 0\} \cup \{\{k_x = 0\} \cap \{k_y > 0\}\} \cup \{\{k_x = k_y = 0\} \cap \{k_z > 0\}\}\}\,. \tag{4.9}$$

is the set of wavevectors $\mathbf{k}$ within the cubic grid, where Δ_k is the distance between two adjacent wavevectors in the grid.
and

$$K^- = -K^+\left\{\mathbf{k}|-\mathbf{k} \in K^+\right\}.$$

To show how we can calculate the energy transfer functions, we apply the so-called *"reality conditions"* on the complex conjugates of velocity and magnetic field, where

$$\mathbf{v}^*(\mathbf{k}) = \mathbf{v}(-\mathbf{k}) \Leftrightarrow \mathbf{v}^*(-\mathbf{k}) = \mathbf{v}(\mathbf{k}) \tag{4.10}$$

$$\mathbf{b}^*(\mathbf{k}) = \mathbf{b}(-\mathbf{k}) \Leftrightarrow \mathbf{b}^*(-\mathbf{k}) = \mathbf{b}(\mathbf{k}) \tag{4.11}$$

These conditions lead to a condition on the transfer function,

$$T(\mathbf{k}|\mathbf{p}|\mathbf{q}) = T^*(-\mathbf{k}| - \mathbf{p}| - \mathbf{q}). \tag{4.12}$$

Thus the information only in the domain K^+ is sufficient to construct the wavevectors field over the entire cube $K^+ \cup K^-$ (see, Fig.4.1).

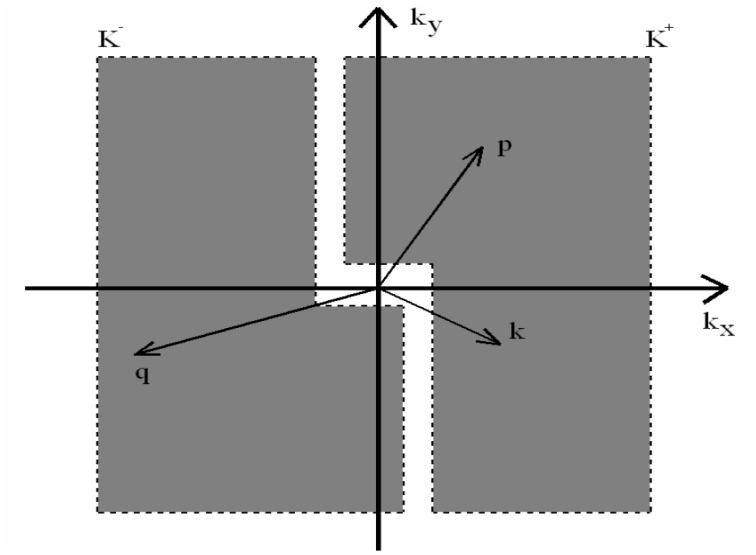

Figure 4.1: K^+ is the domain in Fourier space and the triad $\Delta_{\mathbf{kpq}}$ is in T^+ with $\mathbf{k} < \mathbf{p}$, from [67].

Step 2: Define T^+ as a set of non-collinear triads

$$\Delta_{\mathbf{kpq}} := \{\mathbf{k}, \mathbf{p}, \mathbf{q} : \mathbf{k} + \mathbf{p} + \mathbf{q} = 0\} \tag{4.13}$$

with two wavevectors say $\mathbf{k}$ and $\mathbf{p}$ in the Fourier domain of K^+ and the remaining vector $\mathbf{q}$ in the Fourier domain of K^-.

step 3: Let T^- be the set of triads whose Fourier conjugate in T^+ satisfies

$$T^- = \left\{\Delta_{\mathbf{kpq}} : \Delta_{-\mathbf{k},-\mathbf{p},-\mathbf{q}} \in T^+\right\}. \tag{4.14}$$

Then any triad in T^- has two wavevectors in K^- and the remaining wavevector in the domain K^+. Any non-collinear triad is in either T^+ or T^-, therefore the sum of the full nonlinear term is taken over $T^+ \cup T^-$.

4.5.1 Computing the nonlinear interactions

In this subsection, we describe a numerical procedure to compute the nonlinear interactions over T which is a given subset of $T^+ \cup T^-$. For simplicity, for a fixed triad in the hydrodynamic case, $\Delta_{\mathbf{kpq}}$ is in $T \cap T^+$ with $\mathbf{k}$ and $\mathbf{p}$ are in K^+ and $\mathbf{q}$ is in K^- as shown in Fig.(4.1). We use the modes $\mathbf{v}(\mathbf{k})$, $\mathbf{v}(\mathbf{p})$ and $\mathbf{v}(-\mathbf{q})$ with the wavevectors in K^+, then we compute the nonlinear terms

$$T^{vv}(\mathbf{k}|\mathbf{p},\mathbf{q}) = T^{vv}(\mathbf{k}|\mathbf{q},\mathbf{p}) = T^{vv}(\mathbf{k}|\mathbf{p}|\mathbf{q}) + T^{vv}(\mathbf{k}|\mathbf{q}|\mathbf{p}),$$

$$T^{vv}(\mathbf{p}|\mathbf{k},\mathbf{q}) = T^{vv}(\mathbf{p}|\mathbf{q},\mathbf{k}) = T^{vv}(\mathbf{p}|\mathbf{k}|\mathbf{q}) + T^{vv}(\mathbf{p}|\mathbf{q}|\mathbf{k}),$$

$$T^{vv}(-\mathbf{q}|-\mathbf{k},-\mathbf{p}) = T^{vv}(-\mathbf{q}|-\mathbf{p},-\mathbf{k}) = T^{vv}(-\mathbf{q}|-\mathbf{k}|-\mathbf{p}) + T^{vv}(-\mathbf{q}|-\mathbf{p}|-\mathbf{k}),$$

The term $T^{vv}(\mathbf{q}|\mathbf{k},\mathbf{p})$ is not necessary because the wavevector $\mathbf{q}$ is not in the computation domain of K^+. However, its conjugate $T^{vv}(-\mathbf{q}|-\mathbf{k},-\mathbf{p})$ must be computed because the wavevector $-\mathbf{q}$ is in the domain of K^-. Nonlinear terms are computed using the following

reality conditions,

$$\begin{cases} \mathbf{v}^*(\mathbf{k}) = \mathbf{v}(-\mathbf{k}) \Leftrightarrow \mathbf{v}^*(-\mathbf{k}) = \mathbf{v}(\mathbf{k}), \quad \mathbf{v}^*(\mathbf{p}) = \mathbf{v}(-\mathbf{p}) \Leftrightarrow \mathbf{v}^*(-\mathbf{p}) = \mathbf{v}(\mathbf{p}) \quad \text{and} \\ \mathbf{v}^*(-\mathbf{q}) = \mathbf{v}(\mathbf{q}) \Leftrightarrow \mathbf{v}^*(\mathbf{q}) = \mathbf{v}(-\mathbf{q}) \end{cases} \tag{4.15}$$

In MHD turbulence, for a fixed triad $\Delta_{\mathbf{kpq}}$ in T^+ with $\mathbf{k}, \mathbf{p} \in K^+$, and $\mathbf{q} \in K^-$, we need only the modes $\mathbf{v}(\mathbf{k})$, $\mathbf{v}(\mathbf{p})$, $\mathbf{v}(-\mathbf{q})$, $\mathbf{b}(\mathbf{k})$, $\mathbf{b}(\mathbf{p})$ and $\mathbf{b}(-\mathbf{q})$ to compute the different nonlinear terms, $T^{YX}(\mathbf{k}|\mathbf{p}, \mathbf{q})$, $T^{YX}(\mathbf{p}|\mathbf{k}, \mathbf{q})$ and $T^{YX}(-\mathbf{q}|-\mathbf{k}, -\mathbf{p})$ (where X and Y are v or b field) by using the following *reality conditions*,

$$\begin{cases} \mathbf{v}^*(\mathbf{k}) = \mathbf{v}(-\mathbf{k}) \Leftrightarrow \mathbf{v}^*(-\mathbf{k}) = \mathbf{v}(\mathbf{k}), \quad \mathbf{v}^*(\mathbf{p}) = \mathbf{v}(-\mathbf{p}) \Leftrightarrow \mathbf{v}^*(-\mathbf{p}) = \mathbf{v}(\mathbf{p}), \\ \mathbf{v}^*(-\mathbf{q}) = \mathbf{v}(\mathbf{q}) \Leftrightarrow \mathbf{v}^*(\mathbf{q}) = \mathbf{v}(-\mathbf{q}), \quad \mathbf{b}^*(\mathbf{k}) = \mathbf{b}(-\mathbf{k}) \Leftrightarrow \mathbf{b}^*(-\mathbf{k}) = \mathbf{b}(\mathbf{k}), \\ \mathbf{b}^*(\mathbf{p}) = \mathbf{b}(-\mathbf{p}) \Leftrightarrow \mathbf{b}^*(-\mathbf{p}) = \mathbf{b}(\mathbf{p}), \quad \mathbf{b}^*(-\mathbf{q}) = \mathbf{b}(\mathbf{q}) \Leftrightarrow \mathbf{b}^*(\mathbf{q}) = \mathbf{b}(-\mathbf{q}). \end{cases} \tag{4.16}$$

It remains to discuss how we identify the triads in T. It suffices to solve for the triads in $T \cap T^+$ because of the reality conditions. This requires a systematic procedure to search over all triads in T^+. For this purpose, an order is introduced between wavevectors in the domain K^+, which is

- **(1) in 2D turbulence**

$$\mathbf{k} < \mathbf{p}, \qquad \text{if either}$$
$$\mathbf{k}, \mathbf{p} \in \{\{k_x < p_x\} \cup \{(k_x = p_x) \cap (k_y < p_y)\}\}. \tag{4.17}$$

- **(2) In 3D turbulence**

$$\mathbf{k} < \mathbf{p}, \qquad \text{if either}$$
$$\mathbf{k}, \mathbf{p} \in \{\{k_x < p_x\} \cup \{(k_x = p_x) \cap (k_y < p_y)\} \cup \{(k_x = p_x) \cap (k_y = p_y) \cap (k_z < p_z)\}\}. \tag{4.18}$$

The use of this inequality is ordered to eliminate the collinear triads. Then, being aware of the fact that $\mathbf{q} = -\mathbf{k} - \mathbf{p}$, T^+ is spanned for fixed $\mathbf{k}$ by numerically looping over all $\mathbf{p}$ in K^+ with $\mathbf{p} > \mathbf{k}$. If $\mathbf{p} = \mathbf{k}$, the triad Δ_{kpq} is collinear and the nonlinear interactions among the triad are identically zero. Thus it is sufficient to consider $\mathbf{p}$ that is strictly greater than $\mathbf{k}$.

Chapter 5

Nonlinear tirad interactions in hydrodynamic turbulence

In incompressible hydrodynamic (HD) turbulence, the quadratic ideal invariants are kinetic energy and mean square vorticity (enstrophy) in the 2D case, and kinetic energy and kinetic helicity in the 3D case. In this chapter, the spectral locality or nonlocality of the transfer functions, triad interactions, and the inertial range cascade directions of these ideal invariants in Fourier space are studied. These topics are investigated by computing the dependence of the transfer density function $Q(v)$ of triads on their legs ratio v, and the locality function $W(v)$. The results are reported for both 2D and 3D-HD turbulence.

5.1 Ideal invariants in 2D-HD turbulence

The Navier-Stokes equations for homogenous incompressible fluid are expressed in Eqs.(1.14) and (1.15). By taking the curl of Eq.(1.14) we have

$$\partial_t \boldsymbol{\omega} + \mathbf{v} \cdot \nabla \boldsymbol{\omega} - \boldsymbol{\omega} \cdot \nabla \mathbf{v} = \tilde{\nu} \Delta \boldsymbol{\omega}, \tag{5.1}$$

$$\nabla \cdot \mathbf{v} = 0. \tag{5.2}$$

where $\boldsymbol{\omega} = \nabla \times \mathbf{v}$ is the vorticity, and $\tilde{\nu}$ is the dimensionaless dissipation coefficient. The term $\boldsymbol{\omega} \cdot \nabla \mathbf{v}$ in Eq.(5.1) is the source of vorticity, which is proportional to the velocity gradient along the vorticity. This term is often called the vorticity-stretching term [2]. Equation (5.1) can be reduced to an advection-diffusion equation in two dimensions (restricting the fluid motion with $\partial z = 0$) [2]

$$\partial_t \boldsymbol{\omega} + \mathbf{v} \cdot \nabla \boldsymbol{\omega} = \mathrm{Re}^{-1} \Delta \boldsymbol{\omega}. \tag{5.3}$$

where Re is the classical Reynolds number. Eq.(5.3) implies that in the 2D-HD case the vorticity of a fluid element is constant and there is no source of vortex-stretching. This lead us to rewrite Eq.(5.3)

$$\partial_t \boldsymbol{\omega} + \mathbf{v} \cdot \nabla \boldsymbol{\omega} = \tilde{\nu}_n (-1)^{n-1} \Delta^n \boldsymbol{\omega} + f. \tag{5.4}$$

where $\tilde{\nu}_n$ is the hyperviscous dimensionless dissipation coefficient, which used to extend the inertial range and n is level of hyperviscosity (when $n = 1$, it is the dimensionless kinematic viscosity). The quantity f is a stirring force applied to the system. The Reynolds number Re

can be expressed with the help of macroscopic quantities characteristic of the flow, the total kinetic energy per unit mass, $E^K = \frac{1}{2}\int_S v^2 dS$ (S denotes the surface of the fully periodic domain) and the rate of the kinetic energy dissipation, $\epsilon = -\dot{E}^K$ for decaying turbulence [2]. These allow using dimensional analysis to estimate a characteristic length scale $L_0 = (E^K)^{3/2}/\epsilon$ and large-scale velocity $V_0 = (E^K)^{1/2}$. Then the Reynolds number in a statistically isotropic system can be defined as (cf. subsection 1.2.1)

$$\mathrm{Re} = \frac{L_0 V_0}{\nu} = \frac{(E^K)^2}{\nu\epsilon}. \tag{5.5}$$

Two-dimensional hydrodynamics is a simpler setting than three-dimensional hydrodynamics. High Reynolds number implies a large separation between integral and dissipation scales and thereby a wide inertial range is obtained. Scaling properties are expected to be better in two-dimensional simulations than that in three-dimensional simulations as higher numerical resolutions can be realized. The nonlinear dynamics of hydrodynamic turbulence is less complicated than that of magnetohydrodynamic turbulence, because it does not involve effects of magnetic fields. However, there are important differences between hydrodynamic turbulence in two and three dimensions, mainly due to the inverse cascade of kinetic energy and the special role of enstrophy in 2D-HD turbulence (which we discuss in detail in section 5.2).
In the 2D-HD turbulence case, two conserved ideal quadratic invariants exist, especially for the ideal fluid (ν=0): the kinetic energy

$$E^K = \frac{1}{2}\int_S v^2 dS, \tag{5.6}$$

and the enstrophy (mean square vorticity)

$$\Omega = \frac{1}{2}\int_S \omega^2 dS. \tag{5.7}$$

5.1.1 Scaling of energy and enstrophy spectra in 2D-hydrodynamic turbulence

2D-HD energy and enstrophy spectra can be obtained by solving the 2D-Navier-Stokes equations (5.2)-(5.3) on a 2π-biperiodic square using a standard pseudospectral method with dealiasing according to the 2/3 rule [16]. The simulations with high-resolution conducted by A. Busse and W.-C. Müller is performed with parameters which are shown in Table 5.1.

Parameters	Energy	Enstrophy
Resolution	4096^2	2048^2
$\tilde{\nu_n}$	0.5e-47	0.16e-3
Reynolds number Re	-	6.25×10^3
Level of hyperviscosity, n	8	1
Forcing wavenumber, k_f	600	–

Table 5.1: Simulation parameters for energy and enstrophy cases in 2D-HD turbulence.

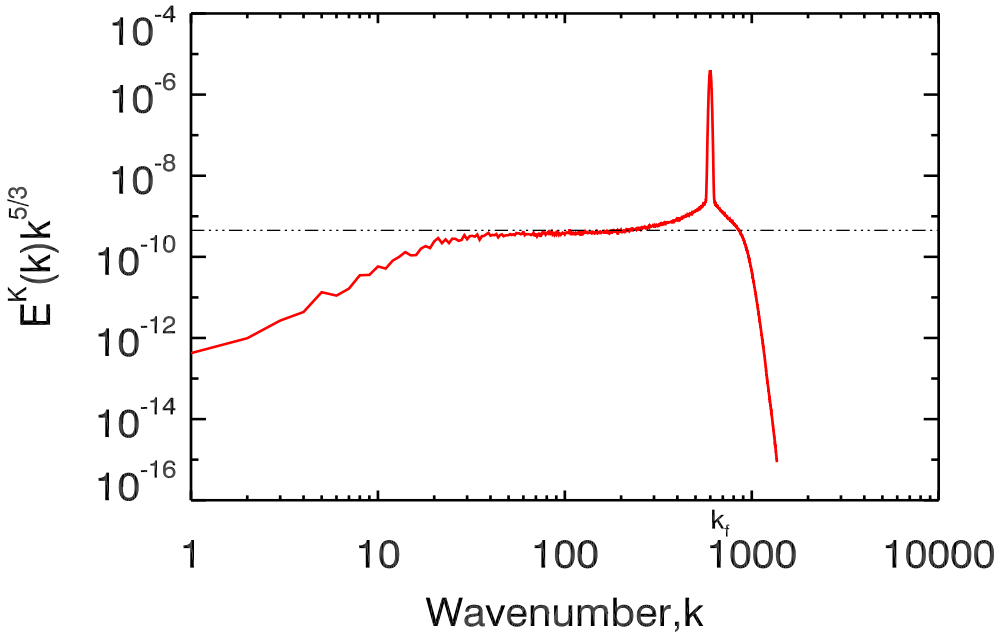

Figure 5.1: Energy spectrum in DNS of 2D-HD turbulence compensated by the inverse Kolmogorov inertial range prediction of $k^{5/3}$. The horizontal dash-dotted line is fitted to the inertial range where Kolmogorov-like $k^{-5/3}$ scaling is observed.

In Fourier space the value of kinetic energy $E^K(\mathbf{k})$ for a given vector $\mathbf{k}$ depends on the value of velocity field $\mathbf{v}(\mathbf{k})$ for this vector:

$$E^K(\mathbf{k}) = \frac{1}{2}|\mathbf{v}(\mathbf{k})|^2. \tag{5.8}$$

The value of the velocity for each given vector $\mathbf{k}$ depends on the vorticity $\boldsymbol{\omega}$. The explicit expression for the velocity, depending on the vorticity, is found using the condition of free divergence of the field ($\nabla \cdot \mathbf{v} = 0$). The vorticity can be expressed in terms of velocity in real space

$$\boldsymbol{\omega}(\mathbf{x}) = \nabla \times \mathbf{v}(\mathbf{x}).$$

In Fourier domain this is

$$\boldsymbol{\omega}(\mathbf{k}) = i\mathbf{k} \times \mathbf{v}(\mathbf{k}).$$

The velocity can then be expressed explicitly via this relation, by calculating the rotation of $\boldsymbol{\omega}$ in Fourier space,

$$\nabla \times \boldsymbol{\omega}(\mathbf{k}) = [\nabla \times (\nabla \times \mathbf{v})](\mathbf{k}).$$

This equation leads us to

$$i\mathbf{k} \times \boldsymbol{\omega}(\mathbf{k}) = -\mathbf{k} \times (\mathbf{k} \times \mathbf{v}(\mathbf{k})).$$

Applying the vector-product relation and using $\nabla \cdot \mathbf{v} = 0$, lead us to

$$\mathbf{v}(\mathbf{k}) = i\frac{\mathbf{k} \times \boldsymbol{\omega}(\mathbf{k})}{k^2}. \tag{5.9}$$

This relation between velocity and vorticity can be used to compute the kinetic energy in Eq.(5.8)

$$E^K(\mathbf{k}) = \frac{1}{2k^2}\boldsymbol{\omega}(\mathbf{k}) \cdot \boldsymbol{\omega}^*(\mathbf{k}) = \frac{1}{k^2}\boldsymbol{\Omega}(\mathbf{k}). \tag{5.10}$$

where $\boldsymbol{\omega}^*(\mathbf{k})$ is the complex conjugate of $\boldsymbol{\omega}(\mathbf{k})$, and $\Omega(\mathbf{k})$ is the enstrophy. The cumulative kinetic energy $E^K(\mathbf{k})$ of homogenous incompressible 2D-hydrodynamic turbulence calculated using Eq.(5.10). The analysis has been done using high-resolution direct numerical simulations (DNS) with parameters which are shown in Table 5.1. In the simulation for the inverse cascade of energy, hyperviscous dissipation with a level of $n = 8$ is used in order to extend the inertial range [74]. The dissipation is not involved in the cascade and has simply the role of removing enstrophy at small scales. Energy is injected into the system by a random forcing delta correlated in time that acts on a band of wavenumbers in the small scales region (large wavenumbers) around $k_f = 600$, adding a friction term removes energy at large scales (small wavenumbers).

According to Kolmogorov's (1941) theory, the inertial ranges of the energy and enstrophy spectra are situated between the driving range and the dissipation range [40] (cf. section 2.1). Through these inertial ranges the energy and enstrophy are cascaded by nonlinear processes to the wavenumbers where they are dissipated. There is a double cascade in 2D-HD turbulence with energy cascading to large length scales and enstrophy cascading to small length scales [75]. Furthermore, the energy and enstrophy spectra in their inertial ranges depend only on the wavenumbes, k and on the rate of their dissipation at which the energy and the enstrophy are cascaded per unit mass. Therefore they have the forms [5, 76]

$$E^K(k) = C\epsilon^{2/3}k^{-5/3}, \qquad \Omega(k) = C'\beta^{2/3}k^{-3}. \tag{5.11}$$

where ϵ is the rate of kinetic energy transfer (cascaded) per unit mass and β is the rate of the enstrophy transfer. C and C' are dimensionless constants.

Fig.5.1 shows the compensated energy spectrum at stationary turbulent flow. This spectrum exhibits Kolmogorov scaling, $E^K(k) \sim k^{-5/3}$ with logarithmic correction [5, 76]. The energy spectrum shows the turbulence in this case is fully-developed in the inertial range. It is clear that this compensated spectrum exhibits an inertial range extended over about one decade in wavenumber space $30 \lesssim k \lesssim 270$.

The enstrophy spectrum of incompressible 2D-HD turbulence is similarly obtained, where the cumulative enstrophy $\Omega(\mathbf{k})$ computed by using Eq.(5.10). The simulation is performed with the parameters specified for enstrophy in decaying isotropic 2D-HD (cf. Table 5.1). Fig.5.2 shows the compensated enstrophy spectrum in DNS of 2D-MHD turbulence. The enstrophy spectrum is compensated by the scaling factor k^3 [5, 76]. The horizontal dashed line in the plot indicates this scaling with the exponent -3. This is in agreement with the scaling prediction k^3 (cf. Eq.5.11). The inertial range of the enstrophy spectrum extends in

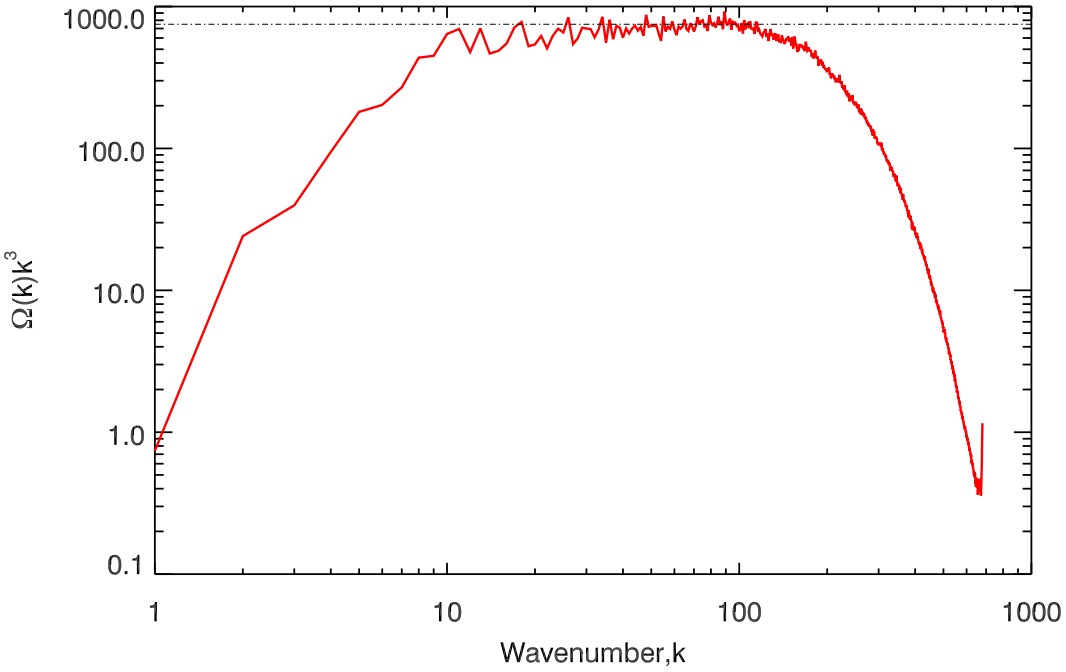

Figure 5.2: Compensated enstrophy spectrum in DNS of decaying isotropic 2D-HD turbulence, the horizontal dash-dotted line indicates the scaling k^{-3}.

wavenumber space $30 \lesssim k \lesssim 100$.

5.2 Nonlinear triad interactions in 2D-hydrodynamic turbulence

5.2.1 $Q(v)$ and $W(v)$ Functions in 2D-HD Turbulence

The locality of the nonlinear energy and mean square vorticity transfer functions, triad interactions, and the type of cascade in the inertial range of incompressible 2D-HD are measured by computing both the transfer density function $Q(v)$ and the locality function $W(v)$ (cf. sections 3.6 and 3.7). The nonlinear terms in the 2D-HD equation (cf. Eq.5.3) conserve both kinetic energy and enstrophy [6].

In order to measure the locality of the nonlinear energy transfer function and the triad interactions in the energy inertial range in 2D-HD turbulence, Kraichnan [5] introduced a function $Q(v)$ that depends on v which is the ratio of the norm of the wavevector with the smallest length of a given triad, and the norm of the wavevector of middle length, in other words it is the ratio of the smallest wavenumber to the middle wavenumber in the interacting triad. This function is derived from the energy flux $\Pi(k)$ which can be expressed as (for more details see section 3.5)

$$\Pi(k) = \int_0^1 dv \int_1^{1+v} dw \left[\ln(w)T(w,1,v) + \ln(v)T(v,1,w)\right]. \tag{5.12}$$

Eq.(5.12) is valid for two and three dimensional hydrodynamic turbulence. The detailed conservation of energy in both two and three dimensions for each triad interaction is expressed by (cf. subsection 3.2.1)

$$T(\mathbf{k}|\mathbf{p},\mathbf{q}) + T(\mathbf{p}|\mathbf{q},\mathbf{k}) + T(\mathbf{q}|\mathbf{k},\mathbf{p}) = 0. \tag{5.13}$$

The quantity $T(\ |\ ,\ )$ in each term of the l.h.s represents the combined energy transfer from two wavenumbers (the second and third) to the first. The term $T(\mathbf{k}|\mathbf{p},\mathbf{q})$ can be split into a sum of two terms as,

$$T(\mathbf{k}|\mathbf{p},\mathbf{q}) = T(\mathbf{k}|\mathbf{p}|\mathbf{q}) + T(\mathbf{k}|\mathbf{q}|\mathbf{p}).$$

where the first nonlinear term of the r.h.s. can be regarded as the rate of the energy transfer from mode $\mathbf{p}$ to mode $\mathbf{k}$ via mode $\mathbf{q}$ which acts as a mediator (*i.e.,* it is responsible for the transfer), and the second term as the rate of the energy transfer from mode $\mathbf{q}$ to mode $\mathbf{k}$ via the mediator $\mathbf{p}$ (cf. subsection 3.2.2). Each of these nonlinear terms is a mode-to-mode energy transfer [39, 61]. The sum of transfer rates of the energy in a triad in 2D-HD turbulence is zero, *i.e.,*

$$T(\mathbf{k}|\mathbf{p}|\mathbf{q}) + T(\mathbf{k}|\mathbf{q}|\mathbf{p}) + T(\mathbf{p}|\mathbf{k}|\mathbf{q}) + T(\mathbf{p}|\mathbf{q}|\mathbf{k}) + T(\mathbf{q}|\mathbf{k}|\mathbf{p}) + T(\mathbf{q}|\mathbf{p}|\mathbf{k}) = 0.$$

This result is detailed conservation of the energy in a triad interaction and means that the energy is conserved in a given triad in 2D-HD turbulence, *i.e.,*

$$T(\mathbf{k}) + T(\mathbf{p}) + T(\mathbf{q}) = \text{const.}$$

Similarly, the detailed conservation of enstrophy for each triad interaction in 2D-HD turbulence can be expressed by

$$k^2 T(\mathbf{k}|\mathbf{p},\mathbf{q}) + p^2\, T(\mathbf{p}|\mathbf{q},\mathbf{k}) + q^2\, T(\mathbf{q}|\mathbf{k},\mathbf{p}) = 0. \tag{5.14}$$

where each term of the l.h.s gives the combined enstrophy transfer function from two modes to the third in the interacting triad. Each of these terms can be split into a sum of two terms, for example $k^2 T(\mathbf{k}|\mathbf{p},\mathbf{q})$ can be written as

$$k^2 T(\mathbf{k}|\mathbf{p},\mathbf{q}) = k^2\, T(\mathbf{k}|\mathbf{p}|\mathbf{q}) + k^2\, T(\mathbf{k}|\mathbf{q}|\mathbf{p}).$$

where the first nonlinear term of the r.h.s. gives the rate of the enstrophy transfer from mode $\mathbf{p}$ to mode $\mathbf{k}$ mediated by mode $\mathbf{q}$, and the second term of the same side gives the rate of the enstrophy transfer from mode $\mathbf{q}$ to mode $\mathbf{k}$ via the mediator $\mathbf{p}$. Each of these nonlinear terms is called a mode-to-mode enstrophy transfer. The sum of the enstrophy transfer rates in a triad in 2D-HD turbulence is zero

$$k^2 T(\mathbf{k}|\mathbf{p}|\mathbf{q}) + k^2\, T(\mathbf{k}|\mathbf{q}|\mathbf{p}) + p^2\, T(\mathbf{p}|\mathbf{k}|\mathbf{q}) + p^2\, T(\mathbf{p}|\mathbf{q}|\mathbf{k}) + q^2\, T(\mathbf{q}|\mathbf{k}|\mathbf{p}) + q^2\, T(\mathbf{q}|\mathbf{p}|\mathbf{k}) = 0.$$

This is the detailed conservation of the enstrophy in a triad interaction and means that that the enstrophy is conserved in a given triad in 2D-HD turbulence,

$$\Omega(\mathbf{k}) + \Omega(\mathbf{p}) + \Omega(\mathbf{q}) = \text{const.}$$

Because of the detailed conservation of the energy and enstrophy in 2D-HD turbulence [6], the over-all conservation laws of them can be written

$$\int_0^\infty T(k)dk = 0, \qquad \int_0^\infty k^2 T(k)dk = 0. \tag{5.15}$$

Eq.(5.15) follows from the detailed conservation of energy and enstrophy in Eqs.(5.13) and (5.14). These equations together give us some properties of an interacting triad formed by three wavenumbers (k, p, q) with $\mathbf{k} = \mathbf{p} + \mathbf{q}$, $k = |\mathbf{k}|$, $p = |\mathbf{p}|$, and $q = |\mathbf{q}|$ in 2D-HD turbulence only written as

$$\begin{aligned} T(p|q,k)/T(k|p,q) &= (q^2 - k^2)/(p^2 - q^2), \\ T(q|k,p)/T(p|q,k) &= (k^2 - p^2)/(q^2 - k^2), \\ T(k|p,q)/T(q|k,p) &= (p^2 - q^2)/(k^2 - p^2). \end{aligned} \tag{5.16}$$

Thus only one of the $T(\ |\ ,\ )$ associated with a given triad interactions is linearly independent [6].

Applying these properties to the nonlinear terms in the energy flux Eq.(5.12), we find

$$T(v,1,w) = T(v,w,1) = \frac{w^2-1}{v^2-w^2}T(1,v,w), \qquad \text{and} \qquad T(w,1,v) = \frac{1-v^2}{v^2-w^2}T(1,v,w).$$

Then Eq.(5.12) for the energy flux $\Pi(k)$, can be simplified in two dimensions only to

$$\Pi(k) = \int_0^1 dv \int_1^{1+v} dw \left[\ln(w)T(1-v^2) + \ln(v)T(w^2-1)\right] \frac{T(1,v,w)}{v^2-w^2}. \tag{5.17}$$

Every pair of v and w values in Eq.(5.12) and Eq.(5.17) corresponds to a possible shape of triangle created by the triad of interacting wavenumbers [6]. We introduce a new function, which is called the transfer density function

$$Q(v) = \frac{v}{\epsilon}\int_1^{1+v} dw \left[\ln(w)T(1-v^2) + \ln(v)T(w^2-1)\right] \frac{T(1,v,w)}{v^2-w^2}. \tag{5.18}$$

Here ϵ is the total rate of kinetic energy dissipation. The integrand in Eq.(5.18) represents the total contribution to the energy transfer across k from all possible triads of a given shape. The T factors in the integrand give the weights of the contribution of the different triangle shapes. Eq.(5.17) for the energy flux in 2D-HD can be written

$$\Pi(k) = \int_0^1 dv \frac{\epsilon}{v} Q(v) = \epsilon \int_0^1 Q(v)\frac{dv}{v}. \tag{5.19}$$

Therefore, $Q(v)$ serves as a measure of the locality of energy transfer. The $Q(v)$ function shows the structure of the inertial range energy transfer.
Repeating this procedure for the enstrophy (details given in Appendix B), the enstrophy flux in 2D-HD can be written

$$Z(k) = \int_0^1 dv \frac{\beta}{v} Q(v) = \beta \int_0^1 Q(v) \frac{dv}{v}. \tag{5.20}$$

Here β is the total rate of enstrophy dissipation.
Kraichnan's approach for measuring the locality energy and enstrophy transfer functions depends on the rule which states that in the inertial range of the energy spectrum, the the total energy flux $\Pi(k)$ is constant and equal to the total rate of energy dissipation ϵ [64] (cf. section 2.2). Similarly, in the inertial range of the enstrophy spectrum, the total enstrophy flux $Z(k)$ is equal to the total rate of enstrophy dissipation β. Eqs.(5.19) and (5.20) can be written :

$$\int_0^1 \frac{dv}{v} Q(v) = 1 \tag{5.21}$$

The above equation shows explicity how $Q(v)$ can be regarded as a probability density function of v (the ratio of the smallest wavenumber to the middle wavenumber in the interacting triad). $Q(v)$ measures the density of contributions to the nonlinear energy or enstrophy transfer of the different shapes of triangles of interacting modes in k-space.
The nature of nonlinear transfer functions and nonlinear triad interactions can be approached based on the geometry of a triad, following Kraichnan's analytical closure model [5]. The part of the total energy transfer function that passes through the inertial-range is measured by our simulation. This part of the energy transfer is due to all triad interactions in which the ratio of the smallest to the middle wavenumber is greater than v. We determine this by the locality function $W(v)$,

$$W(v) = \int_v^1 Q(s) \frac{ds}{s}. \tag{5.22}$$

5.2.2 Locality of the energy in 2D-HD turbulence

To measure the locality of the nonlinear energy transfer function in incompressible isotropic 2D-HD turbulence, the function $Q(v)$ can be used. This transfer density function depends on v, the ratio of the smallest wavenumber to the middle wavenumber for a given interacting triad. In our approach, the normalization of $Q(v)$ in Eq.(5.21) shows how it represents as a probability density function of v. Instead of a numerical integration of $Q(v)$, the distribution of the different triads implied in the energy transfer through the quantity, v is determined. Thus for wavevectors $\mathbf{k}$, $\mathbf{p}$ and $\mathbf{q}$ with $\mathbf{k} = \mathbf{p} + \mathbf{q}$, which form a triad, we compute the ratio v followed by the distribution of this ratio over the interval $[0, 1]$. $Q(v)$ is appropriately normalized over the total number of triads interactions. The normalized histogram of v values shows the density of different wavevectors triangles. This histogram also shows the locality of the nonlinear energy transfer in k-space in the inertial range of 2D-HD turbulence (cf. Fig.5.3).
In our approach, to measure the locality of the nonlinear energy transfer function, the following

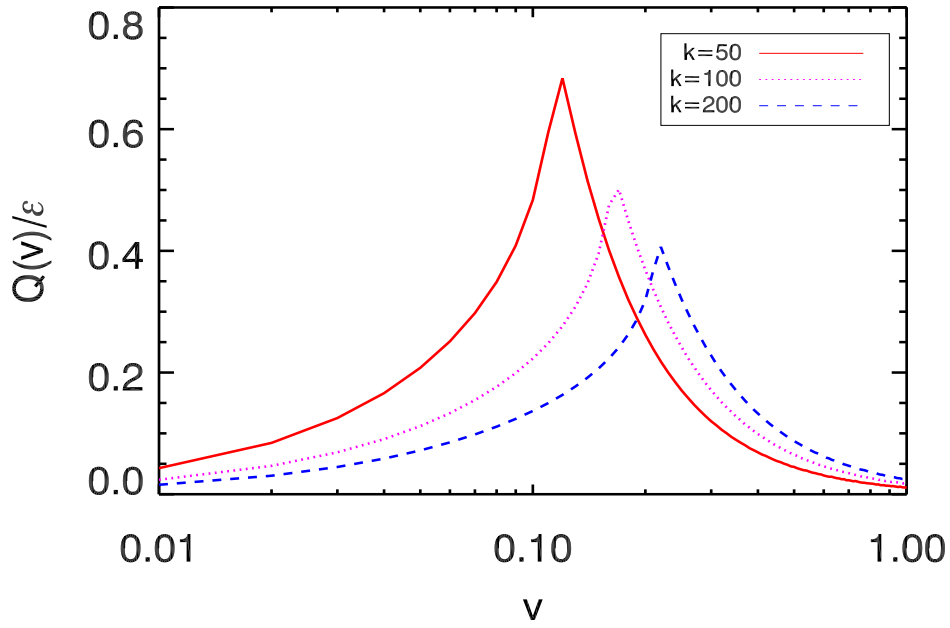

Figure 5.3: Normalized transfer density functions $Q(v)$ of the energy transfer for $k = 50$ (solid line), $k = 100$ (dotted line), and $k = 200$ (dashed line) in the inertial range of homogenous incompressible 2D-HD turbulence.

steps are used:

(1) An extension for Smith and Lee [67] approach is performed (cf. section 4.5 for simulation details) with high resolution 4096^2 grid points of incompressible 2D-HD turbulence.

(2) For an arbitrary fixed **k**-vector in the inertial range, graphs of the distribution of the different shapes of nonlinear triads involved in energy transfer are computed. The distribution give us more information about the interactions which are involved in changing the energy.

(3) Contributions to the kinetic energy transfer associated with the density of the triad interactions $(\mathbf{k}, \mathbf{p}, \mathbf{q})$ are determined (*i.e.,* belonging to each value of v) coming from the combined energy transfer rates from modes belonging to **p** and **q** to mode **k**. For example the kinetic energy transfer from modes belonging to **p** and **q** to the kinetic energy in the third mode **k**, $T^{vv}(\mathbf{k}|\mathbf{p},\mathbf{q})$ (where $T^{vv}(\mathbf{k}|\mathbf{p},\mathbf{q}) = T^{vv}(\mathbf{k}|\mathbf{p}|\mathbf{q}) + T^{vv}(\mathbf{k}|\mathbf{q}|\mathbf{p})$). Thus the value of the combined kinetic energy transfer from two modes **p** and **q** to the kinetic energy in mode **k** for each v-value is computed. The energy contributions normalized over the total amount of energy transfer, due to the histograms of energy transfer for the same arbitrary fixed **k**-vector.

It is important here to mention that all spectral results of the transfer density functions $Q(v)$ in the following sections are obtained by averaging over different independent states of fully developed quasi-stationary turbulence. To separate the local and nonlocal transfer and triad interactions, we used the parameter v (the ratio of the smallest wavenumber to the middle

wavenumber in the interacting triad) to classify the transfer and interactions as local when $v \geq 0.5$ and nonlocal when $v < 0.5$.

Fig.5.3 shows the normalized transfer density functions $Q(v)$ for k-values chosen in the inertial range of the energy spectrum, say $k = 50, 100$, and 200. These k-values are chosen at different positions of the inertial range (see Fig.5.1) to show how the strength of the function $Q(v)$ vary a long the inertial range. The contributions of the transfer density function $Q(v)$ are normalized by the rate of kinetic energy dissipation, $\epsilon = \nu \int_S \boldsymbol{\omega^2} dS$ (cf. subsection 1.7.3). Fig.5.3 shows three peaks with different amplitudes, each for a different value of k. These amplitudes represent the strengths of the energy transfer functions and triad interactions. The peaks of the functions $Q(v)$ appear at v-values are close to zero, ($v = 0.12, 0.18$, and 0.22 for $k = 50, 100$, and 200, respectively). In other words, most of the nonlinear energy transfer takes place in the region $v < 0.5$. This implies that the highest probability of nonlinear kinetic energy transfer takes place between two wavenumbers of different size in any given interacting triad. This indicates that most of the nonlinear kinetic energy transfer is highly nonlocal (cf. section 3.4).

The positions of the peaks of the density functions $Q(v)$ in Fig.5.3 indicate that the magnitudes of energy transfer which come from local triads ($k \approx p \approx q$) are small, while the magnitudes which come from nonlocal triads ($k \neq p \neq q$) are large. The functions $Q(v)$ vanish at $v = 1$, because each triad interaction conserves both energy and enstrophy. This implies that the energy transfer function $T(\mathbf{k}|\mathbf{p}, \mathbf{q})$ is zero if any two of the three wavenumbers are equal (cf. Eq.5.13 and 5.14). Thus it can be envisaged that most of the interacting triads includes three wavenumbers with different sizes in the inertial range. The total energy is exchanged between two small scales (large wavenumbers) and a large scale (small wavenumber) in a given triad. Thus the triad interactions are predominantly nonlocal in the energy inertial range of 2D-HD turbulence. In addition, Fig.5.3 indicates that the strength of the function $Q(v)$ increases with decreasing k-value and v go to zero. This indicates that the kinetic energy is transferred from small scales to large scales in the inertial range. Thus the kinetic energy flux is negative and the nonlinear energy transfer has an inverse cascade. The graphs fall to zero for v-values close to zero. Due to the fact that the triangles are elongated, they can not be represented in a square box anymore. The highest density of triad interactions is given for triangles that are elongated.

The nature of the nonlinear energy transfer functions and nonlinear triad interactions can be quantified by considering the contributions based on the geometry of a triad. This is accomplished by measuring the locality function $W(v)$ in Eq.(5.22). Fig.5.4 depicts the locality functions $W(v)$ for the transfer density functions $Q(v)$ shown in Fig.5.3. Approximately 60% of the total energy transfer comes from triad interactions in which the ratio of the smallest wavenumber to the middle is greater than 0.09, 0.13, and 0.17 at $k = 50, 100$, and 200, respectively. In other words, 40% of the total energy transfer involves wavenumber triads in which the smallest wavenumber is less than 0.09, 0.13, and 0.17 of the middle wavenumber at $k = 50, 100$, and 200, respectively. This implies that most of the nonlinear energy transfer exchanges between two wavenumbers with different sizes in the interacting triad. The triad interactions in this case have a high probability to be between wavenumbers triads with

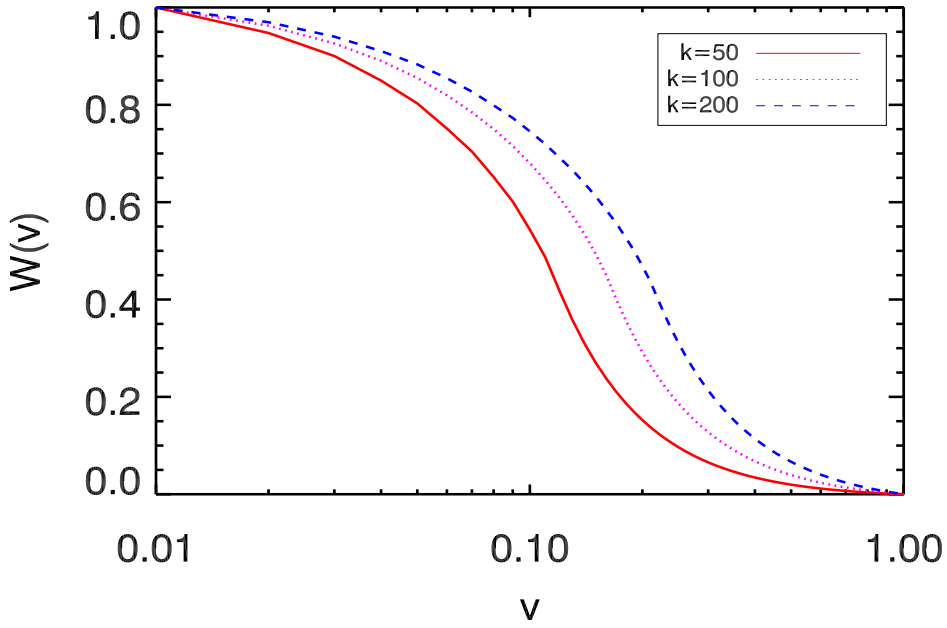

Figure 5.4: The locality-functions $W(v)$ of the energy transfer for $k = 50$ (solid line), $k = 100$ (dotted line), and $k = 200$ (dashed line) in the inertial range of homogenous incompressible 2D-HD turbulence

different size legs. These interactions predominantly occured between one large scale and two small scales in a given triad. These results indicate that the total nonlinear energy transfer in 2D-HD turbulence is nonlocal through nonlocal triad interactions with an inverse cascade direction. The spectral results in this case show that there is no evidence of local transfer or triad interactions between the modes in the inertial range. These results are in good agreement with previous theoretical results of Kraichnan [5]. Kraichnan computed the strength of the energy transfer and triad interactions in 2D-HD turbulence using an "almost Markovian Galilean invariant" turbulence model. He showed that 40% of the total energy transfer involves triads in which the smallest wavenumber is more than one-fifth of the middle wavenumber.

5.2.3 Locality of the enstrophy in 2D-HD turbulence

The locality of the nonlinear enstrophy transfer and nonlinear triad interactions in the inertial range of enstrophy in incompressible 2D-HD turbulence are measured in the same way (that these quantities were measured for energy). In this case the contribution to the enstrophy transfer function associated with the density of the triad interactions is determined. Contributions come from the combined enstrophy transfer rates from modes $\mathbf{p}$ and $\mathbf{q}$ to a third mode $\mathbf{k}$, $k^2 T^{vv}(\mathbf{k}|\mathbf{p},\mathbf{q}) = k^2 T^{vv}(\mathbf{k}|\mathbf{p}|\mathbf{q}) + k^2 T^{vv}(\mathbf{k}|\mathbf{q}|\mathbf{p})$. Fig.5.5 shows the normalized transfer density function $Q(v)$ of the enstrophy for $k = 80$ in the inertial range of the enstrophy spectrum. The function $Q(v)$ is normalized by the rate of enstrophy dissipation $\beta = \nu \int_S dS(\nabla\boldsymbol{\omega})^2$. The graph shows that the locality of the nonlinear transfer of enstrophy is stronger than that of nonlinear energy transfer. Strong local transfer of enstrophy char-

acterized by a strong peak that appears between $v = 0.5$ and 0.8. This implies that the nonlinear enstrophy transfer occurs between two wavenumbers of a given triad that possess nearly similar-size. This indicates that most of the nonlinear enstrophy transfer rates is local in the inertial range. In addition, as in the case of the energy transfer, the $Q(v)$ graph of enstrophy falls to zero for v-values close to zero. Due to the fact that the triangles are elongated in the inertial range, they can not be represented in the square box anymore.
The nonlinear enstrophy is exchanged between three wavenumbers of the interacting triad $(\mathbf{k}, \mathbf{p}, \mathbf{q})$ with $\mathbf{k} = \mathbf{p} + \mathbf{q}$, and $k = |\mathbf{k}|, p = |\mathbf{p}|$, and $q = |\mathbf{q}|$. To determine the type of locality or nonlocality for the triad interactions associated with the enstrophy transfer, the contribution of the combined enstrophy transfer rate $k^2T(\mathbf{k}|\mathbf{p}, \mathbf{q})$ for every wavenumber triad $(\mathbf{k}, \mathbf{p}, \mathbf{q})$ for a fixed $\mathbf{k}$-vector in the inertial range is calculated. Thus the combined enstrophy transfer rate from two modes p and q to the enstrophy in mode k for each v-value in the interval [0,1] is computed. Fig.5.6 shows the normalized contributions of the combined enstrophy transfer rate $k^2T(\mathbf{k}|\mathbf{p}, \mathbf{q})$ for fixed $k = 40, 50$ and 80 in the enstrophy inertial range. The graphs show that most of the nonlinear enstrophy transfer exchanges between wavenumbers of triads interactions at $v \approx 0.06, 0.07$ and 0.09 for $k = 40, 50$ and 80, respectively (here $v < 0.5$) and decreases with v values close to 1. This implies that the magnitudes of interactions for nonlocal triads $k \neq p \neq q$ are larger, while the interactions are small for local triads $k \approx p \approx q$. Thus nonlinear triad interactions occur between three wavenumbers with different sizes in the interacting triad. Most of the total enstrophy has a high probability to transfer between three wavenumbers in the interacting triad with two wavenumbers of similar size that are longer than the third wavenumber ($k \approx p \gg q$, $k \approx q \gg p$, or $p \approx q \gg k$). Thus most nonlinear triad interactions in the enstrophy inertial range is nonlocal (cf. section 3.4). This result indicates that the important triads are elongated in the inertial range. It seems that in such triad interactions the smallest wavenumber acts as a mediator, but does not lose or gain significant enstrophy. Physically, this is consistent with idea that large scale straining of vortex sheets is the mechanism for the enstrophy cascade. One can consider the enstrophy transfer to be local in the sense that enstrophy is transferred only between the two wavenumbers of similar size. Fig.5.6 shows also the enstrophy transfer function $k^2T(\mathbf{k}|\mathbf{p}, \mathbf{q})$ abruptly drops to zero at $v \approx 0.06$. This confirms that the fact which is the nonlinear triads can not be represented in the square box anymore. In addition, Fig.5.6 shows that the combined enstrophy transfer rate is approximately the same for different k-values in the inertial range. Thus the flux of enstrophy is constant, positive and transfers from large scales to small scales (*i.e.,* direct cascade) in the inertial range. Fig.5.7 depicts the locality function $W(v)$ for the function $Q(v)$ was drawn in Fig.5.5. Approximately 60% and 80% of the total enstrophy transfer comes from triad interactions in which the ratio of the smallest wavenumber to the middle is greater than 0.23 and 0.10, respectively. 40% and 20% of the total enstrophy transfer involves wavenumber triads in which the smallest wavenumber is less than one-fifth and one-tenth of the middle wavenumber. This implies that most of nonlinear enstrophy transfer occurs between two wavenumbers of similar size. It is clear that the influence of the large scales may be communicated directly to all scales. In this cascade, information about the forcing scales is gradually lost as enstrophy is transferred in small steps to small scales. The local enstrophy

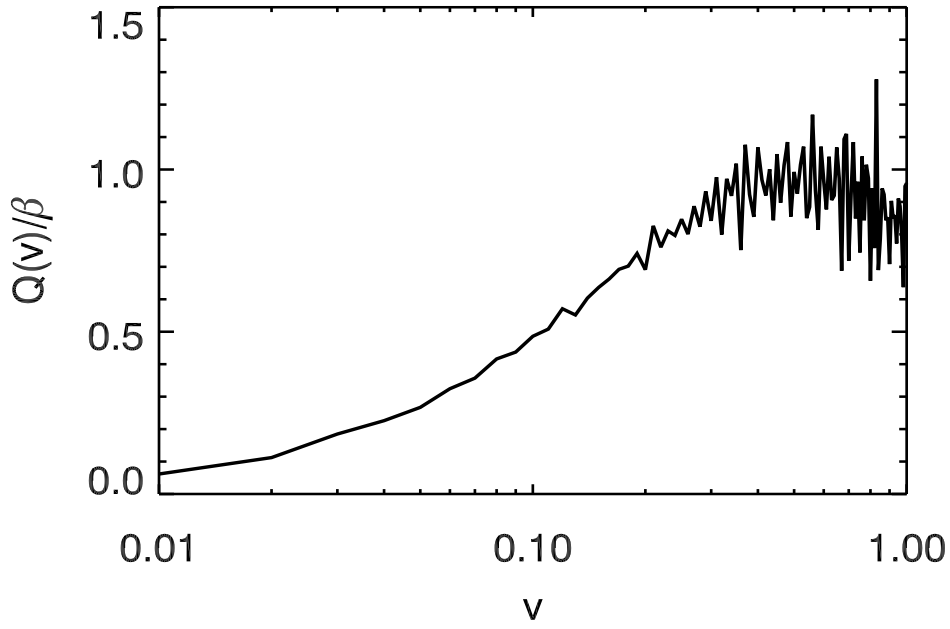

Figure 5.5: Normalized transfer density function $Q(v)$ of enstrophy transfer for $k = 80$ in the inertial range of homogenous incompressible 2D-HD turbulence.

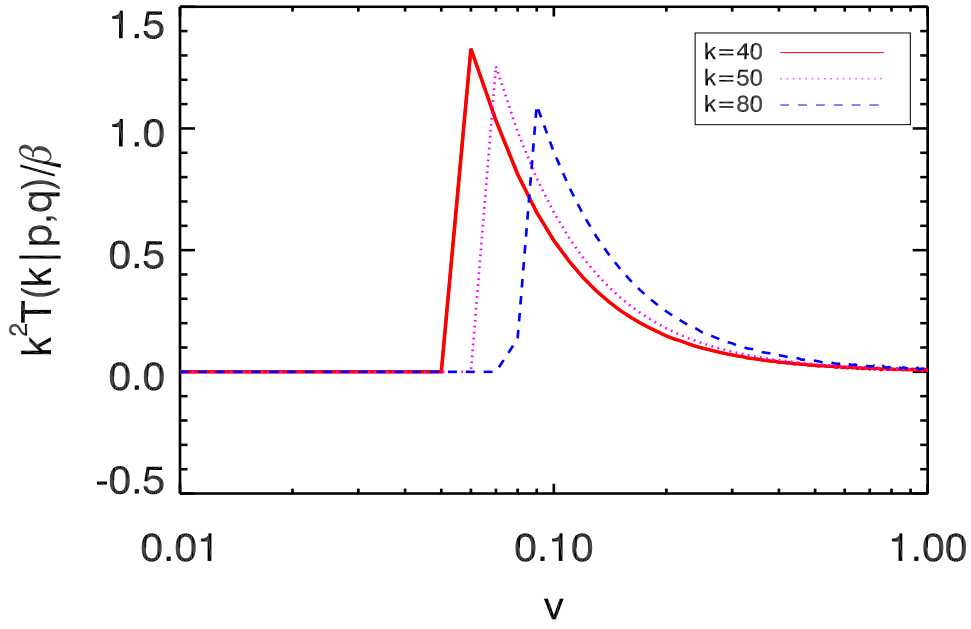

Figure 5.6: Normalized contributions of the combined enstrophy transfer function $k^2 T(\mathbf{k}|\mathbf{p},\mathbf{q})$ for fixed $k = 40, 50$ and 80 in the enstrophy inertial range.

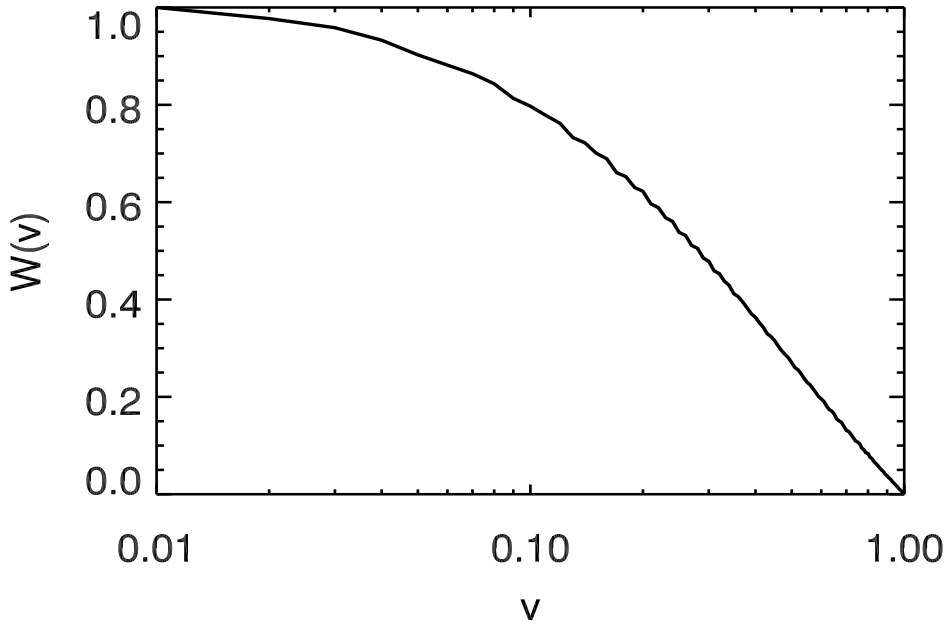

Figure 5.7: The locality-function $W(v)$ of enstrophy transfer for $k = 80$ in the inertial range of homogenous incompressible 2D-HD turbulence.

flux is positive and there is a direct cascade to small scales. These results report that the nonlinear enstrophy transfer in the inertial range of incompressible 2D-HD turbulence is local via nonlocal triad interactions with a direct cascade direction. These reults are in are in good agreement with Maltrud and Vallis [77], they determined the relative importance of the types of wavevector triad interactions that transfer enstrophy in the inertial range using DNS of 2D-HD turbulence. They claimed that the triads are typically elongated and the enstrophy transfer within these triads is directed from large scale to small scales. Our results show that there is a dual cascade with energy cascading to large length scales and enstrophy cascading to small length scales.

In Fig.5.7 approximately 80% of the enstrophy transfer comes from triad interactions in which the ratio of the smallest to the middle wavenumber is greater than 0.10, in contrast to 60% of the energy transfer in the energy inertial range (cf. Fig.5.4). Thus the triads that contribute to the enstrophy transfer are more local than those that contribute to the energy transfer in the energy inertial range in the sense that contributions to the total transfer are significant even as the ratio of the smallest to the middle wavenumber approaches unity. In the next section, the quadratic nonlinearity invariants in incompressible 3D-HD turbulence are discussed, and the spectal properties of their transfer functions, triad interactions, and cascade direction are explained.

5.3 Ideal invariants in 3D-HD turbulence

The nonlinear terms in the vorticity equation (cf. Eq.5.1) include a vortex-stretching term $\boldsymbol{\omega} \cdot \nabla \mathbf{v}$ comparable to that in the 2D-HD case (cf. Eq.5.3). The vortex-stretching term modifies the nonlinear transfer of kinetic energy in the inertial range of 3D-HD turbulence. The vorticity field is stretched in the direction parallel to velocity gradients. This process together with incompressibility and angular momentum conservation leads to an increase of vorticity. According to the Kelvin-Helmholtz theorem, the vorticity flux which is the intensity of the vortex tube is a constant of the motion if the fluid is of uniform density and zero viscosity. If the vortex tube is stretched in such a way that its cross section decreases, its mean vorticity will increase. If one considers a thin vortex tube embedded in turbulence in a slightly viscous flow, it will both be stretched by turbulence, and moved with the fluid particles. One can consider turbulence as a collection of thin vortex tubes stretched by the induced velocity field. This vortex-tube stretching can lead to the formation of regions of space characterized by a high vorticity and high dissipation of kinetic energy. Such a state of the fluid, *i.e.,* highly dissipative structures embedded into an irrotational flow, is called internal intermittency [1]. The DNS results of three dimensional, isotropic, hydrodynamic turbulence have established that the turbulent structures are in fact thin tubes of high vorticity due to the vortex stretching. The phenomenology of vortex-stretching is cannot be applied to 2D-HD case because the vorticity is conserved and no vortex-stretching occurs. This leads to an inverse cascade of kinetic energy (cf. section 5.2 and [2])
Two ideal invariants in three dimensional Navier-Stokes turbulence can be found by neglecting dissipation effect (ν=0) in the set of equations (5.1)-(5.2), kinetic energy and kinetic helicity (cf. section 1.7).

5.3.1 Scaling of energy and kinetic helicity spectra in 3D-HD turbulence

To obtain the spectra of the kinetic energy and kinetic helicity in 3D-HD, the system of 3D Navier-Stokes equations (5.1)-(5.2) is solved on a periodic cube using a standard pseudospectral method with dealiasing according to the 2/3 rule [16]. The simulation has been performed by W.-C. Müller with resolution 1024^3, the dissipation coefficient $\tilde{\nu} = 5.2 \times 10^{-4}$, and the Reynolds number Re ~ 6300.
In the inertial range, both energy and kinetic helicity are cascaded through nonlinear processes. The energy and kinetic helicity spectra in the inertial range depend only on the wavenumbe, k and on the rate of dissipation at which the energy and the helicity are cascaded. Therefore, according to Kolmogorov scaling [40, 41]

$$E^K(k) = C^E \epsilon^{2/3} k^{-5/3}, \qquad H^K(k) = C^{HK} \alpha \epsilon^{-1/3} k^{-5/3}, \tag{5.23}$$

where ϵ is the dissipation rate of kinetic energy, and α is the dissipation rate of the kinetic helicity. C^E and C^{HK} are dimensionless constants.
In Fourier space, the cumulative kinetic energy $E^K(\mathbf{k})$ of incompressible 3D-hydrodynamic turbulence is calculated over spherical shell of radius $k = |\mathbf{k}|$ using Eq.(5.10). Fig.5.8 depicts the compensated kinetic energy spectrum calculated by a DNS of 3D Navier-Stokes turbu-

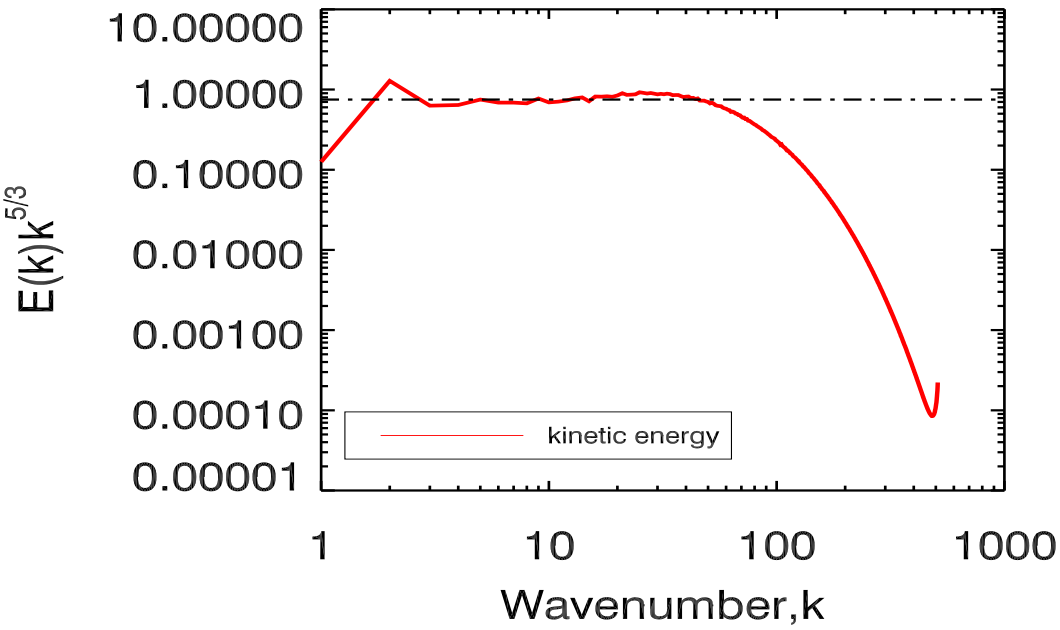

Figure 5.8: Compensated energy spectrum in DNS of 3D-HD turbulence, the horizontal dash-dotted line indicates Kolmogorov-like $k^{-5/3}$ inertial range.

lence. The scaling factor of the energy spectrum agrees with those of the transverse velocity structure functions in the inertial range, consistent with the scaling prediction $E^K(k) \sim k^{-5/3}$ (cf. Eq.5.23). The energy spectrum shows the turbulence is fully-developed inertial range. The spectrum exhibits an inertial range extended over about one decade in wavenumber $3 \lesssim k \lesssim 40$.

The cumulative kinetic helicity $H^K(\mathbf{k})$ in incompressible 3D-hydrodynamic turbulence calculated in Fourier space via the velocity and vorticity by the following equation,

$$H^K(\mathbf{k}) = \omega^*(\mathbf{k}) \cdot \mathbf{v}(\mathbf{k}).$$

The kinetic helicity spectrum is compansated by the same scaling factor $k^{-5/3}$ like energy spectrum to make the inertial range clearly visible. Fig.5.9 depicts the compensated kinetic helicity spectrum from our DNS of 3D Navier-Stokes turbulence. The kinetic helicity spectrum shows the turbulence is fully-developed in the inertial range. It exhibits an inertial range extended in wavenumber $5 \lesssim k \lesssim 50$. Both spectrum of kinetic helicity and the spectrum of energy satsify a $-5/3$ law in the inertial range of 3D Navier-Stokes turbulence. Thus as we will see, there is a joint cascade of the kinetic energy and kinetic helicity to small scales.

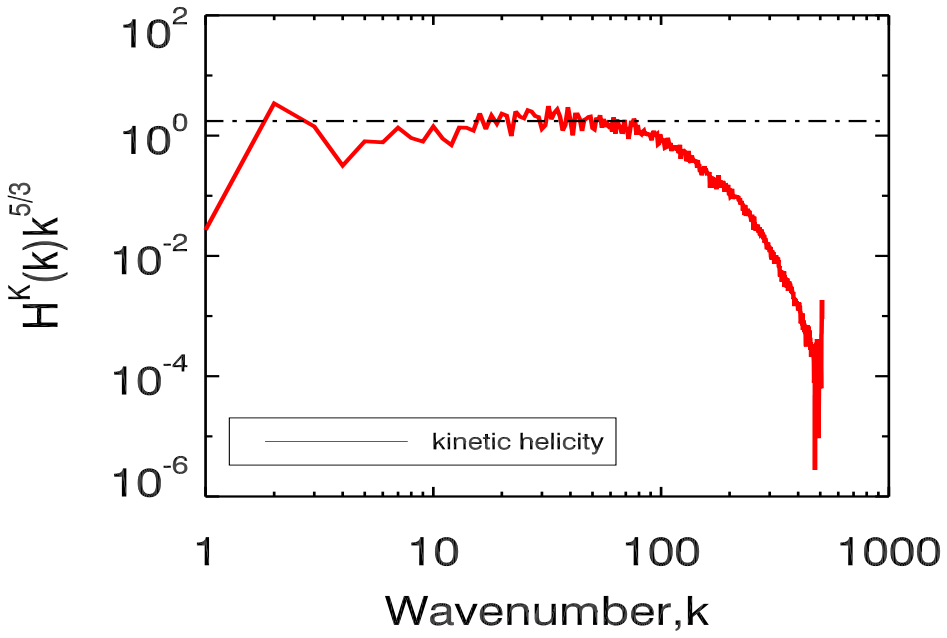

Figure 5.9: Compensated kinetic helicity in DNS of 3D-HD turbulence, the horizontal dash-dotted line indicates the scaling factor in the vicinity of $k^{-5/3}$.

5.4 Nonlinear triad interactions in 3D-hydrodynamic turbulence

5.4.1 $Q(v)$ and $W(v)$ functions in 3D-HD turbulence

The nonlinear terms of 3D Navier-Stokes equations conserves both kinetic energy and the kinetic helicity [2, 58, 78]. To measure the locality of the nonlinear energy transfer function and the triad interactions in the energy inertial range, the same steps used in 2D-HD are repeated. The simulation program is extended from 2D to 3D (cf. section 4.5). The energy is conserved in both 2D and 3D incompressible Navier-Stokes turbulence, thus the detailed conservation of energy in 2D-HD for each triad interaction is also valid in 3D-HD.
To measure the locality of the nonlinear kinetic helicity, the transfer density function $Q(v)$ and locality function $W(v)$ for the kinetic helicity are computed. The kinetic helicity is assumed to be nonzero in our calculation,

$$H^K = \frac{1}{2}\langle \mathbf{v} \cdot \boldsymbol{\omega} \rangle .$$

Both kinetic energy and kinetic helicity are conserved in three dimensions [2, 58]. However, an interesting pattern in the energy transfers among Fourier modes is obtained by focusing on a single triad. For a single interacting triad $(\mathbf{k}, \mathbf{p}, \mathbf{q})$ with $\mathbf{k} + \mathbf{p} + \mathbf{q} = 0$, and $k = |\mathbf{k}|, p = |\mathbf{p}|, q = |\mathbf{q}|$. The evolution equation of kinetic helicity in a triad interaction is

$$\frac{\partial H^K(\mathbf{k})}{\partial t} = \frac{1}{2}\mathcal{R}\left[\boldsymbol{\omega}^*(\mathbf{k}) \cdot \frac{\partial \mathbf{v}(\mathbf{k})}{\partial t} + \mathbf{v}^*(\mathbf{k}) \cdot \frac{\partial \boldsymbol{\omega}(\mathbf{k})}{\partial t}\right] . \tag{5.24}$$

This equation can be written in our triad notation as

$$H^K(\mathbf{k}|\mathbf{p},\mathbf{q}) = H^K(\mathbf{k}|\mathbf{p}|\mathbf{q}) + H^K(\mathbf{k}|\mathbf{q}|\mathbf{p}), \tag{5.25}$$

where

$$H^K(\mathbf{k}|\mathbf{p}|\mathbf{q}) = \frac{1}{2}\Im\left[(\mathbf{k}\cdot\mathbf{v}(\mathbf{q}))\left\{\boldsymbol{\omega}^*(\mathbf{k})\cdot\mathbf{v}(\mathbf{p}) + \boldsymbol{\omega}(\mathbf{p})\cdot\mathbf{v}^*(\mathbf{k})\right\} - (\mathbf{k}\cdot\boldsymbol{\omega}(\mathbf{q}))(\mathbf{v}^*(\mathbf{k})\cdot\mathbf{v}(\mathbf{p}))\right]. \tag{5.26}$$

$\Im$ is the imaginary part. $H^K(\mathbf{k}|\mathbf{p}|\mathbf{q})$ represents the mode-to-mode kinetic helicity transfer from mode $\mathbf{p}$ to mode $\mathbf{k}$ with mode $\mathbf{q}$ acting as a mediator [39]. The sum of transfer rates of kinetic helicity in a triad $(\mathbf{k},\mathbf{p},\mathbf{q})$ in decaying 3D-HD turbulence is zero

$$H^K(\mathbf{k}|\mathbf{p},\mathbf{q}) + H^K(\mathbf{p}|\mathbf{q},\mathbf{k}) + H^K(\mathbf{q}|\mathbf{k},\mathbf{p}) = 0. \tag{5.27}$$

This is equivalent to

$$H^K(\mathbf{k}|\mathbf{p}|\mathbf{q}) + H^K(\mathbf{k}|\mathbf{q}|\mathbf{p}) + H^K(\mathbf{p}|\mathbf{k}|\mathbf{q}) + H^K(\mathbf{p}|\mathbf{q}|\mathbf{k}) + H^K(\mathbf{q}|\mathbf{k}|\mathbf{p}) + H^K(\mathbf{q}|\mathbf{p}|\mathbf{k}) = 0.$$

This result implies that kinetic heicity is conserved in a triad [39, 21], which is also referred to as detailed conservation of kinetic helicity in a triad interaction in decaying 3D-HD turbulence, *i.e.*,

$$H^K(\mathbf{k}) + H^K(\mathbf{p}) + H^K(\mathbf{q}) = \text{const.} \tag{5.28}$$

The detailed conservation of the energy and helicity in 3D-HD turbulence, lead to global conservation of these quantities:

$$\int_0^\infty T(k)dk = 0, \qquad \int_0^\infty H^K(k)dk = 0. \tag{5.29}$$

The kinetic energy is conserved in both 2D and 3D Navier-Stokes turbulence, so the same transfer density function $Q(v)$ which uesd in the 2D case (cf. Eq.5.19 with Eq.3.77), can be used to measure the locality of the energy in the 3D case. Since the kinetic helicity is conserved, the energy and helicity have a joint cascade and their spectra satisfy a $-5/3$ law in the inertial range. By a similar analysis for the kinetic helicity, we obtain the transfer density function $Q(v)$ which serves to measure the locality of kinetic helicity in the inertial range. This function can be derived from the kinetic helicity flux

$$\Pi^{HK}(k) = \alpha\int_0^1 Q(v)\frac{dv}{v} \tag{5.30}$$

where α is the rate of kinetic helicity dissipation.

5.4.2 Locality of the energy in 3D-HD turbulence

The simulation program discussed in subsection 5.3.1 is used to compute the transfer density function $Q(v)$ and the locality function $W(v)$. Thus the locality of kinetic energy in the inertial range of energy spectrum can be measured.

Fig.5.10 shows the normalized transfer density functions $Q(v)$ for chosen k-values in the en-

ergy inertial range (see Fig.5.8). The functions $Q(v)$ are normalized by the rate of kinetic energy dissipation, $\epsilon = \nu \int_V \boldsymbol{\omega}^2 dV$. Fig.5.10 shows that the locality of the kinetic energy is charactericed by three peaks with different amplitudes at v-values are close to 1. The maximum amplitudes appear at approximately $v = 0.7, 0.8$, and 0.85 for $k = 10, 20$, and 30, respectively (note that $v > 0.5$). The inset graphs show a log-log plot of the same normalized transfer density functions. The values of the density functions $Q(v)$ do not vanish at $v = 1$. This means that the energy transfer function $T(\mathbf{k}|\mathbf{p}, \mathbf{q})$ is not zero if any two of the three wavenumbers are equal. This is contrary with the density function of energy in 2D-HD turbulence (cf. Fig.5.3). Thus most of the nonlinear kinetic energy is transferred between two wavenumbers with similar sizes in a given interacting triad. It also indicates that the maximum energy transfer takes place between neighboring wavenumbers. Thus most of the nonlinear kinetic energy transfer is highly local in the energy inertial range of incompressible 3D-HD turbulence.

Fig.5.11 shows the normalized contributions of the combined energy transfer rates $T(\mathbf{k}|\mathbf{p}, \mathbf{q})$ for chosen k in the inertial range (cf. section 3.2). These functions have a maximum amplitudes at $v \approx 0.17, 0.18$ and 0.21 for $k = 10, 20$, and 30, respectively. All graphs fall to zero with v-value close to 1. This implies that the magnitudes of interactions for nonlocal triads $k \approx p \gg q$, $k \approx q \gg p$, or $p \approx \ q \gg k$ are larger than those for local triads $k \approx p \approx q$. Thus most nonlinear triad interactions associated with energy transfer takes place between three wavenumbers with different sizes. Most of these triads have two wavenumbers with similar sizes, longer than the third wavenumber. This indicates that in the triad interaction, the largest scale acts as a mediator only when the energy transfers between the two small scales and the triads are very elongated in the inertial range. Thus triad interactions in 3D-HD energy inertial range are predominantly nonlocal. This result contradicts the classical Kolmogorov phenomenological argument [40], in which Kolmogrov assumed that the energy transferred locally via local triad interactions in the inertial range. Fig.5.10 shows that the strength of the transfer density functions $Q(v)$ increases with k value increases. The kinetic energy is transferred from large scales to small scales with local energy transfer in the energy inertial range. In addition, Fig.5.11 shows that the combined energy transfer rate is approximately the same for different k-values in the inertial range. These results indicates that the flux of the kinetic energy is constant, positive and transfers from large scales to small scales (*i.e,* direct cascade) in the inertial range. The there is no possibility for negative nonlocal flux in the inertial range of homogenous incompressible 3D-HD turbulence. This observation is consistent with recent high Reynolds number simulations such as Mininni *et al.* [79]. Mininni *et al.* reported that the percentage of the nonlocal flux decreases as a power law of the Reynolds number, suggesting that the flux in hydrodynamic turbulence is predominantly local for large Reynolds number. Recent theoretical results of Aluie and Eyink [80] and Eyink and Aluie [81] showed that the energy flux in hydrodynamic turbulence is local in Fourier space in the limit of infinite Reynolds number. They claimed that the energy transfer is dominated by local triad interactions and this in disagreement with our results. Fig.5.12 shows the locality functions $W(v)$ that correspond to the functions $Q(v)$ of Fig.5.10. Approximately 80% of the total energy transfer comes from triad interactions in which the ratio of

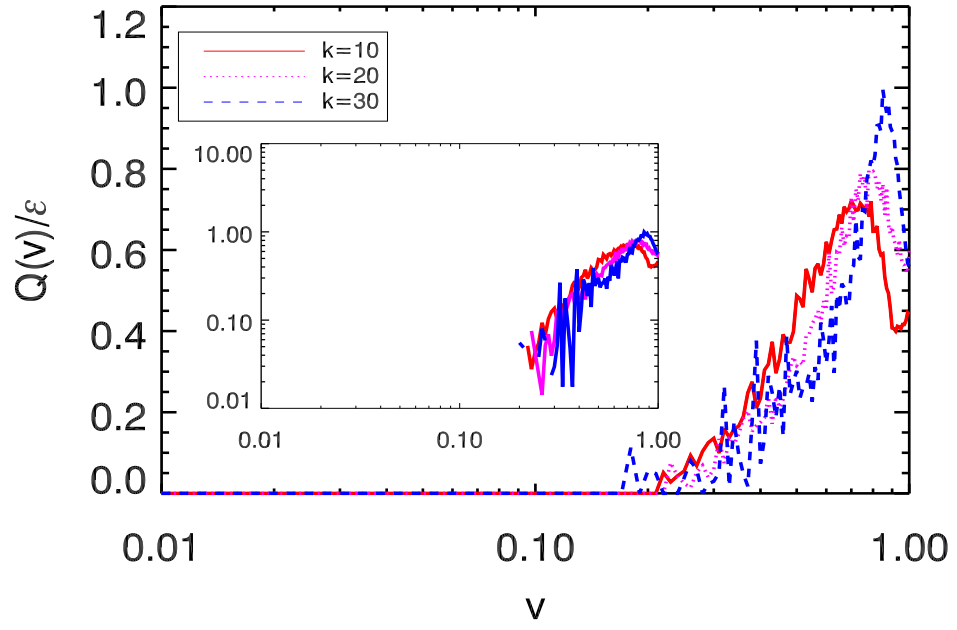

Figure 5.10: Normalized transfer density functions $Q(v)$ of energy transfer for $k = 10$ (solid), 20 (dotted), and 30 (dashed) in the inertial range of homogenous incompressible 3D-HD turbulence. The inset is log-log plot of the same functions.

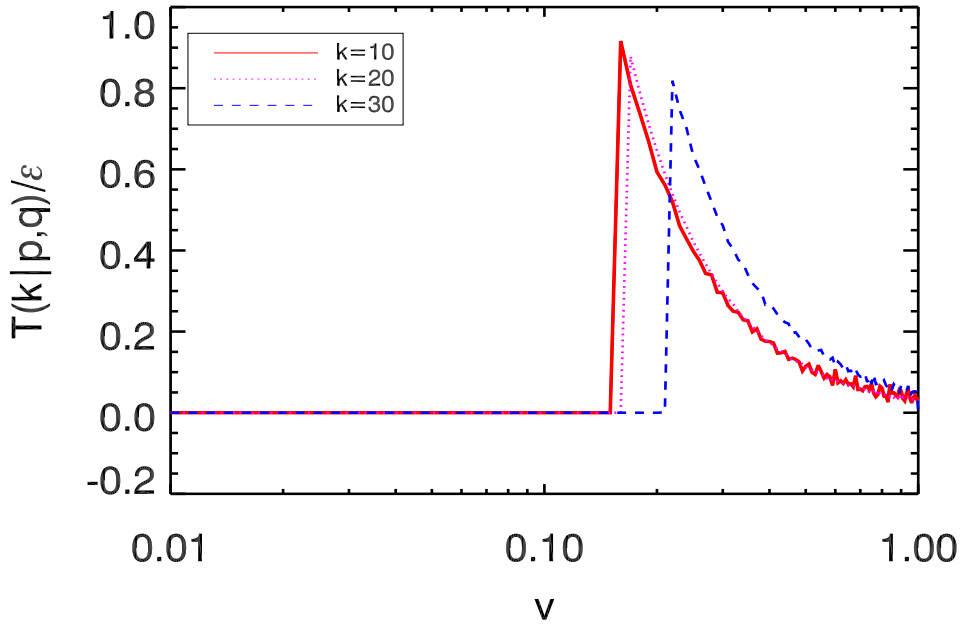

Figure 5.11: Normalized contributions of the combined energy transfer rate $T(\mathbf{k}|\mathbf{p},\mathbf{q})$ for $k = 10$ (solid), 20 (dotted), and 30 (dashed) in the inertial range of homogenous incompressible 3D-HD turbulence.

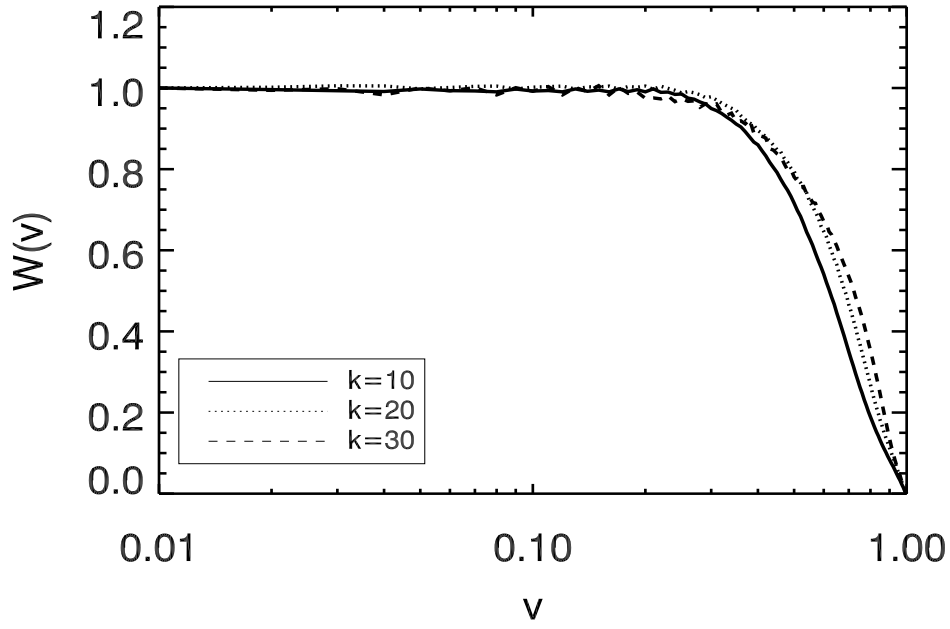

Figure 5.12: The locality functions $W(v)$ of energy transfer for $k = 10$ (solid), 20 (dotted), and 30 (dashed) in the inertial range of homogenous incompressible 3D-HD turbulence.

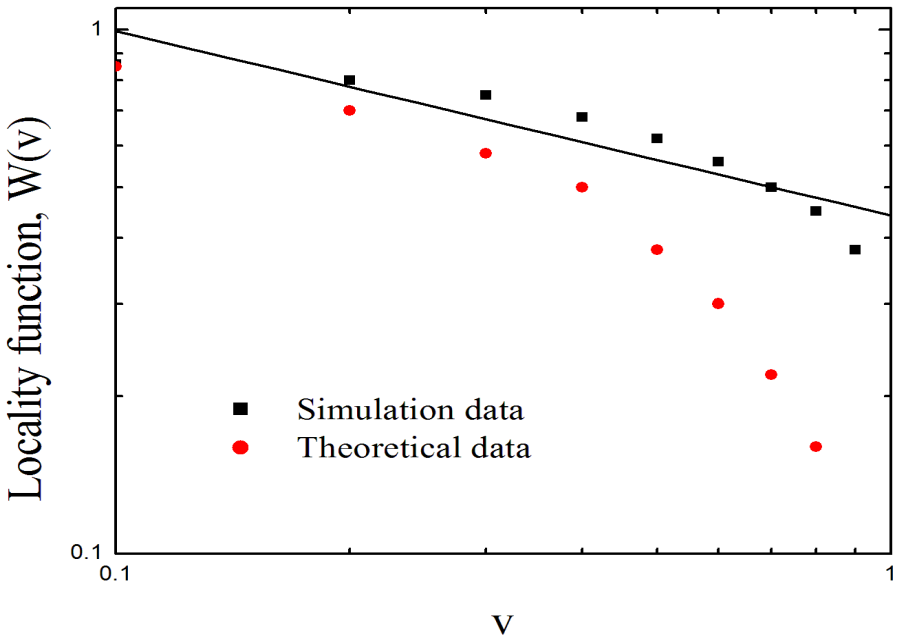

Figure 5.13: Comparison between data from our 1024^3 simulation (black) and Kraichnan's theoretical calculation [5] (red) for the locality function $W(v)$ of energy in 3D-HD turbulence.

the smallest wavenumber to the middle is greater than 0.45, 0.5, and 0.5 for $k = 10, 20$, and 30, respectively. In other words, 20% of the total energy transfer involves wavenumber triads in which the smallest wavenumber is less than 0.45 of the middle wavenumber at $k = 10$ and less than one-half of the middle wavenumber at $k = 20$ and 30. Most of nonlinear energy is transferred between two wavenumbers with similar sizes and the energy is transferred from small wavenumbers to large wavenumbers. Thus the nonlinear energy transfer is predominantly local and exhibits a direct cascade.

Our results in agreement with the established theoretical result of Kraichnan [5], concerning the strength of triad interactions and energy transfers in 2D and 3D fluid turbulence calculated from an "almost Markovian Galilean invariant" turbulence model. Kraichnan showed that in 3D, 35% of the total energy transfer across a unit wavenumber sphere involves triads in which the smallest wavenumber is more than one-half of the middle wavenumber for a given triad. Hence, the energy transfer in 3D fluid turbulence is local. Verma *et al.* [82] also computed the strength of the nonlinear triad interactions and the energy exchange between wavenumbers shells in incompressible 3D fluid turbulence. They used first order perturbative field theory for their computation, they reported that the shell-to-shell energy transfer rate is local with a direct cascade via nonlocal triad interactions. In addition, our results are compatible with the numerical simulations of Domaradzki and Ragallo [7], where they showed that energy transfers in homogenous incompressible 3D fluid turbulence were always local via nonlocal triad interactions. Domaradzki and Ragallo found their numerical results in agreement with an eddy-damped quasi-normal Makrovian (EDQNM)[1] calculation. They conjectured that the observed energy transfer was caused by triads with at least one wavenumber in the energy-containing range. Zhou [83] numerically computed the energy transfers using different wavenumber summation scheme, and found the energy transfers to be local. Waleffe [65] investigated the nonlinear interactions in homogeneous turbulence using a decomposition of the velocity field in terms of helical modes. He reported that the triad energy transfer due to nonlocal interactions is mostly local. Ohkitani and Kida [84] analyzed the triad interactions and concluded that nonlocal interactions were strong, but energy exchanged predominantly between comparable scales. Our results confirm the presence of interactions between disparate scales in a turbulent flow at large Reynolds numbers. Thus our results shed some light on the dynamics of energy transfer, interactions between different scales and a cascade process in a flow which are some fundamental properties of turbulence.

Fig.5.13 depicts a comparison between data from our 1024^3 simulation and Kraichnan's theoretical calculation for the locality function $W(v)$ of the energy in 3D-HD turbulence for all possible ratios $v \leq 1$. Theoretical data from Kraichnan's work is estimated from his results (see, Fig.2 in [5]). Fig.5.13 show that our simulation data has a clear deviation from the classical prediction of Kraichnan which is $W(v) \propto v^{4/3}$ for $v \leq 1$. Our results are shifted upwards from theoretical data, this shift indicates that the influence of the small wavenumbers on the energy transfer to large wavenumbers is equivalent or stronger than that predicted by the classical 4/3 scaling. The prediction of our simulation is $W(v) \propto v^{0.92}$ for $v \leq 1$. This is prediction deviates from DNS results of Domaradzki and Carati [85]. This observation implies

[1] More details about this approximation, see [1, 26].

that the decay of nonlocal contributions in v is even faster than that proved by Eyink [86], where he predicts $W(v) \propto v^{2/3}$ as a rigorous upper bound.

5.4.3 Locality of the kinetic helicity in 3D-HD turbulence

Kinetic helicity is one of two important quadratic invariants of inviscid incompressible 3D fluid turbulence; it plays a role in the dynamics of turbulence. Kinetic helicity is typically present in all rotating fluid systems, *e.g.,* the earth, the sun, and the galaxies. In these astrophysical systems, kinetic helicity generates magnetic fields [87]. Recent numerical calculations of magnetohydrodynamic turbulence showed that kinetic helicity induces additional fluxes of energy and magnetic helicity [70]. Studying the locality of kinetic helicity in incompressible 3D fluid turbulence can provide information about the dynamics of turbulence.
In the following parts of this work, the spectral locality of the nonlinear kinetic helicity transfer function, triad interactions, and type of helicity cascade are studied. To measure the transfer density function $Q(v)$ of kinetic helicity, we determine the strength of the contributions to the kinetic helicity transfer functions. These contributions associated with the density of the triad interactions (*i.e.,* each value of v) coming from the combined kinetic helicity transfer rates from modes belonging to $\mathbf{p}$ and $\mathbf{q}$ to the third one $\mathbf{k}$ as shown in Eq.(5.25) with Eq.(5.26). The kinetic helicity contributions are normalized over the total amount of helicity transfer.
Fig.5.14 shows the normalized transfer density functions $Q(v)$ of the kinetic helicity for k-values $k = 10, 20$, and 30. The functions $Q(v)$ are normalized by the rate of kinetic helicity dissipation, $D_{HK} = \alpha = \nu \int_V dV \boldsymbol{\omega} \cdot (\nabla \times \boldsymbol{\omega})$. Fig.5.14 shows that the transfer density functions of the helicity at k-values have the same behavior as those for kinetic energy in Fig.5.10. The graphs of the functions $Q(v)$ of the helicity are characterized by three peaks with different amplitudes at v-values close to 1. These peaks appear at approximately $v = 0.75, 0.82$, and 0.88 for $k = 10, 20$, and 30, respectively. The positions of the peaks of the transfer density functions of helicity are larger than those for the energy by small values (cf. Fig.5.12). This implies that there is a strong joint between the nonlinear transfer rates of energy and helicity simultaneously in the inertial range. Most of the nonlinear kinetic helicity is transferred between two wavenumbers with similar sizes in a given interacting triad. This implies that the nonlinear kinetic helicity transfer is predominantly local in the inertial range of 3D-HD turbulence. In addition, Fig.5.14 shows that the strength of the transfer density functions $Q(v)$ for helicity increases with k value. The kinetic helicity is transferred from large scales to small scales in the inertial range. Thus the kinetic helicity flux is positive and the nonlinear helicity transfer has a direct cascade in the inertial range of incompressible 3D-HD turbulence. The graphs of the $Q(v)$ are smoother than those found for kinetic energy. Due to the strong joint cascade of both energy and helicity in 3D-HD turbulence, most of the triad interactions associated with helicity transfer is predominantly nonlocal in the inertial range.

Fig.5.15 shows the locality functions $W(v)$ for the nonlinear energy transfer functions at $k = 10, 20$, and 30 in the helicity inertial range. Approximately 80% of the total helicity transfer comes from triad interactions in which the ratio of the smallest wavenumber to the middle is greater than 0.5, 0.6, and 0.7 at $k = 10, 20$, and 30, respectively. Most of nonlinear helicity is transferred between two wavenumbers with similar sizes from small wavenumbers to large wavenumbers. The spectral results for kinetic helicity show that the nonlinear helicity transfer is more local than energy. This result is in contradiction with the result obtained by André and Lesieur [88], which states that the kinetic helicity transfer is less local than the energy transfer in isotropic turbulence at high Reynolds number. Our results of the nonlinear processes of kinetic helicity in isotropic 3D-HD turbulence are in good agreement with the recent works, *e.g.,* the results of Avinash *et al.* [89]. They applied the perturbative field-

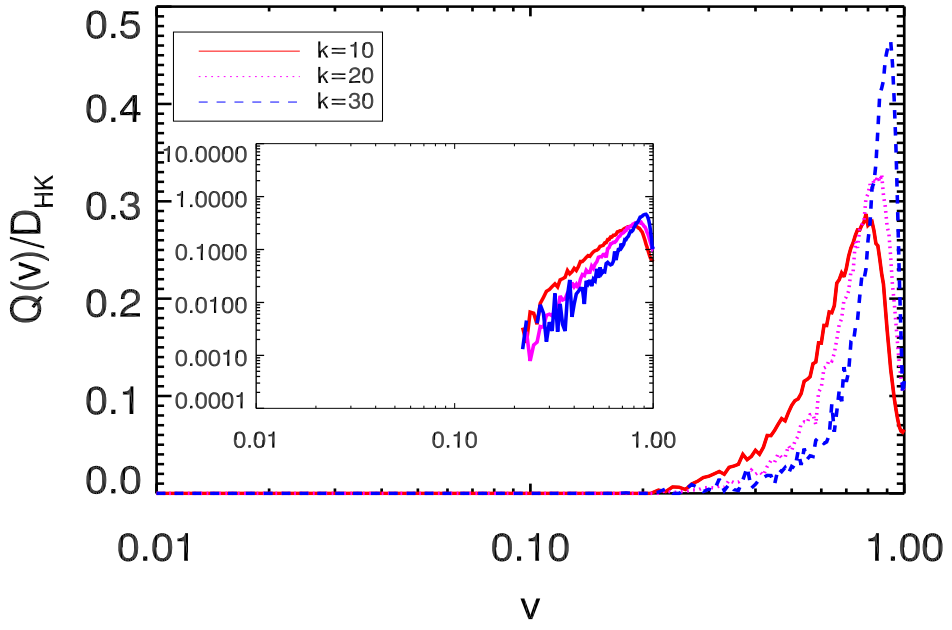

Figure 5.14: Normalized transfer density functions $Q(v)$ of kinetic helicity transfer for $k = 10$ (solid), 20 (dotted), and 30 (dashed) in the inertial range of homogenous incompressible 3D-HD turbulence. The inset is log-log plot of the same functions

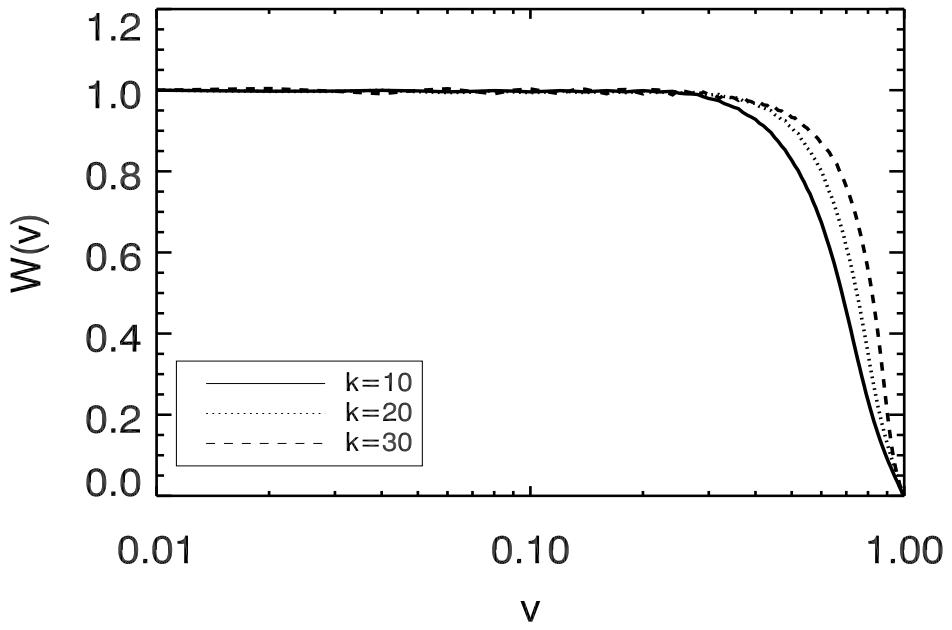

Figure 5.15: The locality functions $W(v)$ of kinetic helicity transfer for $k = 10$ (solid), 20 (dotted), and 30 (dashed) in the inertial range of homogenous incompressible 3D-HD turbulence.

theoretic technique to helical turbulence. They found that the kinetic helicity flux is constant and direct in the inertial range. Chen *et al.* [78] computed the transfer function of both energy and kinetic helicity in 3D-HD turbulence, theoretically. They claimed that there is a joint cascade of both energy and helicity simultaneously to small scales. Our results for the spectral properties of the quadratic nonlinear invariants in both of 2D and 3D-hydrodynamic turbulence are summarized in Table 5.2.

Ideal invariant	Transfer function	Triad interactions	Cascade direction
2D-NS: Energy, E^K	nonlocal	nonlocal	inverse
2D-NS: Enstrophy, Ω	weaker local	nonlocal	direct
3D-NS: Energy, E^K	local	nonlocal	direct
3D-NS: Kinetic helicity, H^K	local	nonlocal	direct

Table 5.2: The spectral properties of the quadratic nonlinear invariants in both of 2D and 3D-hydrodynamic turbulence.

It is important to mention for conclusion, that our approach gives a direct result for the spectral properties of the nonlinear ideal invariants. If the transfer density function $Q(v)$ of a physical quantity has a peak close to one, the transfer of this quantity is local with a direct cascade and the triad interactions are considered as nonlocal (triad interactions occur between two wavenumbers with similar sizes and longer than the third wavenumber in the interacting triad). If the peak of the function $Q(v)$ is close to zero, the transfer is nonlocal with an inverse cascade and the triad interactions are considered as nonlocal (triad interactions occur between three different wavenumbers in the interacting triad). Thus we suggest to apply our approach for different turbulent systems, where it gives a direct results for the spectral properties of these systems.

In the next chapter, the spectral properties of the nonlinear processes for different ideal invariants will be studied both in incompressible isotropic 2D-MHD and isotropic, anisotropic, and forced inverse 3D-MHD turbulence systems.

Chapter 6

Nonlinear triad interactions in magnetohydrodynamic turbulence

Physics of magnetohydrodynamic (MHD) turbulence is more complex than of neutral fluid turbulence. This is because there are two coupled vector fields, velocity and magnetic, and two dissipative parameters, viscosity and resistivity. In addition, when the system is subject to a mean magnetic field $\mathbf{b_0}$, which cannot be transformed away using Galilean transformation, the turbulence becomes anisotropic and thus giving special behavior in different directions. Two-dimensional magnetohydrodynamics (2D-MHD) turbulence is the simplest case of a MHD turbulent system commonly studied. Plasma dynamics in two dimensions can be seen as an approximation to a three-dimensional system with a strong mean magnetic field, because the turbulent dynamics are largely restricted to two-dimensional planes. In this chapter, we begin by treating two-dimensional MHD turbulence simulation without a mean magnetic field. Then isotropic, anisotropic, and forced inverse cascade three-dimensional MHD turbulence systems will be presented. In incompressible MHD turbulence, the nonlinear quadratic invariants are total energy, cross helicity, and mean square magnetic vector potential in the 2D-MHD case. In 3D-MHD case they are total energy, cross helicity, and magnetic helicity. The spectral locality of the transfer functions, triad interactions and the inertial range cascade directions of the ideal invariants in Fourier space are discussed. Both the transfer density function $Q(v)$ and the locality function $W(v)$ are computed. Results are reported for both 2D and 3D-MHD turbulence.

6.1 Ideal invariants in 2D-MHD turbulence

The non-dimensional MHD equations (cf. Eqs.1.38-1.40) are presented in section 1.2. In the 2D-MHD approximation (where $\partial z = 0$), the system of equations can be reduced and written in terms of the vertical vorticity ω and the magnetic field $\mathbf{b}$ [2].

$$\partial_t \omega + \mathbf{v} \cdot \nabla \omega - \mathbf{b} \cdot \nabla j = \hat{\nu} \nabla^2 \omega, \tag{6.1}$$

$$\partial_t \mathbf{b} + \mathbf{v} \cdot \nabla \mathbf{b} = \tilde{\eta} \nabla^2 \mathbf{b}, \tag{6.2}$$

$$\nabla \cdot \mathbf{v} = 0, \quad \nabla \cdot \mathbf{b} = 0. \tag{6.3}$$

Here $j = (\nabla \times \mathbf{b}) \cdot \mathbf{e}_z$ is the current density and $\tilde{\nu}$ and $\tilde{\eta}$ are dimensionless dissipation coefficients related to the kinematic viscosity and magnetic diffusivity, respectively (cf. Eq.1.37). The vorticity and current density are now scalar functions in the direction perpendicular to the xy- plane where turbulent dynamics take place. The magnetic field in the 2D-MHD is usually expressed in terms of one scalar function ψ that corresponds to the modulus of the magnetic vector potential that is perpendicular to the xy-plane. Instead of Eq.(6.2), the following equation for the evolution of this scalar function is used [2]

$$\partial_t \psi + (\mathbf{v} \cdot \nabla)\psi = \tilde{\eta} \nabla^2 \psi. \tag{6.4}$$

The magnetic field and the current density are related to ψ, $\mathbf{b} = \nabla\psi \times \mathbf{e}_z$ and $j = -\nabla^2\psi$, respectively. Eq.(6.4) is an advection-diffusion equation for an active scalar, since ψ influences via the Lorentz force on the time evolution of the velocity field. From the structure of this equation and from the absence of any driving term, clearly ψ decays in time and the magnetic energy is dissipated as well. Therefore, there is no possibility for dynamo action in 2D-MHD [90, 91]. However, it is possible to amplify the magnetic energy during the initial phase when ψ-field is distorted by the velocity field, and may form very steep gradients.
In incompressible 2D-MHD turbulence ($\nu = \eta = 0$), Eqs.(6.1) and (6.4) possess three quadratic nonlinear invariants: the total energy

$$E^{\mathrm{tot}} = E^K + E^M = \frac{1}{2}\int_S dS(v^2 + b^2),$$

the mean square magnetic vector potential

$$A = \frac{1}{2}\int_S dS\psi^2,$$

and the cross helicity

$$H^C = \frac{1}{2}\int_S dS(\mathbf{v} \cdot \mathbf{b}).$$

6.1.1 Spectra of the total energy and mean square magnetic vector potential in 2D-MHD turbulence

To obtain the spectra of energy and mean square magnetic vector potential, the set of Eqs.(6.1)-(6.3) is solved on a 2π-periodic square using a standard pseudospectral method with dealiasing according to the 2/3 rule [16]. The simulation is performed with the resolution 1024^2 (the simulation is conducted by W.-C. Müller and A. Busse). The dissipation coefficients are $\tilde{\nu} = \tilde{\eta} = 5 \times 10^{-4}$, value chosen to obtain the maximal extension of the inertial ranges of both fields. The Reynolds numbers based on the typical velocity $V_0 = (E^K)^{1/2}$ and on the associated length $L_0 = (E^{\mathrm{tot}})^{3/2}/\epsilon$ (ϵ is the total energy dissipation) are approximately $\mathrm{Re} = \mathrm{Rm} \approx 7 \times 10^4$ [2, 4], where

$$\mathrm{Re} \approx \frac{(E^K)^{1/2}(E^{\mathrm{tot}})^{3/2}}{\nu\epsilon}, \qquad \mathrm{Rm} \approx \frac{(E^K)^{1/2}(E^{\mathrm{tot}})^{3/2}}{\eta\epsilon}.$$

This corresponds to magnetic Prandtl number $\mathrm{Pr_m} = 1$ to allow us to achieve a formally symmetric configuration with regard to non-dimensional $\mathbf{v}$ and $\mathbf{b}$ fields. All spectral results presented in the 2D-MHD turbulence case are obtained from this simulation. As discussed in subsection 5.1.1, the kinetic energy in Fourier space is computed from

$$E^K(\mathbf{k}) = \frac{1}{2k^2}\omega(\mathbf{k}) \cdot \omega^*(\mathbf{k}). \tag{6.5}$$

The magnetic energy $E^M(\mathbf{k})$ in Fourier space is computed in terms of the magnetic vector potential $\mathbf{a}$

$$E^M(\mathbf{k}) = \frac{1}{2}\left[\mathbf{a}(\mathbf{k}) \cdot \mathbf{a}^*(\mathbf{k})\right] k^2. \tag{6.6}$$

The magnetic field $\mathbf{b}(\mathbf{k})$ in Fourier space is

$$\mathbf{b}(\mathbf{k}) = i\left[\mathbf{k} \times \mathbf{a}(\mathbf{k})\right],$$

where $\mathbf{b} = \nabla \times \mathbf{a}$. In addition, the mean square magnetic vector potentail $A(\mathbf{k})$ is expressed in terms of the magnetic vector potential $\mathbf{a}$ in spectral space

$$A(\mathbf{k}) = \frac{1}{2}\left[\mathbf{a}(\mathbf{k}) \cdot \mathbf{a}^*(\mathbf{k})\right]. \tag{6.7}$$

The cumulative total energy $E^{\mathrm{tot}}(\mathbf{k}) = E^K(\mathbf{k}) + E^M(\mathbf{k})$ of incompressible decaying isotropic 2D-MHD turbulence is calculated using Eqs.(6.5) and (6.6) for the cumulative kinetic energy $E^K(\mathbf{k})$ and magnetic energy $E^M(\mathbf{k})$, respectively. Kinetic and magnetic energy are injected into the system over a narrow band of large wavenumbers. If no magnetic energy is injected into the system, the inverse cascade could not take place since the mean square magnetic vector potential $\langle A \rangle$ would decrease. Through the energy and mean square magnetic vector potential inertial ranges, these quantities are cascaded nonlinearly to large wavenumbers, where they are dissipated. Furthermore, the spectra of energy and mean square magnetic vector potential in the inertial ranges depend only on the wavenumbers k and on the rate of dissipation. Therefore, the energy and mean square magnetic vector potential have the forms [2, 56]

$$E^{\mathrm{tot}}(k) = C_{IK}(b_0\epsilon)^{1/2}k^{-3/2}, \qquad A(k) = C_A D_A^{2/3} k^{-7/2}.$$

Here b_0 is the magnetic field guide, $\epsilon = \int_S dS(\nu\omega^2 + \eta j^2)$ is the rate of the total energy dissipation, and $D_A = \eta \int_S dS\mathbf{b}^2$ is the rate of the mean square magnetic vector potential dissipation. The dimensionless constants are determined numerically to be $C_{IK} = 1.8$ and $C_A = 2.6$ (see, *e.g.,* [2]).

In Fig.6.1a total energy spectrum of decaying 2D-MHD turbulence is compensated to make the inertial range clearly visible. The spectrum of total energy denoted by the solid line exhibits approximate Iroshnikov and Kraichnan (IK) behavior $E(k) \sim k^{-3/2}$ [43, 25] (see section 2.2). The total energy spectrum shows a well-developed inertial range with an associated scaling exponent of $-3/2$. The initial ratio E^K/E^M is unity. The total energy spectrum exhibits an inertial range extended over $5 \lesssim k \lesssim 20$, see some related work, *e.g,* D. Biskamp [92] and D.

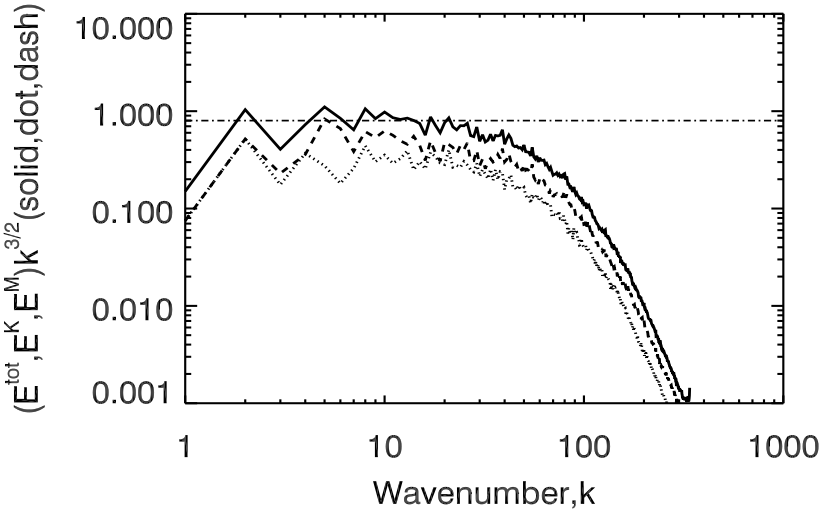

a)

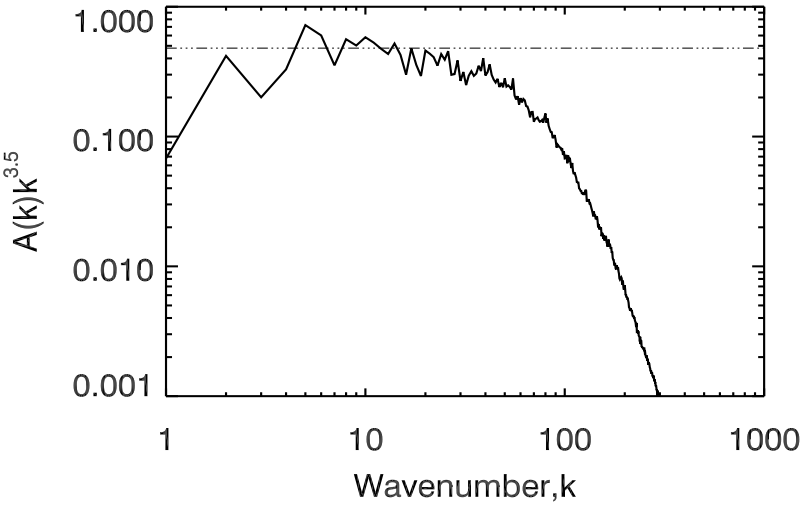

b)

Figure 6.1: a) Compensated energy spectra produced from DNS of 2D-MHD turbulence: total energy (solid line), kinetic energy (dotted line) and magnetic energy (dashed line). The horizontal dash-dotted line indicates an IK-like $\sim k^{-3/2}$ inertial range. b) Compensated mean square magnetic vector potential produced from DNS of 2D-MHD turbulence, the horizontal dash-dotted line indicates the scaling $k^{-3.5}$.

Škandera [93]. The spectra of kinetic energy $E^K(\mathbf{k})$ and magnetic energy $E^M(\mathbf{k})$ exhibit comparable amplitudes and scaling consistent with the IK picture. The validity of this 2D-MHD turbulence phenomenology is somewhat controversial because it neglects anisotropies caused by the magnetic field. However, we find that direct numerical simulation of two dimensional MHD turbulence [92] agree well with established scalings.
Fig.6.1b shows the spectrum of the mean square magnetic vector potential, obtained by computing the cumulative mean square magnetic vector potential of incompressible decaying isotropic 2D-MHD (cf. Eq.6.7). The spectrum is compensated by $k^{-3.5}$. The magnetic potential A exhibits roughly an inertial-range scaling as well. In Fig.6.1b, the horizontal dash-dotted line indicates the scaling $k^{-3.5}$. The scaling exponent is found close to the value -3.5 and the spectrum of the mean square magnetic vector potential has a well-developed inertial range. The spectrum of the mean square magnetic vector potential exhibits an inertial range for wavenumbers $7 \lesssim k \lesssim 20$. In the next section, the spectral properties of the nonlinear processes of the ideal invariants in the 2D-MHD turbulence are discussed.

6.2 Nonlinear triad interactions in 2D-MHD turbulence

6.2.1 Locality of the total energy in 2D-MHD turbulence

The locality of total energy is studied by computing the strength of the nonlinear transfer function and its triad interactions in the inertial range. Both the transfer density function $Q(v)$ and locality function $W(v)$ are computed in the same way as for hydrodynamic turbulence. For a fixed $\mathbf{k}$-vector, various graphs of the distributions of the different shapes of nonlinear triads implicated in the total energy transfer are computed. The contributions to the total energy transfer associated with the density of the triad interactions $(\mathbf{k}, \mathbf{p}, \mathbf{q})$ are determined. We compute the combined kinetic energy transfer from modes belonging to $\mathbf{p}$ and $\mathbf{q}$ to the magnetic energy in the third mode $\mathbf{k}$, $T^{bv}(\mathbf{k}|\mathbf{p}, \mathbf{q})$; also we examine the analogously defined $T^{vv}(\mathbf{k}|\mathbf{p}, \mathbf{q})$, $T^{bb}(\mathbf{k}|\mathbf{p}, \mathbf{q})$, and $T^{vb}(\mathbf{k}|\mathbf{p}, \mathbf{q})$. These functions are computed for the ratio between the smallest and middle wavenumbers, v in the interacting triads. The sum of these quantities gives the total nonlinear energy transfer for each v-value. These contributions are normalized over the total amount of energy transfer using histograms of the total energy transfer for the same arbitrary fixed $\mathbf{k}$-vector in the inertial range.

All spectral results for the transfer density functions $Q(v)$ in this section are obtained by averaging over different independent states of fully developed quasi-stationary turbulence. Fig.6.2a shows the normalized transfer density function $Q(v)$ for a chosen value $k = 10$ in the total energy inertial range. The function $Q(v)$ is normalized by the rate of total energy dissipation $\epsilon = \int_S dS(\nu\omega^2 + \eta j^2)$. The inset graph shows a log-log plot for the normalized transfer density function $Q(v)$. The locality of the nonlinear transfer of the total energy is characterized by a strong peak that appears close to $v = 1$. Because $v \sim 1$ means that two wavenumbers are of the same size, most of the total nonlinear energy transfer takes place between two wavenumbers of similar size and a negligible energy is transferred between wavenumbers with different sizes. Thus the nonlinear energy transfer is predominantly local. Total energy is exchanged between three wavenumbers of the interacting triad $(\mathbf{k}, \mathbf{p}, \mathbf{q})$ with $\mathbf{k} = \mathbf{p} + \mathbf{q}$, and $k = |\mathbf{k}|, p = |\mathbf{p}|, q = |\mathbf{q}|$. To determine the type of triad interactions in which

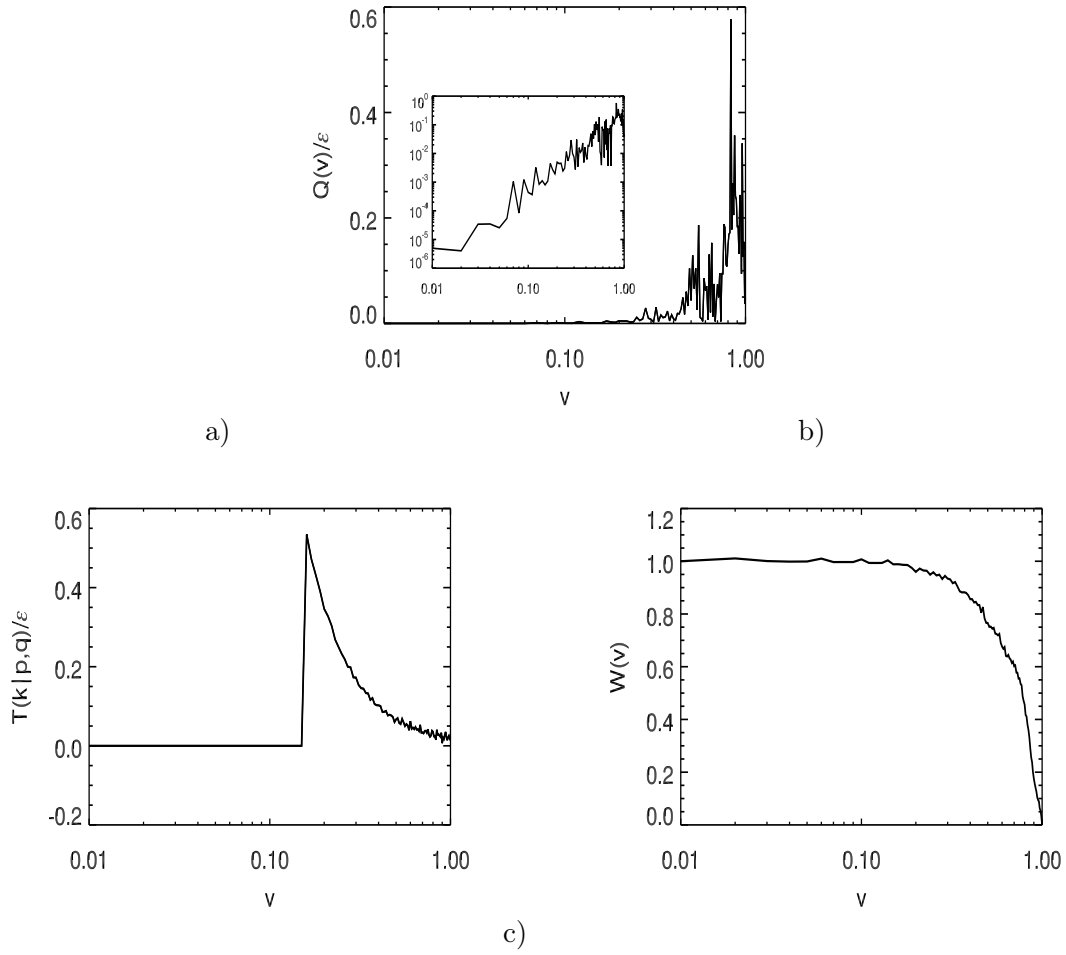

Figure 6.2: a) Normalized transfer density function $Q(v)$ of the total energy transfer in decaying 2D-MHD turbulence. The inset is log-log plot for the same function. b) Normalized contributions of the combined total energy transfer function $T(\mathbf{k}|\mathbf{p},\mathbf{q})$ for $k = 10$ in the inertial range of 2D-MHD turbulence. c) The locality function $W(v)$ of the total energy transfer in decaying 2D-MHD turbulence.

the total energy can be transferred, the contribution from the combined total energy transfer rate for every wavenumber triad for a fixed **k**-vector in the inertial range is computed. Fig.6.2b shows the normalized contributions of the combined total energy transfer rate $T(\mathbf{k}|\mathbf{p},\mathbf{q})$ for $k = 10$ in the inertial range. The function $T(\mathbf{k}|\mathbf{p},\mathbf{q})$ is characterized by a high amplitude peak at $v \approx 0.17$ and falls to zero for v-values close to 1. Thus the highest probabilty of nonlinear total energy is exchanged between three wavenumbers with different sizes in the interacting triad. Most of these triads are formed by two wavenumbers with similar sizes that are longer than the third wavenumber, *i.e.*, $k \approx p \gg q$, $k \approx q \gg p$, or $p \approx q \gg k$. It is likely that the total energy is exchanged only between two similar small scales without affecting the remaing large scale in the interacting triad. The smallest wavenumber in the interacting triad acts as a mediator only between the largest wavenumbers. Thus most of the interacting triads are nonlocal. Note that most of the nonlinear triad interactions associated with total energy transfer appears in the region of $v < 0.5$. In Fig.6.2b, the function $T(\mathbf{k}|\mathbf{p},\mathbf{q})$ abruptly drops to zero to the left of $v \approx 0.15$. This occurs because the nonlinear triads can not be represented

in the square box anymore. The position of the peak of the transfer density function $Q(v)$ in Fig.6.2a indicates that most of the total energy transferred from large scales to small scales in the inertial range. Thus the total energy flux is positive and transferred with a direct cascade. This result is in a agreement with well-established by theoretical results from Pouquet [56]. Pouquet used a statistical model, the eddy-damped quasi-normal Markovian (EDQNM) approximation. She showed that the energy cascades to small scales. Our approach of performing a DNS of the 2D-MHD equations with high resolution leads to a good understanding of the small scale structures of fully-developed turbulence. Fig.6.2c shows the locality function $W(v)$ for the density function $Q(v)$ that is plotted in Fig.6.2a. Approximately 60% of the total energy transfer comes from triad interactions in which the ratio of the smallest to the middle wavenumber is greater than 0.7. Most of the total energy transfer occurs between two wavenumbers of similar size. In addition, this notation indicates that the total energy is transferred from small wavenumbers to large wavenumbers. The total nonlinear energy transfer in decaying 2D-MHD turbulence is local with a direct cascade direction through nonlocal triad interactions. Our results are compatible with Dar *et al.,* [61]. They computed the cascade rates (or flux) and shell-to-shell energy transfers using the formalism of the effective mode-to-mode transfer by DNS in 2D-MHD turbulence (see section 3.3). They showed that the flux of the nonlinear total energy transfer is positive and transferred from large scales to small scales in the inertial range.

6.2.2 Locality of the cross helicity in 2D-MHD turbulence

Cross helicity is a conserved ideal invariant and plays an important role in the dynamics of MHD turbulence [2, 39, 94]. The phenomenon of scale-dependent dynamic alignment is closely related to the conservation of cross helicity. Cross helicity has only recently become an object of systematic study, as it becomes clear that it plays a fundamental role in driven MHD turbulence [95, 94].
Cross helicity is assumed to be nonzero in the inertial range of decaying 2D-MHD

$$H^C = \frac{1}{2} \langle \mathbf{v} \cdot \mathbf{b} \rangle . \tag{6.8}$$

Here $\langle ..... \rangle$ represents the ensemble average. Both total energy and cross helicity are conserved in 2D-MHD turbulence [2, 21, 39]. However, if we focus on a single triad a pattern in the energy transfers among Fourier modes can be obtained. For a single interacting triad $(\mathbf{k}, \mathbf{p}, \mathbf{q})$ with $\mathbf{k} = \mathbf{p} + \mathbf{q}$, and $k = |\mathbf{k}|, p = |\mathbf{p}|, q = |\mathbf{q}|$, the evolution equation of cross helicity in a triad interaction is [39]

$$\frac{\partial H^C(\mathbf{k})}{\partial t} = \frac{1}{2} \mathcal{R} \left[\mathbf{b}^*(\mathbf{k}) \cdot \frac{\partial \mathbf{v}(\mathbf{k})}{\partial \mathbf{t}} + \mathbf{v}^*(\mathbf{k}) \cdot \frac{\partial \mathbf{b}(\mathbf{k})}{\partial \mathbf{t}} \right] . \tag{6.9}$$

This equation can be simplified in our triad notation as

$$H^C(\mathbf{k}|\mathbf{p}, \mathbf{q}) = H^C(\mathbf{k}|\mathbf{p}|\mathbf{q}) + H^C(\mathbf{k}|\mathbf{q}|\mathbf{p}). \tag{6.10}$$

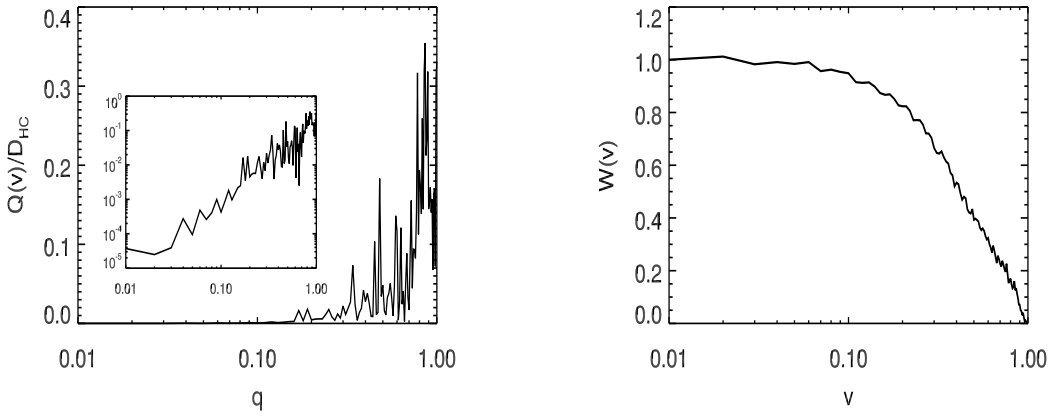

a) b)

Figure 6.3: a) Normalized transfer density function $Q(v)$ of cross helicity for $k = 10$ in the 2D-MHD inertial range. The inset is log-log plot for the same function. b) The locality function $W(v)$ of cross helicity at $k = 10$ in the 2D-MHD inertial range.

where the transfer rate of cross helicity in a triad is

$$H^C(\mathbf{k}|\mathbf{p}|\mathbf{q}) = \frac{1}{2}\Im\left[(\mathbf{k}\cdot\mathbf{v}(\mathbf{q}))\left\{\mathbf{b}^*(\mathbf{k})\cdot\mathbf{v}(\mathbf{p}) + \mathbf{b}(\mathbf{p})\cdot\mathbf{v}^*(\mathbf{k})\right\} - (\mathbf{k}\cdot\mathbf{b}(\mathbf{q}))(\mathbf{v}^*(\mathbf{k})\cdot\mathbf{v}(\mathbf{p}))\right]. \tag{6.11}$$

This formula stands for the mode-to-mode cross helicity transfer from mode $\mathbf{p}$ to mode $\mathbf{k}$ with mode $\mathbf{q}$ acting as a mediator [39]. Here $\Im$ represents the imaginary part of the argument. The sum of transfer rates of cross helicity in a triad $(\mathbf{k}, \mathbf{p}, \mathbf{q})$ is zero

$$H^C(\mathbf{k}|\mathbf{p}|\mathbf{q}) + H^C(\mathbf{k}|\mathbf{q}|\mathbf{p}) + H^C(\mathbf{p}|\mathbf{k}|\mathbf{q}) + H^C(\mathbf{p}|\mathbf{q}|\mathbf{k}) + H^C(\mathbf{q}|\mathbf{k}|\mathbf{p}) + H^C(\mathbf{q}|\mathbf{p}|\mathbf{k}) = 0. \tag{6.12}$$

This is the detailed conservation of cross helicity, which implies that cross helicity is conserved in a triad [39, 21], *i.e.,*

$$H^C(\mathbf{k}) + H^C(\mathbf{p}) + H^C(\mathbf{q}) = \text{const.} \tag{6.13}$$

The locality of cross helicity is measured using an analysis similar to that discussed above for the total energy. Fig.6.3a shows the normalized transfer density function $Q(v)$ of the nonlinear cross helicity transfer for $k = 10$ in the inertial range. The density function is normalized by the rate of cross helicity dissipation $D_{HC} = -\frac{\nu+\eta}{2}\int_S dS(\mathbf{j}\cdot\boldsymbol{\omega})$. The locality of the cross helicity transfer function is characterized by a strong peaks close to $v \approx 1$. Most of the nonlinear cross helicity is transferred between two wavenumbers with similar sizes. Thus most of the nonlinear cross helicity transfer is local in the inertial range. Also, Fig.6.3a shows that the behavior of the cross helicity dynamics is similar to that of the total energy. The positions of the peaks indicate that most of the nonlinear cross helicity is transferred from large scales to small scales. This implies that the cross helicity transfer has a direct cascade. In addition, most of the nonlinear triads associated with cross helicity transfer is formed by two wavenumbers with similar sizes, longer than the third wavenumber, *i.e.,* $k \approx p \gg q$, $k \approx q \gg p$, or $p \approx q \gg k$. Thus most of the interacting triads are nonlocal in the inertial

range. Fig.6.3b shows the locality function $W(v)$ for the transfer density function $Q(v)$ of the cross helicity in the inertial range. Approximately 40% of the cross helicity transfer involves wavenumber triads in which the smallest wavenumber is less than 0.40 of the middle wavenumber. This implies that most of the cross helicity is transferred locally between two wavenumbers with similar legs through nonlocal triad interactions. In Fig.6.2c approximately 60% of the total energy transfer comes from triad interactions in which the ratio of the smallest to the middle wavenumber is greater than 0.7, in contrast to 25% of the cross helicity transfer in the inertial range (cf. Fig.6.3b). This is because the cross helicity decays more slowly than energy in the inertial range. There is a strong local alignment between the velocity fields and magnetic field, so the cross helicity plays an important role in dynamo action. Our calculation supports the results obtained by Hattori [96], who studied the alignment structure of 2D-MHD turbulence using DNS with high resolution.

6.2.3 Locality of the mean square magnetic vector potential in 2D-MHD turbulence

The enstrophy as well as the energy is an ideal invariant of 2D-HD turbulence due to the lack of vortex stretching. As a result, the energy is transferred from small to large scale (inverse cascade direction) as mentioned in section 5.2. In 2D-MHD turbulence, a magnetic field allows the possibility of generation of vorticity by the Lorentz force, breaking the conservation of enstrophy [56]. The mean square magnetic vector potential becomes an ideal invariant in 2D-MHD turbulence. The spectral locality of the mean square magnetic vector potential in its inertial range is measured by using our approach.
The nonlinear terms of the set of equations of incompressible decaying 2D-MHD (cf. Eqs.6.1-6.3) conserve the total energy and the mean square magnetic vector potential [56]

$$E^{\rm tot} = \int_0^\infty (E^K(k) + E^M(k))dk. \tag{6.14}$$

and

$$A = \int_0^\infty k^{-2} E^M(k)dk. \tag{6.15}$$

The total energy and the mean square magnetic vector potential satisify detailed conservation for each triad interaction

$$T(\mathbf{k}|\mathbf{p},\mathbf{q}) + T(\mathbf{p}|\mathbf{q},\mathbf{k}) + T(\mathbf{q}|\mathbf{k},\mathbf{p}) = 0, \tag{6.16}$$

$$k^{-2}T^{bb}(\mathbf{k}|\mathbf{p},\mathbf{q}) + p^{-2}\,T^{bb}(\mathbf{p}|\mathbf{q},\mathbf{k}) + q^{-2}\,T^{bb}(\mathbf{q}|\mathbf{k},\mathbf{p}) = 0. \tag{6.17}$$

Here $T(\mathbf{k}|\mathbf{p},\mathbf{q})$ in Eq.(6.16) is the combination of the total energy transfer from modes $\mathbf{p}$ and $\mathbf{q}$ to mode $\mathbf{k}$. The global conservation of the total energy and mean square magnetic vector potential implies:

$$\int_0^\infty T(k)dk = 0, \qquad \int_0^\infty k^{-2}T^{bb}(k)dk = 0. \tag{6.18}$$

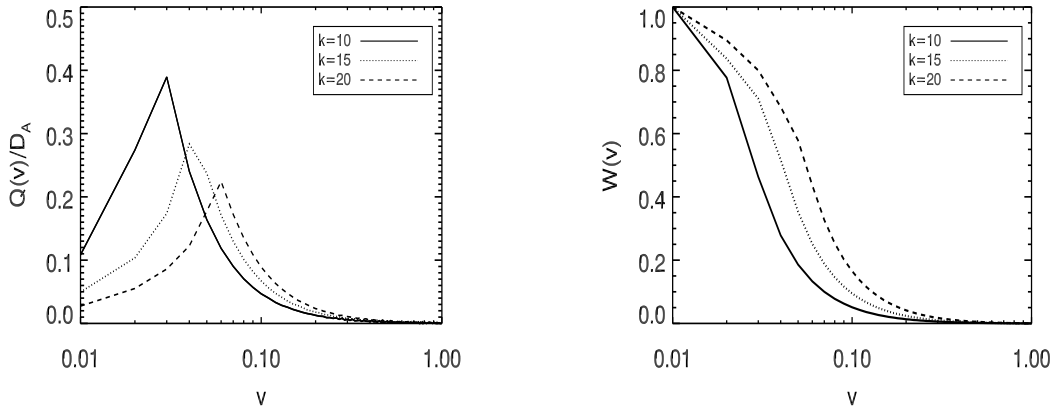

a) b)

Figure 6.4: a) Normalized density transfer functions $Q(v)$ of the mean square magnetic vector potential for $k = 10, 15$, and 20 in the inertial range of 2D-MHD turbulence. b) The locality functions $W(v)$ for the density functions in (a).

Following the detailed properties of the energy transfer rate for each triad [39], the detailed properties of the mean square magnetic vector potential transfer rate can be derived

$$A(\mathbf{k}|\mathbf{p},\mathbf{q}) = k^{-2}\,T^{bb}(\mathbf{k}|\mathbf{p},\mathbf{q}). \tag{6.19}$$

This equation represents the nonlinear term of combined mean square magnetic vector potential transfer rate from two modes $\mathbf{p}$ and $\mathbf{q}$ to mode $\mathbf{k}$, which can be split into a sum of two terms

$$A(\mathbf{k}|\mathbf{p},\mathbf{q}) = \mathrm{A}(\mathbf{k}|\mathbf{p}|\mathbf{q}) + \mathrm{A}(\mathbf{k}|\mathbf{q}|\mathbf{p}) = k^{-2}\,T^{bb}(\mathbf{k}|\mathbf{p}|\mathbf{q}) + k^{-2}\,T^{bb}(\mathbf{k}|\mathbf{q}|\mathbf{p}). \tag{6.20}$$

The first nonlinear term on the r.h.s. of Eq.(6.20) gives the rate of the mean square magnetic vector potential transfer from the mode $\mathbf{p}$ to mode $\mathbf{k}$ through the mediator $\mathbf{q}$. The second term gives the rate of the mean square magnetic vector potential transfer from the mode $\mathbf{q}$ to mode $\mathbf{k}$ via the mediator $\mathbf{p}$. Each of these nonlinear terms is called mode-to-mode mean square magnetic vector potential transfer. The sum of transfer rates of the mean square magnetic vector potential in a triad is zero, *i.e.,*

$$k^{-2}T^{bb}(\mathbf{k}|\mathbf{p}|\mathbf{q})+k^{-2}\,T^{bb}(\mathbf{k}|\mathbf{q}|\mathbf{p})+p^{-2}\,T^{bb}(\mathbf{p}|\mathbf{k}|\mathbf{q})+p^{-2}\,T^{bb}(\mathbf{p}|\mathbf{q}|\mathbf{k})+q^{-2}\,T^{bb}(\mathbf{q}|\mathbf{k}|\mathbf{p})+q^{-2}\,T^{bb}(\mathbf{q}|\mathbf{p}|\mathbf{k}) = 0. \tag{6.21}$$

Eq.(6.21) expresses that the mean square magnetic vector potential is conserved in a given triad, which is also referred to as detailed conservation of the mean square magnetic vector potential in a triad interaction

$$A(\mathbf{k}) + A(\mathbf{p}) + A(\mathbf{q}) = \text{const.} \tag{6.22}$$

The locality of the mean square magnetic vector potential transfer is measured by computing the transfer density function $Q(v)$ and the locality function $W(v)$. More details for the mean

square magnetic vector potential transfer density and locality functions, see Appendix B. Fig.6.4a shows the normalized transfer density functions $Q(v)$ of the mean square magnetic vector potential for k-values in the inertial range (see Fig.6.1b). The density functions are normalized by the rate of the mean square magnetic vector potential dissipation $D_A = \eta \int_S dS\mathbf{b}^2$. $Q(v)$ is characterized by three peaks with different amplitude at v-values close to zero: $v = 0.03, 0.035$, and 0.06 for $k = 10, 15$, and 20, respectively. Most of the interacting triads are in the region of $v < 0.5$. Thus mean square magnetic vector potential is transferred between two wavenumbers of the interacting triad with different sizes. In addition, the most probability of the mean square magnetic vector potential is exchanged between three wavenumbes with different sizes in the interacting triad. Most of the transfer takes place between one large scale and two small scales in the interacting triad. The transfer of the mean square magnetic vector potential is predominantly nonlocal with nonlocal triad interactions (cf. section 3.4). Fig.6.4a shows that the amplitude of the density functions $Q(v)$ increases with v value close to zero and decreasing k-value. The cascade rate of the mean square magnetic vector potential is negative and transferred from small scales to large scales in the inertial range, *i.e,* the mean square magnetic vector potential has an inverse cascade. Fig.6.4b shows the locality functions $W(v)$ that correspond to the density functions $Q(v)$ of Fig.6.4a. Approximately 60% of the total mean square magnetic vector potential transfer comes from triad interactions in which the ratio of the smallest wavenumber to the middle is greater than 0.025, 0.035, and 0.048 for $k = 10, 15$, and 20, respectively. The mean square magnetic vector potential is transferred from large wavenumbers to small wavenumbers with nonlocal transfer through nonlocal triad interactions in the inertial range of 2D-MHD turbulence. These results also agree with the work of Pouquet [56]. Pouquet suggested that the mean square manetic potential is transferred from small scales to large scales (*i.e.,* an inverse cascade) using the EDQNM closure approximation. The locality functions for the total energy, cross helicity, and squared magnetic potential (cf. Figs.6.2c, 6.3b and 6.4b) show that the triads that contribute to the total energy and cross helicity transfer are more local than triads that contribute to the mean squared potential in the inertial range, especially for v close to 1.

Our results for the spectral properties of the nonlinear ideal invariants in the inertial range of decaying 2D-MHD turbulence are summarized in Table 6.1.

Ideal invariant	Transfer function	Triad interactions	Cascade direction
Total energy, E^{tot}	local	nonlocal	direct
Cross helicity, H^C	local	nonlocal	direct
Mean square magnetic vector potential, A	nonlocal	nonlocal	inverse

Table 6.1: The spectral properties of nonlinear ideal invariants in the inertial range of incompressible 2D-MHD turbulence.

Our approach toward the transfer density function and locality function is a direct technique to shed light on the nature of transfer functions, triad interactions, and small scale structure of fully developed turbulence. In the next part of this work, the spectral properties for different quadratic nonlinear invariants in incompressible 3D-MHD turbulence will be studied.

6.3 Nonlinear triad interactions in 3D-MHD turbulence

Motions of plasma in 3D-MHD are not restricted to a two-dimensional plane as in the setup studied in section 6.1, so the turbulent flow is able to explore the third direction dragging the magnetic field with it. Thus magnetic field becomes twisted and stretched, receiving energy from the velocity field. Such motions are supposed to be responsible for an amplification of magnetic energy, a process called a turbulent dynamo. This work does not focus on the amplification process itself, but investigates the dynamics of the nonlinear processes of incompressible 3D-MHD turbulence.

6.3.1 Conservative forms of the nonlinear terms and ideal invariants in 3D-MHD turbulence

From the structure of the individual MHD equations in the set of Eqs.(1.32)-(1.36), the nonlinear dynamics, especially of the magnetic field, differs in three dimensional MHD from the two-dimensional case. It is therefore important from the point of view of nonlinear dynamics to recall the main consequence of this difference. The nonlinear terms from the equation for velocity fluctuations (cf. Eq.1.32) multiplied by $\mathbf{v}$ can be expressed as

$$\mathbf{v}\cdot\left[-\mathbf{v}\left(\mathbf{v}\cdot\nabla\right)\mathbf{v}+\mathbf{j}\times\mathbf{b}\right]=-\mathbf{v}\cdot\left[\left(\mathbf{v}\cdot\nabla\right)\mathbf{v}\right]-\frac{1}{2}\nabla\cdot\left(\mathbf{b}^2\mathbf{v}\right)+\mathbf{v}\cdot\left[\left(\mathbf{b}\cdot\nabla\right)\mathbf{b}\right]. \tag{6.23}$$

where,

$$\begin{aligned}-\mathbf{v}\cdot\left[\left(\mathbf{v}\cdot\nabla\right)\mathbf{v}\right]&=-\frac{1}{2}\nabla\cdot\left(\mathbf{v}^2\mathbf{v}\right),\\ \mathbf{v}\cdot\left[\left(\mathbf{b}\cdot\nabla\right)\mathbf{b}\right]&=\nabla\cdot\left(\mathbf{v}\cdot\mathbf{bb}\right)-\mathbf{b}\cdot\left[\left(\mathbf{b}\cdot\nabla\right)\mathbf{v}\right].\end{aligned} \tag{6.24}$$

Similarly, the nonlinear term from the equation for magnetic field fluctuations (cf. Eq.1.33) multiplied by $\mathbf{b}$ can be also reformulated

$$\mathbf{b}\cdot\left[\nabla\times\left(\mathbf{v}\times\mathbf{b}\right)\right]=\mathbf{b}\cdot\left[\left(\mathbf{b}\cdot\nabla\right)\mathbf{v}\right]-\mathbf{b}\cdot\left[\left(\mathbf{v}\cdot\nabla\right)\mathbf{b}\right]. \tag{6.25}$$

where,

$$\begin{aligned}-\mathbf{b}\cdot\left[\left(\mathbf{v}\cdot\nabla\right)\mathbf{b}\right]&=-\frac{1}{2}\nabla\cdot\left(\mathbf{b}^2\mathbf{v}\right),\\ \mathbf{b}\cdot\left[\left(\mathbf{b}\cdot\nabla\right)\mathbf{v}\right]&=\nabla\cdot\left(\mathbf{v}\cdot\mathbf{bb}\right)-\mathbf{v}\cdot\left[\left(\mathbf{b}\cdot\nabla\right)\mathbf{b}\right].\end{aligned} \tag{6.26}$$

The above relations imply an important difference with respect to the two-dimensional case. Over a period of long-term evolution, the magnetic field can gain energy from the velocity field through the magnetic field stretching term on the l.h.s. of Eq.(6.26). The equation for the magnetic potential contains a source of stretching term, so it cannot be expressed in the form of an advection-diffusion equation as in the two-dimensional case. The second term on the r.h.s. of Eq.(6.26) is identical to the term on the l.h.s. of Eq.(6.24). Therefore, the terms that exchange energy, *i.e.,* the terms on the l.h.s. of Eqs.(6.24) and (6.26), summed together can be expressed in a divergence form. This means that the energy is exchanged between the velocity and the magnetic field, and is conserved during this process. Moreover, in the limit of infinite electrical conductivity, the magnetic flux through a surface moving with the fluid

remains constant and magnetic field is "frozen into" the velocity field [97, 98].
In the case of pure magnetohydrodynamics, there exist three ideal invariants: the total energy, cross helicity, and magnetic helicity (cf. subsection 1.7.2).

6.3.2 Energy spectra of isotropic and anisotropic 3D-MHD turbulence

The scaling of the energy spectra of incompressible isotropic and anisotropic 3D-MHD turbulence is obtained by analyzing data from pseudospectral DNS conducted by W.-C. Müller. This is acomplished by extending the program which used for analysis in the case of 2D-MHD to 3D-MHD (cf. section 4.5). In the decaying isotropic case, the simulation is performed using a high-resolution DNS (512^3 grid points). The dissipation coefficients are $\tilde{\mu} = \tilde{\eta} = 3 \times 10^{-4}$. The Reynolds numbers are approximately $\mathrm{Re} = \mathrm{Rm} \approx 3300$, and magnetic Prandtl number $\mathrm{Pr_m} = 1$. Initially the ratio E^K/E^M is unity so that we treat a formally symmetric configuration with regard to velocity and magnetic fields.
Fig.6.5 depicts the compensated energy spectra in DNS of decaying isotropic 3D-MHD turbulence. The horizontal dash-dotted line indicates a Kolmogorov-like $\sim k^{-5/3}$ inertial range. The total energy spectrum shows the turbulence in this case is fully-developed as well as a region of wavenumbers that correspond to the self-similar $-5/3$ - inertial range, this in agreement with solar wind measurements (see, *e.g.,* [38]). The same observation has been obtained in previous related work (see, *e.g.,* [35, 68]. The spectrum of total energy exhibits an inertial range for wavenumbers $k \approx (4 - 28)$.

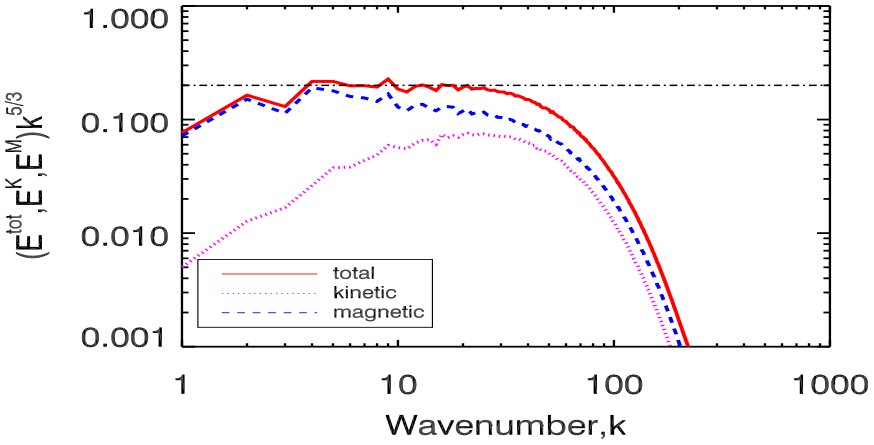

Figure 6.5: Compensated energy spectra from DNS of decaying isotropic MHD turbulence: total energy (solid line), kinetic energy (dotted line), and magnetic energy (dashed line). The horizontal dash-dotted line indicates a Kolmogorov-like $\sim k^{-5/3}$ inertial range.

In case of incompressible anisotropic 3D-MHD turbulence, a $1024^2 \times 256$ grid points pseudospectral forced turbulence simulation with an imposed constant mean magnetic filed of strength $b_0 = |\mathbf{b_0}| = 5$ in units of the large-scale rms (root mean square) magnetic field $b_{\mathrm{rms}} = v_{\mathrm{rms}} \approx 1$ conducted by W.-C. Müller is carried out. The simulation is performed with dissipation coefficients $\tilde{\mu} = \tilde{\eta} = 9 \times 10^{-5}$. A strongly anisotropic system is generated due to the depletion of small scale turbulent fluctuations along the mean magnetic field $\mathbf{b_0}$. This allows for reduced numerical resolution along the corresponding axis. The forcing

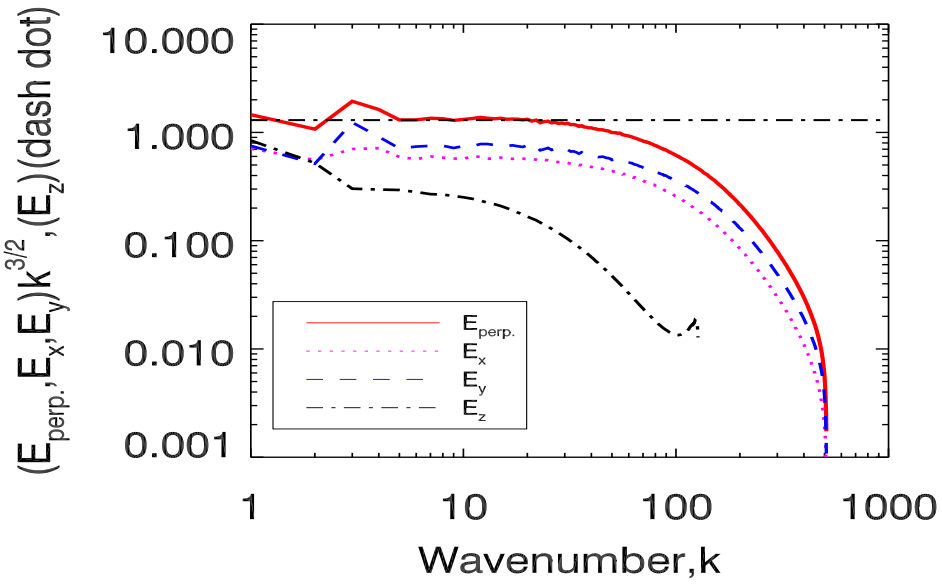

Figure 6.6: Compensated total energy spectrum in field-perpendicular (solid line), total energy in x-direction (dotted line), total energy in y-direction (dashed line), and total energy spectrum in field-parallel (dash-dotted line) produced by DNS of 3D-MHD turbulence with a strong mean magnetic field. The dash-dotted line indicates IK-like scaling $\sim k^{-3/2}$.

keeps the ratio of fluctuations to mean field approximately constant. The cumulative total energy in different directions is computed. The compensated field-perpendicular and parallel spectra for the kinetic and magnetic energy are measured, which are defined as; $E(k_\perp) = \int d\mathbf{k}' \delta(|\mathbf{k}'_\perp| - k_\perp)(|\hat{\mathbf{v}}(\mathbf{k}')|^2 + |\hat{\mathbf{b}}(\mathbf{k}')|^2)$ and $E(k_\parallel) = \int d\mathbf{k}' \delta(|\mathbf{k}'_\parallel| - k_\parallel)(|\hat{\mathbf{v}}(\mathbf{k}')|^2 + |\hat{\mathbf{b}}(\mathbf{k}')|^2)$ (where $k_\perp = (k_x^2 + k_y^2)^{1/2}$ and $k_\parallel = |k_z|$). Iroshnikov [43] and Kraichnan [25] postulated that the time-scale for the nonlinear interactions of incompressible anisotropic MHD turbulence is proportional to the mean magnetic field strength $\mathbf{b_0}$. This leads to the Iroshnikov and Kraichnan energy spectrum of incompressible anisotropic MHD turbulence (IK)-like scaling $\sim k^{-3/2}$ (cf. section 2.2). The IK scaling is well-established for $E_\perp$ (see, [35, 50, 51, 99]). Fig.6.6 depicts the compensated total energy spectra in one-dimensional parallel and perpendicular to the mean magnetic field. The kinetic and magnetic energy as well as the ratio E^K/E^M are approximately unity. Müller and Grappin [35] observed that the field-parallel dissipation length is larger than in field-perpendicular directions, because the magnetic field-lines are stiff and the magnetic field intensity is in cascade. This leads to a steepening spectrum in the field-parallel direction ($k_\parallel$) [11]. There is no distinguishable inertial range for the field-parallel spectrum. For the field-perpendicular spectrum, the inertial range is more clear $k \approx (5 - 28)$. The spectral properties of the nonlinear transfer functions, triad interactions and cascade directions of ideal invariants in the energy inertial range of isotropic and anisotropic 3D-MHD are studied in the next sections.

6.4 Locality of the total energy in isotropic and anisotropic 3D-MHD turbulence

The locality of the nonlinear total energy transfer of incompressible isotropic and anisotropic 3D-MHD turbulence is studied by computing the strength of the nonlinear total energy exchanges between the wavenumbers (*i.e.,* the total energy transfer function) and the nonlinear triad interactions in the interacting triads in the energy inertial range. For this purpose, both the transfer density function $Q(v)$ and locality function $W(v)$ are computed using our approach.

6.4.1 Locality of the total energy in isotropic 3D-MHD turbulence

Fig.6.7 shows the normalized transfer density functions $Q(v)$ of the total energy at independent states of fully developed quasi-stationary turbulence $t = 0.5 - 9$ for fixed k in the energy inertial range. The density fumctions are normalized by the total energy dissipation $\epsilon = \int_V dV(\nu\omega^2 + \eta j^2)$. The graphs with different colors from black at $t = 0.5$ to red at $t = 9$ correspond to amplitudes of the density functions $Q(v)$ (from low to high). As time progress, the amplitude of the function $Q(v)$ increases. The total energy transfer and triad interactions increase in turbulent flow. For simplicity, Fig.6.8a depicts the strength of the density function at time $t = 9$. The function $Q(v)$ is characterized by a high-amplitude peak at v-value close to 1. Most of the nonlinear total energy is transferred between two wavenumbers of similar size and a negligible amount of the total energy is transferred between two different scales in the interacting triad. Thus the nonlinear total energy transfer is predominantly local in the inertial range.

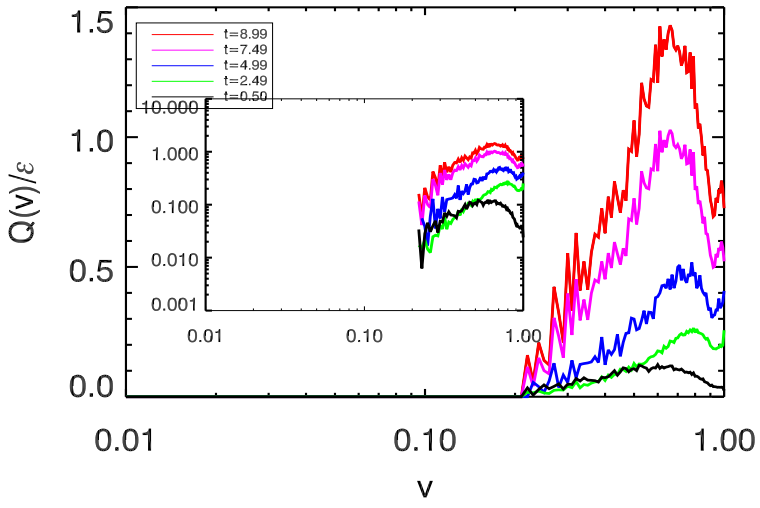

Figure 6.7: The normalized transfer density functions $Q(v)$ of the total energy in decaying isotropic MHD turbulence taken at regular time intervals in the simulation. The inset is a log-log plot for the same functions.

In Fig.6.8a, the peak of $Q(v)$ shows that the total energy is transferred from samll wavenumbers to large wavenumbers. So the nonlinear total energy transfer is a direct cascade in the inertial range with a constant and positive flux.

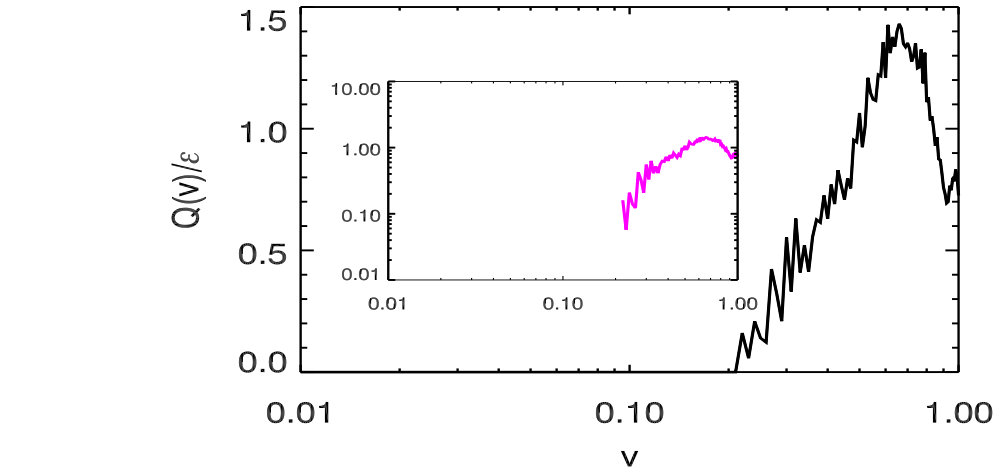

a)

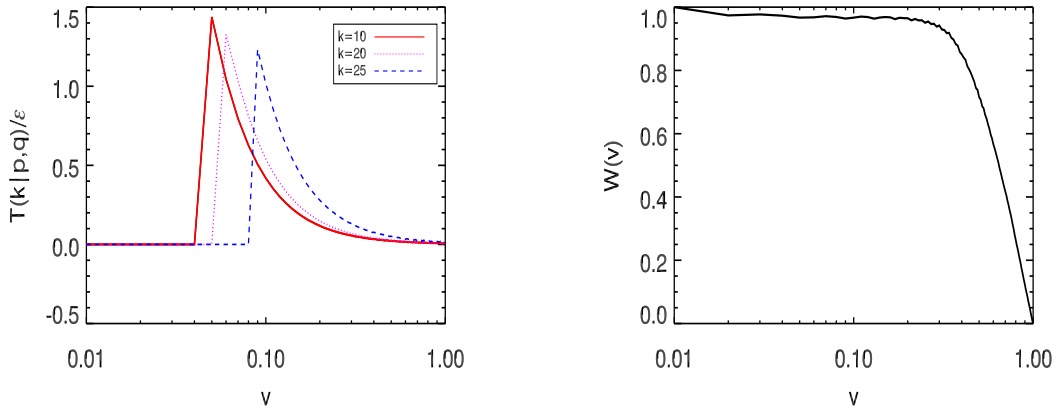

b) c)

Figure 6.8: a) Normalized transfer density function $Q(v)$ for the total energy in decaying isotropic 3D-MHD turbulence at $t = 9$. The inset is a log-log plot for the same function. b) Normalized contributions of the combined total energy transfer rate $T(\mathbf{k}|\mathbf{p},\mathbf{q})$ for for $k = 10$ (solid), 20 (dotted), and 25 (dashed) in the inertial range of decaying isotropic 3D-MHD turbulence. c) The locality-function $W(v)$ of the total energy in decaying isotropic MHD turbulence in (a).

Fig.6.8b shows the normalized contributions of the combined total energy transfer rate $T(\mathbf{k}|\mathbf{p},\mathbf{q})$ for k-values in the inertial range. These functions have a maximum amplitudes at $v \approx 0.05, 0.06$ and 0.09 for $k = 10, 20$, and 25, respectively. All graphs fall to zero with v-value close to 1. The magnitudes of interactions for nonlocal triads $k \approx p \gg q$, $k \approx q \gg p$, or $p \approx q \gg k$ are larger than those for local triads $k \approx p \approx q$. Thus most nonlinear triad interactions associated with total energy transfer takes place between three wavenumbers with different sizes. These triads have two wavenumbers with similar sizes, longer than the third wavenumber. This indicates that in the triad interaction, the largest scale acts as a mediator only when the energy transfers between the two small scales and the triads are very elongated in the inertial range. Thus triad interactions in isotropic 3D-MHD energy inertial range are predominantly nonlocal. In Fig.6.8b, the combined total energy functions $T(\mathbf{k}|\mathbf{p},\mathbf{q})$ abruptly drops to zero, thus nonlinear triads can no longer be represented in the cubic box. The spec-

tral properties of the total energy in decaying isotropic 3D-MHD turbulence are similar to those of kinetic energy in decaying isotropic 3D-HD turbulence. The interacting triads in the inertial range of isotropic 3D-MHD are more nonlocal compared to the triads in the inertial range of 3D-HD turbulence (cf. Fig.5.11). Fig.6.8b shows that the combined total energy transfer rate is approximately the same for different k-values in the inertial range. These results indicates that the flux of the total energy is constant, positive and transfers from large scales to small scales.

These results are compatible with the result of Alexakis *et al.* [8, 54], who investigated the transfer of energy from large scales to small scales in fully developed 3D-MHD turbulence using a shell-to-shell approach. The DNS of Alexakis *et al.* is not used to examine the situation of an externally imposed uniform magnetic field. They showed that the transfer of energy from large scales to small scales is local with a highly nonlocal process in Fourier space. The contributions of the total energy transfer could depend on the geometry of the triad. The locality function $W(v)$ is computed to express the nature of the locality of the total energy transfer. Fig.6.8c shows the locality function $W(v)$ for the transfer density function $Q(v)$ in Fig.6.8a. Approximately 60% of the total energy transfer comes from triad interactions in which the ratio of the smallest to the middle wavenumber is greater than 0.58. This implies that most of the total energy transfer takes place between two wavenumbers with similar sizes. Our results report that the total nonlinear energy transfer in the inertial range of isotropic 3D-MHD turbulence is predominantly local through nonlocal triad interactions with a direct cascade to small scales.

Fig.6.9 shows the normalized transfer density functions and the locality functions for the nonlinear energy transfer, $T^{vv}(\mathbf{k}|\mathbf{p},\mathbf{q})$ and $\mathbf{k}$, $T^{bb}(\mathbf{k}|\mathbf{p},\mathbf{q})$. Similarly, Fig.6.10 shows the normalized transfer density functions and the locality functions for the nonlinear energy transfer, $T^{bv}(\mathbf{k}|\mathbf{p},\mathbf{q})$ and $T^{vb}(\mathbf{k}|\mathbf{p},\mathbf{q})$. The transfer density function $Q(v)$ for each quantity is characterized by a peak close to 1. The transfer of these quantities is predominantly local between two wavenumbers of similar size with positive flux in the inertial range. This set of figures indicates that there are transfers of kinetic energy from large scales to small scales, magnetic energy from large scales to small scales, kinetic energy from large scales to magnetic energy at small scales, and magnetic energy from large scales to kinetic energy at small scales. These types of transfers are local with a direct cascade in the inertial range of isotropic 3D-MHD turbulence and there is no possibility for nonlocal transfers. These results are compatible with simulation results by Debliquy *et al.* [62], who have studied the energy fluxes and shell-to-shell interactions in decaying 3D-MHD turbulence using a high-resolution (512^3) DNS. They claimed that the energy transfer from one field to another is local with a direct cascade. Recently, Aluie and Eyink [100] have shown that the velocity to velocity and magnetic to magnetic fluxes are local in the limit of infinite Reynolds number. The fluxes coupling velocity and magnetic fields are also local. Our results are in contradiction compared with Verma results in [60, 10]. Verma used the field-theoretic calculations to compute the shell-to-shell transfers and concluded that the transfers T^{vv} and T^{bb} were local, but the transfers T^{vb} and T^{bv} were nonlocal.

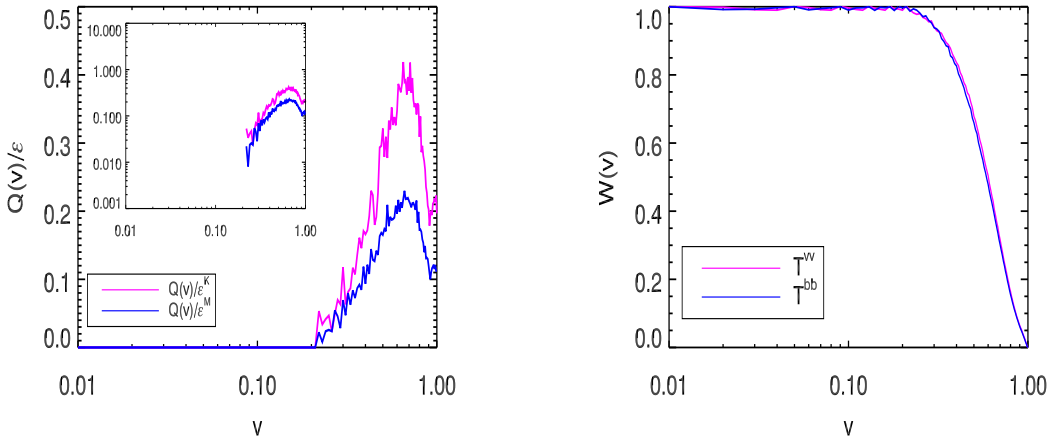

a) b)

Figure 6.9: a) Normalized transfer density function $Q(v)$ of kinetic-to-kinetic, T^{vv} (magenta) and magnetic-to-magnetic, T^{bb} (blue) energy transfer in isotropic 3D-MHD turbulence. The inset is a log-log plot for the same functions. b) The locality-functions $W(v)$ of kinetic-to-kinetic, T^{vv} (magenta), and magnetic-to-magnetic, T^{bb} (blue) in isotropic 3D-MHD turbulence.

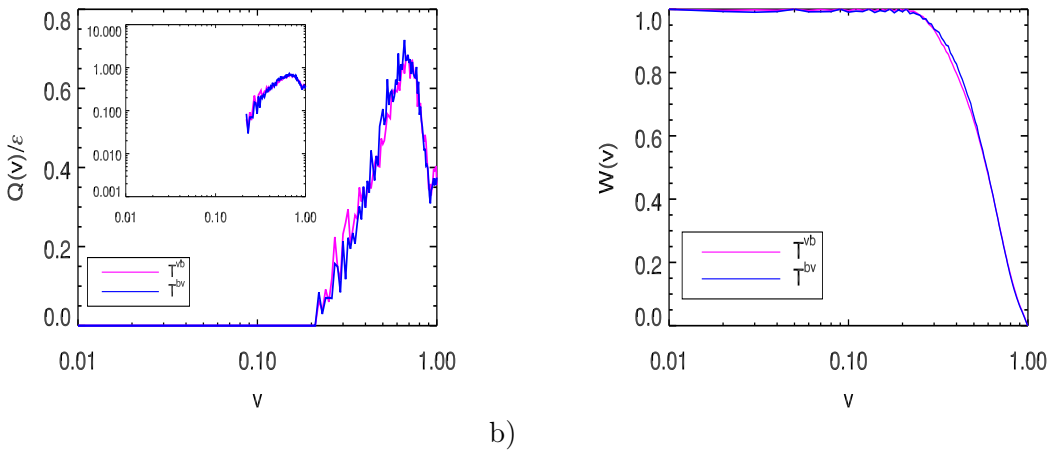

a) b)

Figure 6.10: a) Normalized transfer density functions $Q(v)$ of kinetic-to-magnetic, T^{bv} (magenta), and magnetic-to-kinetic, T^{vb} (blue) energy transfer in isotropic 3D-MHD turbulence. The inset is a log-log plot for the same functions. b) The locality-functions $W(v)$ of kinetic-to-magnetic, T^{bv} (magenta), and magnetic-to-kinetic, T^{vb} (blue) in isotropic 3D-MHD turbulence.

6.4.2 Locality of the total energy in anisotropic 3D-MHD turbulence

The transfer density functions $Q(v)$ and locality functions $W(v)$ of the total energy transfer perpendicular to the mean magnetic field, $k_\perp = 25$ (where k_z=0 and k_x and k_y are chosen in the inertial range of the field-perpendicular spectrum) and parallel, $k_\parallel = 5$ (where $k_\parallel = |k_z|$, $k_x = 0$, and k_y is chosen in the inertial range) are computed.

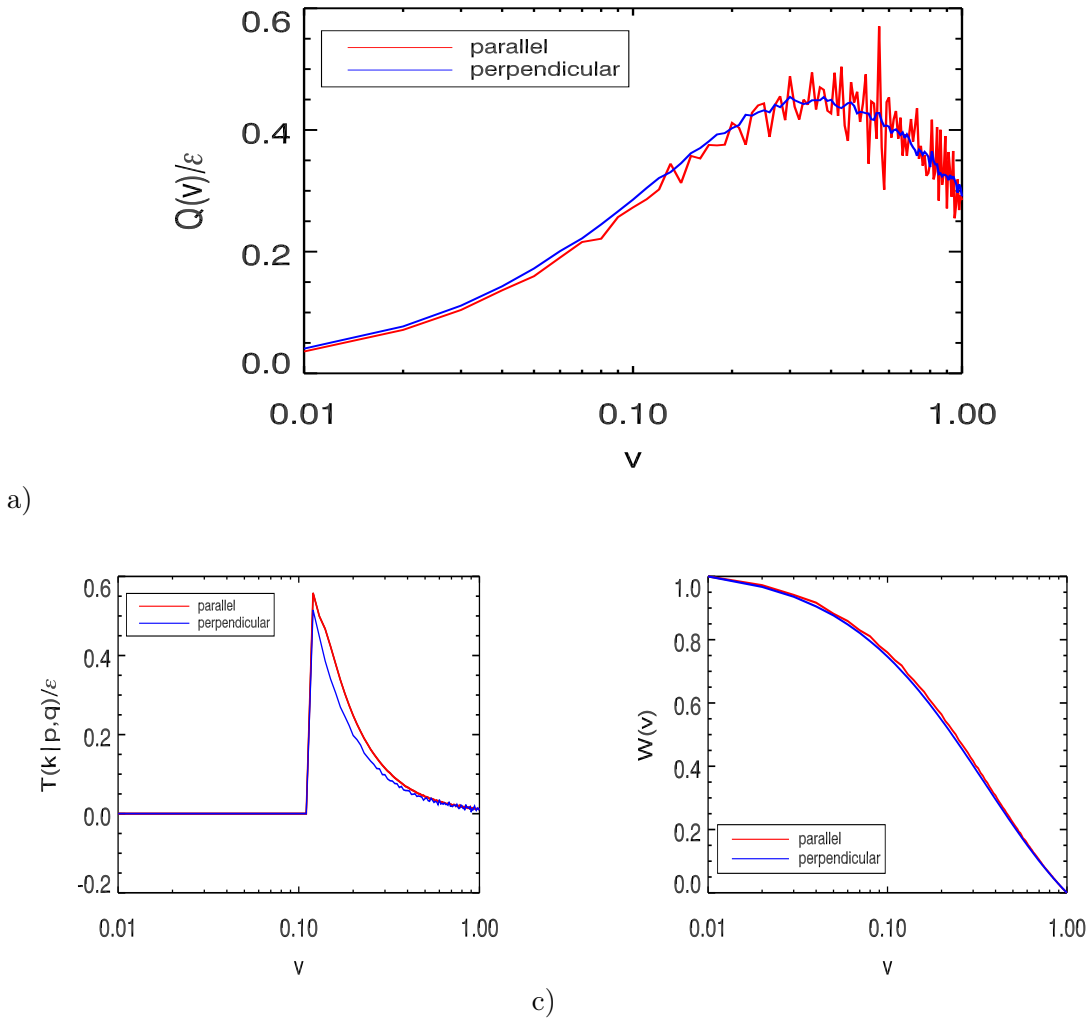

Figure 6.11: a) Normalized transfer density functions $Q(v)$ of the total energy in both parallel (red line) and perpendicular (blue line) directions in anisotropic 3D-MHD turbulence. b) Normalized contributions of the combined total transfer rates $T(\mathbf{k}|\mathbf{p},\mathbf{q})$ in both parallel (red line) and perpendicular (blue line) directions to the mean magnetic field. c) The locality-functions $W(v)$ of the total energy in both parallel (red line) and perpendicular (blue line) directions in anisotropic 3D-MHD turbulence.

Fig.6.11a shows the normalized transfer density functions in the parallel and perpendicular directions. These functions are normalized by the total energy dissipation. In Fig.6.11a, $Q(v)$ in both parallel and perpendicular directions has the same strength and amplitude, and is characterized by peaks at v-values between 0.4 and 0.5. This can be explained by a significant a mount of magnetic helicity in the system. The transfer of magnetic helicity is predominantly nonlocal with an inverse cascade (will be shown in section 6.6). The magnetic helicity pulls magnetic energy along with it to large scales. The maximum value of the total energy transfer

appears at a v-value, at which the middle wavenumber is $1-2$ times larger than the smallest wavenumber. This observation implies that the transfer of total energy between modes that travel in the same direction is local where the energy is exchanged between two wavenumbers with approximately similar sizes. The positioning of the peaks in Fig.6.11a shows that most of the energy is transfered from large scales to small scales. The total energy transfer is predominantly a direct cascade in both perpendicular and parallel directions, but it is weaker than that in the isotropic case (cf. Fig.6.8a). When the injected magnetic field increases the energy transfer function becomes nonlocal with nonlocal triad interactions in both parallel and perpendicular directions. Also, Fig.6.11a shows that the density function $Q(v)$ in the parallel direction has more fluctuation than that in the perpendicular direction. This is because of the stiffness of magnetic field-lines and the turbulent depletion along the mean magnetic field that reduces the extent field-parallel Fourier ensemble. This is in agreement with the fact that, in incompressible anisotropic MHD turbulence the turbulent fluctuations are elongated along the guiding magnetic field lines [44, 7]. These results confirm the claim by Alexakis *et al.* [11], who investigated the locality of the energy transfer and the spectral interactions for anisotropic 3D-MHD for varying intensity. They claimed that the energy transfer functions are local in the parallel and perpendicular directions to the magnetic guide field regardless of magnetic field strength.

Fig.6.11b depicts the normalized contributions of the combined total transfer rates $T(\mathbf{k}|\mathbf{p},\mathbf{q})$ parallel to the mean magnetic field ($k_{\parallel}$) and perpendicular ($k_{\perp}$). These functions are characterized by a maximum value at approximately $v \approx 0.12$ and falls to zero for v-values close to 1. The magnitudes of interactions for nonlocal triads, which formed by two wavenumbers with similar sizes and longer than the third wavenumber are larger than those for local triads (note that most of these nonlocal triads are in the region $v < 0.5$). Thus nonlinear triad interactions are found to be nonlocal in both the parallel and perpendicular directions.

Fig.6.11c shows the locality functions $W(v)$ that correspond to the $Q(v)$ in Fig.6.11a. 60% of the total energy transfer comes from triad interactions in which the ratio of the smallest to the middle wavenumber is greater than 0.20. Most of the total energy transfer is exchanged between two wavenumbers with similar sizes. Thus most of the total nonlinear energy transfer in anisotropic 3D-MHD turbulence is local through nonlocal triad interactions with a direct cascade for both parallel and perpendicular quantities. Our results for the spectral properties of the total energy transfer in the inertial range of 3D-MHD are summarized in Table 6.2.

—	Decaying isotropic	Forced anisotropic
Total energy transfer function	local	local
Triad interaction	nonlocal	nonlocal
Cascade direction	direct	direct

Table 6.2: The spectral properties of nonlinear total energy transfer in the inertial range of 3D-MHD turbulence.

6.5 Locality of the cross helicity in isotropic and anisotropic 3D-MHD turbulence

Cross helicity is a nonlinear quadratic invariant of the 3D-MHD system. The locality of nonlinear transfer function and triad interactions, and the cascade of cross helicity are discussed.

Since the sum of transfer rates of the cross helicity in a MHD triad is zero, the cross helicity is conserved in a MHD triad. The locality properties of the cross helicity in incompressible 3D-MHD turbulence is measured by extending the simulation program used for cross helicity calculations in the case of 2D-MHD to 3D-MHD with the same parameters specified for the incompressible isotropic and the anisotropic 3D-MHD turbulence (cf. subsection 6.3.2).

6.5.1 Locality of the cross helicity in isotropic 3D-MHD turbulence

Fig.6.12a shows the normalized transfer density function $Q(v)$ of the nonlinear cross helicity transfer function for $k = 25$ in the inertial range. The density function $Q(v)$ for the cross helicity exhibits properties similar to the density function for the total energy in isotropic 3D-MHD. $Q(v)$ is characterized by a high-amplitude peak close to $v \approx 1$. Most of the nonlinear cross helicity is transferred between two wavenumbers with similar sizes. Thus nonlinear cross helicity transfer is local. In addition, Most of nonlinear triads associated with cross helicity transfer arew formed by three wavenumbers with different sizes. These triads have two wavenumbers with similar sizes, longer than the third wavenumber. Thus nonlinear triad interactions are predominantly nonlocal in the inertial range of isotropic 3D-MHD turbulence.

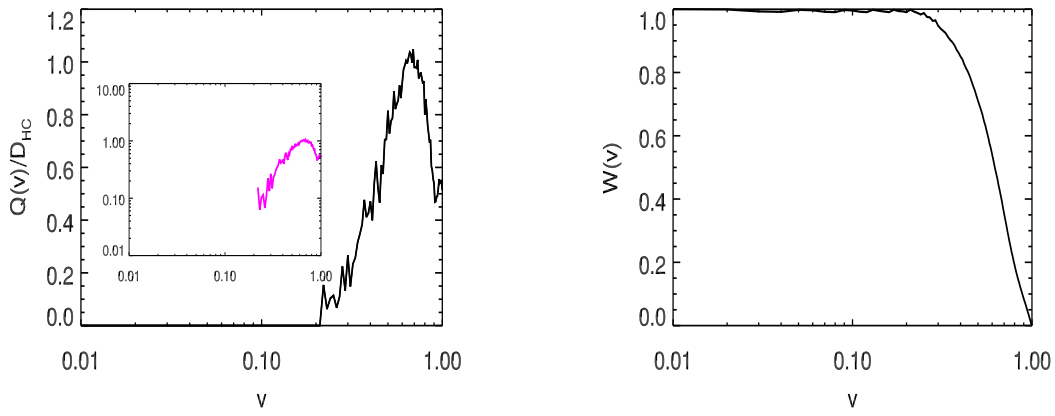

a) b)

Figure 6.12: a) The normalized transfer density function $Q(v)$ of the cross helicity for $k = 25$ in isotropic 3D-MHD turbulence. b) The locality function $W(v)$ of cross helicity for $Q(v)$ in (a).

Fig.6.12b shows the locality function $W(v)$ for the function $Q(v)$ in Fig.6.12a. Approximately 60% of the cross helicity transfer comes from triad interactions in which the ratio of the smallest to the middle wavenumber is greater than 0.55. 40% of the cross helicity transfer involves wavenumber triads in which the smallest wavenumber is less than one-half of the middle wavenumber. Thus most of the cross helicity transferred between two wavenumbers of similar size. Our results show that the nonlinear cross helicity transfer in isotropic 3D-MHD turbulence is local through nonlocal triad interactions with a direct cascade.

6.5.2 Locality of the cross helicity in anisotropic 3D-MHD turbulence

Figs.6.13a and b show the normalized transfer density functions $Q(v)$ and their correspond locality functions $W(v)$ for the nonlinear cross helicity transfer parallel and perpendicular to the mean magnetic field guide. These figures look similar to those of total energy transfer in anisotropic MHD (cf. subsection 6.4.2). This similarily can be explained by the fact that field is imposed on a MHD system, most of the nonlinear cross helicity transfer becomes local with a direct cascade. Most of the triads interactions are nonlocal. Thus when a small magnetic field is imposed, the cross helicity is transfered from large sclaes to small scales with local direct cascade, but when the injected magnetic field increases the cross helicity transfer function becomes more nonlocal with nonlocal triad interactions in both parallel and perpendicular directions.

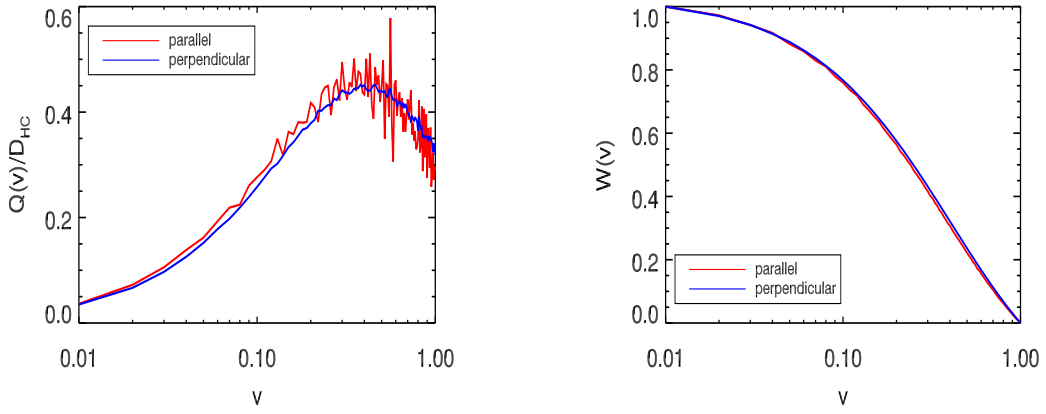

a) b)

Figure 6.13: a) The normalized transfer density functions $Q(v)$ for cross helicity in both parallel and perpendicular directions of anisotropic MHD. b) The locality W-functions for cross helicity in both parallel and perpendicular directions of anisotropic MHD.

Our results for the spectral properties of the nonlinear cross helicity in the inertial range of 3D-MHD are summarized in Table 6.3.

—	Decaying isotropic	Forced anisotropic
Cross helicity transfer function	local	local
Triad interaction	nonlocal	nonlocal
Cascade direction	direct	direct

Table 6.3: The spectral properties of the nonlinear cross helicity transfer in the inertial range of 3D-MHD turbulence.

6.6 Locality of the magnetic helicity in 3D-MHD turbulence

Magnetic helicity is an ideal invariant of 3D-MHD turbulence. The magnetic helicity in a given volume is the volume integral of the dot product of the magnetic vector potential **a** and the magnetic field **b** (cf. subsection 1.7.2). The name helicity is thus appropriate as it gauges the relative curling or braiding of the lines of **a** and **b**. Magnetic fields can include many types

of structures that have high magnetic helicity: twisted, kinked, knotted or linked magnetic flux tubes, sheared layers of magnetic flux and force-free fields. Magnetic helicity quantifies various aspects of the magnetic field structure. Magnetic helicity is conserved in ideal MHD and is approximately conserved during magnetic reconnection[1]. In a confined volume, widespread reconnection may reduce the magnetic energy of a field while approximately conserving its magnetic helicity [102]. As a result, the field relaxes to a minimum energy state, called the Taylor state, where the current is parallel to the force-free field [102]. Such relaxation processes are important to both fusion (especially in reversed field pinch devices) and astrophysical plasmas [103]. Inverse cascade of magnetic helicity in 3D-MHD turbulence is believed to be responsible for the formation of large-scale magnetic structures in the universe. In celestial bodies with rotation, the difference between kinetic helicity (twists in the velocity field) and magnetic helicity (twists in the magnetic field) results in the so called α-dynamo. An α-dynamo results when kinetic helicity injection enhances the magnetic field [2], but does not necessarily lead to stable large-scale magnetic structure formation.
The total magnetic helicity is given by

$$H^M = \frac{1}{2} \langle \mathbf{a} \cdot \mathbf{b} \rangle , \tag{6.27}$$

where $\mathbf{b} = \nabla \times \mathbf{a}$ and $\mathbf{a}$ is the magnetic vector potential. For a single triad $(\mathbf{k}, \mathbf{p}, \mathbf{q})$ with $\mathbf{k} = \mathbf{p} + \mathbf{q}$, $k = |\mathbf{k}|$, $p = |\mathbf{p}|$, and $q = |\mathbf{q}|$, the evolution equation of magnetic helicity in a triad interaction is [39]

$$\frac{\partial H^M(\mathbf{k})}{\partial t} = \frac{1}{2} \mathcal{R} \left[\mathbf{b}^*(\mathbf{k}) \cdot \frac{\partial \mathbf{a}(\mathbf{k})}{\partial t} + \mathbf{a}^*(\mathbf{k}) \cdot \frac{\partial \mathbf{b}(\mathbf{k})}{\partial t} \right] . \tag{6.28}$$

Eq.(6.28) can be simplified to

$$H^M(\mathbf{k}|\mathbf{p}, \mathbf{q}) = H^M(\mathbf{k}|\mathbf{p}|\mathbf{q}) + H^M(\mathbf{k}|\mathbf{q}|\mathbf{p}). \tag{6.29}$$

where

$$\begin{aligned} H^M(\mathbf{k}|\mathbf{p}|\mathbf{q}) = & \frac{1}{4} \mathcal{R} \left[\mathbf{b}(\mathbf{k}) \cdot (\mathbf{v}(\mathbf{p}) \times \mathbf{b}(\mathbf{q})) \right] \\ & + \frac{1}{4} \Im \left[(\mathbf{k} \cdot \mathbf{b}(\mathbf{q}))(\mathbf{a}(\mathbf{k}) \cdot \mathbf{v}(\mathbf{p})) - (\mathbf{k} \cdot \mathbf{v}(\mathbf{q}))(\mathbf{a}(\mathbf{k}) \cdot \mathbf{b}(\mathbf{p})) \right] . \end{aligned} \tag{6.30}$$

The quantity $H^M(\mathbf{k}|\mathbf{p}|\mathbf{q})$ in Eq.(6.30) represents the mode-to-mode magnetic helicity transfer from mode $\mathbf{p}$ to mode $\mathbf{k}$ with mode $\mathbf{q}$ acting as a mediator [39]. We can define the second term in the r.h.s of Eq.(6.29) similarly.
The sum of magnetic helicity transfer rates in a triad is zero,

$$H^M(\mathbf{k}|\mathbf{p}|\mathbf{q}) + H^M(\mathbf{k}|\mathbf{q}|\mathbf{p}) + H^M(\mathbf{p}|\mathbf{k}|\mathbf{q}) + H^M(\mathbf{p}|\mathbf{q}|\mathbf{k}) + H^M(\mathbf{q}|\mathbf{k}|\mathbf{p}) + H^M(\mathbf{q}|\mathbf{p}|\mathbf{k}) = 0. \tag{6.31}$$

[1] Magnetic reconnection is a process in which there is a change of magnetic connectivity of plasma elements due to the presence of a localized diffusion region where ideal MHD breaks down [101].

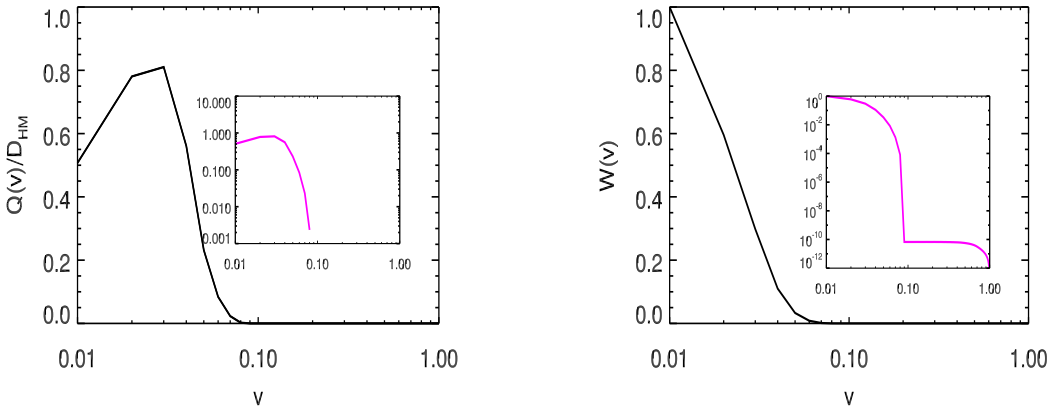

a) b)

Figure 6.14: a) The normalized transfer density function $Q(v)$ for magnetic helicity for $k = 25$. The inset is a log-log plot for the same function. b) The locality function $W(v)$ for magnetic helicity at $k = 25$. The inset is a log-log plot for the same function.

Magnetic helicity is conserved in a triad, also referred to as detailed conservation of magnetic helicity in a triad interaction,*i.e.*,

$$H^M(\mathbf{k}) + H^M(\mathbf{p}) + H^M(\mathbf{q}) = \text{const.} \tag{6.32}$$

The locality of the magnetic helicity in isotropic and anisotropic 3D-MHD turbulence can be measured by using our approach. To this end, the transfer density function $Q(v)$ and the locality function $W(v)$ of magnetic helicity transfer are computed.

6.6.1 Locality of the magnetic helicity in isotropic 3D-MHD turbulence

Fig.6.14a shows the normalized transfer density function $Q(v)$ of the nonlinear magnetic helicity transfer function for $k = 25$ in the inertial range. The density function is normalized by the rate of the magnetic helicity dissipation $D_{HM} = -\eta \int_V (\mathbf{j} \cdot \mathbf{b}) \mathbf{dV}$. Here most of the nonlinear magnetic helicity transfer occurs in the region $v < 0.5$. The density function $Q(v)$ is characterized by a peak with a high amplitude at $v \approx 0.03$. Thus most of the magnetic helicity is transferred between two wavenumbers with different sizes. The transfer of magnetic helicity is dominantly nonlocal. Most of the triads associated with magnetic helicity transfer are formed by three wavenumbers with different sizes. Thus the triad interactions are nonlocal in the inertial range of incompressible isotropic 3D-MHD turbulence. The locality function that correspond to the transfer density function $Q(v)$ is shown in Fig.6.14b. This cumulative function shows that approximately 60% of the total magnetic helicity transfer comes from triad interactions in which the ratio of the smallest to the middle wavenumber is greater than 0.024. Thus most of the magnetic helicity transfer occurs between two sides with different lengths in the interacting triad. The transfer of magnetic helicity is nonlocal through nonlocal triad interactions.

Fig.6.15a shows the normalized transfer density functions $Q(v)$ for k-values chosen in the

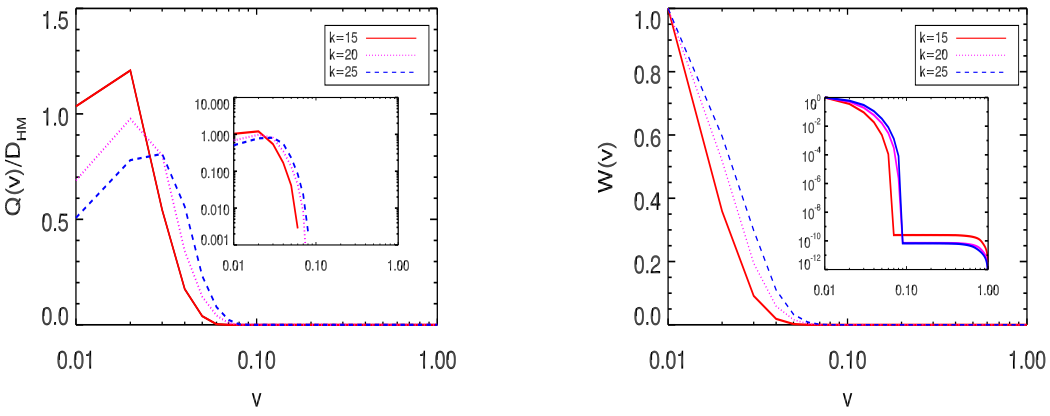

a) b)

Figure 6.15: a) The normalized transfer density functions $Q(v)$ for magnetic helicity at $k = 15, 20$, and 25. The inset is a log-log plot for the same functions. b) The locality functions $W(v)$ for magnetic helicity at $k = 15, 20$, and 25. The inset is a log-log plot for the same functions.

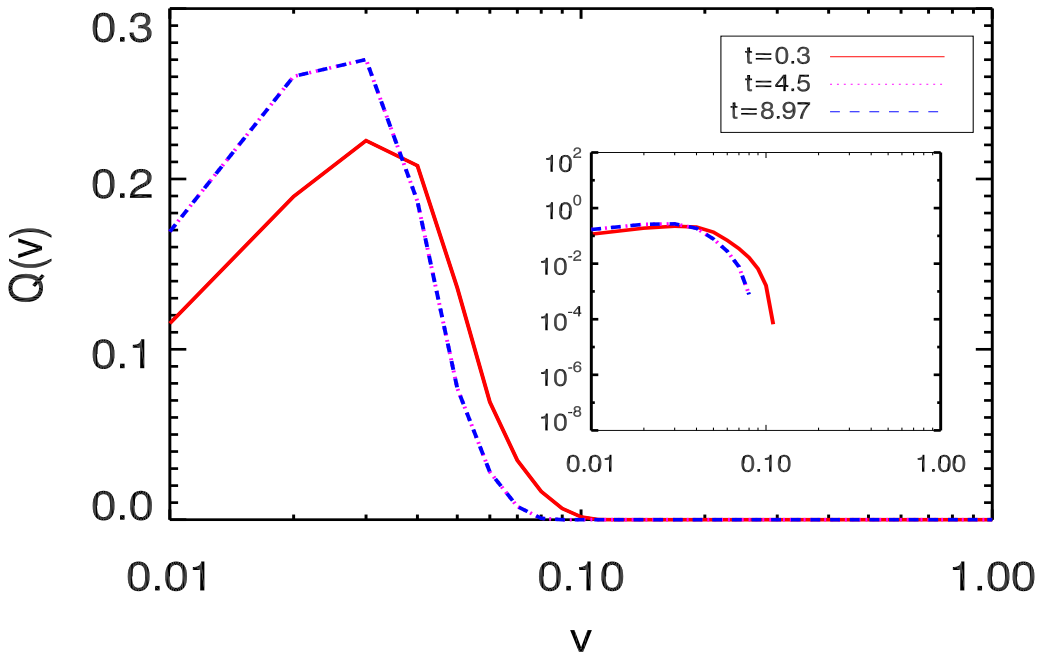

Figure 6.16: Time evolution of transfer density functions $Q(v)$ of magnetic helicity. Red solid line: $Q(v)$ at initial state at t=0.3, magenta dotted line: $Q(v)$ at t=4.5, dashed blue line: $Q(v)$ at t=9. The inset is a log-log plot for the same functions.

inertial range. In this figure, the strength of the density function $Q(v)$ increases with v value close to zero, and also increases as the k-value decreases. Fig.6.15b shows the locality functions $W(v)$ for the functions $Q(v)$ in Fig.6.15a. 40% of the total magnetic helicity transfer involves wavenumber triads in which the ratio of the smallest wavenumber to the middle is greater than 0.020, 0.022, and 0.024 at $k = 15, 20$, and 25, respectively. The nonlinear magnetic helicity is transferred from large wavenumbers to small wavenumbers, so the cascade direction of the magnetic helicity transfer is inverted in incompressible decaying 3D-MHD turbulence. These results agree with the works of Pouquet *et al.* and Alexakis *et al.* [26, 104].
In the above discussion, we focus on the transfer and triad interactions of magnetic helicity in a particular instant of time (selected from a quasi-stationary or stationary state of the turbulent flow). We now focus on how the transfer and interactions evolve through time to reach their final states. The time evolution of $Q(v)$ for magnetic helicity in isotropic turbulence is shown in Fig.6.16. From an initial state in which the transfer functions of magnetic helicity are less nonlocal, they reach a state over time that is maximally nonlocal and remain in that state for the rest of the simulation time. Thus for magnetic helicity, the strength of transfer and the triad interactions in the initial states are different but when a quasi-stationary state is reached in the turbulent flow, the average nature of these transfers and interactions does not change any further.

6.6.2 Locality of the magnetic helicity in anisotropic 3D-MHD turbulence

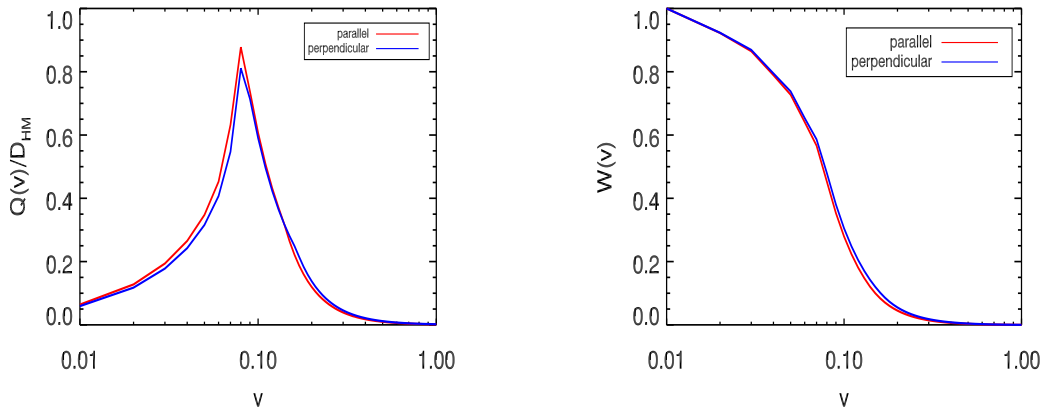

Figure 6.17: a) The normalized transfer density function $Q(v)$ for magnetic helicity in both parallel and perpendicular directions at $t = 49.225$. b) The locality function $W(v)$ for magnetic helicity in both parallel and perpendicular directions at $t = 49.225$.

The locality of the magnetic helicity parallel and perpendicular to the mean magnetic field is measured. This accomplished by computing the transfer density functions $Q(v)$ and the locality functions $W(v)$ of magnetic helicity transfer in both directions.
Fig.6.17 shows the normalized density functions $Q(v)$ and their correspond locality functions $W(v)$ parallel and perpendicular to the mean magnetic field. In these figures, the density function of the magnetic helicity transfer in both directions is characterized by the typical peak at the same v-value ≈ 0.08. Most of the magnetic helicity transfer takes place between two wavenumbers with different sizes. Thus the transfer of magnetic helicity is nonlocal through nonlocal triad interaction with an inverse cascade. When the mean magnetic field

increases, the nonlinear transfer of magnetic helicity becomes more nonlocal through nonlocal triad interactions in the parallel and perpendicular directions. Our results for the spectral properties of the magnetic helicity transfer in the inertial range of 3D-MHD turbulence are summarized in Table 6.4.

—	Decaying isotropic	Forced anisotropic
Magnetic helicity transfer function	nonlocal	nonlocal
Triad interaction	nonlocal	nonlocal
Cascade direction	inverse	inverse

Table 6.4: The spectral properties of the nonlinear magnetic helicity transfer in the inertial range of 3D-MHD turbulence.

We conclude that the fluxes of the total energy and cross helicity are dominated by local transfer with direct cascade directions. Flux of magnetic helicity is dominated by nonlocal transfer through nonlocal triad interactions with an inverse cascade. Also, the magnetic stretching term is dominated by nonlocal triads interactions with local magnetic energy transfer. Our results for magnetic helicity, magnetic energy transfer, and triad interactions are in agreement with Aluie and Eyink [100].
In the next part of this work, the locality of some quadratic nonlinear invariants with forced inverse cascade for magnetic helicity in 3D-MHD turbulence are studied by using high-resolution (1024^3) direct numerical simulation.

6.7 Nonlinear triad interactions in forced inverse cascade turbulence

In most DNS of 3D-MHD turbulence, the forcing mechanisms and initial conditions are in small wavenumber region. The energy containing scales usually the large scales [105, 106]. In this section, we explore the nature of the transfer functions and triad interactions of ideal invariants in a forced inverse cascade turbulence system based on DNS conducted by S. K. Malapaka [107]. We particularly examine the magnetic helicity when the forcing and initial conditions of the DNS are placed in large wavenumber k of the spectra by using our approach for the density function $Q(v)$ and locality function $W(v)$. Such a system would help toward understand the true nature of local transfer, triad interactions and how the inverse cascade operates.
The forcing occurs at small scales of 3D-MHD turbulence system, and this results in two inertial ranges one to the left and one to the right of the forcing [107]. The nature of the transfer functions and triad interactions in each of these spectral ranges are studied using a reference wavenumber from each region. Two cases are discsussed, one in which both kinetic and magnetic helicities are supplied by the forcing, and a second where only magnetic helicity is supplied.

6.7.1 Supplying both magnetic and kinetic helicities through the forcing

In this case, the forcing terms in the equations of the MHD turbulence system supply both kinetic and magnetic helicities [107]. Fig.6.18a shows the transfer density functions $Q(v)$ of magnetic helicity, kinetic helicity, total energy, and magnetic energy generated using the high

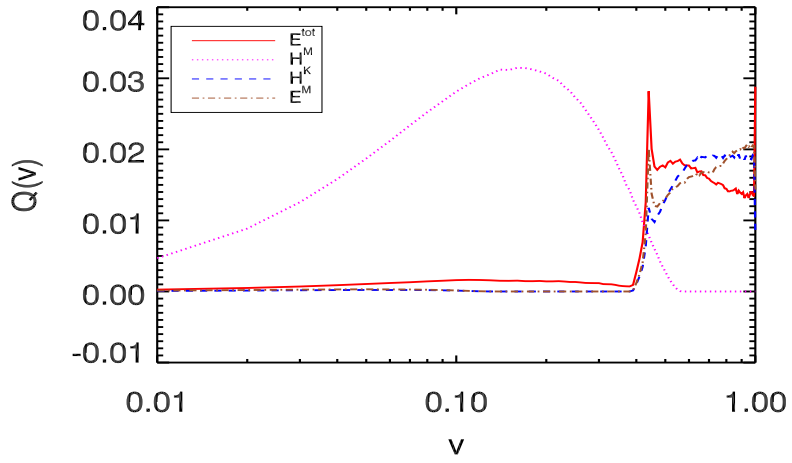

a)

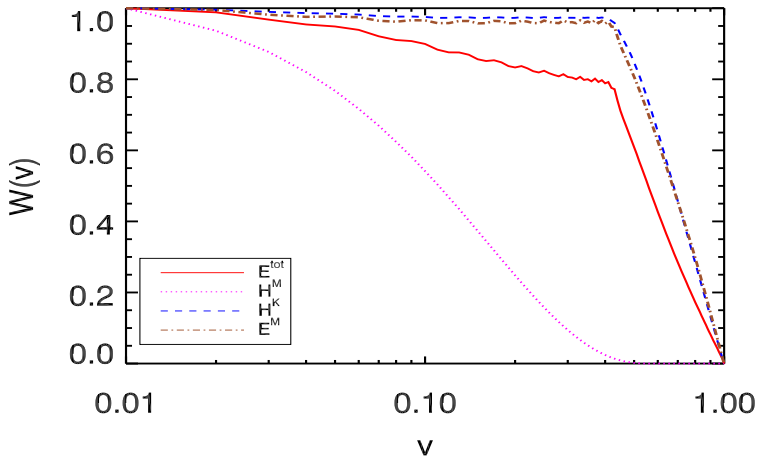

b)

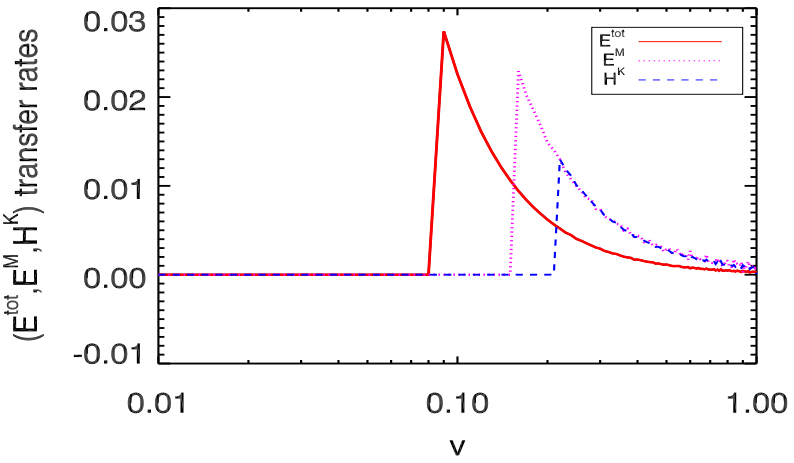

c)

Figure 6.18: a) The transfer density functions $Q(v)$ of magnetic helicity (magenta dotted line), kinetic helicity (dashed blue line), total energy (red solid line), and magnetic energy (brown dashed-dotted line) with large $k = 300$ as the reference wavenumber. b) The locality functions $W(v)$ of the quantities in (a). c) The contributions of the combined transfer rates for total energy (red solid line), magnetic energy (magenta dotted line), and kinetic helicity (blue dashed line) with large $k = 300$ as the reference wavenumber. The time at which this analysis was done is t=6.28.

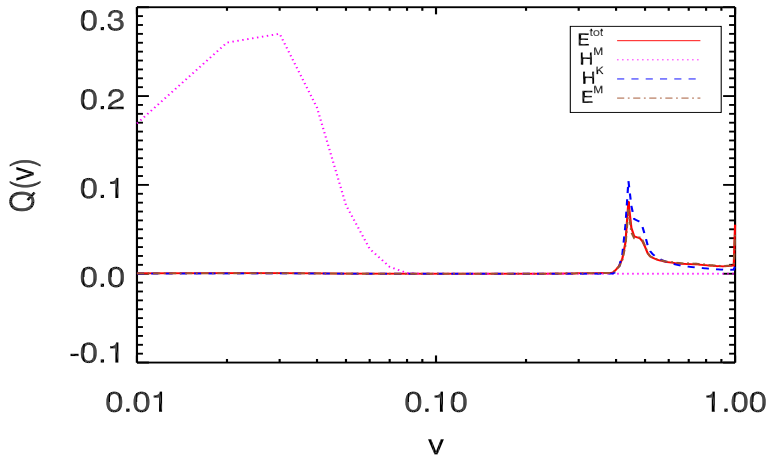

Figure 6.19: The transfer density functions $Q(v)$ of magnetic helicity (magenta dotted line), kinetic helicity (dashed blue line), total energy (red solid line), and magnetic energy (brown dashed-dotted line) with small $k = 30$ as the reference wavenumber. The time at which this analysis was done is t=6.28.

wavenumber as reference. Fig.6.18b shows the locality functions $W(v)$ of the same quantities as the functions $Q(v)$ in Fig.6.18a. In Fig.6.18a, the strength of magnetic helicity density function is in the range $0.1 < v < 0.2$, while the strengths of the total energy and magnetic energy are $0.4 < v < 0.5$, and for the kinetic helicity $0.6 < v < 0.8$. This implies that the transfer of magnetic helicity is the most nonlocal of all the quantities. The transfer of total energy and magnetic energy have nearly the same level of locality (they are more local than magnetic helicity). The transfer of kinetic helicity is the most local one of all the quantities. In addition, the positions of the functions $Q(v)$ in Fig.6.18a indicate that the nonlinear triad interactions of magnetic helicity are the most nonlocal of all the quantities. Triad interactions in total energy and magnetic energy show similar levels of nonlocality. The triad interactions in kinetic helicity show the least nonlocal behavior, because the kinetic helicity is transferred locally between the wavenumber triads with two wavenumbers of approximately similar size (small scale) that are much larger than the third wavenumber (large scale). The triad interactions of magnetic helicity occur betwen three wavenumbers with disparate sizes. In Fig.6.18b, it is clearly seen that for the locality functions, the amplitudes of the quantities are converse to that of the values in the density functions and the spread of the function also is complementary. Thus magnetic helicity which has the highest amount of nonlocal interactions, has the least amount of spread followed by total energy, magnetic energy and kinetic helicity. In other words, approximately 50% of the magnetic helicity spread occurs in the area in which $v > 0.1$ compared to 90% of total energy, 94% of magnetic energy, and 96% of kinetic helicity.
Fig.6.18c shows the contributions of transfer rates for total energy $T(\mathbf{k}|\mathbf{p},\mathbf{q})$, magnetic energy $T^{bb}(\mathbf{k}|\mathbf{p},\mathbf{q})$, and kinetic helicity $H^K(\mathbf{k}|\mathbf{p},\mathbf{q})$ for the triad interactions associated with the transfer of these quantities. These functions have maximum amplitudes at $v = 0.09, 0.16$ and 0.20 for total energy, magnetic energy, and kinetic helicity, respectively. All graphs fall to zero with v-value close to 1. Thus the magnitudes of interactions for nonlocal triads $k \neq p \neq q$

are larger than those for local triads $k \approx p \approx q$. Most nonlocal triads have two wavenumbers of similar size that are much larger than the third wavenumber ($k \approx p \gg q$, $k \approx q \gg p$, or $p \approx q \gg k$). Triad interactions in total energy is more nonlocal than those in magnetic energy and kinetic helicity (all peaks are in the region $v < 0.5$).

From Figs.6.18a, b, and c, the important conclusions that could be drawn are: the nonlinear transfer of magnetic helicity is highly nonlocal. The triad interactions in magnetic helicity are predominantly nonlocal and thus, it is possible that these nonlocal interactions drive the magnetic helicity flux towards the large scales resulting in the so called inverse cascade. The transfer of the other quantities predominantly local with a direct cascade. Although it is possible to have few nonlocal interactions for magnetic helicity (from the non-zero amplitude of the density function $Q(v)$), other quantities have a significant for highly nonlocal triad interactions (see Fig.6.18c). Our results show that nonlocality of the nonlinear total and magnetic energy transfer functions in forced MHD turbulence is more pronounced as in both freely decaying isotropic HD and MHD turbulence (cf. Figs.5.10 and 6.8a). Fig.6.19 depicts the functions $Q(v)$ for the same quantities in Fig.6.18a with the reference wavenumber in the small k region. Both the nonlocality and amplitude of the same magnetic helicity transfer are more than in the large k (cf. Fig.6.18a). The amplitude of the functions $Q(v)$ of the other quantities (total energy, magnetic energy, and kinetic helicity) also show a slight increase but not as strongly as magnetic helicity, in which the amplitude almost shows an order of increase from about 0.03 to 0.3. The nature of nonlinear transfer and triad interactions in these quantities remains the same as in the large k case.

6.7.2 Supplying only magnetic helicity through the forcing

Figs.6.20a shows the transfer density functions $Q(v)$ of the same quantities as in Fig.6.18a, when only magnetic helicity is supplied through the forcing, keeping the fraction of kinetic helicity at zero. The same reference wavenumbers that were used in large k and small k regions above are used here for computing the density functions.

Fig.6.20a shows $Q(v)$ when large k is used as reference number. This figure shows the strength of the nonlocal transfer and nonlocal triad interactions in magnetic helicity is larger than that when both kinetic and magnetic helicities are supplied, when the reference wavenumber is in the large k (cf. Fig.6.18a). The nature of transfer functions and triad interactions in the other three quantities is different from the case in Fig.6.18a. They do not exhibit any significant peak but have a flat profile, that indicates local transfer functions with nonlocal triad interactions. This result is shown in Fig.6.20b which depicts the contributions of transfer rates for total energy, magnetic energy, and kinetic helicity. These functions show that triad interactions in these quantitiesre are nonlocal. Fig.6.20c shows that the transfer function and triad interactions in magnetic helicity in small k are similar to that in Fig.6.19, but the interactions in the other three quantities are negligible compared with Fig.6.19.

From Figs.6.18a, 6.19, 6.20a, and 6.20c, we can conclude that when both magnetic and kinetic helicities are supplied through the forcing at small scales, there are two means of transfer and types of triad interactions in magnetic helicity, which bring down the strength of these interactions. When only magnetic helicity is supplied through the forcing, the interaction strength is significantly larger. The transfer functions and triad interactions in the

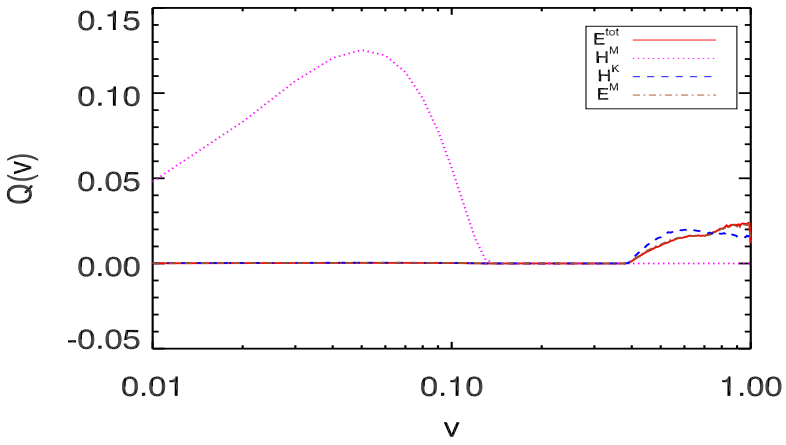

a)

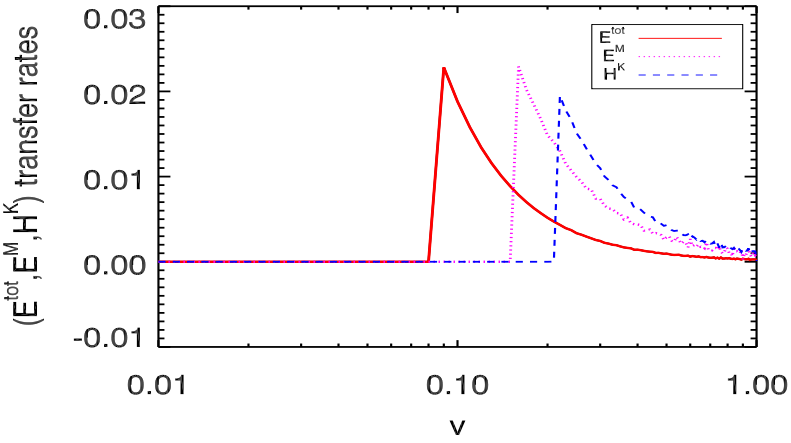

b)

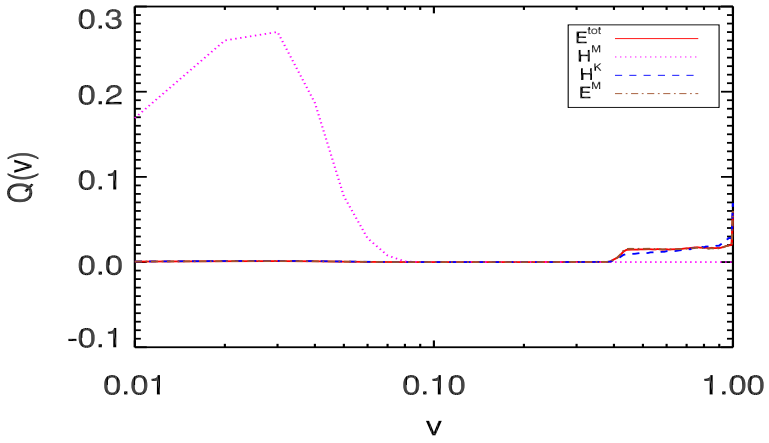

c)

Figure 6.20: a) The transfer density functions $Q(v)$ of magnetic helicity (magenta dotted line), kinetic helicity (dashed blue line), total energy (red solid line), and magnetic energy (brown dashed-dotted line) with large $k = 300$ as the reference wavenumber. The time at which this analysis was done is t=6.9. b) The contributions of the combined transfer rates for total energy (red solid line), magnetic energy (magenta dotted line), and kinetic helicity (blue dashed line) with large $k = 300$ as the reference wavenumber. c) The same as in (a) with small $k = 30$ as the reference wavenumber.

small scales for total energy, magnetic energy and kinetic helicity are significant when both magnetic and kinetic helicities are supplied through the forcing. But when only magnetic helicity is supplied through the forcing, this affect is absent. This behavior is similar for the transfer functions and triad interactions in the large scales. When kinetic helicity is supplied through the forcing along with the magnetic helicity, it increases the transfer and triad interactions in the small scales compared to the normal triad interactions in magnetic helicity. At the same time a signficant nonlocal presence, increasing the nonlocal triad interactions in the three quantities mentioned above. In the large scales, the effect of triad interactions of kinetic helicity are negligible. In this region, the triad interactions of magnetic helicity show a similar behavior to the case where only magnetic helicity is supplied through the forcing.
From our results for the spectral properties of magnetic helicity and other quantities (total energy, magnetic energy, and kinetic helicity) in the forced inverse cascade system, we conclude that several quantities show inverse spectral transfer. This is mainly due to the inverse spectral transfer of magnetic helicity which pulls all these quantities along with it. In Figs.6.19 and 6.20c, strong nonlocal transfer with nonlocal triad interactions are present in magnetic helicity. These transfers are predominantly local with nonlocal triad interactions in the other quantities. Thus our results support the argument that, because of the magnetic helicity has inverse cascade with predominantly nonlocal transfer, other quantities get transferred to large scales. The same behavior is also expected for the decaying MHD turbulence case. Even at small scales (see Figs.6.18a and 6.20a) magnetic helicity is highly nonlocal while all other quantities have less nonlocal transfers with nonlocal triad interactions. These nonlocal triad interactions are responsible for a small-scale dynamo that can operate and enhance magnetic energy at the expense of kinetic energy, while the flux of magnetic helicity is an inverse cascade.
While magnetic energy itself has a strong local transfer with several degrees of nonlocal triad interactions, linkages and twists in the magnetic field-lines could span several scales and are mostly nonlocal. In the large scale magnetic structure formation process, the twisted field lines play a more significant role than the local strength of the magnetic field itself. Malapaka [107] observes that the velocity of the flow slows down and kinetic helicity becomes weaker as the simulation progresses. This was explained in terms of magnetic energy gain at the expense of kinetic energy. The twists in the velocity field (which would be represented by kinetic helicity) aid in the enhancement of the nonlocality of triad interactions of magnetic field lines. The same process hinders the flow, thus keeping the twists in the velocity field local.
In this analysis for the forced inverse cascade MHD-turbulence case, we find that the transfer function and triad interactions of the nonlinear magnetic helicity are highly nonlocal in both small scales and large scales. Transfer functions and triad interactions of other quantities are significantly less nonlocal in nature. The strength of nonlocal transfer and triad interactions in large scales region for magnetic helicity do not change in any of the simulations we performed. However, in small scales region, the strength of these transfers and interactions varied depending on whether only magnetic helicity was applied through the forcing or both kinetic and magnetic helicities are supplied. In addition, our results show that the nature

of the transfer for other ideal invariants such as total energy, magnetic energy, and kinetic helicity changes from highly nonlocal, when the forcing is present to significantly local when the decaying turbulence takes over.

Chapter 7

Summary and Conclusions

The main objective of this thesis is to better understand the nonlinear dynamical processes of hydrodynamic (HD) and magnetohydrodynamic (MHD) turbulence. These processes play an important role in understanding the nature of energy transfer and structure formation in a turbulent flow. For this purpose, the spectral properties of transfer functions, triad interactions, and cascade directions of ideal quadratic invariants of incompressible two and three-dimensional HD and MHD turbulent flows are studied by analyzing data from high-resolution direct numerical simulations. High resolution is necessary to resolve the inertial range of a turbulent flow, where the nonlinear dynamics of turbulence are dominant and non-universal large- and small-scale effects can be neglected. All turbulent systems studied in this thesis are investigated using analysis of fully-developed, driven turbulence produced by large direct numerical pseudospectral simulations. The main advantage of the DNS method is that it does not use any additional physical approximations to solve the underlying equations. This point is of fundamental importance for turbulence investigations because no simplification of the nonlinear terms is employed. In addition, the DNS approach has the possibility of comprehensive diagnostics since calculated turbulent fields are known at all grid points in a computional box at all time steps. The nonlinear terms in the differential equations of Navier-Stokes and MHD turbulent flows lead to the property that three wavevectors $\mathbf{k}$, $\mathbf{p}$ and $\mathbf{q}$ are involved in any basic triad interaction between turbulent fluctuations with $\mathbf{k} + \mathbf{p} + \mathbf{q} = 0$, $k = |\mathbf{k}|$, $p = |\mathbf{p}|$, and $q = |\mathbf{q}|$. The transfer of an ideal invariant is typically between two Fourier modes with the third mode being regarded as responsible for the transfer; thus the triad interaction takes place between three wavenumbers.

We introduce an accurate approach for analyzing nonlinear turbulent transfer functions, triad interactions, and cascade processes in systems of incompressible HD and MHD turbulence. This approach involves a direct numerical examination of every wavenumber triad in the inertial range associated with the nonlinear terms in the differential equations of Navier-Stokes and MHD turbulent flows. The technique allows us to compute the spectral transfer functions, fluxes, and the spectral locality of the transfer functions and triad interactions. Our approach computes the transfer density functions $Q(v)$ and locality functions $W(v)$ for all triads with regard to the shape of the underlying wavenumber triads for each ideal invariant. The density function indicates the locality of the nonlinear transfer and triad interactions

between different scales of the wavenumber triads. The cascade direction of ideal invariant quantities in the inertial range can also be inferred from this diagnostic.

Ananlysis of $Q(v)$ and $W(v)$ helps us to understand the different types of cascade directions, which are useful for diagnostic astrophysical settings such as solar wind, interstellar clouds and intergalactic media. Our DNS results confirm the theoretical results of Kriachnan. Thus DNS illustrates the theory of energy transfer due to the nonlinear interactions of the modes in wavevectors space. The transfer density function $Q(v)$ and locality function $W(v)$ analysis is a powerful and straightforward tool for understanding the nature of transfer of physical invariants like energy, and the interaction of different spatial scales in triads. The density function analysis along with analysis of fluxes (see, O. Debliquy *et al.* [62]) could shed light on the nature of energy cascades or spectral transfer.

As a simple case of incompressible turbulence, isotropic hydrodynamic turbulence (two dimensions) is considered first. The simulation in this case is performed at high resolution (4096^2 grid points). The spectral properties of energy and enstrophy are studied. Results show that the nonlinear energy transfer is predominantly nonlocal from small scale (large wavenumbers) to large scales (small wavenumbers) with nonlocal triad interactions. There is a dual cascade with energy cascading toward large length-scales and enstrophy cascading toward small length-scales. Thus the nonlinear enstrophy transfer is characterized by local transfer through nonlocal triad interactions and a direct cascade direction. These results agree with the theoretical predictions of Kraichnan [5, 6] and the numerical analysis of Chen *et al.* [108] and Boffetta [75].

To understand the nonlinear dynamics of turbulent flow in real observable systems, a simulation is performed for three-dimensional hydrodynamic turbulence at a resolution of 1024^3 and Reynolds number, $\mathrm{Re} \approx 6300$. We observe Kolmogorov's 5/3 power-law for both energy and kinetic helicity spectra. In the inertial range, spectrally local transfer between two similar-size wavenumbers in a triad is dominant for both energy and kinetic helicity. The energy and kinetic helicity fluxes are positive and cascading from large scales to small scales in the inertial range. Thus there is a strong joint cascade of energy and helicity simultaneously in the inertial range.

The simplest model that involves the effects of a magnetic field on turbulent flow is the two-dimensional magnetohydrodynamic turbulence system. This configuration is attractive because it allows us to apply higher Reynolds numbers than the three-dimensional case. The dynamics of plasma in 2D-MHD systems can be seen as an approximation to fully 3D-MHD systems with a strong mean magnetic fields, where the turbulent dynamics are restricted to planes perpendicular to the mean magnetic field. In an incompressible isotropic 2D-MHD turbulent system, the simulation is performed with high resolution of 1024^2 and Reynolds number, $\mathrm{Re} = \mathrm{Rm} \approx 7 \times 10^4$. The transfers of energy and cross helicity are highly local between two similar-size wavenumbers in a given triad, with nonlocal triad interactions in the inertial range. The cross helicity cascades more slowly than the energy. The mean square magnetic vector potential is characterized by nonlocal transfer with inverse cascade from small scales to large scales through highly nonlocal triad interactions.

In 3D-MHD turbulence, the dynamics of the nonlinear processes are studied for three

cases: isotropic, anisotropic and forced-inverse cascade turbulence. For isotropic 3D-MHD turbulence, the simulation is performed with a resolution of 512^3 and Reynolds numbers $\mathrm{Re} = \mathrm{Rm} \approx 3300$. The initial ratio between kinetic and magnetic energy is unity. The statistics of the transfer density function $Q(v)$ and locality function $W(v)$ evidence both energy and cross helicity transfer between two similar-size wavenumbers. The total, kinetic, and magnetic energy transfer is local with a direct cascade through nonlocal triad interactions in the inertial range of decaying macroscopically isotropic MHD turbulence. The transfer of magnetic helicity is dominantly nonlocal through nonlocal triad interaction with an inverse cascade.

When the system is subject to a strong mean magnetic field, the turbulence becomes anisotropic. The simulation of anisotropic 3D-MHD is performed at a resolution of $1024^2 \times 256$ forced turbulence is simulated. The nonlinear transfer of the total energy and cross helicity is weaker and exhibits a moderate increase of nonlocality in both perpendicular and parallel directions compared to the isotropic case. Statistically, the total energy and cross helicity transfer functions are weakly local with a direct cascade through nonlocal triad interactions compared to the isotropic case. Magnetic helicity is characterized by nonlocal transfer through nonlocal triad interactions with an inverse cascade in both perpendicular and parallel directions to the mean magnetic field.

Studies of the spectral properties of ideal quadratic invariants in two approximate scaling ranges are performed for the first time for forced-inverse cascade 3D-MHD turbulence using high resolution of 1024^3. Forcing is applied to the system in two different ways, one in large wavenumber region and other in small wavenumber region for all quantities in the forced turbulent system. Two cases are studied: one in which both kinetic and magnetic helicities are injected by the forcing and one in which only magnetic helicity is injected. Analyses of the transfer density function $Q(v)$ and locality function $W(v)$ show that the nonlinear transfer of magnetic helicity is highly nonlocal with an inverse cascade. Transfer of other quantities (*i.e.,* total, magnetic energy, and kinetic helicity) is significantly local in nature. The strength of nonlocal interactions at large scales for magnetic helicity is the same in both cases studied. At small scales, the strength of the interactions vary depending on whether only magnetic helicity is forced, or both kinetic and magnetic helicities are forced.

From the spectral results of several different cases of turbulence investigated in the presented work, the transfer functions for kinetic energy in 2D-HD, mean-square magnetic vector potential in 2D-MHD, and magnetic helicity in 3D-MHD are nonlocal through nonlocal triad interactions with an inverse cascade. For all other quantities (*e.g.,* total energy and cross helicity in 2D and 3D-MHD), the transfer functions are predominantly local through nonlocal triad interactions with a direct cascade. The transfer between velocity and magnetic modes is local and there is no evidence of nonlocal transfer. The results show that nonlocal triad interactions dominate for all studied cases. Indeed, nonlocal triad interactions in MHD turbulence are significantly more pronounced than in HD turbulence. Thus nonlocal interactions have an effect on the dynamics of a turbulent cascade. Moreover, our results could be of interest to experimentalists working on 3D hydrodynamic turbulence, since we can perform

diagnostics that would be difficult to develop in laboratory experiments. The investigation of three-dimensional magnetohydrodynamic turbulence system is particularly attractive because it represents a useful model for a detailed study of the spectral properties of nonlinear turbulent dynamics. Understanding the turbulent dynamics in MHD could impact such diverse scientific fields as Fusion or satellite design.

We use two different forcing techniques and find that the type of forcing leaves a unique signature in both the density function and locality function. An analysis of these two functions could determine where and how energy is entering a turbulent system. An inverse cascade of magnetic helicity can create large-scale magnetic structures. Thus the development of large-scale magnetic structure is because of the highly nonlocal triad interactions in the twists of the field-lines rather than slightly nonlocal interactions of the magnetic field itself. We see an evidence of the formation of these large-scale structure in our simulation of 3D-MHD with highly nonlocal triad interactions. It is suggested that performing the transfer density function $Q(v)$ analysis for the magnetic field data obtained from different space missions. Such an analysis would help in better understanding of the physics of large-scale magnetic structure formation in the universe. Also, it is suggested that it is important to extend the analysis of the density function $Q(v)$ to various possible turbulent flow systems to shed light on the fundamental spectral properties of turbulent flows.

Appendix A

The Fourier transformed energy equation and conservation theory of kinetic energy in fluid turbulence

In order to show the theorem of detailed conservation of the kinetic energy in fluid turbulence, firstly the Fourier transformed of the energy equation must be shown. Since we are interested in a statistical form of the Fourier transformed Navier-Stokes equations, in this appendix the velocity will be replaced in this equation by its pair correlation function.
However, from sections 1.5 and 3.1, the Fourier transformed Navier-Stokes equations can be written as

$$(\frac{\partial}{\partial t} + \nu k^2)v_i(\mathbf{k}) = -\frac{i}{2}P_{ijm}(\mathbf{k}) \iint_{\mathbb{R}^6} \hat{v}_j(\mathbf{p})\hat{v}_m(\mathbf{q})\delta(\mathbf{k}-\mathbf{p}-\mathbf{q})d^3pd^3q, \tag{A.1}$$

where

$$P_{ijm} := [k_m(\delta_{ij} - \frac{k_ik_j}{k^2}) + k_j(\delta_{im} - \frac{k_ik_m}{k^2})]. \tag{A.2}$$

The operator P_{ijm} has thus been converted from a differential operator to an algebraic one, which makes calculations much easier. Eq.(A.1) do not completely describe stationary turbulence although time did not yet appear explicitly in it. A turbulent flow is said to be stationary if its velocity statistics do not change with time, *i.e.,* if its probability density function is invariant under a shift of time. Like in the case of homogeneity of space, the moments of higher order of the velocity only depend on the velocity differences over time intervals, and the velocity correlation function becomes

$$\langle v_i(\mathbf{k},t)v_j(\mathbf{k}',t')\rangle = w_{ij}(\mathbf{k},t-t')\delta_{\mathbf{k},\mathbf{k}'} = P_{ij}(\mathbf{k})w(k,t-t')\delta_{\mathbf{k},\mathbf{k}'}. \tag{A.3}$$

where $w_{ij}(\mathbf{k})$ is the tensor describing the pair correlation function and it must be depend on the vector direction and it must have the general form

$$w_{ij}(\mathbf{k}) = A(k)\delta_{ij} + B(k)k_ik_j + C(k)\epsilon_{ijl}k_l,$$

where A, B and C depend on the norm of the vector $\mathbf{k}$, $k = |\mathbf{k}|$. the symmetry condition $w_{ij}(\mathbf{k}) = w_{ji}(-\mathbf{k})$ and the incompressibility condition in Fourier space $k_j w_{ij} = 0$ lead $C = 0$ and $Ak_i + Bk_i k^2 = 0$, thus $B = -A/k^2$. Taking w instead A, the tensor w_{ij} finally written as

$$w_{ij}(\mathbf{k}) = w(k)(\delta_{ij} - \frac{k_i k_j}{k^2}),$$

Introducing, $(\delta_{ij} - \frac{k_i k_j}{k^2}) = P_{ij}(\mathbf{k})$ is the projection tensor, then we can write

$$w_{ij}(\mathbf{k}) = P_{ij}(\mathbf{k}) w(k).$$

This lead us to write the velocity correlation function with time intervals by Eq.A.3
In other hand, in non-stationary turbulent flows, the dissipative effects of viscosity usually transform these flows rapidly into laminar flows. In order to keep the flow turbulent, thus stationary, a hypothetical (homogeneous isotropic) stirring force[1] $f_i(\mathbf{k})$ is introduced into Eq.(A.1)

$$(\frac{\partial}{\partial t} + \nu k^2) v_i(\mathbf{k}) = -\frac{i}{2} P_{ijm}(\mathbf{k}) \iint v_j(\mathbf{p}) v_m(\mathbf{q}) \delta(\mathbf{k} - \mathbf{p} - \mathbf{q}) d^3p d^3q + f_i(\mathbf{k}). \tag{A.4}$$

But since the nature of the force is not known, authors leave it away[29] in the remaining calculations. In order to compute the evolution equation for the density of kinetic energy for the stationary case, multiply Eq.(A.1) by $v_i(\mathbf{k}', t)$ (for the non-stationary case, by $v_i(\mathbf{k}', t')$). We omit writing the time-dependance of the velocity components for brevity in the following computations, but we keep in mind the presence of the time variable t in the latter. Then we have

$$\begin{aligned}
\frac{\partial}{\partial t}(v_i(\mathbf{k}) v_i(\mathbf{k}')) &= v_i(\mathbf{k}) \frac{\partial v_i(\mathbf{k}')}{\partial t} + v_i(\mathbf{k}') \frac{\partial v_i(\mathbf{k})}{\partial t} \\
&= v_i(\mathbf{k}) \left[-\nu k'^2 v_i(\mathbf{k}') - \frac{i}{2} P_{ijm}(\mathbf{k}') \iint_{\mathbb{R}^6} v_j(\mathbf{p}) v_m(\mathbf{q}) \delta(\mathbf{k}' - \mathbf{p} - \mathbf{q}) d^3p d^3q \right] \\
&+ v_i(\mathbf{k}') \left[-\nu k^2 v_i(\mathbf{k}) - \frac{i}{2} P_{ijm}(\mathbf{k}) \iint_{\mathbb{R}^6} v_j(\mathbf{p}) v_m(\mathbf{q}) \delta(\mathbf{k} - \mathbf{p} - \mathbf{q}) d^3p d^3q \right].
\end{aligned} \tag{A.5}$$

Averaging gives

$$\begin{aligned}
(\frac{\partial}{\partial t} + \nu(k^2 + k'^2)) \langle v_i(\mathbf{k}) v_i(\mathbf{k}') \rangle = -\frac{i}{2} \iint_{\mathbb{R}^6} \big[& P_{ijm}(\mathbf{k}') \langle v_i(\mathbf{k}) v_j(\mathbf{p}) v_m(\mathbf{q}) \rangle \delta(\mathbf{k}' - \mathbf{p} - \mathbf{q}) \\
& + P_{ijm}(\mathbf{k}) \langle v_i(\mathbf{k}') v_j(\mathbf{p}) v_m(\mathbf{q}) \rangle \delta(\mathbf{k} - \mathbf{p} - \mathbf{q}) d^3p d^3q.
\end{aligned} \tag{A.6}$$

Since the ensemble averages on the r.h.s. are proportional to delta-functions, we can momentarily set them to

$$\langle v_i(\mathbf{k}) v_j(\mathbf{p}) v_m(\mathbf{q}) \rangle =: f(\mathbf{p}, \mathbf{q}) \delta(\mathbf{k} + \mathbf{p} + \mathbf{q}), \tag{A.7}$$

[1] This force has a "non-real" character, since in real life it arises by effects that are in contradiction with homogeneity and isotropy

$$\langle v_i(\mathbf{k}')v_j(\mathbf{p})v_m(\mathbf{q})\rangle =: f(\mathbf{p},\mathbf{q})\delta(\mathbf{k}'+\mathbf{p}+\mathbf{q}). \tag{A.8}$$

and replace the averages on the l.h.s. by the expression for the correlation tensor (cf. Eq.A.3), which is the standard form of the correlation function in homogeneous isotropic turbulence,

$$\langle v_i(\mathbf{k})v_j(\mathbf{k}')\rangle = P_{ij}(\mathbf{k})w(k)\delta(\mathbf{k}+\mathbf{k}').$$

Thus Eq.(A.6) can be written as

$$\begin{aligned}(\frac{\partial}{\partial t}+\nu(k^2+k'^2))&2w(k)\delta(\mathbf{k}+\mathbf{k}')\\ &= -\frac{i}{2}\iint_{\mathbb{R}^6}\left[P_{ijm}(\mathbf{k}')f(\mathbf{p},\mathbf{q})\delta(\mathbf{k}+\mathbf{p}+\mathbf{q})\delta(\mathbf{k}'-\mathbf{p}-\mathbf{q})\right.\\ &+\left. P_{ijm}(\mathbf{k})f(\mathbf{p},\mathbf{q})\delta(\mathbf{k}'+\mathbf{p}+\mathbf{q})\delta(\mathbf{k}-\mathbf{p}-\mathbf{q})\right]d^3p\,d^3q\\ &= -\frac{i}{2}\delta(\mathbf{k}+\mathbf{k}')\int_{\mathbb{R}^3}\left[P_{ijm}(\mathbf{k}')f(\mathbf{k}'-\mathbf{q},\mathbf{q})+P_{ijm}(\mathbf{k})f(\mathbf{k}'-\mathbf{q},\mathbf{q})\right]d^3q.\end{aligned} \tag{A.9}$$

At this stage, the $\delta(\mathbf{k}+\mathbf{k}')$-function can be cancelled out on both sides of the equation. Reintroducing the ensemble averages on the r.h.s. using (A.7) for $\mathbf{k}'=-\mathbf{k}$, we get

$$\begin{aligned}&(\frac{\partial}{\partial t}+2\nu k^2)2w(k)\\ &= -\frac{i}{2}\iint_{\mathbb{R}^6}\left[P_{ijm}(-\mathbf{k})f(\mathbf{p},\mathbf{q})\delta(\mathbf{k}+\mathbf{p}+\mathbf{q})+P_{ijm}(\mathbf{k})f(\mathbf{p},\mathbf{q})\delta(\mathbf{p}-\mathbf{k}+\mathbf{q})\right]d^3q\,d^3p\\ &= -\iint_{\mathbb{R}^6}P_{ijm}(\mathbf{k})\frac{i}{2}\left[-\langle v_i(\mathbf{k})v_j(\mathbf{p})v_m(\mathbf{q})\rangle+\langle v_i(-\mathbf{k})v_j(\mathbf{p})v_m(\mathbf{q})\rangle\right]d^3qd^3p.\end{aligned} \tag{A.10}$$

Since the integrals are symmetric with respect to $\mathbf{p}$ and $\mathbf{q}$, they remain unchanged by a change of variables in the second summ and of the integrals into $-\mathbf{p}$ and $-\mathbf{q}$,

$$\begin{aligned}&(\frac{\partial}{\partial t}+2\nu k^2)w(k)\\ &= -\frac{1}{2}\iint_{\mathbb{R}^6}P_{ijm}(\mathbf{k})\frac{i}{2}\left[-\langle v_i(\mathbf{k})v_j(\mathbf{p})v_m(\mathbf{q})\rangle+\langle v_i(-\mathbf{k})v_j(-\mathbf{p})v_m(-\mathbf{q})\rangle\right]d^3q\,d^3p\\ &= -\frac{1}{2}\iint_{\mathbb{R}^6}P_{ijm}(\mathbf{k})\frac{i}{2}\left[\langle v_i^*(\mathbf{k})v_j^*(\mathbf{p})v_m^*(\mathbf{q})\rangle-\langle v_i(\mathbf{k})v_j(\mathbf{p})v_m(\mathbf{q})\rangle\right]d^3q\,d^3p\end{aligned} \tag{A.11}$$

Taking $z := \langle v_i(\mathbf{k})v_j(\mathbf{p})v_m(\mathbf{q})\rangle$ and using the expression $Im(z)=\frac{i}{2}(z^*-z)$, we finally have

$$(\frac{\partial}{\partial t}+2\nu k^2)w(k) = -\frac{1}{2}P_{ijm}(\mathbf{k})\iint_{\mathbb{R}^6}Im\left[\langle v_i(\mathbf{k})v_j(\mathbf{p})v_m(\mathbf{q})\rangle\right]d^3q\,d^3p \tag{A.12}$$

The ensemble average on the r.h.s. in equation (A.12) already contains a delta-function, $\delta(\mathbf{k}+\mathbf{p}+\mathbf{q})$, according to equation (A.7). This implies that the integrals vanish if the vectors $\mathbf{k}$, $\mathbf{p}$ and $\mathbf{q}$ do not form a triangle, *i.e.,* if their sum is nonzero.
Using the characteristic notations of (A.3) for stationary flows, the resulting equation with

reintroduced time variables

$$(\frac{\partial}{\partial t} + \nu k^2)w(k, t - t') = \frac{1}{2}S(k, t - t'), \tag{A.13}$$

where

$$S(k, t - t') := -P_{ijm}(\mathbf{k}) \iint_{\mathbb{R}^6} Im\left(\langle v_i(\mathbf{k}, t')v_j(\mathbf{p}, t)v_m(\mathbf{q}, t)\rangle\right) d^3p\, d^3q, \tag{A.14}$$

describes the evolution of the density of kinetic energy[2].
In order to get an equation for non-stationary flows as well, we write t' as a full variable by replacing $w(k, t - t')$ and $S(k, t - t')$ by $w(k, t, t')$ and by $S(k, t, t')$ respectively. Then, since $w(k, t, t')$ is symmetric for fixed k with respect to an interchange of its variables t and t' [109], the partial derivative $\frac{\partial}{\partial t}w(k, t, t)$ is

$$\begin{aligned}\frac{\partial}{\partial t}w(k, t, t) &= \frac{\partial}{\partial t_1}w(k, t_1, t_2)|_{t_1=t_2=t} + \frac{\partial}{\partial t_2}w(k, t_1, t_2)|_{t_1=t_2=t} \\ &= 2\frac{\partial}{\partial t_1}w(k, t, t) = -2(\nu k^2 w(k, t, t) - \frac{1}{2}S(k, t, t)),\end{aligned} \tag{A.15}$$

where we used equation (A.13) to derive the last equality.
Thus, in the non-stationary case and for $t = t'$, the evolution equation for the density w of kinetic energy per unit mass is

$$(\frac{\partial}{\partial t} + 2\nu k^2)w(k, t, t) = S(k, t, t), \tag{A.16}$$

where

$$S(k, t, t) = -\frac{1}{2}P_{ijm}(\mathbf{k}) \iint_{\mathbb{R}^6} Im\left(\langle v_i(\mathbf{k}, t)v_j(\mathbf{p}, t)v_m(\mathbf{q}, t)\rangle\right)\, d^3p\, d^3q. \tag{A.17}$$

For simplicity of notation, let us write $S(k, t)$ instead of $S(k, t, t)$ when necessary. S is called the kinetic energy transfer. It has to be emphasized that this nonlinear term in wavenumber space only appears if the three vectors $\mathbf{p}, \mathbf{k}, \mathbf{q}$ form a triangle, *i.e.,* if their sum is zero. In this case, they form a so-called **triad**. These triads are the key of understanding the phenomenon of energy transfer in turbulent flows, representing the fundamental object of interest in the study of Navier-Stokes turbulence. The triads existence comes from the presence, under the integral sign, of the delta-function, because the triple correlation is proportional to a delta function in the case of isotropy. If these vectors do not form a triangle, then the nonlinear term vanishes.
The nonlinear term on the r.h.s of the evolution equation (A.16), $S(k, t, t)$, can be brought into a form which shows an interesting kind of conservation of the kinetic energy. Recall the expression for the transfer function

$$S(k, t, t) = -\frac{1}{2}P_{ijm}(\mathbf{k}) \iint_{\mathbb{R}^6} Im\left(\langle v_i(\mathbf{k}, t)v_j(\mathbf{p}, t)v_m(\mathbf{q}, t)\rangle\right)\, d^3p\, d^3q, \tag{A.18}$$

[2]It can been shown in [29] (see the Appendix) that the expression for S in fact depends on the modulus of the vector $\mathbf{k}$. We therefore use the notation $S(k, t - t')$ introduced by Leslie.

where

$$P_{ijm}(\mathbf{k}) = [k_m(\delta_{ij} - \frac{k_i k_j}{k^2}) + k_j(\delta_{im} - \frac{k_i k_m}{k^2})]. \tag{A.19}$$

Neglecting time for the present calculations, using the convention of summation for double indices and the incompressibility condition in Fourier space $k_i v_i(\mathbf{k}) = 0$, we have

$$\begin{aligned} P_{ijm}(\mathbf{k}) &\langle v_i(\mathbf{k}) v_j(\mathbf{p}) v_m(\mathbf{q}) \rangle \\ &= \left\langle [k_m(\delta_{ij} - \frac{k_i k_j}{k^2}) + k_j(\delta_{im} - \frac{k_i k_m}{k^2})] v_i(\mathbf{k}) v_j(\mathbf{p}) v_m(\mathbf{q}) \right\rangle \\ &= \left\langle k_m(\delta_{ij} - \frac{k_i k_j}{k^2}) v_i(\mathbf{k}) v_j(\mathbf{p}) v_m(\mathbf{q}) \right\rangle \\ &+ \left\langle k_j(\delta_{im} - \frac{k_i k_m}{k^2}) v_i(\mathbf{k}) v_j(\mathbf{p}) v_m(\mathbf{q}) \right\rangle \\ &= \langle (\mathbf{k} \cdot \mathbf{v}(\mathbf{q}))\, (\mathbf{v}(\mathbf{p}) \cdot \mathbf{v}(\mathbf{k})) \rangle + \langle (\mathbf{k} \cdot \mathbf{v}(\mathbf{p}))\, (\mathbf{v}(\mathbf{q}) \cdot \mathbf{v}(\mathbf{k})) \rangle \,. \end{aligned} \tag{A.20}$$

Thus the evolution equation of energy becomes

$$\begin{aligned} (\frac{\partial}{\partial t} + 2\nu k^2) w(k,t,t) = \\ - \frac{1}{2} \iint_{\mathbb{R}^6} Im\left[\langle (\mathbf{k} \cdot \mathbf{v}(\mathbf{q}))(\mathbf{v}(\mathbf{p}) \cdot \mathbf{v}(\mathbf{k})) \rangle + \langle (\mathbf{k} \cdot \mathbf{v}(\mathbf{p}))(\mathbf{v}(\mathbf{q}) \cdot \mathbf{v}(\mathbf{k})) \rangle \right] d^3p d^3q. \end{aligned} \tag{A.21}$$

Using the following abbreviation

$$T(\mathbf{k}|\mathbf{p},\mathbf{q}) = -Im\left[\langle (\mathbf{k} \cdot \mathbf{v}(\mathbf{q}))(\mathbf{v}(\mathbf{p}) \cdot \mathbf{v}(\mathbf{k})) \rangle + \langle (\mathbf{k} \cdot \mathbf{v}(\mathbf{p}))(\mathbf{v}(\mathbf{q}) \cdot \mathbf{v}(\mathbf{k})) \rangle \right], \tag{A.22}$$

a cyclic permutation of $\mathbf{k}$, $\mathbf{p}$ and $\mathbf{q}$ results in

$$T(\mathbf{k}|\mathbf{p},\mathbf{q}) + T(\mathbf{p}|\mathbf{q},\mathbf{k}) + T(\mathbf{q}|\mathbf{k},\mathbf{p}) = 0. \tag{A.23}$$

This is the "theorem of detailed conservation" [76], which shows that for a single triad

$$\{\mathbf{v}(\mathbf{k}), \mathbf{v}(\mathbf{p}), \mathbf{v}(\mathbf{q}); \mathbf{k} + \mathbf{p} + \mathbf{q} = 0\}, \tag{A.24}$$

and this implies that the kinetic energy is conservatively exchanged between these modes[3]. In other words, energy is not lost within the triad, thus rendering the meaning of "detailed" conservation more explicit. A consequence of detailed conservation is the conservation of kinetic energy in a certain region of wavenumbers called inertial range, where the energy spectrum exhibits self-similar behaviour and where turbulent energy production and dissipation are negligible. The key information throughout these considerations is the fact that the turbulent energy is conserved by the non-linear terms of the Navier-Stokes equations.

[3]Note that Rose and Sulem ([76], p.447) derived this "theorem" using the evolution equation for the quantity $|v(\mathbf{k})|^2$ and starting with the Fourier transformed, incompressible Euler equation, instead of using the evolution equation for the averaged energy density.

The energy equation (cf. Eq.A.21) can now be written as

$$(\frac{\partial}{\partial t} + 2\nu k^2)w(k,t) = \frac{1}{2}\iint_{\mathbb{R}^6} T(\mathbf{k}|\mathbf{p},\mathbf{q})\,d^3p d^3q, \tag{A.25}$$

where

$$T(\mathbf{k}|\mathbf{p},\mathbf{q}) = -Im\left[\langle(\mathbf{k}\cdot\mathbf{v}(\mathbf{q}))(\mathbf{v}(\mathbf{p})\cdot\mathbf{v}(\mathbf{k}))\rangle + \langle(\mathbf{k}\cdot\mathbf{v}(\mathbf{p}))(\mathbf{v}(\mathbf{q})\cdot\mathbf{v}(\mathbf{k}))\rangle\right].$$

This expression for the nonlinear term is in fact the starting point of the models made for numerical calculations. The quantity, $T(\mathbf{k}|\mathbf{p},\mathbf{q})$ has been interpreted by Lesieur [1] as the "combined energy transfer" rate from the modes $\mathbf{p}$ and $\mathbf{q}$ to the mode $\mathbf{k}$, then used by many authors (see, for example [53, 26, 54, 55, 56, 57]).

Appendix B

Transfer density function, $Q(v)$ of the enstrophy

The enstrophy (mean square vorticity), $\Omega(k)$ balance equation in 2D-HD is given by Kriachnan [6]

$$\Omega(k) = \int_0^\infty \int_0^\infty k^2 T(k,p,q) dpdq. \tag{B.1}$$

with $k = |\mathbf{k}|, p = |\mathbf{p}|$, $q = |\mathbf{q}|, \mathbf{k} = \mathbf{p} + \mathbf{q}$ in the ineracting triad.
where the quantity $k^2T(k,p,q) = k^2T(k,q,p)$ is the net rate of enstrophy transfer into mode k from interactions with modes p and q. Then the mean rate of transfer of enstrophy from below k to above k is

$$\begin{aligned} Z(k) &= \int_k^\infty (k^{'})^2 T(k^{'}) dk^{'} = \int_k^\infty \left(\int_0^\infty \int_0^\infty (k^{'})^2 T(k^{'},p,q) dpdq \right) dk^{'}. \\ &= \int_k^\infty (k^{'})^2 dk^{'} \int_0^k \int_0^k T(k^{'},p,q) dpdq - \int_0^k (k^{'})^2 dk^{'} \int_k^\infty \int_k^\infty T(k^{'},p,q) dpdq. \end{aligned} \tag{B.2}$$

where the first integral on the r.h.s. of Eq.(B.2) gives the total rate of enstrophy gained into the range $k^{'} > k$ after triad interactions with p and q that are smaller than k, while the second integral gives the total rate loss of enstrophy in the range $k^{'} < k$ after triad interactions with p and q that are bigger than k.
Repeating the procedure which showed in section 3.5 for the enstrophy flux, $Z(k)$ in Eq.(B.2), with putting $n = 3$ as a power of the scaling factor in Kraichman's assumption [6], we can obtain

$$Z(k) = \int_0^1 dv \int_1^{1+v} dw \left[\ln(w) w^2 T(w,1,v) + \ln(v) v^2 T(v,1,w) \right]. \tag{B.3}$$

Again by applying the properties of 2D-HD, which in Eq.(5.16) into Eq.(B.3), we obtain

$$Z(k) = \int_0^1 dv \int_1^{1+v} dw \left[\ln(w) w^2 T(1-v^2) + \ln(v) v^2 T(w^2-1) \right] \frac{T(1,v,w)}{v^2 - w^2}. \tag{B.4}$$

Introducing a new function,

$$Q(v) = \frac{v}{\beta} \int_1^{1+v} dw \left[\ln(w) w^2 T(1-v^2) + \ln(v) v^2 T(w^2-1) \right] \frac{T(1,v,w)}{v^2 - w^2}. \tag{B.5}$$

where β is the total rate of enstrophy dissipation, then Eq.(B.4) for the enstrophy flux in 2D-HD can be written by

$$Z(k) = \int_0^1 dv \frac{\beta}{v} Q(v) = \beta \int_0^1 Q(v) \frac{dv}{v}. \tag{B.6}$$

The function $Q(v)$ in Eq.(B.6) serves as a measure of the locality or nonlocality of enstrophy transfer of a given interacting triad in 2D-HD turbulence, showing the structure of the inertial range enstrophy transfer in 2D-HD.

Appendix C

Transfer density function, $Q(v)$ of the mean square magnetic vector potential

The mean square magnetic vector potential A balance equation in 2D-MHD is given by [56]

$$A(k) = \int_0^\infty \int_0^\infty k^{-2} T^{bb}(k,p,q) dpdq. \tag{C.1}$$

where the quantity $k^{-2}T^{bb}(k,p,q) = k^{-2}T^{bb}(k,q,p)$ is the net rate of mean square magnetic vector potential transfer into mode k from interactions with modes p and q. Then the mean rate of transfer (the flux) of the squared magnetic vector potential from below k to above k is

$$\begin{aligned} Y(k) &= \int_k^\infty (k^{'})^{-2} T^{bb}(k^{'}) dk^{'} = \frac{1}{2} \int_k^\infty \left(\int_0^\infty \int_0^\infty (k^{'})^{-2} T^{bb}(k^{'},p,q) dpdq \right) dk^{'}. \\ &= \frac{1}{2} \int_k^\infty (k^{'})^{-2} dk^{'} \int_0^k \int_0^k T^{bb}(k^{'},p,q) dpdq - \frac{1}{2} \int_0^k (k^{'})^{-2} dk^{'} \int_k^\infty \int_k^\infty T^{bb}(k^{'},p,q) dpdq. \end{aligned} \tag{C.2}$$

where the first integral on the r.h.s. of Eq.(C.2) gives the total rate of the mean square magnetic vector potential gained into the range $k^{'} > k$ after triad interactions with p and q that are smaller than k, while the second integral gives the total rate loss of the mean square magnetic vector potential in the range $k^{'} < k$ after triad interactions with p and q that are bigger than k.
Using the symmetry of $T^{bb}(k^{'},p,q)$, where $T^{bb}(k^{'},p,q)$=$T^{bb}(k^{'},q,p)$ we can write $2\int_0^k dp \int_0^p dq$ instead of $\int_0^k dp \int_0^k dq$ in the first integral and $2\int_k^\infty dp \int_p^\infty dq$ instead of $\int_k^\infty dp \int_k^\infty dq$ in the second integral, then we can write

$$\begin{aligned} Y(k) = &\int_k^\infty (k^{'})^{-2} dk^{'} \int_0^k \int_0^p T^{bb}(k^{'},p,q) dpdq \\ &- \int_0^k (k^{'})^{-2} dk^{'} \int_k^\infty \int_p^\infty T^{bb}(k^{'},p,q) dpdq. \end{aligned} \tag{C.3}$$

Choosing the following variable changes, $p = \frac{k}{u}$, $k^{'} = pw$, $q = pv$ in the first term and $p = \frac{k}{u}$, $k^{'} = pv$, $q = pw$ in the second term of the right hand side of Eq.(C.3), we have

$$Y(k) = \int_0^1 dv \int_1^\infty du \int_u^\infty dw \frac{1}{u}\left(\frac{k}{u}\right) w^{-2} T^{bb}(\frac{k}{u}w, \frac{k}{u}, \frac{k}{u}v) - \int_0^1 du \int_1^\infty dw \int_0^u dv \frac{1}{u}\left(\frac{k}{u}\right) v^{-2} T^{bb}(\frac{k}{u}v, \frac{k}{u}, \frac{k}{u}w). \tag{C.4}$$

Kraichnan assumed that the double and triple moments at the instant considered satisfy [6]

$$\frac{T(ak, ap, aq)}{T(k, p, q)} = a^{-(1+3n)/2}.$$

where a is an arbitrary scaling factor and n is unknown. Putting $n = 1/3$, where the magnetic energy spectrum can be expressed in terms of the mean square magnetic vector potential by [110]

$$E_k^M = k^2 A_k \propto k^{-1/3}. \tag{C.5}$$

then we obtain

$$\frac{T(ak, ap, aq)}{T(k, p, q)} = a^{-1} \Rightarrow T(ak, ap, aq) = a^{-1} T(k, p, q). \tag{C.6}$$

Using Eq.(C.6) with $a = k/u$, then Eq.(C.4) can be written by

$$\begin{aligned} Y(k) &= \int_0^1 dv \int_1^\infty du \int_u^\infty dw \frac{1}{u} a w^{-2} T^{bb}(aw, a, av) - \int_0^1 du \int_1^\infty dw \int_0^u dv \frac{1}{u} a v^{-2} T^{bb}(av, a, aw). \\ &= \int_0^1 dv \int_1^\infty du \int_u^\infty dw \frac{1}{u} w^{-2} T^{bb}(w, 1, v) - \int_0^1 du \int_1^\infty dw \int_0^u dv \frac{1}{u} v^{-2} T^{bb}(v, 1, w). \end{aligned} \tag{C.7}$$

Because of $\int_1^\infty du \int_u^\infty dw$ is equivalent to $\int_1^\infty dw \int_1^w du$ in first integral and $\int_0^1 du \int_0^u dv$ is equivalent to $\int_0^1 dv \int_v^1 du$ in the second integral, Eq.(C.7) can be written by

$$\begin{aligned} Y(k) &= \int_0^1 dv \int_1^\infty dw \int_1^w du \frac{1}{u} w^{-2} T^{bb}(w, 1, v) - \int_0^1 dv \int_1^\infty dw \int_v^1 du \frac{1}{u} v^{-2} T^{bb}(v, 1, w) \\ &= \int_0^1 dv \int_1^\infty dw \ln(w) w^{-2} T^{bb}(w, 1, v) + \int_0^1 dv \int_1^\infty dw \ln(v) v^{-2} T^{bb}(v, 1, w) \\ &= \int_0^1 dv \int_1^\infty dw \left[\ln(w) w^{-2} T^{bb}(w, 1, v) + \ln(v) v^{-2} T^{bb}(v, 1, w)\right]. \end{aligned} \tag{C.8}$$

With the consideration that T^{bb} is non-zero only if w, 1 and v are form a triangle, so in Eq.(C.8) the integration border ∞ replaced by $1 + v$, then we can write

$$Y(k) = \int_0^1 dv \int_1^{1+v} dw \left[\ln(w) w^{-2} T^{bb}(w, 1, v) + \ln(v) v^{-2} T^{bb}(v, 1, w)\right] \tag{C.9}$$

The above equation expresses for the flux (the cascade rate) of the mean square magnetic vector potential as integrals over contributions from all possible shapes of the triangles formed

by the wavenumbers k, p, q in Eq.(C.2). If we introduce a new function, which is

$$Q(v) = \frac{v}{D_A} \int_1^{1+v} dw \left[\ln(w) w^{-2} T^{bb}(w, 1, v) + \ln(v) v^{-2} T^{bb}(v, 1, w) \right]. \tag{C.10}$$

we get

$$Y(k) = D_A \int_0^1 \frac{dv}{v} Q(v). \tag{C.11}$$

where D_A is the rate of the mean square magnetic vector potential dissipation. Therefore, the function $Q(v)$ serves as a measure of the localness of the mean square magnetic vector potential transfer.

Bibliography

[1] M. Lesieur. Turbulence in fluids. *Kluwer Academic Publishers*, 1997.

[2] D. Biskamp. Magnetohydrodynamic turbulence. *Cambridge University Press, Cambridge, England*, 2003.

[3] Ya. B. Zeldovich, A. A. Ruzmaikin, and D. D. Sokoloff. Magnetic field in astrophysics. *(Gordon& Breach Science Publications, New york)*, 1990.

[4] W.-C. Müller. Magnetohydrodynamic turbulence. *Lec. Notes Phys.*, 756:223–254, 2009.

[5] R. H. Kraichnan. Inertial-range transfer in two- and three-dimensional turbulence. *J. Fluids Mech.*, 47:525–535, 1971.

[6] R. H. Kraichnan. Inertial ranges in two dimensional turbulence. *Phys. Fluids*, 10:1417–1423, 1967.

[7] J. Domaradzki and R. Rogallo. Local energy transfer and nonlocal interactions in homogenous, isotropic turbulence. *Phys. Fluids A*, 2:413–426, 1990.

[8] A. Alexakis, P. D. Mininni, and A. Pouquet. Shell-to-shell energy transfer in magnetohydrodynamics. I. Steady state turbulence. *Phys. Rev. E*, 72:046301, 2005.

[9] M. K. Verma. Field theoretic calculation of renormalized viscosity, renormalized resistivity, and energy fluxes of magnetohydrodynamic turbulence. *Phys. Rev. E*, 64:026305, 2001.

[10] M. K. Verma. Field theoretic calculation of energy cascade rates in non-helical magnetohydrodynamic turbulence. *Pramana J. Phys.*, 61:577–494, 2003.

[11] A. Alexakis, B. Bigot, H. Politano, and S. Galtier. Anisotropic fluxes and nonlocal interactions in magnetohydrodynamic turbulence. *Phys. Rev. E*, 76:056313, 2007.

[12] T. Hertkorn. Nonlinear triad interactions in two-dimensional turbulence. *Diplomarbeit, Universität Bayreuth, Germany*, 2007.

[13] M. Haslehner. Fourier space structure of nonlinear interactions in navier-stokes turbulence. *Diplomarbeit, Ludwig-Maximilians-Universität, München, Germany*, 2008.

[14] L. D. Landau and E. M. Lifshitz. Fluid mechanics. *Pergamon Press, Oxford*, 1987.

[15] C. Foias, O.Manley, R. Rosa, and R. Temam. Navier-Stokes equations and turbulence. *Cambridge University Press, Cambridge, England*, 2004.

[16] C. Canuto, M. Y. Hussaini, A. Quateroni, and T. A. Zang. Spectral methods in fluid dynamics. *Springer-Verlag, New York*, 1988.

[17] P. K. Kundu and I. M. Cohen. Fluid mechanics. *Academic Press, San Diego*, 1990.

[18] W.-C. Müller. Makroskopische und statistische eigenschaften dreidimensionaler magnetohydrodynamischer turbulenz. *IPP-Report, Max-Planck-Institut für Plasmaphysik*, IPP 5/90, 2000.

[19] D. Škandera. Statistical properties and structure of turbulent convection. *Fakultät für Physik der Technischen Universität München*, Dissertation, 2007.

[20] A. Brandenburg and K. Subramanian. Astrophysical magnetic fields and nonlinear dynamo theory. *Phys. Rep.*, 417:1–209, 2005.

[21] D. Biskamp. Nonlinear magnetohydrodynamics. *Cambridge University Pres, Cambridge, UK*, 1997.

[22] Y. Lithwick and P. Goldreich. Imbalanced weak magnetohydrodynamic turbulence. *Astrophys. J.*, 582:1220–1240, 2003.

[23] W. M. Elsässer. The hydromagnetic equations. *Phys. Rev.*, 79:183, 1950.

[24] S. B. Pope. Turbulent flows. *Cambridge University Press, Cambridge, UK*, 2000.

[25] R. H. kraichnan. Inertial-range spectrum of hydromagnetic turbulence. *Phys. fluids*, 8:1385–1387, 1965.

[26] A. Pouquet, U. Frisch, and J. Léorat. Strong MHD helical turbulence and the nonlinear dynamo effect. *J. Fluid Mech.*, 77:321–354, 1976.

[27] S. A. Orszag. Lectures on the statistical theory of turbulence, Les Houches lectures, fluid dynamics. *editors R.Balian and J.L. Peube*, 1973.

[28] Simmons and Salter. Experimental investigation and analysis of the velocity variations in turbulent flow. *Proc. Roy. Soc. Lond. A*, 145(854):212–234, 1934.

[29] D. C. Leslie. Developments in the theory of turbulence. *Oxford University Press, Clarendon*, 1973.

[30] W.-C. Müller and D. Biskamp. The evolving phenomenological view on magnetohydrodynamic turbulence. *Lecture Notes in Physics,614, edited by E. Flagarone, T. Passot*, Springer, 2003.

[31] H. K. Moffatt. The degree of knottedness of tangled vortex lines. *J. Fluid Mech.*, 35(1):117–129, 1969.

[32] A. Tsinober. An informal introduction to turbulence. *Kluwer Academic Publishers*, 2001.

[33] P. Sagaut, S. Deck, and M. Terracol. Multiscale and multiresolution approaches in turbulence. *Imperial College Press*, 2006.

[34] U. Frisch. Turbulence: The legacy of *A.N.Kolmogorov*. *Cambridge University Press*, 1996.

[35] W.-C. Müller and R. Grappin. Spectral energy dynamics in magnetohydrodynamic turbulence. *Phys. Rev. Lett.*, 95:114502, 2005.

[36] W.-C. Müller and D. Biskamp. Scaling properties of three-dimensional magnetohydrodynamic turbulence. *Phys. Rev. Lett.*, 84:475–478, 2000.

[37] D. Biskamp and W.-C. Müller. Scaling properties of three dimensional isotropic magnetohydrodynamic turbulence. *Phys. Plasmas*, 7(12):4889–4900, 2000.

[38] R. J. Leamon, C. W. Smith, N. F. Ness, W. H. Matthaeus, and H. K. Wong. Observational constraints on the dynamics of the interplanetary magnetic field dissipation range. *J. Geophys. Res.*, 103(A3):4775–4787, 1997.

[39] M. K. Verma. Statistical theory of magnetohydrodynamic turbulence:recent results. *Phys. Rep.*, 401:229–380, 2004.

[40] A. N. Kolmogorov. The local structure of turbulence in incompressible viscous fluid for very large Reynolds numbers. *Proceedings of the Royal Society A*, 434:9 (1991), [Dokl. Akad. Nauk SSSR, 30(4), 1941].

[41] A. N. Kolmogorov. Dissipation of energy in the locally isotropic turbulence. *Proceedings of the Royal Society A*, 434:15 (1991), [Dokl. Akad. Nauk SSSR, 32(1), 1941].

[42] A.N. Kolmogorov. On degeneration (decay) of isotropic turbulence in an incompressible viscous liquid. *Dokl. Akad. Nauk SSSR*, 31:538–540, 1941.

[43] P. S. Iroshnikov. Turbulence of a conducting fluid in a strong magnetic field. *Astron. Zh.*, 40:742, 1963, [Sov. Astron. 7, 566 (1964)].

[44] J. V. Shebalin, W. H. Matthaeus, and D. J. Montgomery. Anisotropy in mhd turbulence due to a mean magnetic field. *J. Plasma Phys.*, 29:525–547, 1983.

[45] W.-C. Müller, D. Biskamp, and R. Grappin. Statistical anisotropy of magnetohydrodynamic turbulence. *phys. Rev. E*, 67:066302, 2003.

[46] S. Galtier, H. Politano, and A. Pouquet. Self-similar energy decay in magnetohydrodynamic turbulence. *Phys. Rev. Lett*, 79(15):2807–2810, 1997.

[47] R. Grappin. Onset and decay of two-dimensional magnetohydrodynamic turbulence with velocity-magnetic field correlation. *Phys. Fluids*, 29(8):2433–2443, 1986.

[48] P. Goldreich and S. Sridhar. Toward a theory of interstellar turbulence. ii: Strong alfvénic turbulence. *Astrophys. J*, 438:763–775, 1995.

[49] S. Sridhar and P. Goldreich. Toward a theory of interstellar turbulence. i: Weak alfvénic turbulence. *Astrophys. J.*, 432:612–621, 1994.

[50] J. Maron and P. Goldreich. Simulations of incompressible magnetohydrodynamic turbulence. *Astrophys. J.*, 554:1175–1196, 2001.

[51] S. Boldyrev. On the spectrum of magnetohydrodynamic turbulence. *Astrophys. J.*, 626:L37, 2005.

[52] G. Gogoberidze. On the nature of incompressible magnetohydrodynamic turbulence. *Phys. Plasmas*, 14:022304, 2007.

[53] M. K. Verma, M. Goldstein, S. Ghosh, and W. Stribling. A numerical study of nonlinear cascade of energy in magnetohydrodynamic turbulence. *J. Geophys. Res.*, 101:21619–21625, 1996.

[54] A. Alexakis, P. D. Mininni, and A. Pouquet. Turbulent cascades, transfer, and scale interactions in magnetohydrodynamics. *New JOURNAL of Physics*, 9:298, 2007.

[55] F. Plunian and R. Stepanov. A non-local shell model of hydrodynamic and magnetohydrodynamic turbulence. *New JOURNAL of Physics*, 9:294, 2007.

[56] A. Pouquet. On two-dimensional magnetohydrodynamic turbulence. *J. Fluid Mech.*, 88:1–16, 1978.

[57] A. Ishizawa and Y. Hattori. Wavelet analysis of two-dimensional mhd turbulence. *J. Phys. Soc. Jpn.*, 67(2):441–450, 1998.

[58] M. Lesieur. Turbulence in fluids - stochastic and numerical modelling. *Kluwer Academic Publishers, Dordrecht*, 1990.

[59] M. M. Stanišic. Mathematic theory of turbulence. *Springer, New York*, 1988.

[60] M. K. Verma, A. Ayyer, and A. V. Chandra. Energy transfers and locality in magnetohydrodynamic turbulence. *Phys. Plasmas*, 12:82307, 2005.

[61] G. Dar, M. K. Verma, and V. Eswaran. Energy transfer in two-dimensional magnetohydrodynamic turbulence: formalism and numerical results. *Physica D*, 157:207–225, 2001.

[62] O. Debliquy, M. K. Verma, and D. Carati. Energy fluxes and shell-to-shell transfers in three-dimensional decaying magnetohydrodynamic turbulence. *Phys. Plasmas*, 12:042309, 2005.

[63] G. Dar, M. K.Verma, and V. Eswaran. A new approach to study energy transfer in magnetohydrodynamic turbulence. *ArXiv e-prints, physics/0006012*, 2000.

[64] R. H. Kraichnan. The structure of isotropic turbulence at very high Reynolds numbers. *J. Fluid Mech.*, 5:497–543, 1959.

[65] F. Waleffe. The nature of triad interactions in homogeneous turbulence. *Phys. Fluids A*, 4(2):350–363, 1992.

[66] V. N. Tsytovich. Theory of turbulent plasma. *Consultants Bureau. New York and London*, 1977.

[67] L. M. Smith and Y. Lee. On near resonances and symmetry breaking in forced rotating flows at moderate rossby number. *J. Fluid Mech.*, 535:111–142, 2005.

[68] N. E. L. Haugen, A. Brandenburg, and W. Dobler. Is nonhelical hydromagnetic turbulence peaked at small scales? *Astrophys. J.*, 597:L141–L144, 2003.

[69] P. Frick and D. Sokoloff. Cascade and dynamo action in a shell model of magnetohydrodynamic turbulence. *Phys. Rev. E*, 57:4155–4164, 1998.

[70] A. Brandenburg. Computational aspects of astrophysical mhd and turbulence. *Advances in nonlinear dynamos (The Fluid Mechanics of Astrophysics and Geophysics) eds. A.Ferriz-Mas and M.Nunez, Taylor & Francis, London and New York*, 9:269, (2003).

[71] E. O. Brigham. The fast fourier transform. *Prentice-Hall, Inc.,Englewood Cliffs, US*, 1974.

[72] A. Pouquet and G. S. Patterson. Numerical simulation of helical magentohydrodynamic turbulence. *J. Fluid Mech.*, 85(2):305, 1978.

[73] D. O. Gómez, P. D. Mininni, and P. Dmitruk. Parallel simulations in turbulent MHD. *Physica Scripta*, T116:123, (2005).

[74] G. Boffetta and S. Musacchio. Predictability of the inverse energy cascade in 2D turbulence. *Phys. Fluids*, 13(4):1060–1062, 2001.

[75] G. Boffetta. Energy and enstrophy fluxes in the double cascase of two-dimensional turbulence. *J. Fluid Mech.*, 589:253–260, 2007.

[76] H. A. Rose and P. L. Sulem. Fully developed turbulence and statistical mechanics. *JOURNAL de Physique*, 39(5):441–484, 1978.

[77] M. E. Maltrud and G. K. Vallis. Energy and enstrophy transfer in numerical simulations of two-dimensional turbulence. *Phys. Fluids A*, 5(7):1760–1775, 1993.

[78] Q. Chen, S. Chen, and G. L. Eyink. The joint cascade of energy and helicity in three-dimensional turbulence. *Phys. Fluids*, 15(2):361, 2003.

[79] P. D. Mininni, A. Alexakis, and A. Pouquet. Nonlocal interactions in hydrodynamic turbulence at high Reynolds numbers: The slow emergence of scaling laws. *Phys. Rev. E*, 77:036306, 2008.

[80] H. Aluie and G. L. Eyink. Localness of energy cascade in hydrodynamic turbulence. II. Sharp spectral filter. *Phys. Fluids*, 21:115108, 2009.

[81] G. L. Eyink and H. Aluie. Localness of energy cascade in hydrodynamic turbulence.I. Smooth coarse graining. *Phys. Fluids*, 21:115107, 2009.

[82] M. K. Verma, A. Ayyer, O. Debliquy, S. Kumar, and A. V. Chandra. Local shell-to-shell energy transfer via nonlocal interactions in fluid turbulence. *Pramana J. Phys.*, 65(2):297–310, 2005.

[83] Y. Zhou. Degrees of locality of energy transfer in the inertial range. *Phys. Fluids A*, 5:1092–1094, 1993.

[84] K. Ohkitani and S. Kida. triad interactions in a forced turbulence. *Phys. Fluids A*4, pages 794–802, 1992.

[85] J. Domaradzki and D. Carati. An analysis of the energy transfer and the locality of nonlinear interactions in turbulence. *Phys. Fluids*, 19:085112, 2007.

[86] G. Eyink. Locality of turbulent cascades. *Physica D*, 207:91–116, 2005.

[87] E. N. Parker. Hydromagnetic dynamo models. *Astrophys. J.*, 122:293, 1955.

[88] J. C. André and M. Lesieur. Influence of helicity on the evolution of isotropic turbulence at high Reynolds number. *J. Fluid. Mech.*, 81:187–207, 1977.

[89] V. Avinash, M. K. Verma, and A. V. Chandra. Field-theoretic calculation of kinetic helicity flux. *Pramana JOURNAL of Physics*, 66(2):447–453, 2006.

[90] Ya. B. Zeldovich. The magnetic field in the two-dimensional motion of a conducting turbulent liquid. *Sov. Phys. JETP*, 4:460–462, 1957.

[91] T. G. Cowling. Dynamo theories of cosmic magnetic fields. *Vistas Astr.*, 1, 1955.

[92] D. Biskamp and E. Schwarz. On two-dimensional magnetohydrodynamic turbulence. *Phys. Plasmas*, 8:3282–3292, 2001.

[93] D. Škandera and W.-C. Müller. Nonlinear cascades in two-dimensional turbulence magnetoconvection. *Phys. Rev. Lett.*, 102:224501, 2009.

[94] J. C. Perez and S. Boldyrev. Role of cross-helicity in magnetohydrodynamic turbulence. *Phys. Rev. Lett.*, 102:025003, 2009.

[95] J. Mason, F. Cattaneo, and S. Boldyrev. Dynamic alignment in driven magnetohydrodynamic turbulence. *Phys. Rev. Lett.*, 97:255002, 2006.

[96] Y. Hattori. Cross helicity and alignment structure in two-dimensional mhd turbulence. *J. Phys. Soci. Japan*, 62(8):2541–2544, 1993.

[97] H. K. Moffatt. Magnetic field generation in electrically conducting fluids. *Cambridge University Press, Cambridge, UK*, 1978.

[98] L. Mestel. Stellar magnetism. *Clarendon Press, Oxford, US*, 1999.

[99] J. Cho and E. T. Vishniac. The anisotropy of magnetohydrodynamic alfvénic turbulence. *Astrophys. J.*, 539:273, 2000.

[100] H. Aluie and G. L. Eyink. Scale locality of magnetohydrodynamic turbulence. *Phys. Rev. Lett.*, 104:081101, 2010.

[101] T. Forbes. Magnetic reconnection MHD theory and applications. *Cambridge University Press*, (2000).

[102] S. Ortolani. Reversed field pinch confinement physics. *Plasma Physics and Controlled Fusion*, 31(10):1665, (1989).

[103] M.A. Berger. Introduction to magnetic helicity. *Plasma Phys. Control. Fusion*, 41:B167–B175, 1999.

[104] A. Alexakis, P.D. Mininni, and A.Pouquet. On the inverse cascade of magnetic helicity. *The Astrophysical JOURNAL*, 640:335–343, 2006.

[105] P. D. Mininni, D. C. Montgomery, and A. Pouquet. Numerical solutions of the three-dimensional magnetohydrodynamic alpha-model. *Phys.Rev.E*, 71:046304, (2005).

[106] A. Brandenburg. The inverse cascade in turbulent dynamos. *arxiv:astro-ph/0012112v1*, (2000).

[107] S. K. Malapaka. A study of magnetic helicity in decaying and forced 3D-MHD turbulence. *IPP-Report, Max-Planck-Institut für Plasmaphysik*, IPP 5/121, 2010.

[108] S. Chen, R. E. Ecke, G. L. Eyink, M. Rivera, M. Wan, and Z. Xiao. Physical mechanism of the two-dimensional inverse energy cascade. *Phys. Rev. Lett.*, 96:084502, 2006.

[109] L. D. Landau and E. M. Lifshitz. Statistical physics. volume V, 1st part, Pergamon Press, 1979.

[110] D. Biskamp and U. Bremer. Dynamics and statistics of inverse cascade processes in 2D magnetohydrodynamic turbulence. *Phys. Rev. Lett.*, 72(24):3819, 1993.

Acknowledgments

My deep gratitude and sincere appreciation from the depths of my heart to priv.-Doz. Dr. Wolf-Christian Müller who is my thesis supervisor for inviting me to Garching Campus and for giving me the opportunity to become a member of his group (Independent Junior Research Group "Computational Studies of Nonlinear (Magneto-) Fluid Dynamics") at Max-Planck-für Plasmaphysik (IPP), Garching, Germany. Thanks to him for suggesting the topics, formulating the objects, and encouragement and standing beside me to overcome the problems during this work. I also thank him for his beneficial help, supporting my work, and answering my numerous questions.

I would like to offer a special thanks to Prof. Dr. Sibylle Günter for supervising my thesis, beneficial help to finish my thesis and for the possibility to submit it at the Technical University of Munich.

Also, I would like to thank all other members of our group, particularly Dr. Angela Busse for her suggesting, supporting, and providing the necessary facilities in every stage of my work and I remain thankful to her for her great assistances with my numerous doubts and mistakes. I would like to express my great thanks to Dr. Jane Pratt who is post-doctoral in our group for her help on issues like manuscript reading towards the end of my thesis and other subjects. I am thankful to Mr. Christian Vogel, who was my junior for his beneficial help, good assistances and advices during this work. I am also thankful to Dr. Dan Škandera who was my senior for his helping and advices during this work. I remain to thank Dr. Shiva Kumar Malapaka for his great assistances, advices during this work and his co-operation after his finishing. My great thanks to both Mr. Tobias Hertkorn and Mrs. Myléne Haslehner for their helping and understanding more subjects via their diploma thesis. I wish to thank Mr. Johannes Griesshammer, who is my room colleague for his supporting and encouragement. I also wish to thank all other members of my group for their understanding and support.

I wish to thank the supper computing team at the RZG for their efforts and helpful in providing, solving the problems in the necessary computing resources for my progress. I also would like to thank the librarians, administrative staff and security at IPP for helping me whenever I need them.

Great thanks and appreciation to both the Ministry of Higher Eductation and Cultural Affairs and Missions Sector in Arab Republic of Egypt, where they allow me to get one of the Ph.D. missions to Germany. I also thank them for their good co-operation and exchange in the Cultural and scientific with Germany univeristies.

I would like to express my thanks and appreciation to Prof. Dr. El Sayed Tag Eldin, the

Egyptain attache in the cultural office in Berlin for his contacts, follow-up and encouragement during this work. I wish to thank all members of the Egyptian Eductional Mission office for their helping in all administrative subjects and encouragement.
All my great thanks to Minufiya University, Egypt. Especially Faculty of Science, Physics Department where I have my work position.
I would like to express my deep thanks to Prof. Dr. Hussein M. El-Samman, Head of Phys. Dep., Minufiya Uni., Egypt for his helping, teaching more useful subjects in physics and encouragement for me all time.
My deep gratitude and sincere appreciation to Prof. Dr. El-Sayed M. Awad who is my Prof. and great brother for his supporting, beneficial help, and teaching how I can make scientific research.
I remain thankful to Prof. Dr. Abdel-Azeem. M. Hussien, prof. Dr. Anwar. A. Hegazy, and Prof. Dr. Mahmoud Ewaida for their great helping and encouragment.
Special thanks to Prof. Dr. Meawad El-Kholy, Vice Dean for student affairs and Prof. Dr. Amin El-Adawy for their great helping and encouragement for studying in Germany. I also would like to express my deep thanks to all staff members, colleagues, and laboratories assistants in Phys. Dep., Minufiya Uni., Egypt.
I wish to thank my wife and children from the depth of my heart for their helping and encouragement during this work. I would like to thank my parents, brothers, sisters, friends and dear relatives in Egypt for their encouragement.
Last but not least, I wish to thank the Almighty GOD, for having given me strength, courage, patience and health to complete this work.